ARTTU ERÄRANTA

Hyperuricemia and Calcium-Phosphate Metabolism in Experimental Renal Insufficiency

Effects on Oxidative Stress and the Renin-Angiotensin-Aldosterone System

ACADEMIC DISSERTATION
To be presented, with the permission of
the Board of the School of Medicine of the University of Tampere,
for public discussion in the Jarmo Visakorpi Auditorium
of the Arvo Building, Lääkärinkatu 1, Tampere,
on April 4th, 2014, at 12 o'clock.

UNIVERSITY OF TAMPERE

ARTTU ERÄRANTA

Hyperuricemia and Calcium-Phosphate Metabolism in Experimental Renal Insufficiency

Effects on Oxidative Stress and the Renin-Angiotensin-Aldosterone System

Acta Universitatis Tamperensis 1915
Tampere University Press
Tampere 2014

UNIVERSITY OF TAMPERE

ACADEMIC DISSERTATION
University of Tampere, School of Medicine
Minerva Institute for Medical Research, Helsinki
University of Helsinki, Department of Clinical Chemistry
Etelä-Pohjanmaa Central Hospital Laboratory, Department of Clinical Chemistry
Finland

Supervised by
Professor Ilkka Pörsti
University of Tampere
Finland

Reviewed by
Docent Risto Kerkelä
University of Oulu
Finland
Docent Risto Tertti
University of Turku
Finland

Cover design by
Mikko Reinikka

Distributor:
kirjamyynti@juvenes.fi
http://granum.uta.fi

Acta Universitatis Tamperensis 1915
ISBN 978-951-44-9398-0 (print)
ISSN-L 1455-1616
ISSN 1455-1616

Acta Electronica Universitatis Tamperensis 1399
ISBN 978-951-44-9399-7 (pdf)
ISSN 1456-954X
http://tampub.uta.fi

Suomen Yliopistopaino Oy – Juvenes Print
Tampere 2014

TABLE OF CONTENTS

LIST OF ORIGINAL COMMUNICATIONS

This thesis is based on the following original communications, which are referred to in the text using roman numerals I-V:

I Arttu Eräranta, Venla Kurra, Anna M. Tahvanainen, Tuija I. Vehmas, Peeter Kööbi, Päivi Lakkisto, Ilkka Tikkanen, Onni J. Niemelä, Jukka T. Mustonen and Ilkka H. Pörsti: Oxonic acid-induced hyperuricemia elevates plasma aldosterone in experimental renal insufficiency. Journal of Hypertension 2008; 26: 1661-1668.

II Venla Kurra, Arttu Eräranta, Pasi Jolma, Tuija I. Vehmas, Asko Riutta, Eeva Moilanen, Anna Tahvanainen, Jarkko Kalliovalkama, Onni Niemelä, Juhani Myllymäki, Jukka Mustonen and Ilkka Pörsti: Hyperuricemia, Oxidative Stress, and Carotid Artery Tone in Experimental Renal Insufficiency. American Journal of Hypertension 2009; 22: 964-970.

III Arttu Eräranta, Päivi J. Lakkisto, Ilkka Tikkanen, Jukka T. Mustonen and Ilkka H. Pörsti: Paricalcitol and renin-angiotensin components in remnant kidneys. Kidney International 2009; 75: 339-340.

IV Arttu Eräranta, Asko Riutta, Meng Fan, Jenni Koskela, Ilkka Tikkanen, Päivi Lakkisto, Onni Niemelä, Jyrki Parkkinen, Jukka Mustonen and Ilkka Pörsti: Dietary Phosphate Binding and Loading Alter Kidney Angiotensin-Converting Enzyme mRNA and Protein Content in 5/6 Nephrectomized Rats. American Journal of Nephrology 2012; 35: 401-408.

V Arttu Eräranta, Suvi Törmänen, Peeter Kööbi, Tuija Vehmas, Päivi Lakkisto, Ilkka Tikkanen, Eeva Moilanen, Jukka Mustonen and Ilkka Pörsti: Phosphate Binding with Calcium Carbonate Reduces Aortic Angiotensin Converting Enzyme and Enhances Bioactivity of Endothelium-derived Nitric Oxide in Experimental Renal Insufficiency. Submitted.

MOST IMPORTANT ABBREVIATIONS

$1,25(OH)_2D_3$	1,25-dihydroxycholecalciferol, calcitriol
18S	18S ribosomal ribonucleic acid
$25(OH)D_3$	25-hydroxycholecalciferol, calcidiol
8-iso-$PGF_{2\alpha}$	8-isoprostaglandin $F_{2\alpha}$
ACE	Angiotensin-converting enzyme
ACE2	Angiotensin-converting enzyme 2
ACEI	Angiotensin-converting enzyme inhibitors
Ach	Acetylcholine
ADMA	Asymmetric dimethylarginine
AMP	Adenosine monophosphate
Ang	Angiotensin
ANOVA	Analysis of variance
ARB	Angiotensin II receptor type 1 blockers
AT_{1R}	Angiotensin II receptor type 1
AT_{1aR}	Angiotensin II receptor subtype 1a
AT_{1bR}	Angiotensin II receptor subtype 1b
AT_{2R}	Angiotensin II receptor type 2
AT_{4R}	Angiotensin IV receptor
bFGF	Basic fibroblast growth factor
BP	Blood pressure
BSA	Bovine serum albumin
CaSR	Ca^{2+}-sensing receptor
cGMP	Cyclic guanosine monophosphate
CKD	Chronic kidney disease
CKD-EPI	CKD-Epidemiology Collaboration GFR equation
COX-2	Cyclooxygenase-2
CRI	Chronic renal insufficiency
C-Src	Cellular Src tyrosine kinase
CTGF	Connective tissue growth factor
CVD	Cardiovascular disease
EDTA	Ethylenediaminetetraacetic acid

ERK	Extracellular signal-regulated kinase
ESA	Erythropoiesis-stimulating agent
ESRD	End-stage renal disease
ET-1	Endothelin-1
ETA	Endothelin-1 receptor type A
FGF23	Fibroblast growth factor 23
GAPDH	Glyceraldehyde 3-phosphate dehydrogenase
HDL	High-density lipoprotein
HO-1	Heme oxygenase-1
LDL	Low-density lipoprotein
L-NAME	NG-nitro-l-arginine methyl ester
MAP	Mitogen-activated protein (kinase)
Mas	Mas proto-oncogene
MDRD	Modification of Diet in Renal Disease GFR equation
MGP	Matrix Gla protein
mRNA	Messenger ribonucleic acid
NE	Norepinephrine (noradrenaline)
NF-κB	Nuclear factor-κB
NO	Nitric oxide
NX	5/6 nephrectomy
Oxo	2.0% oxonic acid diet
PCR	Polymerase chain reaction
Pi	Phosphate (inorganic)
PPAR-γ	peroxisome proliferator-activated receptor γ (gamma)
PRA	Plasma renin activity
PRR	(Pro)renin receptor
PTH	Parathyroid hormone
RAAS	Renin-angiotensin-aldosterone system (circulating)
RAS	Renin-angiotensin system (tissue-level and intracellular)
RIA	Radioimmunoassay
RNA	Ribonucleic acid
ROS	Reactive oxygen species
RT	Room temperature

RT-PCR	Reverse transcription polymerase chain reaction
Runx2	Runt-related transcription factor 2
RXR	Retinoid X receptor
SD	Sprague-Dawley rats
SDS	Sodium dodecyl sulphate
SHPT	Secondary hyperparathyroidism
SOD	Superoxide dismutase
TRAP	Total peroxyl radical-trapping capacity
UA	Uric acid
URAT1	Uric acid transporter 1
VDR	Vitamin D receptor
XO	Xanthine oxidase

ABSTRACT

Chronic kidney disease is linked to several disturbances of the normal homeostasis. Progressing kidney damage may lead to decreased renal filtration capacity and alter cardiovascular physiology in a way that favors inflammation, arterial remodeling, elevated blood pressure, and increased oxidative stress. When the loss of renal function continues unabated, chronic renal insufficiency (CRI) develops.

Experimental models offer a flexible tool to study disorders that cannot be investigated in a cell culture, or are not feasible or ethical for a clinical setting. The present series of studies featured a rat model of experimental chronic renal insufficiency induced by the surgical ablation of 5/6 of total renal mass (NX). Decapsulation of both kidneys was performed in the sham rats (Sham). Dietary and pharmacological interventions included 2.0% oxonic acid-induced hyperuricemia, paricalcitol treatment, and phosphate loading or phosphate binding with 3.0% calcium carbonate. Elevated circulating level of uric acid, hyperuricemia, is commonly associated with the initiation of multiple pathophysiological processes, whereas uric acid also functions as an antioxidant protecting from oxidative stress. Paricalcitol is a vitamin D receptor activator, which is used to treat secondary hyperparathyroidism, while calcium-based phosphate binders have been traditionally used to lower serum phosphate levels. The studies were designed to mimic some of the most common complications associated with kidney disease.

The aim of this investigation was to determine the potential changes in the renin-angiotensin-aldosterone (RAAS) system gene expression and in the markers of oxidative stress during stage 3 experimental CRI. The two studies on experimental hyperuricemia were designed to specifically focus on the circulating RAAS and the renal tissue renin-angiotensin system (RAS), carotid artery tone, and antioxidant capacity. In the third study, the effects of paricalcitol on the kidney RAS component gene transcription were studied. The final two studies examined altered calcium-phosphate metabolism in CRI, and concentrated on the kidney and vascular RAS gene expression, as well as the effects on vascular function and nitric oxide (NO) metabolites in conduit-size arteries.

The principal measurement methods used in this series of studies were quantitative *in vitro* autoradiography, Western blotting, real-time quantitative RT-PCR, radioimmunoassay, histological analysis, and *in vitro* vascular function determinations. The duration of the

studies was 12 or 27 weeks, which were chosen to influence the severity of CRI. The experimental models were found suitable for the study designs, and successfully produced the previously reported characteristics of each disorder.

Experimental hyperuricemia activated the circulating RAAS, reflected as increased plasma renin activity and aldosterone concentration, as well as reduced oxidative stress and increased antioxidant capacity *in vivo*, as evidenced by reduced 24-hour urinary 8-isoprostaglandin $F_{2\alpha}$ excretion and increased plasma total peroxyl radical-trapping capacity, respectively. Hyperuricemia also caused elevated K^+ to Na^+ ratio in the urine and enhanced NO-mediated vasorelaxation of the carotid artery in the NX rats. According to the findings of these two 12-week studies, the role of aldosterone seems pivotal in the hyperuricemia-induced Na^+ retention and blood pressure elevation, whereas the increased uric acid level may contrarily provide beneficial effects on oxidative stress.

Fifteen-week paricalcitol treatment, initiated 12 weeks after the initial insult, did not influence the transcription levels of the kidney RAS component genes, which were elevated in the NX rats. This result was contrary to an earlier experimental report, which found a suppressing influence on several kidney RAS components following initiation of paricalcitol treatment only four days after surgery. Without doubt, the situation in the included study more resembles the clinical renal disease, and may explain the inconsistency in comparison with the earlier findings.

Dietary phosphate loading was associated with elevated kidney, cardiac, and aortic angiotensin-converting enzyme (ACE) expression, increased tissue damage, and lower angiotensin II receptor subtype 1a transcription in the NX rats. Phosphate binding had opposite effects on kidney, cardiac, and aortic ACE, as well as kidney damage and nitrated proteins in the aorta, while it also enhanced vasorelaxation via increased bioactivity of endothelium-derived NO. The hypertension in the NX rats was associated with elevated levels of plasma and urine NO metabolites, decreased endothelial NO synthase, increased ACE and nitrated proteins in the aorta, as well as impaired vasorelaxation via endothelium-derived NO in the mesenteric artery. These findings underline the importance of effective phosphate control in chronic kidney disease.

In conclusion, the present studies provide a broad assessment of common complications associated with CRI. The differing effects on the RAAS and oxidative stress highlight the multifaceted metabolic modulation in stage 3 kidney disease.

TIIVISTELMÄ

Krooninen munuaistauti aiheuttaa monia häiriöitä kehon normaalissa homeostaasissa. Edetessään munuaisvaurio vähentää munuaisten suodatuskapasiteettia, nostaa virtsahapon pitoisuutta verenkierrossa ja aiheuttaa verenkiertoelimistössä muutoksia, jotka suosivat tulehdustilaa, verisuonten rakenteellisia muutoksia (jäykistyminen, seinämän paksuuntuminen), kohonnutta verenpainetta ja lisääntynyttä hapetusstressiä. Jos munuaisten suodatuskapasiteetin lasku jatkuu esteittä, on seurauksena lopulta terminaalinen munuaisten vajaatoiminta.

Kokeelliset mallit tarjoavat mahdollisuuden tutkimuksiin, joita ei voi toteuttaa soluviljelymalleissa tai kliinisissä hankkeissa. Tässä tutkimussarjassa käytettiin munuaisten vajaatoiminnan rottamallia, joka aiheutettiin vähentämällä kirurgisesti 5/6 munuaismassasta (NX). Verrokkien toimenpiteenä oli munuaiskapselien poisto (Sham). Tutkimusasetelmina olivat kokeellinen hyperurikemia, parikalsitolihoito, fosfaattilisä sekä fosforinsitomishoito 3.0% kalsiumkarbonaatilla. Hyperurikemia aiheutettiin ravinnon 2.0% oksonihappolisällä, joka estää virtsahappoa metaboloivaa urikaasi-entsyymiä. Vaikka hyperurikemian on esitetty olevan monien patofysiologisten prosessien taustalla, toimii virtsahappo myös hapetusstressiltä suojaavana antioksidanttina. D-vitamiinireseptoria aktivoivalla parikalsitolilla hoidetaan sekundaarista hyperparatyreoosia, kun taas kalsiumperäisiä fosforinsitojia käytetään vähentämään elimistön fosforipitoisuutta.

Tutkimuksessa selvitettiin reniini-angiotensiini-aldosteroni -järjestelmän (RAAS) komponenttien geeni-ilmentymisen muutoksia sekä muutoksia hapetusstressitasossa. Kokeellisissa hyperurikemiatutkimuksissa tärkeimpinä kohteina olivat kiertävä RAAS ja munuaiskudoksen reniini-angiotensiini -järjestelmä (RAS), kaulavaltimon tonus sekä hapetusstressi. Kolmannessa osatyössä tutkittiin parikalsitolihoidon vaikutusta munuaisen RAS-geenien luentaan. Kaksi viimeistä osatyötä käsittelivät kalsium-fosfori -tasapainon muutoksia kokeellisessa munuaisten vajaatoiminnassa, tutkimuskohteina munuaisten ja verisuoniston RAS-geenien ekspression muutokset, verisuonen supistustilan säätely (suolilievevaltimo) ja verenkierron sekä virtsan typpioksimetaboliitit.

Pääasiallisina mittausvälineinä käytettiin *in vitro* autoradiografiaa, Western blot -menetelmää, reaaliaikaista käänteis-PCR -menetelmää, radioimmunoassay -menetelmää, histologista analyysiä sekä *in vitro* verisuonifunktion rekisteröintiä. Osatutkimusten

kestona oli 12 tai 27 viikkoa, millä vaikutettiin munuaisten vajaatoiminnan asteeseen. Kokeelliset mallit toimivat odotetusti, ja niissä havaitut ominaisuudet olivat linjassa aiemman tiedon kanssa.

Kokeellinen hyperurikemia aktivoi kiertävän RAAS:n eli lisäsi plasman reniiniaktiivisuuttta ja aldosteronipitoisuutta. Samanaikaisesti se vähensi hapetusstressiä ja lisäsi antioksidanttikapasiteettia, mikä voitiin havaita vuorokausivirtsan vähentyneenä 8-iso-$PGF_{2\alpha}$ -erityksenä sekä lisääntyneenä plasman TRAP-arvona. Vaikka hyperurikemia nosti verenpainetta ja lisäsi kaliumin hukkaa virtsaan, havaittiin samalla parantunut kaulavaltimon typpioksidivälitteinen verisuonen laajeneminen. Näiden 12 viikkoa kestäneiden tutkimusten löydökset viittaavat aldosteronin rooliin hyperurikemian aiheuttamien natriumretention ja kohonneen verenpaineen taustalla. Toisaalta löydökset osoittavat myös hyperurikemian aiheuttamia myönteisiä vaikutuksia hapetusstressin tasoon.

Viidentoista viikon parikalsitolihoito, joka aloitettiin 12 viikkoa NX- ja Sham-leikkausten jälkeen, ei vaikuttanut munuaiskudoksen RAS-geenien luentaan, joka lisääntyi NX rotissa. Tämä löydös ei vastaa aiemmin julkaistua laajan huomion saanutta kokeellista tutkimusta, jossa parikalsitolihoito vähensi munuaisten RAS-geenien luentaa, kun hoito aloitettiin heti neljä päivää leikkausten jälkeen. Tutkimussarjaan kuuluvan osatyön asetelma muistuttaa enemmän kliinistä munuaistautia, mikä voi selittää eriävät löydökset.

Ravinnon fosfaattilisä aiheutti lisääntynyttä munuaisten, sydämen ja valtimoiden angiotensiiniä konvertoivan entsyymin (ACE) ilmentymistä, lisäsi kudosvauriota ja vähensi angiotensiini II:n reseptori 1a:n luentaa NX rotissa. Fosforinsidonta aiheutti päinvastaisen vasteen tutkittujen kudosten ACE-ekspressiossa. Lisäksi se vähensi munuaisvaurioita ja nitroproteiinien määrää valtimoissa sekä paransi typpioksidivälitteistä verisuonen laajenemista. NX rottien kohonnut verenpaine oli yhteydessä typpioksidin metaboliittien lisääntymiseen plasmassa ja virtsassa sekä vähentyneeseen endoteelin typpioksidisyntaasi-entsyymiin. ACE-ekspressio ja nitroproteiinien määrä lisääntyi valtimoissa ja typpioksidivälitteinen vasorelaksaatio heikentyi suolilievevaltimossa.

Kaikkiaan tutkimussarja mallintaa kroonisen munuaisten vajaatoiminnan tyypillisiä komplikaatioita ja niihin vaikuttavia tekijöitä. Tutkimuslöydökset korostavat veren fosfaattipitoisuuden hallinnan merkitystä munuaisten vajaatoiminnassa sekä komplikaatioiden taustalla olevan säätelyjärjestelmän monimuotoisuutta.

INTRODUCTION

Chronic kidney disease (CKD), with the associated disturbances in mineral metabolism and cardiovascular complications, has become a common public health issue in all modern countries (KDIGO 2013). CKD predisposes to chronic renal insufficiency (CRI) and is a major risk factor for the leading global cause of premature death – cardiovascular disease (CVD) (Mendis et al. 2011, Talreja et al. 2013). The principal contributors to kidney damage are rapidly increasing diabetes mellitus type II, lifestyle factors such as dietary habits and excessive salt intake, as well as chronically aging population (Lopez-Vargas et al. 2013).

Uric acid (UA) metabolism and elevated serum UA, hyperuricemia, have been increasingly studied in recent years. This is mainly due to the elusive role of UA behind hypertension and metabolic disorders. There has been a multitude of studies linking hyperuricemia to endothelial dysfunction, microvascular disease, increased inflammation, and the initiation of metabolic syndrome (Johnson et al. 2013a, Kanbay et al. 2013). However, it has long been known that UA can act as an antioxidant (Ames et al. 1981), while low circulating concentrations have been linked to several neurological disorders (Spitsin and Koprowski 2008) and even premature death in hemodialysis patients (Hsu et al. 2004). No clear-cut consensus has yet formed on whether hyperuricemia is harmful or beneficial.

Experimental CRI studies using 5/6 nephrectomized (NX) remnant kidney rats have been performed since the early 1960's, when Morrison published the article describing this model (Morrison 1962). In the NX, removal of one kidney and two-thirds of the remaining kidney results in progressive hyperfiltration and hypertrophy (Morrison and Howard 1966, Shimamura and Morrison 1975). This model features low circulating concentration of renin, as the loss of juxtaglomerular mass decreases renin synthesis and secretion. One of the most important reasons for the widespread use of NX is its flexibility. The duration of the disease progression can easily be tailored to meet the criteria of different study designs, while the mechanisms of progression closely follow that of human CKD.

Calcium-phosphate metabolism is one of the key targets for pharmacological treatment of CKD (Slatopolsky 2011). Disturbances in renal handling of phosphate rapidly develop with the loss of filtration capacity. Parathyroid hormone (PTH) levels rise already in the early stages of CKD due to phosphate retention. The ensuing secondary

hyperparathyroidism (SHPT) is an early and major complication of CKD (Slatopolsky et al. 2001). As active vitamin D synthesis decreases, the vitamin D receptor (VDR) activation is suppressed. Paricalcitol is a third-generation VDR activator, which combats SHPT by lowering PTH concentration and suppressing its expression in the parathyroid gland (Coyne et al. 2006). Contrary to supplementation with calcitriol ($1,25(OH)_2D_3$), paricalcitol does not induce hypercalcemia, renal stones, and increased hyperphosphatemia, making it more suitable for SHPT treatment.

The aim in this series of studies was to investigate the effects of experimental hyperuricemia, altered calcium-phosphate metabolism, and paricalcitol treatment in experimental renal insufficiency. The principal focus was on oxidative stress, and the components of the renin-angiotensin-aldosterone system (RAAS), as determined by various different methods including *in vitro* autoradiography, Western blotting, real-time RT-PCR, radioimmunoassay (RIA), and *in vitro* vascular function measurements. Combined together, these investigations aim to provide further insight into the elaborate modulation of metabolism during stage 3 experimental CRI.

REVIEW OF THE LITERATURE

1. CHRONIC KIDNEY DISEASE AND CHRONIC RENAL INSUFFICIENCY

The global prevalence of CKD and CRI is increasing rapidly (Lopez-Vargas et al. 2013). Together with immense public health concerns, it brings profound economic implications that make suppression of kidney diseases a major health-care priority (Khwaja et al. 2007, Salonen et al. 2007). CKD predisposes to end-stage renal disease (ESRD) and is a major risk factor for CVD, the leading global cause of premature death (Mendis et al. 2011, Talreja et al. 2013). Studies suggest that over 10% of the population in Europe (Lameire et al. 2005, de Jong et al. 2008) and almost 17% of the population in the USA (Rosamond et al. 2008) are affected by some stage of CKD. The rising global prevalence of CKD is largely attributable to increased rates of diabetes and hypertension, as well as ageing population, which further complicates successful treatment and prevention (Lopez-Vargas et al. 2013).

1.1. Chronic kidney disease

The Kidney Disease Outcome Quality Initiative (K/DOQI) of the National Kidney Foundation published the first internationally accepted definition and classification of CKD in 2002 (K/DOQI 2002). Eleven years after the first publication, the Kidney Disease: Improving Global Outcomes (KDIGO) organization published an update (KDIGO 2013). The new guidelines apply to all patients with CKD not receiving renal replacement therapy (RRT) and include both children and adults (Stevens and Levin 2013). According to both guidelines, CKD is defined as structural or functional abnormalities of the kidneys or glomerular filtration rate (GFR) of <60 ml/min/1.73m^2 for 3 months or more (K/DOQI 2002, KDIGO 2013).

It has long been known that the best overall indicator of renal function is the GFR (Smith 1951). However, the structural damage in CKD can be present without a decrease in GFR, and may include pathological abnormalities or markers of kidney damage such as urinary, blood, and imaging abnormalities (Levey et al. 2007b). Kidney damage can be ascertained in many cases by the presence of albuminuria, defined as albumin-to-creatinine ratio >30 mg/g in two of three spot urine specimens (Levey et al. 2005). GFR value can be estimated

by measuring serum creatinine or the amount of creatinine excreted in 24-hour urine sample, and also by the use of estimating equations to determine clinically applicable value. Serum creatinine is a well-known marker of muscular mass in steady state, and thus correlates with age, gender and ethnicity (Delanaye et al. 2013).

Directly measuring the GFR is often cumbersome and costly, which is why estimation of GFR has become essential for the diagnosis and evaluation of renal function (Delanaye et al. 2013). Many different equations to estimate GFR based on serum creatinine concentration have been published (Cockcroft and Gault 1976, Levey et al. 1999, Kemperman et al. 2002, Levey et al. 2009). The first of these equations was developed by Cockcroft and Gault in 1976 (Cockcroft and Gault 1976). It was popular for many years because of its simplicity and ease of use. However, this equation estimates creatinine clearance and not true GFR, and was too inaccurate for CKD diagnosis. An equation derived from measured GFR was developed 23 years later in the Modification of Diet in Renal Disease (MDRD) Study (Levey et al. 1999). This equation takes into account the concentration of serum creatinine and 6 other variables. The K/DOQI selected MDRD as the equation of choice, and it is currently in worldwide clinical use (K/DOQI 2002). Recently, some concern has been raised whether the MDRD equation systematically underestimates GFR in different populations in ranges over 60 ml/min/1.73m^2, thus overestimation the prevalence of CKD (Rule et al. 2006, Delanaye et al. 2011a, Delanaye et al. 2011b). In 2009, a new equation was developed by the CKD-Epidemiology Collaboration (CKD-EPI) with the aim to better estimate GFR levels in this range (Levey et al. 2009). It remains to be seen whether the putative benefits of CKD-EPI will make it the equation of choice in the future (Inker and Levey 2013).

The severity of kidney disease is classified according to the level of GFR into five stages in which lower stage number represents a less severe form of the disease (Table 1) (Levey et al. 2007b). The first stage exhibits kidney damage with normal GFR of ≥90 ml/min/1.73m^2, whereas the second stage features a slightly decreased GFR of 89-60 ml/min/1.73m^2. The most common findings in these two stages are albuminuria, proteinuria, and hematuria, depending on the symptoms and manifestations of the renal damage. Kidney disease progression leads to the third stage when GFR drops to values <60 ml/min/1.73m^2. This stage is commonly described as early CRI. The fourth stage is late CRI or pre-ESRD with a severely decreased GFR of 29-15 ml/min/1.73m^2. The fifth, and

the last, stage of CKD is ESRD or kidney failure, and patients going through this stage have a GFR under 15 ml/min/1.73m^2 and need RRT (Levey et al. 2005). In Finland, the Finnish Registry for Kidney Diseases publishes a yearly report of patients undergoing RRT (2012). The newest report published in 2012 states that the total prevalence of RRT had increased by 31% from 2001 and by 10% from 2006. Somewhat surprisingly the incidence of RRT was 7% lower than 2001. Geographically the prevalence of RRT was highest in the southwestern region and lowest in the northern region of Finland.

Table 1. The current classification of chronic kidney disease.

Stage:	Description:	GFR (ml/min/1.73m$^{2)}$	Description:
1	Kidney damage with normal or increased GFR	≥90	Albuminuria, proteinuria, hematuria
2	Kidney damage with mildly decreased GFR	60-89	Albuminuria, proteinuria, hematuria
3	Moderately decreased GFR	30-59	Early chronic renal insufficiency
4	Severely decreased GFR	15-29	Late chronic renal insufficiency
5	Kidney failure	<15 (or dialysis)	Renal failure, uremia, end-stage renal disease

GFR = glomerular filtration rate; Table adapted from Levey et al. (Levey et al. 2007b)

1.1.1. Disease progression

Progressing CKD is characterized by histological findings of glomerulosclerosis, vascular sclerosis and tubulointerstitial fibrosis, leading to a shared final pathway of injury (Fogo 2007). Podocyte damage and loss is a key step at which many pathogenic mechanisms unite to result in glomerulosclerosis (Kriz et al. 1998, Lemley 2012). Glomerulosclerosis initiates with damage to the endothelial cells, which may be caused by several different mechanisms (Figure 1). Consequently the damaged endothelial cells lose their anti-coagulant, anti-inflammatory and anti-proliferative properties and begin to synthesize cell adhesion molecules (Johnson 1994). These changes rapidly lead to increased influx of platelets and inflammatory cells into the glomerular capillaries. Subsequently, mesangial

cell proliferation is stimulated by infiltrating monocytes (Johnson 1994). Mesangial cells are the major extracellular matrix (ECM) forming cell type in the glomerulus and vital to the glomerulosclerotic process, while the activated interstitial fibroblast or myofibroblast is central to the development of tubulointerstitial fibrosis (Khwaja et al. 2007). These cells derive from diverse origins, such as residential fibroblasts, vascular pericytes, epithelial-to-mesenchymal transition, and circulating fibrocytes in bone marrow (He et al. 2013). It is also worth noting that the degree of tubulointerstitial damage has been shown to be a better predictor of decline in renal function than glomerulosclerosis (Schainuck et al. 1970).

The response to the initial glomerular and tubulointerstitial cell injury involves changes in cell number via necrosis, apoptosis, and cell proliferation, as well as cell size via cellular hypertrophy (Khwaja et al. 2007). These changes trigger the growth of ECM, and their interplay determines whether the initial kidney damage results in mending the injury and subsequent healing, or in scarring via progressive fibrosis (Fogo 2007, Khwaja et al. 2007). Many different growth factors appear to modulate progression of glomerular and tubulointerstitial scarring (Bohle et al. 1992). These factors and their roles may change at the different stages of injury. Previous studies have reported altered levels of RAAS components; especially angiotensin II (Ang II), as well as basic fibroblast growth factor (bFGF), endothelin-1 (ET-1), PDGF, TGF-β, and many chemokines among others, in progressive renal scarring (Fogo 2007). So far, no clinical therapies specifically targeting kidney remodeling and the ensuing fibrotic process has been available, but potential new drugs such as cysteamine (Okamura et al. 2013) and relaxin (Sasser 2013) have been reported to slow down harmful fibrosis in experimental settings.

As CKD progresses, new disorders and symptoms add up. Chronic kidney injury depletes endogenous intracellular and extracellular antioxidant systems, resulting in increased tissue oxidative stress (Okamura et al. 2013). Chronic renal failure, the last stage of CKD, is associated with increased cardiovascular morbidity and mortality, with the underlying causes including anemia, acidosis, hypertension, volume overload, and accumulation of uremic toxins (Luke 1998, Rostand and Drüeke 1999, Pörsti et al. 2004). Notably, in many CKD patients the disease never progresses this far. Longitudinal studies clearly show that patients with CKD are far more likely to die from CVD than to develop kidney failure (Keith et al. 2004, Levey et al. 2007b).

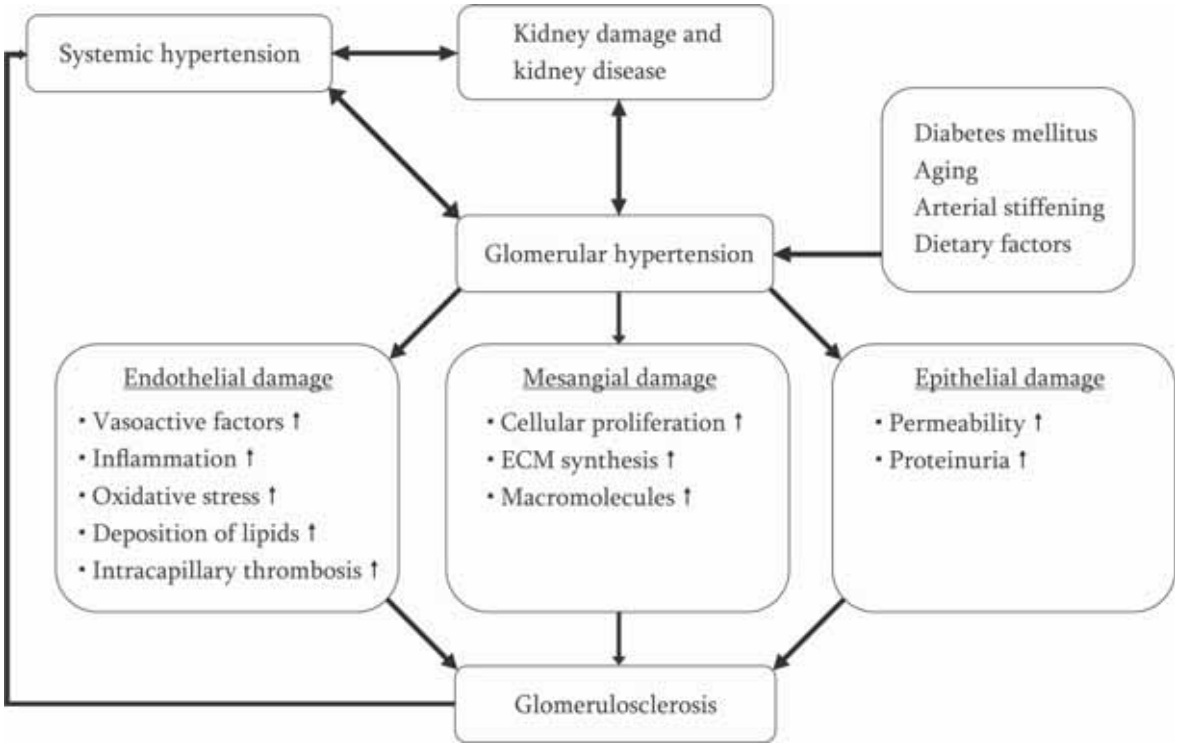

Figure 1. *Mechanisms of kidney damage and glomerulosclerosis.* Various factors lead to initial kidney damage and systemic hypertension via an increase in glomerular pressure. Glomerular hypertension causes endothelial, mesangial, and epithelial damage contributing to glomerulosclerosis. ECM = Extracellular matrix; Figure adapted from Johnson et al. (Johnson 1994) and Fogo (Fogo 2007).

1.1.2. Pharmacological treatment

Treatment of CKD is currently divided into pharmacological therapies that aim to treat the causes of CKD and therapies to maintain kidney function (Levey et al. 2007a). The main treatment to decrease the rate of disease progression is aggressive control of hypertension with the primary focus on RAAS inhibitors (Remuzzi et al. 2005). Systemic hypertension commonly accompanies renal disease and may both result from, and contribute to, CKD. Hypertension is known to accelerate the progression of CKD, and to achieve recommended BP targets, the majority of CKD patients require three or more BP lowering drugs (Talreja et al. 2013). The choice of second line drug should be based on specific comorbidities along with consideration of complementary method of action. Commonly a calcium-channel blocker or a diuretic is selected, as both have additive synergistic effects in combination with RAAS blockade (Talreja et al. 2013).

The RAAS has been a key focal point in studies of CKD progression mainly because the inhibition of its components provides major therapeutic effect in CKD (Remuzzi et al. 2005). Angiotensin-converting enzyme (ACE) inhibitors (ACEI) decrease glomerular capillary pressure by preferential dilation of the efferent arteriole (Brown and Vaughan 1998), likely mediated by inhibition of Ang II and also by increasing the vasodilatory bradykinin, which is degraded by ACE (Fogo 2007). Indeed, Ang II type 1 receptor blockers (ARB), which do not have this ability to increase bradykinin, do not preferentially dilate the efferent arteriole or decrease glomerular pressure to the extent that is seen with ACEI in most studies. However, both ACEI and ARB have shown superior efficacy in slowing progressive CKD in experimental models and in human CKD when compared with other BP-lowering agents. (MacKinnon et al. 2006, Fogo 2007). It is also worth noting that ARB leave the Ang II type 2 receptor (AT_{2R}) active, and may in theory lead to augmented beneficial effects by allowing unbound Ang II to bind this receptor (Fogo 2007).

Recently, a new treatment option to block RAAS has emerged in the form of direct renin inhibition (Morishita and Kusano 2013). Aliskiren is the most commonly used orally active non-peptide direct renin inhibitor, which acts by binding to the active site of renin and directly inhibits plasma renin activity (PRA). This effect is contrary to the reactive rise in PRA observed with ACEI and ARB. Direct renin inhibition appears to be generally efficient and safe, however, several studies have reported symptomatic hypotension following aliskiren treatment in patients with CKD. This is why careful observation of BP is needed with aliskiren treatment in early stage CKD patients (Morishita and Kusano 2013).

One of the common complications in progressive CKD is anemia, which develops to most patients at stages 3-4. Mechanistically this happens when enough renal erythropoietin-producing cells switch from a physiologic, erythropoietin-producing state, to a pathologic ECM-producing phenotype in response to inflammatory injury (Xiao and Liu 2013). As anemia becomes severe, the administration of erythropoiesis-stimulating agents (ESA) is generally required, along with the repletion of iron stores and the correction of other causes of anemia (Drüeke 2013). The introduction of ESAs three decades ago markedly improved the lives of many CKD patients, who until then had severe, often transfusion-dependent anemia (Watson 1989). Today there are three generations of ESAs used in CKD-associated

anemia (Magwood et al. 2013). Two types of recombinant human erythropoietin, epoetin α and epoetin β, have been available since ESAs were first developed. Both are highly effective but short-acting, as dosing is needed three times a week. Subsequently, two second-generation ESAs with an extended duration of action were approved, darbepoetin α and methoxy polyethylene glycol-epoetin β, with dosing interval of up to a month (Drüeke 2013). The third generation features peptide-based ESAs, such as peginesatide (Macdougall 2012), which is effective but highly expensive. These peptide-based ESAs are not homologous with erythropoietin and therefore exhibit no antibody cross-activity, which makes them also suitable for patients suffering from pure red cell aplasia (Drüeke 2013).

1.2. Vascular complications and oxidative stress

In CKD patients, the arterial remodeling is characterized by dilatation and intima-media hypertrophy of conduit arteries, as well as hypertrophy in the walls of peripheral muscular-type conduit arteries (Morris et al. 2001). These changes are mainly induced by oxidative stress, inflammation, homocysteine, endogenous nitric oxide (NO) synthase inhibitors, as well as the accumulation of oxidized low-density lipoproteins (LDL) (Annuk et al. 2003). Elevated plasma levels of ET-1 may also contribute to the cardiovascular remodeling in CKD patients (Demuth et al. 1998), as ET-1 type A receptor (ETA) antagonism has been successful in suppressing the increase in intimal and medial thickness of small mesenteric arteries (Amann et al. 2001). The remodeling of conductance vessels includes medial calcifications, increased ECM content and hyperplasia of smooth muscle (Amann et al. 1997). It is noteworthy that the vascular phenotype of even young dialysis patients may be comparable with that of 80-year-old subjects without kidney disease (Foley et al. 1998). Arterial remodeling and increased arterial stiffness measured from aortic pulse wave velocity are strong independent predictors of cardiovascular mortality (Blacher et al. 1999).

Vascular oxidative stress with an increased production of reactive oxygen species (ROS) contributes to mechanisms of vascular dysfunction (Förstermann 2010). Oxidative stress is mainly caused by an imbalance between the activity of endogenous pro-oxidative enzymes such as NADPH oxidase, xanthine oxidoreductase, or the mitochondrial respiratory chain, and anti-oxidative enzymes such as superoxide dismutase (SOD), glutathione peroxidase, and heme oxygenase (HO) (Puca et al. 2013). Also, small molecular weight antioxidants may play a role in the defense against oxidative stress (Chen et al. 2001). Increased ROS

concentrations reduce the amount of bioactive NO by chemical inactivation to form toxic peroxynitrite. Peroxynitrite can, in turn, uncouple the endothelial NO synthase (eNOS) to become a dysfunctional superoxide-generating enzyme that contributes to vascular oxidative stress (Kuzkaya et al. 2003). Oxidative stress and endothelial dysfunction can promote atherogenesis. Therapeutically, drugs in clinical use such as ACEI, ARB, and statins may have pleiotropic actions that can improve endothelial function (Souza-Barbosa et al. 2006). Also, dietary polyphenolic antioxidants can reduce oxidative stress, whereas clinical trials with antioxidant vitamins C and E failed to show an improved cardiovascular outcome (Förstermann 2010).

1.2.1. Nitric oxide

NO is a paracrine factor that controls vascular tone, inhibits platelet function, prevents adhesion of leukocytes, and reduces proliferation of the intima (Förstermann 2010). The endothelial cells continuously synthesize NO from L-arginine by the constitutive eNOS (Moncada and Higgs 1993). NO is able to activate guanylate cyclase, thereby increasing the production of cyclic guanosine monophosphate (cGMP) and reducing intracellular Ca^{2+}, subsequently relaxing the smooth muscle (Behrendt and Ganz 2002). It is well known that NO protects against vascular injury, inflammation, and thrombosis, which are all key events in the genesis and progression of atherosclerosis (Behrendt and Ganz 2002).

Several factors are involved in reduced NO bioactivity, such as mechanical disruption of the endothelium by atherosclerosis, as well as increased inactivation of NO by ROS (Ohara et al. 1993). This condition is known as endothelial dysfunction, which can promote vasospasm, thrombosis, vascular inflammation, and proliferation of vascular smooth muscle cells (VSMC) (Förstermann 2010). Endothelial dysfunction may also predispose the patient to accelerated atherosclerosis and may be involved in the pathogenesis of secondary hypertension in CRI (London et al. 2004). When compared with small vessels, the contribution of eNOS to vasomotion seems to be greater in conduit-size arteries, as the NO-mediated relaxation is more pronounced in large arteries (Garland et al. 1995, Geiger et al. 1997). The interaction between activation of vascular renin-angiotensin system (RAS) and the bioavailability of endothelium-derived NO is an important regulator of vascular tone (Raij 2001).

1.3. Experimental chronic renal insufficiency

The NX model (Morrison 1962, Morrison and Howard 1966) has been extensively used to investigate CRI. In this model, removal of 5/6 of total renal mass; one kidney and two-thirds of the remaining kidney, results in progressive hyperfiltration and nephron hypertrophy (Morrison and Howard 1966, Shimamura and Morrison 1975, Hostetter et al. 1981). Direct micropuncture studies have demonstrated that single nephron function is increased after subtotal nephrectomy (Olson and Heptinstall 1988). When renal mass is reduced, the remaining nephrons undergo functional as well as structural hypertrophy. Adaptations in the microcirculation of the spared nephrons result in an increased driving force for filtration and subsequent increase in GFR (Hostetter et al. 1981).

The magnitude of increase in single nephron filtration rate closely correlates with the amount of renal mass that has been lost. In short, greater degrees of removal result in greater increases in single nephron filtration at the residual nephrons. This adaptation is generally considered beneficial because it seemingly negates the reduction in total GFR that would otherwise occur. Studies have, however, shown that pathological sclerosis eventually occurs in the glomeruli of these residual nephrons (Morrison and Howard 1966, Shimamura and Morrison 1975, Purkerson et al. 1976). Experimental studies have reported that after NX operation, eventual sclerotic destruction of remnant glomeruli is accompanied by progressive proteinuria and arterial hypertension. With severe reduction in renal mass, alterations in glomerular structure are detected as early as two weeks. By week 7 more than 50% of glomeruli exhibit morphological changes, and all animals tended to die by 90 days (Purkerson et al. 1976). Notably, the amount of lost renal mass seems to be crucial, as clinical studies have shown that only patients with greater than 50% loss of renal mass have an increase in long-term risk for proteinuria and renal insufficiency (Novick et al. 1991).

Persistent proteinuria, which is an independent risk factor of CKD progression, has garnered much attention in the pathophysiology of CRI (Klahr et al. 1994, Williams and Coles 1994). Proteinuria results from glomerular capillary hypertension and damage to the permeability barrier in the glomerulus. Damaged barrier leaks proteins and overloads the proximal tubular cells, quickly leading to increased activation of the intrarenal ACE (Largo et al. 1999), ET-1, and other cytokines inducing apoptosis, inflammation, and fibrosis. It has also been suggested that proteinuria directly increases the influx of growth factors such

as TGF-ß and hepatocyte growth factor into tubular fluid (Wang et al. 2000). There these factors promote interstitial fibrosis by interacting with receptors located at the apical membrane of the tubular cells (Wang and Hirschberg 2000). Consistent with its important role in CRI pathophysiology, the severity of proteinuria correlates well to the rate of GFR decline also in clinical settings (GISEN-group 1997).

The 5/6 NX rat model is a flexible tool for studying different stages of CKD, as the duration of disease progression can be designed to meet the specific criteria of the study. Early stages of CKD are immediately present after recovery from the NX operation. Subsequent glomerulosclerosis and tubulointerstitial fibrosis then cause natural disease progression and concomitant loss of renal function with exactly the same mechanisms that are present in human CKD (Morrison and Howard 1966). Even though kidneys have a remarkable degree of functional reserve, a decrease in number of functioning nephrons beyond a certain limit leads to an overload on the remaining functioning nephrons, causing disease progression irrespective of the cause of the renal disease (Shimamura and Morrison 1975).

2. HYPERTENSION AND CARDIOVASCULAR DISEASE

Hypertension is the most common form of CVD, and it is currently present in 33% of US adults ≥20 years of age (Go et al. 2014). That adds up to staggering 78 million hypertensive people in the United States alone. The overall prevalence increases dramatically with age, affecting the majority of population over the age of 60 (Watanabe et al. 2002, Rosamond et al. 2008). In the USA, the prevalence of hypertension is nearly equal between men and women, while African American adults have among the highest prevalence of hypertension in the world, 44% (Go et al. 2014). In CKD patients the prevalence of hypertension varies with the etiology of the kidney disease and the stage of CKD. However, it is known to be notably higher in comparison with general population (Ridao et al. 2001) To support this, there is a recent study on stage 2-4 CKD patients showing an enormous 86% overall prevalence of hypertension (Muntner et al. 2010, Talreja et al. 2013). CVD remains the number one cause of death worldwide, contributing to over 33% of global mortality (Mendis et al. 2011). Nearly 2200 Americans die of CVD each day - an average of 1 death every 40 seconds (Go et al. 2014). In Europe, CVD currently causes 46% of total deaths, but CVD mortality rates vary greatly between

countries (Nichols et al. 2013). The highest CVD mortality rates, >900 deaths per 100 000 men and >510 deaths per 100 000 women, is seen in Turkmenistan and Russia, with other countries of former Soviet Union not far behind. In Finland, the CVD mortality rates were 275 deaths per 100 000 men and 146 deaths per 100 000 women in 2011 (Nichols et al. 2013).

In the past 100 years, the prevalence of hypertension in the USA has effectively more than tripled (Johnson et al. 2005c). This increase correlates with the epidemic increase in obesity, metabolic syndrome, type II diabetes, and ESRD, raising the likelihood that these conditions are pathogenetically related and intricately linked to environmental and especially dietary changes that have occurred in the world population during the 100 year span (Johnson et al. 2005c). Hypertension markedly increases the risk for myocardial infarction, stroke, congestive heart failure, and peripheral vascular disease, while successful early treatment reduces these complications and can reduce the number of cardiovascular deaths as well as improve overall quality of life (Watanabe et al. 2002, Rosamond et al. 2008).

2.1. Essential hypertension

According to the newest guidelines, published jointly by the European Society of Hypertension and the European Society of Cardiology in 2013, hypertension is defined as systolic BP of ≥140mmHg or diastolic BP of ≥90mmHg, or both, measured in a relaxed, sitting position (Mancia et al. 2013). The same classification is used in young, middle-aged and elderly subjects, whereas different criteria, based on percentiles, are adopted in children and teenagers. BP measurements should always be associated with measurement of heart rate, as resting heart rate values independently predict cardiovascular morbidity and mortality in several conditions, including hypertension (Benetos et al. 1999, Julius et al. 2012).

For ambulatory BP monitoring, hypertension is defined when the average BP values for a 24-hour period are ≥130/80mmHg, day-time average of ≥130/85mmHg, or night-time average of ≥120/70mmHg (Mancia et al. 2013). The original cut-off of 140/90mmHg was chosen in the early 1900s based on the fact that less than 10% of the US population had BPs in that range (Johnson et al. 2008a). In addition, it was recognized from the start that BPs in the hypertensive range were almost inevitably accompanied with arteriolosclerosis

as well as kidneys that were markedly contracted and granular in appearance, with glomerular and tubular changes visible in microscope. This confirms that hypertension should not simply be defined as an elevation in BP, but considered a syndrome featuring microvascular disease and renal involvement (Johnson et al. 2008a). Afferent arteriolopathy and concomitant microvascular disease narrows glomerular afferent arteriolar lumens via hypercellularity and thickening, thereby causing glomerular hypertension (Johnson et al. 2003)

Further support for the key role of kidneys in the initiation of hypertension has come from transplant studies in experimental models of hypertension (Dahl and Heine 1975, Rettig et al. 1990) and in clinical setting (Curtis et al. 1983). Dahl and Heine (Dahl and Heine 1975) demonstrated that the transplantation of a kidney from a rat with salt-sensitive hypertension to a normotensive rat will transfer the salt sensitivity. It was later shown in hypertension-induced ESRD patients that the transplantation of a kidney from a normotensive donor could cure the hypertension (Curtis et al. 1983). This finding along with a more recent study (Kvist and Mulvany 2003) demonstrated that systemic vascular disease cannot be the cause of hypertension (Johnson et al. 2008a). However, the primary importance of kidneys in essential hypertension does not negate the role of non-renal mechanisms in its pathophysiology. For example, the elevation in peripheral vascular resistance is mediated by vasoconstriction that is dependent on Ang II receptors and other mediator systems (Crowley et al. 2005). Persistent activation of the sympathetic nervous system may also cause chronic hypertension (Johnson et al. 2008a).

It has been observed that salt restriction causes some individuals with essential hypertension to have a greater fall in BP than others, and this has led to the concept of further classifying essential hypertension as salt-sensitive or salt-resistant. Intricately associated with the vascular lesion in the kidney is an infiltration into the interstitium of inflammatory cells consisting of T-cells and macrophages, many of which are producing oxidants and Ang II (Johnson et al. 2008a). Because renal microvascular disease is non-uniform, the rise in systemic BP results in some nephrons being overperfused whereas others are underperfused. Peritubular capillaries may also be damaged. The net effect is that ischemia is not completely relieved, and this leads to continued stimulation of sodium reabsorptive mechanisms by renin-dependent and renin-independent mechanisms (Sealey

et al. 1988). Consequently, the pressure natriuresis curve is shifted to the right and flattened, and the hypertension becomes salt-sensitive (Johnson et al. 2008a).

2.2. Secondary hypertension in chronic kidney disease

Impairment of renal sodium handling has been implicated in both experimental and human hypertension (Talreja et al. 2013). Hypertension secondary to early-stage CKD is mainly related to an impairment of Na^+-excretion leading to an expansion of circulating volume and total Na^+-content. This leads to increased secretion of endogenous factors that induce alterations in cytosolic Ca^{2+} homeostasis of VSMCs, followed by elevated peripheral resistance and BP (Schiffl et al. 1993). Thus, the expansion of extracellular fluid volume is the initial driver of hypertension, which is subsequently maintained by elevated vascular resistance (Talreja et al. 2013).

In addition to extracellular volume overload, increased sympathetic activity and the action of the RAAS contribute to hypertension in CKD, even in the presence of normovolemia (Talreja et al. 2013). Increased sympathetic outflow to kidney induces several pro-hypertensive effects including stimulation of renin release, Na^+ and water reabsorption, and an increase in renal vascular resistance (Converse et al. 1992). These effects point to a critical role of renal sympathetic afferents in the maintenance of hypertension and high central sympathetic activity in patients with CKD. A small randomized controlled trial has shown that renal sympathetic denervation therapy by high frequency radioablation can result in significant short-term reduction in BP among patients with resistant hypertension and preserved renal function (Esler et al. 2010). However, more studies are needed to assess the safety and efficacy of these procedures.

Disturbed balance between endothelium-derived vasodilators and vasoconstrictors in CKD has also been implicated as a mechanism leading to elevated BP (Shultz 1992). Suppressed synthesis of vasodilators such as NO and kinins, as well as increased production of vasoconstrictors such as ET-1 may also induce increased vascular resistance by their direct action on the VSMCs, and intracellular Ca^{2+}-metabolism (Förstermann 2010). Adipose tissue cytokines adiponectin and visfatin also potentially contribute to endothelial dysfunction (Zoccali 2008). ETA-antagonists have shown some efficacy in the treatment of resistant hypertension in the general population, but with significant fluid retention, which makes their therapeutic use questionable in CKD (Weber et al. 2009).

3. THE RENIN-ANGIOTENSIN-ALDOSTERONE SYSTEM

The critical role of the circulating RAAS in the regulation of arterial pressure and sodium homeostasis has been recognized for many years (Zhuo et al. 1999, Navar and Nishiyama 2001, Bernstein 2006, Paul et al. 2006). The RAAS is the best known regulator of BP and determinant of target-organ damage from hypertension. It also controls fluid and electrolyte balance through coordinated effects on the heart, blood vessels, and kidneys (Remuzzi et al. 2005). Ang II is the most powerful biologically active product of the RAAS, although there are other bioactive Ang peptides, including Ang III, Ang IV, and Ang 1-7. Ang II directly constricts VSMCs, enhances myocardial contractility, stimulates aldosterone production, stimulates release of catecholamines from the adrenal medulla and sympathetic nerve endings, increases sympathetic nervous system activity, and stimulates thirst and salt appetite (Kobori et al. 2007b). Ang II also regulates sodium transport by epithelial cells in the intestine and kidney. There has also been a growing appreciation of the organ-specific roles exerted by Ang II acting as a paracrine factor (Paul et al. 2006). In addition to its physiological roles, locally produced Ang II induces inflammation, cell growth, mitogenesis, apoptosis, cell migration, and differentiation, regulates the gene expression of bioactive substances, and activates multiple intracellular signaling pathways; all of which might contribute to tissue injury (Navar 1997, Kobori et al. 2007a).

3.1. The classic circulating renin-angiotensin-aldosterone system

The first enzyme of the classic systemic RAAS, renin, is produced by the juxtaglomerular cells of the afferent renal arteriole in a series of steps (Simoes e Silva and Flynn 2012). Gene transcription in the cell nucleus creates pre-prorenin, which is cleaved to produce prorenin in the endoplasmic reticulum. The Golgi apparatus then packs prorenin into secretory granules, where a portion appears to be converted into active renin (Griendling et al. 1993). The release of both peptides is mainly triggered by the stimulation of renal juxtaglomerular cells. Major stimuli for secretion of renin from the juxtaglomerular apparatus include glomerular hypoperfusion, reduced sodium intake, and increased activity of the sympathetic nervous system (Figure 2). Local sites of renin conversion have been shown in several organs, including the ovaries, placenta, testes, adrenal glands, and retina (Griendling et al. 1993, Simoes e Silva and Flynn 2012). Prorenin was long considered to

function solely as an inactive precursor to renin synthesis, but this view has rapidly changed with the introduction of (pro)renin receptor (PRR) in 2002 (Nguyen et al. 2002).

Angiotensinogen is an alpha-2-globulin, which is primarily formed and constitutively secreted by the hepatic cells into the circulation, where it functions as the principal substrate for renin (Brasier and Li 1996). Plasma angiotensinogen levels are increased by corticosteroids, estrogen, thyroid hormone, and Ang II (Basso and Terragno 2001, Stavreus-Evers et al. 2001). On release into the circulation, renin cleaves angiotensinogen at the N-terminus to form the decapeptide Ang I (Navar 1997). The circulating concentrations of angiotensinogen are abundant, being more than 1000 times greater than the plasma Ang I and Ang II concentrations (Navar and Nishiyama 2001). Although some variation between species exists, changes in renin activity determine the rate of Ang I formation in the plasma from the huge stores of circulating angiotensinogen, effectively making it the rate-limiting step of the RAAS (Ichihara et al. 2004, Paul et al. 2006).

Renin is stored in substantial quantities in the granules of juxtaglomerular cells (Paul et al. 2006), and thus large changes in plasma renin levels can occur rapidly, leading to changes in Ang I generation. Ang I is easily converted to Ang II, due not only to the circulating ACE, but also to the widespread presence of ACE on endothelial cells of many vascular beds including the lung (Navar 1997, Ichihara et al. 2004, Paul et al. 2006). Although other pathways for Ang II formation have been identified in certain tissues, the circulating levels of Ang II reflect primarily the consequences of the renin and ACE enzymatic cascade on angiotensinogen (Johnston 1994, Kobori et al. 2007a). The resultant increases in plasma Ang II exert powerful actions throughout the body through activation of Ang II receptors (Paul et al. 2006). Several angiotensinases and peptidases are then able to metabolize Ang II further (Kobori et al. 2007a). It is currently recognized that several of the down-stream peptides, including Ang III, Ang IV, and Ang 1-7, have biological activity, but their plasma levels are much lower than those of Ang II (Kobori et al. 2007a).

3.1.1. Plasma renin and aldosterone

The plasma renin concentration or activity is often used as a measure of the overall activity of the RAAS. In most species, renin synthesized by the juxtaglomerular apparatus cells is the primary source of both circulating and intrarenal renin levels. The secreted active form of renin contains 339 to 343 amino acid residues after proteolytic removal of the 43-amino acid residue at the N-terminus of prorenin. Circulating active renin and prorenin are released mainly from the kidney, but other tissues also secrete prorenin into the circulation (Sealey et al. 1986). Besides serving as the precursor for active renin and binding PRR, it has been suggested that circulating prorenin is taken up by some tissues where it may contribute to the local synthesis of Ang peptides (Prescott et al. 2002). Although renin or prorenin may directly induce cellular effects via PRR, the best-established role of renin is to act on angiotensinogen to form Ang I.

The mineralocorticoid aldosterone is synthesized by a series of enzymatic reactions from cholesterol in the zona glomerulosa of the adrenal gland. In addition, extra-adrenal synthesis of aldosterone has been reported in different tissues (Takeda et al. 2000, Cachofeiro et al. 2008). The extra-adrenal production of aldosterone appears to be regulated by the same stimuli that regulate adrenal synthesis. At the vascular level, its production has been reported in both endothelial cells and VSMCs. However, the physiological relevance of this production is still under discussion (Cachofeiro et al. 2008). High circulating aldosterone concentration is acknowledged as a significant cardiovascular risk factor (Schmidt and Schmieder 2003, Schmidt et al. 2006), and independently of the circulating or local origin, aldosterone exerts actions in the vascular wall through genomic and non-genomic effects.

Genomic actions imply the binding of aldosterone to cytoplasmatic mineralocorticoid receptors, a member of the nuclear receptor superfamily, and involve transcription and protein synthesis (Fuller and Young 2005). These receptors have been found in both endothelial cells and VSMCs and their expression can be increased in certain pathological situations such as hypertension (Fuller and Young 2005). The direct targets for aldosterone are the late distal convoluted tubules, the connecting tubules, and the principal cells of the cortical and medullary collecting ducts. Aldosterone binds to the receptor and translocates into the nucleus. The ligand-receptor complex then forms a homodimer, binds to the

specific DNA sequences and stimulates the transcription of its target genes (Nagase and Fujita 2008).

The non-genomic effects of aldosterone are observed quickly after secretion or administration, and are insensitive to transcription inhibitors. To date, two different non-genomic responses have been reported (Cachofeiro et al. 2008). One appears to involve mineralocorticoid receptors, whereas the second involves an unidentified membrane receptor. The signaling pathways include the modulation of intracellular calcium, Na^+/H^+-exchanger activity, and phosphorylation of signaling molecules, including protein kinase C, epidermal growth factor receptor, mitogen-activated protein (MAP) kinases, and cellular Src tyrosine kinase (C-Src) (Cachofeiro et al. 2008, Nagase and Fujita 2008). In fact, it was reported recently that aldosterone-induced activation of C-Src, extracellular signal-regulated kinases 1 and 2 (ERK1/2), and p38 MAP kinase is increased in spontaneously hypertensive rat vascular cells, suggesting that aldosterone plays an important role through the upregulation of C-Src signaling in vascular alterations observed in hypertensive rats (Cachofeiro et al. 2008).

3.1.2. Angiotensin-converting enzyme and angiotensin II receptors

Ang I is rapidly converted into the major effector of the RAAS, Ang II, by ACE, which is located on endothelial cells in many vascular beds and on membranes of various other cells including brush border membranes of proximal tubules (Mezzano et al. 2003). The localization of ACE within the kidney in various species has been well characterized. However, there are some important differences between humans and commonly used experimental animals. Indeed, it has been reported that kidneys from normal human subjects predominantly expressed ACE in the brush border of proximal tubular segments, and very little ACE expression was observed on vascular endothelial cells. ACE was not detectable in the vasculature of the glomerular tuft or even in the basolateral membranes of epithelial cells. In contrast, there was intense labeling on the endothelial cells of almost all of the renal microvasculature of rats (Kobori et al. 2007a). It has been reported that less than 10% of arterially delivered Ang I is converted to Ang II, which along with the reduced ACE expression on renal vascular endothelial cells in humans implies that the influence of intrarenal Ang II formed from circulating precursors may not be of major significance (Paul et al. 2006).

Most of the actions of Ang II on renal function are the consequence of activation of Ang II receptors, which are widely distributed in various regions and cell types of the kidney. Two major categories of Ang II receptors, type 1 (AT_{1R}) and type 2 (AT_{2R}), have been described, pharmacologically characterized, and cloned (Kobori et al. 2007a). Additionally, AT_{1R} features two well characterized subtypes: 1a (AT_{1aR}) and 1b (AT_{1bR}), although recent evidence suggests that humans only express AT_{1aR} (Higuchi et al. 2007). In literature, most of the hypertension-causing actions of Ang II are generally attributed to the AT_{1R}, marking it as the bad receptor regarding the pathogenesis of hypertension (Ito et al. 1995). AT_{1R} transcript has been localized to proximal tubules, the thick ascending limb of the loop of Henle, glomeruli, arterial vasculature, vasa recta, arcuate arteries, and juxtaglomerular cells (Tufro-McReddie and Gomez 1993). In rodents AT_{1aR} is the predominant subtype in all nephron segments, whereas AT_{1bR} is more abundant than AT_{1aR} only in the glomerulus. In mature kidneys, AT_{1aR} have been localized to the luminal and basolateral membranes of several segments of the nephron, as well as on the renal microvasculature in both cortex and medulla, VSMCs of afferent and efferent arterioles, epithelial cells of the thick ascending limb of Henle, proximal tubular apical and basolateral membranes, mesangial cells, distal tubules, collecting ducts, and macula densa cells (Harrison-Bernard et al. 1999). This evidence is consistent with the localization of the transcript for the AT_{1R} subtypes in all of the renal tubular and vascular segments in rats (Miyata et al. 1999).

The AT_{2R} is highly expressed in human and rodent kidney mesenchyme during fetal life and decreases dramatically after birth (Kobori et al. 2007a). AT_{2R} protein has been localized to the glomerular epithelial cells, proximal tubules, collecting ducts, and parts of the renal vasculature of the adult rat (Miyata et al. 1999). Although the role of AT_{2R} in regulating renal function remains uncertain, it has been suggested that AT_{2R} activation counteracts AT_{1R} effects by stimulating formation of bradykinin and NO, thereby leading to increases in interstitial fluid concentration of cGMP (Siragy and Carey 1999). AT_{2R} activation seems to influence proximal tubule sodium reabsorption either by a cell membrane receptor-mediated mechanism or by an interstitial NO-cGMP pathway (Jin et al. 2001). Ang II infusion into AT_{2R}-knockout mice leads to exaggerated hypertension and reductions in renal function, probably due to decreased renal interstitial fluid levels of bradykinin and cGMP available that counteract the direct effect of Ang II (Siragy and

Carey 1999). AT_{2R} can thus be regarded as a protective component of RAAS that inhibits vasoconstriction.

3.2. Novel components

A little over a decade age, the RAAS was considered a linear process. However, this view first started to change in 2000, as the RAAS gained a new member called angiotensin-converting enzyme 2 (ACE2) (Donoghue et al. 2000). Today, the conventional view of the RAAS has undergone significant change at several levels, with the identification of PRR (Nguyen et al. 2002), Mas oncogene, and AT_{4R} receptor, as well as recognition of functionally active Ang II-derived peptides and intracellular RAS, and finally, the existence of locally regulated tissue RAS (Nguyen Dinh Cat and Touyz 2011) (Figure 2).

ACE2 is expressed predominantly in vascular endothelial cells of the heart and kidney. ACE2 and ACE have different biochemical activities, as ACE2 converts Ang I to Ang 1–9 with nine amino acids, whereas ACE converts it to Ang II with eight amino acids (Figure 2). Ang II is a potent blood vessel constrictor. Ang 1–9 has no known effect on blood vessels but can be converted by ACE to a shorter peptide, Ang 1–7, which is a vasodilator (Pörsti et al. 1994). ACE2 can also produce Ang 1–7 by converting Ang II (Nguyen Dinh Cat and Touyz 2011). Thus, it has been suggested that ACE2 functions as one of the protective components of the RAAS suppressing the formation of the vasopressor Ang II (Boehm and Nabel 2002). The catalytic efficiency of ACE2 against Ang II is 400-fold higher than for Ang I, whereas it does not metabolize bradykinin (Simoes e Silva and Flynn 2012). CKD has been associated with a reduction in renal ACE2 expression. As Ang II is the primary substrate for ACE2 in renal tissue, the reduction of ACE2 expression and activity leads to local elevation of Ang II concentrations, which may contribute to development of renal damage (Simoes e Silva and Flynn 2012).

The PRR is a multifunctional receptor that also mediates effects independent of the RAAS (Hitom et al. 2010). PRRs are abundant in heart, brain and placenta, lower levels being found in the kidney and liver (Nguyen 2007). Visceral adipose tissue also expresses PRR, whereas less PRRs are expressed in the subcutaneous adipose tissue (Achard et al. 2007). PRR works by activating signaling molecules, and promoting cell growth and fibrosis, independently of Ang II, in cardiomyocytes, mesangial cells, podocytes, distal tubular cells, vascular endothelial cells and VSMCs (Danser and Nguyen 2008). The exact

physiological significance of the PRR remains unclear although it may act as an amplifier of tissue RAS (Nguyen Dinh Cat and Touyz 2011).

The effects of Ang 1-7 are mainly relayed via the Mas proto-oncogene, which was first implicated as Ang 1-7 receptor by Santos et al. (Santos et al. 2003). Mas functions as the main effector conveying the vasodilatory, antiproliferative, anti-inflammatory and antifibrotic effects of Ang 1-7 (Simoes e Silva et al. 2013). In the proximal tubule Ang 1–7 displays growth inhibitory properties and antagonizes the effects of Ang II, whereas in mesangial cells, it appears to stimulate cell growth pathways (Simoes e Silva and Flynn 2012). The renoprotective effects of Ang 1-7 seem to involve the modulation of oxidative stress, leukocyte influx and activation, and fibrosis in renal tissues (Esteban et al. 2009). The data provided by human studies also indicate a beneficial role for the activation of this alternative RAS axis in patients with renal diseases (Simoes e Silva et al. 2013). In addition, it is hypothesized that the beneficial effects of ACEI and ARB in renal diseases might involve, at least in part, the elevation of plasma Ang 1-7 levels. These effects imply a counter-regulatory role against Ang II for this peptide within the RAAS (Simoes e Silva and Flynn 2012).

The biologically active Ang IV peptide raised new interest with the founding of new a receptor, AT_{4R} or originally transmembrane enzyme called insulin-regulated aminopeptidase (IRAP) (Albiston et al. 2007). Actions of Ang IV mediated by AT_{4R} include renal vasodilation, hypertrophy and activation of nuclear factor-κB (NF-κB) leading to increased expression of platelet activator inhibitor-I, monocyte chemoattractant protein, interleukin-6 and tumor necrosis factor-α (Chai et al. 2004). Ang IV also exerts a wide range of neural effects including the ability to enhance learning and memory recall, anti-convulsant and anti-epileptogenic properties and protection against cerebral ischemia. Some of these actions are mediated via the AT_{1R}, but others are due to binding to AT_{4R}. Exact mechanisms of action whereby Ang IV induces effects via AT_{4R} are unclear and the biological significance remains to be elucidated (Nguyen Dinh Cat and Touyz 2011).

Of all the novel components, the Ang III peptide is possibly the most potent effector of the RAAS. It is not exactly newly discovered, having been known to cause vasoconstriction and release of aldosterone for almost 40 years (Saito et al. 1978a), however, its importance has only very recently been appreciated. Ang III is generated from Ang II by aminopeptidase A. Ang III exerts its actions via AT_{1R} and AT_{2R}. While Ang II is

considered the main effector of RAAS, Ang III may be equally or even more important in some actions mediated by AT_{1R}, such as the release of anti-diuretic hormone vasopressin (Fyhrquist and Saijonmaa 2008). *In vitro*, Ang III stimulates proliferation, production of pro-inflammatory mediators and deposition of ECM proteins (Wang et al. 2010).

3.3. The intrarenal renin-angiotensin-system

In recent years, the focus of interest on the role of the RAAS in the pathophysiology of hypertension and organ injury has changed to a major emphasis on the role of the local RAS in specific tissues. In the kidney, all of the RAS components are present, and intrarenal Ang II is formed by multiple independent mechanisms (Navar and Nishiyama 2001). Proximal tubular angiotensinogen, collecting duct renin, and tubular Ang II receptors are positively augmented by intrarenal Ang II. In addition to the classic RAAS pathways, PRR and chymase are also involved in local Ang II formation in the kidney (Prescott et al. 2002, Miyazaki and Takai 2006). Moreover, circulating Ang II is actively internalized into proximal tubular cells by Ang II receptor-dependent mechanisms (Higuchi et al. 2007). Consequently, Ang II is compartmentalized in the renal interstitial fluid and the proximal tubular compartments with much higher concentrations than those existing in the circulation. Recent evidence has also revealed that inappropriate activation of the intrarenal RAS is an important contributor to the pathogenesis of hypertension and renal injury (Kobori et al. 2007a). Thus, it is necessary to understand the mechanisms responsible for independent regulation of the intrarenal RAS.

The RAAS has been acknowledged as an endocrine, paracrine, autocrine, and intracrine system, and because of that, it has been almost impossible to distinguish the different contributions of the classic RAAS versus the local RAS (Navar et al. 2002, Kobori et al. 2007a). Emerging evidence suggests that local formation is of major significance in the regulation of the Ang II levels in many organs and tissues. For example, there is substantial evidence that the Ang peptide levels in the brain are regulated in an autonomous manner (Kobori et al. 2007a). Although every organ system in the body has elements of the RAS, the kidney is unique in having every component of the RAS with compartmentalization in the tubular and interstitial networks as well as intracellular accumulation. Recent attention has been focused on the existence of unique RASs in various organ systems. Various studies have demonstrated the importance of the tissue RAS in the brain, heart, adrenal glands, and vasculature as well as in the kidney (Navar et al. 1995, Bader 2010). There is

substantial evidence that the major fraction of Ang II present in renal tissues is generated locally from angiotensinogen delivered to the kidney as well as from angiotensinogen locally produced by proximal tubule cells. Ang I delivered to the kidney can also be converted to Ang II (Komlosi et al. 2003). Renin secreted by the juxtaglomerular apparatus cells and delivered to the renal interstitium and vascular compartment also provides a pathway for the local generation of Ang I (Hackenthal et al. 1990, Kobori et al. 2007a). ACE is abundant in the rat kidney and has been located in the proximal and distal tubules, the collecting ducts, and renal endothelial cells. Therefore, all components necessary to generate intrarenal Ang II are present along the nephron (Paul et al. 2006, Kobori et al. 2007a).

Although most of the circulating angiotensinogen is produced and secreted by the liver, the kidneys also produce angiotensinogen (Kobori et al. 2007b). Intrarenal angiotensinogen mRNA and protein have been localized to proximal tubule cells, indicating that the intratubular Ang II could be derived from locally formed and secreted angiotensinogen. The angiotensinogen produced in proximal tubule cells seems to be secreted directly into the tubular lumen in addition to producing its metabolites intracellularly and secreting them into the tubule lumen (Lantelme et al. 2002). Proximal tubule angiotensinogen concentrations in rats have been reported in the range of 300 to 600 nM, which greatly exceed the free Ang I and Ang II tubular fluid concentrations (Navar and Nishiyama 2001). Because of its substantial molecular size, it seems unlikely that much of the plasma angiotensinogen filters across the glomerular membrane, further supporting the concept that proximal tubule cells secrete angiotensinogen directly into the tubule (Kobori et al. 2007a).

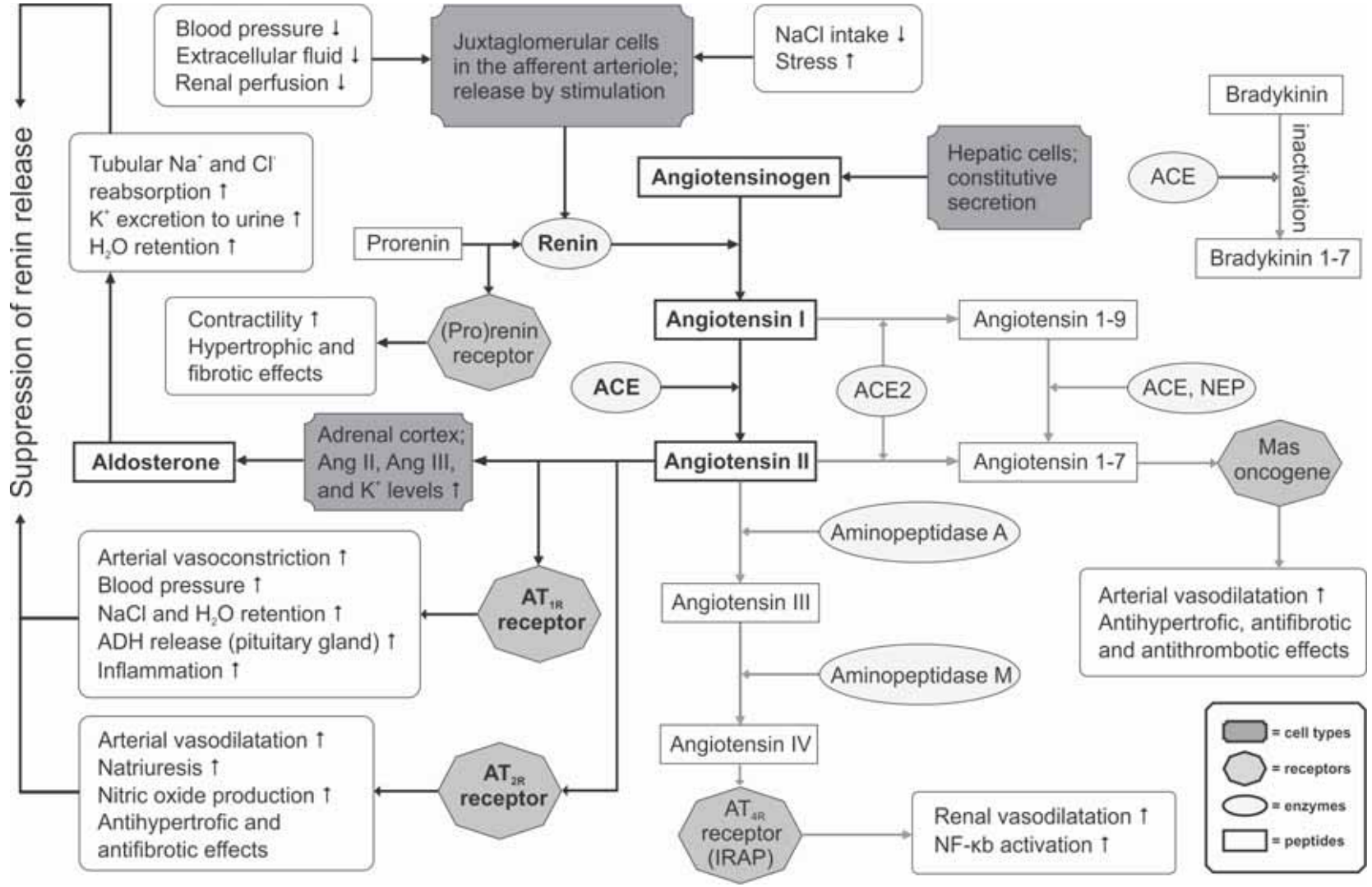

Figure 2. *The renin-angiotensin-aldosterone system overview.* The modern RAAS comprises many components. In addition to its function in the RAAS, ACE also participates in the kinin-kallikrein system by inactivating the vasodilatory bradykinin. ADH = Anti-diuretic hormone, IRAP = Insulin-regulated aminopeptidase; Figure by the author with data by Fyhrquist et al., Simoes et al., and Ngyen Dinh et al. (Fyhrquist and Saijonmaa 2008, Nguyen Dinh Cat and Touyz 2011, Simoes e Silva and Flynn 2012).

3.4. The vascular renin-angiotensin system

All the elements of the RAS are present also in the vasculature, indicating that the vascular system may act independently to generate Ang II (Nguyen Dinh Cat and Touyz 2011). Expression of renin, angiotensinogen, ACE, Ang I and Ang II has been demonstrated at the mRNA and protein levels within the endothelium of veins, large conduit arteries, and small resistance arteries (Nguyen Dinh Cat and Touyz 2011). The levels of Ang II and its metabolites may differ between tissues, and may even be higher in microvessels than in the plasma, because of local regulation of vascular RAS (Danser 2003).

4. URIC ACID AND HYPERURICEMIA

4.1. Uric acid synthesis and metabolism

UA is generated during the catabolism of purines obtained by ingestion or from the breakdown of DNA, RNA and ATP (Watanabe et al. 2002, Johnson et al. 2008b). UA is a weak acid (pK_a=5.75) distributed throughout the extracellular fluid compartment as sodium urate, and cleared from the plasma mainly by glomerular filtration (Waring et al. 2000). The synthesizing enzyme is xanthine oxidoreductase, which promotes the last catalytic steps by converting hypoxanthine to xanthine and xanthine to UA (Doehner and Anker 2005). The substrates for hypoxanthine formation by adenine deaminase are adenine and adenosine, whereas inosine phosphorylase uses inosine as its substrate. Guanine also functions as a precursor for UA synthesis, but it is metabolised straight to xanthine by the guanine deaminase (Waring et al. 2000).

Xanthine oxidoreductase is a flavoprotein that contains both iron and molybdenum and uses NAD^+ as an electron acceptor. It exists in two interconvertible forms: xanthine dehydrogenase and xanthine oxidase (XO). In its XO form, this enzyme can function as a redox partner to molecular oxygen, generating free oxygen radicals superoxide anion and hydrogen peroxide, which may be converted to free hydroxyl radicals (Doehner and Anker 2005). In 1968, the cytosolic XO was the first documented putative biologic generator of oxygen-derived free radicals, and since then, it is well known that XO is a major source of free oxygen radical production in the human body (Terada et al. 1992, Harrison 1997). This metabolic pathway is of particular significance in conditions of tissue hypoxia and ischemia/reperfusion because the increased degradation of ATP via adenosine leads to

increased substrate load for XO. Accordingly, an increase in serum UA level has been observed in hypoxic states such as obstructive pulmonary disease, neonatal hypoxia, cyanotic heart disease, and acute heart failure (Doehner and Anker 2005). Simultaneously, in ischemia and hypoxia, xanthine dehydrogenase increasingly transforms to XO, which further adds to accelerated radical production (Terada et al. 1992).

In most mammals UA is further degraded to allantoin by the enzyme urate oxidase (uricase), resulting in serum UA levels in the range of 30-90 μmol/l (Watanabe et al. 2002, Johnson et al. 2008b). Uricase is localized predominantly in liver and is associated with the peroxisome as a tetramer with a subunit molecular mass of 32-33 kDa (Wu et al. 1989). Depending on the species, allantoin may be further degraded by allantoinase to generate ammonia (Johnson et al. 2008b). The serum UA concentration of apes and humans and some New World monkeys is markedly higher than in other mammals. This increase is due to distinct mutations in the uricase gene that rendered it non-functional during the Miocene era (Wu et al. 1992). Elevated serum UA concentration is called hyperuricemia when it exceeds 360 μmol/l in women, or 420 μmol/l in men (Johnson et al. 2003).

Hyperuricemia might be best known for its association with gout, which is a disease recognized for centuries (Terkeltaub 2006, Rivard et al. 2013). Gout is the most common inflammatory arthritis in men, affecting almost 2% of adult men in the Western world (Lee et al. 2006). Gout is caused by deposition of urate crystals in the joints in which they induce chronic inflammation and tissue damage. However, hyperuricemia is also known to be present without crystal formation in many CKD and CVD patients. Characteristically, patient groups with the highest cardiovascular risk coincidentally have highest mean serum UA concentrations. These include heavy alcohol users with increased UA generation and decreased excretion, as well as diuretic users with decreased UA excretion. Because of lower nephron count, people of African descent also have an increased risk for hyperuricemia (Johnson et al. 2003). Additionally, serum UA is typically higher in men and postmenopausal women than premenopausal women because of the uricosuric actions of estrogen, whereas high insulin concentration has been reported to decrease UA excretion (Muscelli et al. 1996).

Altered serum UA concentrations, both above and below normal levels, have been linked to a number of disease states. Hyperuricemia has been associated with gout, hypertension, CVD, and CKD, whereas lower than normal UA concentration, hypouricemia, has been

linked to Parkinson's disease, Alzheimer's disease, and optic neuritis (Kutzing and Firestein 2008). Several recent studies have also reported lower levels of UA in multiple sclerosis patients, while other studies found no such correlation (Spitsin and Koprowski 2008). Historically, elevated UA has been considered a marker of the above disease states, but recently published studies have provided evidence that UA may actually play a role in the development or progression of such diseases (Kutzing and Firestein 2008). As a result, the manipulation of UA concentrations is now either included in, or being investigated for, the treatment of a variety of disease states (Kutzing and Firestein 2008).

4.1.1. The benefits of uricase mutations

In humans, the chimpanzee, and the gorilla, three uricase mutations have been identified. These include a nonsense mutation of codon 33, a nonsense mutation of codon 187, and a splice mutation in exon 3, while the human uricase gene totals 304 codons – 8 exons and 8 introns. The mutation at codon 33 is also found to be present in the orangutan, whereas none of these mutations are present in the gibbon, in which a separate 13 bp reading-frame-changing deletion was identified between codons 72 and 76 of exon 2 (Wu et al. 1992). Based on the phylogeny of hominoid evolution as assessed by DNA-DNA hybridization, it was proposed that the nonsense mutation affecting the hominoid lineage at codon 33 occurred between 24 and 13 to 16 million years ago, and the 13 bp deletion in exon 2 occurred sometime after the split of the gibbon from the other hominoids, which occurred around 22 to 24 million years ago (Wu et al. 1992, Watanabe et al. 2002). The current evidence now suggests that the loss of uricase in humans may have been stepwise, with a progressive loss in activity due to mutations in the promoter region followed by complete silencing of the gene (Oda et al. 2002, Johnson et al. 2008b).

The biological reason for the loss of urate oxidase activity in hominoids is unknown, but there are a few reasonable hypotheses that are in agreement with the existent UA evidence. An evolutionary fact is that when a mutation completely silences the function of an enzyme, it either hampers its carrier, or gives the carrier an advantage over the wild-type population. When this kind of mutation sweeps all over the population and becomes the wild-type, we can safely assume that the mutation was highly advantageous in the contemporary environment. During the Miocene this was the situation that happened with the uricase gene. Non-functional uricase presented a new kind of survival advantage that

eventually lead to its complete precipitation in later hominoids (Watanabe et al. 2002, Johnson et al. 2008b).

The most quoted hypothesis explaining the advantage associated with the non-functional uricase is that originally proposed by Ames et al. (Ames et al. 1981), who suggested that the uricase mutation may have occurred as a means to replace serum antioxidant activity after the loss of ascorbate, vitamin C, synthesis. Indeed, UA is a water-soluble antioxidant that can help maintain ascorbate levels and is also considered to be one of the most important antioxidants in the plasma (Ames et al. 1981, Johnson et al. 2008b). However, UA is not solely an antioxidant as it can also function as a pro-oxidant on a variety of cell types and *in vivo*, as evidenced by its reactions with peroxynitrite (Santos et al. 1999). According to the hypothesis, it was also suggested that the reason humans have longer life expectancy compared to other mammals may relate to the antioxidant benefits provided by the higher UA levels. Challenging this hypothesis, however, is the observation that neither ascorbate nor UA levels correlate with maximum life span in vertebrates (Lopez-Torres et al. 1993, Johnson et al. 2008b).

Another hypothesis is that the increase in UA resulted in better reaction time and higher mental performance due to its putative neurostimulant properties based on its similarity in chemical structure with caffeine (Johnson et al. 2008b). While some epidemiological and experimental studies have supported this, the evidence has been weak at best. Other alternative hypotheses have linked the increase in UA with improved innate immune function and the ability to ward off infections or tumors. Specifically, UA is reported to aid in the immune recognition of dying cells, help activate the inflammasome critical for interleukin-1 β release, and participate in the immune rejection of tumor cells (Shi et al. 2003, Hu et al. 2004, Johnson et al. 2008b).

The latest uricase hypothesis was postulated by Watanabe et al. in 2002 (Watanabe et al. 2002) and it has generated mixed opinions in different medical fields (Ellman and Becker 2006, Johnson et al. 2008a). According to this hypothesis, elevated UA would have benefited the hominoids of the Miocene by causing sodium retention, concurrently helping to maintain BP during the times of low sodium ingestion. Hominoids that could better conserve sodium and maintain BP might have prevailed during the harsh environment of the Miocene (Watanabe et al. 2002). In fact, there is evidence that during the early Miocene there was a marked increase in the number of ape species (Begun 2003).

However, by the mid Miocene there was global cooling called the Miocene Disruption, which caused extinction of numerous species, likely including many species of apes. During this period, large rain forests dried out leaving only deserts and grasslands, thus forcing early hominoids to elevate their posture and to modify their diet (Johnson et al. 2008b).

The Paleolithic diet was low in sodium (Eaton and Konner 1985), and hence survival would have been better with those species that could maintain BP and salt sensitivity. The increase in serum UA acutely increases BP and maintains sodium conservation because of the action of UA to enhance activation of the RAAS in response to a low-salt diet. However, UA can also induce renal microvascular disease by stimulating VSMC-proliferation with the activation of MAP kinase and stimulation of platelet-derived growth factor, cyclooxygenase-2 (COX-2), and the RAAS (Watanabe et al. 2002). Microvascular disease, preglomerular arteriolar disease, and interstitial inflammation are associated with narrowing of renal afferent arteriolar lumens, thereby causing local vasoconstriction, glomerular hypertension, and salt sensitivity with a chronic increase in BP (Sanchez-Lozada et al. 2002). The activation of these two main pathways, the RAAS and microvascular disease, results in a persistent elevation in BP with concurrent maintenance of sodium balance (Watanabe et al. 2002). Indeed, there is also clinical evidence that high serum UA levels are associated with increased proximal tubular sodium reabsorption in men (Cappuccio et al. 1993), while sodium sensitivity is considered a characteristic feature in hyperuricemia (Ward 1998).

Extensive studies showing that hyperuricemia independently predicts the development of hypertension (Johnson et al. 2005a, Sundstrom et al. 2005) have been carried out recently. Hyperuricemia has been shown to be prevalent in early hypertension, and in one study it was present in almost 90% of hypertensive adolescents (Feig and Johnson 2003). Furthermore, recent clinical trials have found that lowering UA lowers BP in both adolescents and adults with hypertension (Feig et al. 2004, Feig and Johnson 2007). In addition to elevating BP, recent studies support UA as having a role in insulin resistance and obesity (Nakagawa et al. 2006, Sanchez-Lozada et al. 2007). It has been reported that fructose, which rapidly raises UA, induces metabolic syndrome in animals and this can be ameliorated by lowering serum UA (Nakagawa et al. 2006). The mechanism by which UA mediates features of the metabolic syndrome may result from the ability to block some of

the actions of insulin by reducing eNOS synthesis as well as due to direct effects of UA on the glomerular adipocytes (Sautin et al. 2007, Johnson et al. 2008b).

The consequence of the uricase mutation is that humans not only have higher serum UA levels than most other mammals, but they also cannot regulate UA levels as effectively (Johnson and Rideout 2004, Johnson et al. 2005d). Interestingly, as the current Western diet is high in meats and fructose which both generate UA, humans today have higher UA levels (range 240-600 μmol/l) compared to primates that lack uricase (typically 180-240 μmol/l range) (Johnson et al. 2005d). However, the most compelling finding is the elevation of mean serum UA levels in the USA during the last century. In men, mean serum UA levels reportedly increased from <210 μmol/l in the 1920s to approximately 300 μmol/l in the 1950's, and to 350-390 μmol/l in the 1970's (Nakagawa et al. 2008). Recent studies have shown that the Yanomamo Indians living in their original habitat and with their primitive diet have serum UA levels in the 120-240 μmol/l range, suggesting that primitive humans had even lower UA levels than those in the beginning of the 1900 (Johnson et al. 2008b). In our modern daily diets, we are ingesting significantly more fructose-containing sweeteners and purine-loaded meats than in the past, and those who obtain the highest UA levels could end up developing hypertension, kidney disease, insulin resistance and obesity (Johnson et al. 2008b), leading to significantly increased cardiovascular mortality (Fang and Alderman 2000).

4.1.2. Uric acid excretion

In humans, UA is mainly excreted through glomerular filtration, although bacterial degradation in the intestine also plays a small role in the elimination (Figure 3). The regulation of urinary UA excretion is complex. According to the classic notion, UA is freely filtrated at glomerulus, but almost completely reabsorbed in the proximal tubulus. As a consequence, only 10% of urate is excreted in urine (Nakagawa et al. 2008). Recent studies have focused on the specific transporters in the proximal tubules that are involved in reabsorption, and UA transporter 1 (URAT1) seems to be one of the major UA transporters present in the luminal border of human proximal tubular cells (Anzai et al. 2007). URAT1 is an organic anion transporter that exchanges organic anions for urate. A key role for URAT1 in regulation of serum UA levels has been suggested, as mutation of URAT1 is known to cause hypouricemia in humans (Nakagawa et al. 2008).

4.1.3. Gout

Gout is one of the most common inflammatory arthritis conditions, affecting up to 1–2% of men in Western countries, and causing morbidity, disability and poorer quality of life (Lee et al. 2006, Sivera et al. 2014). It has been recognized since antiquity, and commonly struck royalty, the rich and educated, and affected many leaders of the day. That is why gout was lovingly known in the 17th century England as "the king of diseases, and the disease of kings" (Rivard et al. 2013).

Gout is the consequence of deposition of monosodium urate crystals in joints and other tissues as a result of persistent hyperuricemia. The metatarsal-phalangeal joint is the most commonly affected site for gouty inflammation at the base of the big toe (Sivera et al. 2014). The principal aim in gout treatment is to reduce serum UA levels, thereby allowing urate crystals to dissolve. This should lead to the elimination of acute episodes of inflammation, the disappearance of tophi, and eventual cure of the disease (Pascual and Sivera 2007).

4.2. Experimental hyperuricemia

Experimental crystal-independent hyperuricemia model based on uricase inhibition was first published in 2001 by Mazzali et al. (Mazzali et al. 2001). Since then it has been used numerous times to model the events associated with non-gouty hyperuricemia. Experimental studies, where rats were made hyperuricemic by the ingestion of uricase inhibitor oxonic acid, 2.0% in diet for 4-7 weeks, have suggested that high UA may play a causal role in the development of hypertension (Mazzali et al. 2001, Kang et al. 2002, Mazzali et al. 2002, Sanchez-Lozada et al. 2002, Nakagawa et al. 2003, Sanchez-Lozada et al. 2005). The oxonic acid model of hyperuricemia has been shown to induce preglomerular arteriolar disease leading to tubular ischemia, interstitial infiltration of lymphocytes and macrophages, oxidant generation, and local vasoconstriction. These changes are associated with decreased GFR and lowered sodium filtration, as well as increased sodium reabsorption, which together result in salt sensitivity (Johnson et al. 2002).

The initial increase in BP in hyperuricemic rats is associated with increased number of renin-positive cells in the juxtaglomerular apparatus (Johnson et al. 2005b), and a direct correlation of serum UA with the percentage of renin-positive juxtaglomerular cells has

been reported in this model (Mazzali et al. 2001). Treatment of hyperuricemia with XO inhibitor allopurinol and uricosuric agents such as benziodarone have been repeatedly shown to prevent the pathological and pathophysiological changes induced by oxonic acid feeding (Mazzali et al. 2001, Kang et al. 2002, Mazzali et al. 2002, Sanchez-Lozada et al. 2002, Nakagawa et al. 2003, Sanchez-Lozada et al. 2005). This effectively validates the model, as any possible harmful changes induced independently by the oxonic acid feeding would not have been prevented with UA-lowering treatment.

4.2. Treatment of hyperuricemia

The current treatment of hyperuricemia is mainly tailored for gout patients, as there is still no consensus on whether lowering of UA in CVD is necessary. Several drugs are known to lower UA. These drugs can influence uricosuria and increase UA excretion, block the final step in UA production via XO inhibition, or lead to direct UA breakdown (Figure 3). The most effective uricosuric drugs are probenecid and sulfinpyrazone, while fenofibrate and losartan, a common ARB, also have uricosuric activity (Dawson and Walters 2006). Rasburicase, on the other hand, is a recombinant uricase which converts UA to allantoin (Herrington and Dinh 2014). It is used in association with some anticancer treatments and is not suitable for repeated dosing (McBride et al. 2013). There are also two commercially available XO inhibitors, allopurinol and oxypurinol, which both are purine analogs. Allopurinol is rapidly metabolized to oxypurinol that binds to XO, thereby inhibiting its activity (Dawson and Walters 2006). A new non-purine XO inhibitor called febuxostat has also been developed (Sanchez-Lozada et al. 2008). It differs from allopurinol because it does not inhibit other enzymes in purine and pyrimidine metabolism pathways. Moreover, the XO inhibiting effect exerted by febuxostat *in vitro* and *in vivo* is more potent than that of allopurinol (Takano et al. 2005). Studies show that febuxostat inhibits the activity of XO simply by obstructing substrate binding and the inhibition is not influenced by changes in the redox status of the system (Okamoto et al. 2003, Sanchez-Lozada et al. 2008, Ye et al. 2013).

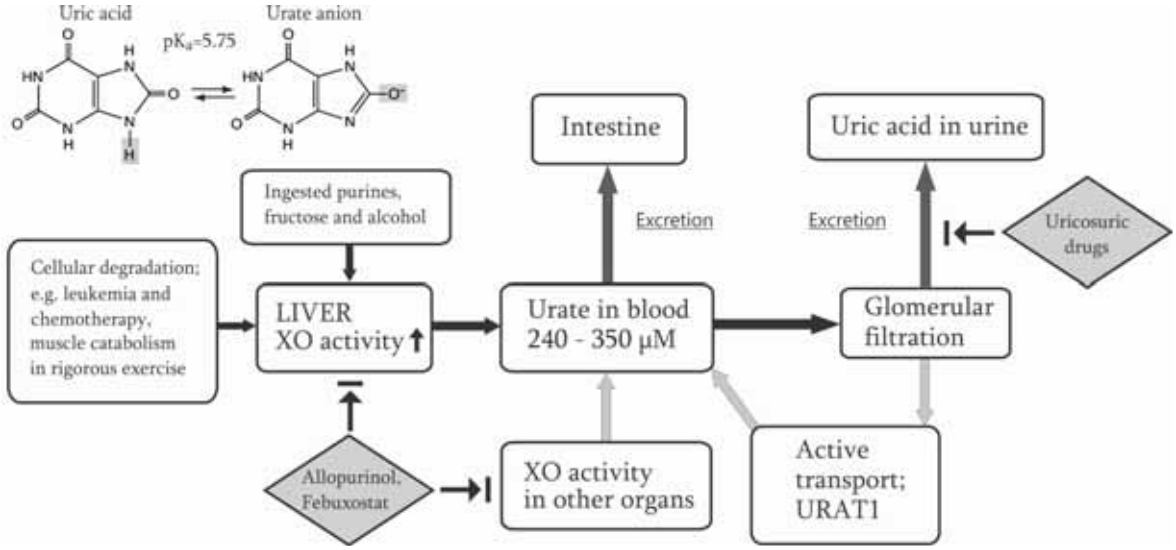

Figure 3. *Uric acid metabolism and the key target points for hyperuricemia treatment.* Uric acid (UA) is present in the form of urate anion in blood. It is mainly produced in the liver by the enzyme xanthine oxidoreductase in its xanthine oxidase (XO) isoform. Additionally, XO in other organs (lung, intestine etc.) contributes to the urate reservoir in blood. UA is excreted mainly through glomerular filtration, while bacterial degradation in the intestine also contributes to the elimination. UA is actively reabsorbed from the proximal tubule by UA transporter 1 (URAT1), which exchanges organic anions for UA. Consequently, only 10% of UA is normally excreted. Allopurinol and febuxostat decrease UA synthesis by inhibiting XO activity. Uricosuric drugs function by inhibiting the tubular reabsorption of UA; Figure by the author with data from Nakagawa et al. and Johnson et al. (Johnson et al. 2008b, Nakagawa et al. 2008).

5. CALCIUM-PHOSPHATE METABOLISM

Many of our essential physiological functions depend on tight control of plasma calcium and phosphorus (Renkema et al. 2008). Phosphorus is essential for the production and function of cell membranes and DNA synthesis (Takeda et al. 2004), as well as intracellular signal transduction and energy exchange (Tonelli 2013). Neuronal excitation, muscle contraction, and blood clotting all require Ca^{2+} ions (Renkema et al. 2008). Without doubt, the importance of both minerals on our bones is paramount (Tejwani and Qian 2013). Although more than 80% of total body phosphorus is stored in bone and teeth, phosphorus is also found in the intracellular compartment and in serum, primarily in the form of anions such as $H_2PO_4^-$ and HPO_4^{2-}, commonly referred to as phosphate (Blumsohn 2004, Tonelli et al. 2010). Calcium is stored in large amounts as the mineral hydroxyapatite ($Ca_{10}(PO_4)_6(OH)_2$) in the skeleton. In the circulation, calcium exists in

three forms: 50% as ionized Ca^{2+}, 40% protein-bound, primarily to albumin, and 10% complexed. The ionized Ca^{2+} is the functional fraction (Tejwani and Qian 2013).

Serum phosphate content is mainly controlled by the regulation of bone formation and resorption, dietary absorption, and renal excretion (Takeda et al. 2004). Many hormones are needed to control these processes, and the roles of the classic regulators such as PTH, calcitonin, and the active form of vitamin D, $1,25(OH)_2D_3$, are already well established (Carney 1997, Holick 2000, Silver and Naveh-Many 2009). However, new factors such as Klotho and fibroblast growth factor 23 (FGF23) have been recently identified as essential to the regulation of calcium and phosphate homeostasis (Kuro-o 2006, Kurosu and Kuro-o 2008).

In a healthy individual, the phosphate balance is primarily maintained by renal excretion. When kidney function is impaired, the excretion of phosphate declines (Tonelli et al. 2010). Notably, a drop in GFR below 30 ml/min/1.73m^2 is usually needed for a substantial elevation in serum phosphate level (Levin et al. 2007). The regulation is so strict that large changes in calcium and phosphate ingestion only lead to small fluctuations in the circulating levels (Renkema et al. 2008). A Western adult consumes 1000 to 1200 mg of dietary phosphate daily, of which approximately 800 mg is ultimately absorbed (Hruska et al. 2008). The phosphate comes mainly from meats, dairy products, and whole grains. Sodium phosphate and other food additives may also contribute to dietary phosphate load, with intakes sometimes reaching as high as 500 mg per day (Sherman 2007). On the other hand, the normal adult daily diet contains roughly 1000 mg of Ca^{2+}. Approximately 300 mg of ingested Ca^{2+} is absorbed from the intestine, promoted by $1,25(OH)_2D_3$. Bone mineral metabolism influences Ca^{2+} concentration by releasing or absorbing circulating Ca^{2+}. When in balance, bone Ca^{2+} absorption equals bone Ca^{2+} resorption. Absorbed dietary Ca^{2+} is excreted by both the colon (100–150 mg/day) and the kidneys (150–200 mg/day) (Tejwani and Qian 2013).

5.1. Fibroblast growth factor 23 and Klotho

Fibroblast growth factors comprise a family of 22 molecules, which can be grouped into 7 subfamilies with the common ability to bind one of the four receptors, typically in a paracrine manner (Kovesdy and Quarles 2013). FGF23 is a 32 kDa protein secreted from osteocytes and osteoblasts, and it is one of the few endocrine fibroblast growth factors

(Kuro-o 2011). It reduces serum inorganic phosphorus and $1,25(OH)_2D_3$ by stimulating endocytosis of the renal sodium-phosphate cotransporters NPT_{2a} and NPT_{2c} and by inhibiting 1-α-hydroxylase and stimulating the catabolic 24-hydroxylase, respectively (Olauson and Larsson 2013). A more acute effect is achieved in parathyroid glands in which FGF23 stimulation suppresses PTH synthesis and release within minutes (Quarles 2012). Excess FGF23 production results in hypophosphatemia and suppressed $1,25(OH)_2D_3$, as well as impaired bone and cartilage mineralization. FGF23 deficiency, on the other hand, results in hyperphosphatemia, elevated $1,25(OH)_2D_3$ level, and soft tissue calcification (Liu and Quarles 2007). PTH levels generally align with the FGF23 concentration in CKD, as high PTH is commonly concomitant to high FGF23, whereas low PTH is observed with low FGF23.

FGF23 cell-target specificity is defined by the presence of receptor complexes formed between FGF receptors and Klotho. While FGF receptors are ubiquitously expressed, Klotho is largely confined to the renal distal tubuli and parathyroid chief cells, making the kidney and parathyroid gland the primary FGF23 target organs (Kovesdy and Quarles 2013) (Figure 4). Klotho, named after an ancient Greek goddess of fate, is a putative aging suppressor gene. A defect in Klotho gene expression in mice confers penetrant phenotypes resembling human premature aging syndromes, whereas Klotho overexpression confers longevity exceeding the wild type (Kuro-o 2011). The Klotho gene encodes a single-pass transmembrane protein expressed predominantly in the kidney and parathyroid gland (Kuro-o 2006). Klotho is also released into circulation through ectodomain shedding from the cell surface by proteases, and independently of FGF23 mediates phosphaturic effects. Furthermore, soluble Klotho promotes calcium reabsorption by stabilization of the renal calcium channel TRPV5 (Olauson and Larsson 2013).

The regulation of FGF23 is complex and incompletely understood. PTH, $1,25(OH)_2D_3$, secreted Klotho, glucocorticoids, calcium and phosphate appear to regulate FGF23 production, but the response is context dependent and the molecular mechanism underlying the transcriptional regulation of FGF23 remain unclear (Kovesdy and Quarles 2013). The principal regulator of FGF23 appears to be $1,25(OH)_2D_3$, which stimulates FGF23 production in the bone (Figure 4), whereas the role of other regulators of FGF23 remains controversial (Liu and Quarles 2007). Stimulation of FGF23 production by PTH has been shown in some, but not all studies. Recent investigations also suggest that bone

mineralization and remodeling may have a direct effect on FGF23 production, and mutations in genes that regulate bone mineralization increase FGF23 gene transcription (Quarles 2012). These local regulators may allow FGF23 to control renal phosphate metabolism according to the actual transport of calcium and phosphate to and from the bone. In addition, leptin, estrogen and glucocorticoids also regulate FGF23 (Tsuji et al. 2010). Interestingly, although phosphate correlates with FGF23 levels in some settings, such as ESRD, changes in serum phosphate content does not appear to have a consistent effect on FGF23 production (Kovesdy and Quarles 2013).

Klotho expression declines progressively in CKD as FGF23 expression increases, while high serum phosphate, PTH, and low $1,25(OH)_2D_3$ accompany these changes (Kuro-o 2011). The first measurable decline in urinary secreted Klotho expression occurs as early as stage 1 CKD and is potentially an early clinical marker of acute renal damage (Hu et al. 2011). Klotho decline precedes FGF23 increase in CKD, and reducing FGF23 increases serum $1,25(OH)_2D_3$ and renal Klotho expression. Parathyroidectomy, $1,25(OH)_2D_3$ supplementation, peroxisome proliferator-activated receptor γ (PPAR-γ) agonists, and RAAS inhibitors can also increase Klotho expression (Kuro-o 2011).

FGF23 and Klotho play crucial roles in the endocrine regulation of mineral metabolism (Kuro-o 2006, Liu and Quarles 2007). Today, pathological elevation of FGF23 and suppressed Klotho are recognized as hallmarks in CKD patients, and these factors appear to present promising biomarkers for prediction of adverse outcome and possibly therapeutic decision making in future treatment of CKD (Olauson and Larsson 2013). However, more research is needed to conclusively determine whether it is Klotho decline or increased FGF23 that is more important in the vicious cycle of phosphate pathology in CKD (Kuro-o 2011).

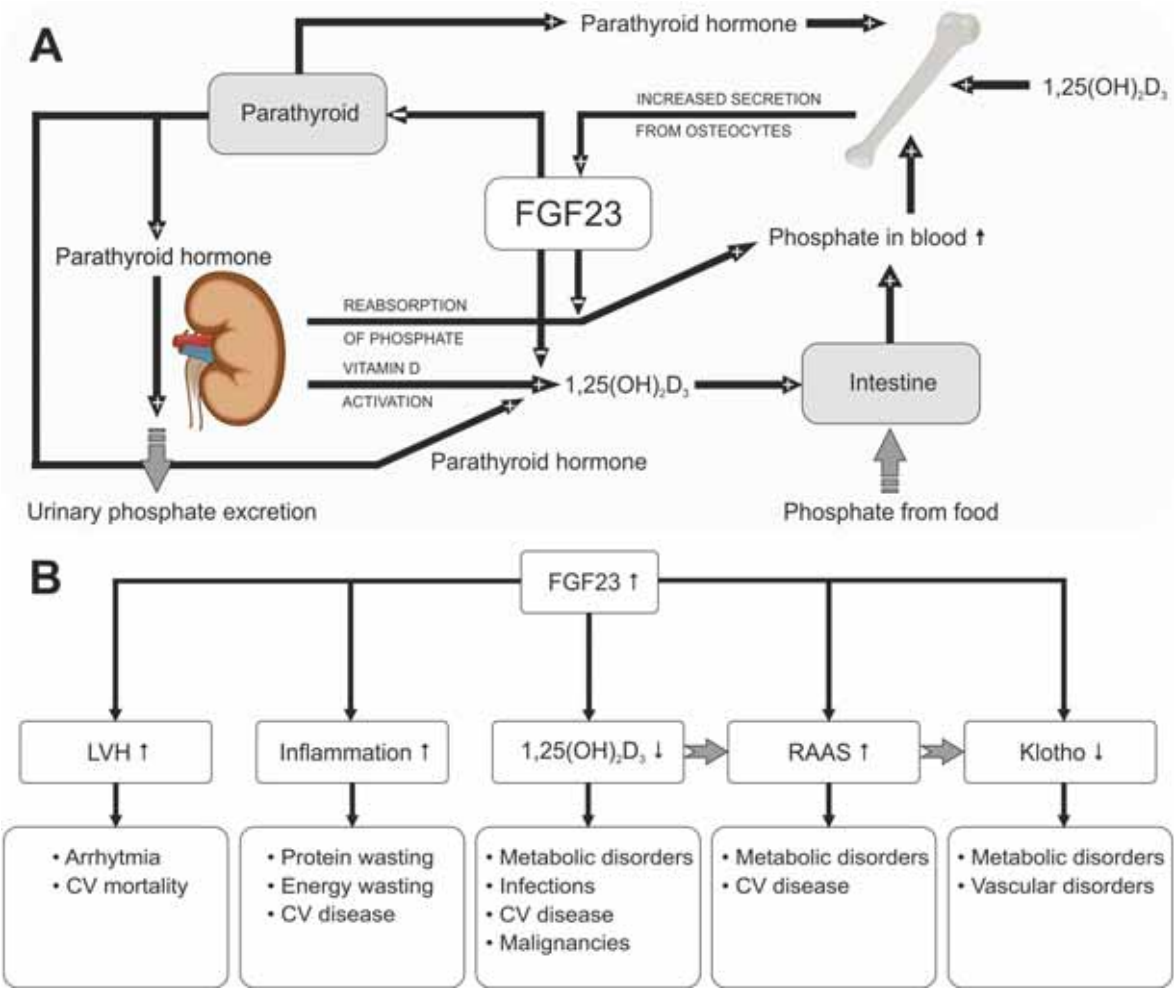

Figure 4. *Fibroblast growth factor 23.* In panel A, fibroblast growth factor 23 (FGF23) is secreted from the bone osteocytes with multiple stimuli. Via Klotho, FGF23 inhibits parathyroid hormone (PTH) secretion in the parathyroid gland, as well as reabsorption of phosphate and calcitriol ($1,25(OH)_2D_3$) synthesis in the kidney. PTH in turn increases phosphaturia, $1,25(OH)_2D_3$ synthesis, and FGF23 secretion from the bone. $1,25(OH)_2D_3$ is responsible for increasing intestinal phosphate absorption. In panel B, increased FGF23 levels induce several pathophysiological processes; CV = cardiovascular, LVH = left ventricular hypertrophy. Figure by the author with data by Nanes (Nanes 2013) and Kovesdy et al. (Kovesdy and Quarles 2013).

5.2. Secondary hyperparathyroidism

CRI is associated with several alterations in calcium-phosphate homeostasis (Slatopolsky 2011). When renal function is impaired, reduced phosphate excretion leads to the elevation of plasma phosphate, and this together with reduced $1,25(OH)_2D_3$ synthesis result in the development of SHPT (Slatopolsky et al. 2001). SHPT is an early and major complication in CKD, and progresses as GFR decreases (Slatopolsky et al. 1999). SHPT is already

present in stage 2-3 CKD and leads to the development of high bone turnover, pathological fractures, vascular calcification, and other systemic alterations (Slatopolsky 2011).

Decreased synthesis of $1,25(OH)_2D_3$ contributes to the characteristic lowering of plasma Ca^{2+} levels in CKD. In the parathyroid cells, reduced expression of VDR and Ca^{2+}-sensing receptors (CaSR) have been reported, which may lead to hypocalcemia (Mihai and Farndon 2000). The extracellular Ca^{2+} concentration plays an important role in the regulation of plasma PTH levels via CaSR, which belongs to the G-protein-coupled receptor family and is present in the membrane of the parathyroid cells (Drüeke 2001, Silver et al. 2002). The synthesis and release of PTH are increased in response to low serum $1,25(OH)_2D_3$, low Ca^{2+} content, and high serum phosphate (Slatopolsky et al. 1999). Along with reduced intestinal calcium absorption due to low $1,25(OH)_2D_3$ levels, hypocalcemia in CKD is frequently exacerbated by the decrease in dietary calcium intake (Drüeke 2001). Therefore, oral calcium supplementation is initiated early in order to combat the calcium deficiency, and to slow the development of SHPT. Supplemented calcium salts also bind phosphate in the intestine, thereby increasing its elimination and helping to suppress hyperphosphatemia (Drüeke 2001).

Extracellular calcium is the main parathyroid regulator. Low levels stimulate PTH secretion, while elevated levels inhibit hormone release and induce degradation within the parathyroid gland (Silver et al. 2002, Cannata-Andia et al. 2010). PTH secretion from the parathyroid can rapidly react to hypocalcemia via CaSR-mediated mechanisms (Silver and Naveh-Many 2009). The Ca^{2+} content in extracellular fluid is recognized by the parathyroid CaSR, and even a small persistent decrease in Ca^{2+} concentration results in relaxation of CaSR, allowing the unrestrained secretion and synthesis of PTH with concomitant parathyroid cell proliferation (Silver and Naveh-Many 2009). The response of the parathyroid gland depends on the rapidity and duration of the hypocalcemic stress. PTH release in response to calcium occurs within seconds to minutes after signaling through the CaSR. Chronic hypocalcemia and hyperphosphatemia stimulate PTH expression and PTH synthesis within hours to days, while parathyroid cells proliferate over days to weeks (Naveh-Many et al. 1990, Naveh-Many et al. 1995, Brown 2000).

The continuous stimulation of the parathyroid gland results in gland enlargement and uncontrolled excess of PTH. Until now, in order to control this situation, calcium supplements and high doses of VDR activators have been used in ESRD patients, inducing

unwelcome increases in serum Ca^{2+}, which has consistently been associated with increased risk of death in observational studies (Block et al. 2004). Notably, a new class of drugs that stimulate CaSR has been developed to combat this issue. Calcimimetics interact with CaSR allosterically at different sites of the molecule, not at the calcium binding site (Mizobuchi et al. 2004, Rodriguez et al. 2007). They change the spatial form of CaSR, and increase the sensitivity of CaSR to calcium. Additionally, calcimimetics upregulate CaSR and VDR, thus, they are able to prevent or attenuate parathyroid hyperplasia (Mizobuchi et al. 2004). Calcimimetics can induce persistent long-term suppression of PTH release. However, due to its half-life, they also induce short-term suppression of PTH synthesis, allowing circadian fluctuations of the circulating PTH with potential anabolic effects on bone (Cannata-Andia et al. 2010).

5.2.1. Vitamin D, vitamin D receptor, and paricalcitol

Vitamin D is a prohormone that is metabolically converted to the active metabolite, $1,25(OH)_2D_3$, which is the endogenous activator of cellular VDR (Dusso et al. 2005). VDR is a cytoplasmic ligand-dependent transcription factor, which is activated upon binding to $1,25(OH)_2D_3$ or other VDR activators, followed by rapid translocation to the nucleus along microtubules (Barsony and McKoy 1992). Subsequent recruitment of cofactors such as the retinoid X receptor (RXR) results in the VDR-RXR cofactor complex. The complex then binds to the vitamin D response element in the promoter region of its target genes, thereby regulating gene transcription (Dusso et al. 2005, Xiong et al. 2012). Vitamin D can be obtained from the diet and by the action of sunlight on the skin. Only a few natural food sources contain significant amounts, but many foods are now fortified with vitamin D_3. Nonetheless, vitamin D insufficiency persists in most of the world due to nutritional deficit, as well as avoidance of sunlight and the use of sunscreens (Dusso et al. 2005).

Vitamin D_3 is produced in the skin by the photolytic cleavage of 7-dehydrocholesterol followed by thermal isomerization (Holick 2013). It is transported by the vitamin D binding protein to the liver, where it is converted to 25-hydroxycholecalciferol ($25(OH)D_3$), the major circulating metabolite of vitamin D_3 (Dusso et al. 2005). This reaction is not well regulated, and thus, the levels of $25(OH)D_3$ increase in proportion to vitamin D intake. For this reason, plasma 25(OH)D-levels are commonly used as an indicator of vitamin D status (Holick 1981). The final activation step,

1α-hydroxylation, occurs primarily in the kidney with 1α-hydroxylase. The reaction forms $1,25(OH)_2D_3$, the active hormonal form of the vitamin (Fraser and Kodicek 1970). Inactivation of $1,25(OH)_2D_3$ is carried out by 24-hydroxylase, which catalyzes a series of oxidation steps resulting in side chain cleavage (Dusso et al. 2005).

In CKD, the diseased kidneys progressively lose their ability to hydroxylate the 1α-position of $25(OH)D_3$ (Coyne et al. 2006). The resulting lack of $1,25(OH)_2D_3$ plays a major role in the early development of SHPT by decreasing intestinal absorption of calcium, and resulting in increased PTH production and hyperproliferation of parathyroid cells (Slatopolsky et al. 1999). The PTH gene transcription in parathyroid glands is decreased by $1,25(OH)_2D_3$ via VDR activation (Slatopolsky et al. 1999). The density of VDR in the parathyroid glands has been reported to markedly reduce in both clinical and experimental CRI (Korkor 1987, Merke et al. 1987). During the progressive loss of renal function, the amount of VDR is further decreased, resulting in desensitization of the parathyroid to the effects of $1,25(OH)_2D_3$ (Slatopolsky 2011).

Paricalcitol, chemically 19-nor-$1,25(OH)_2D_2$, is a third-generation VDR activator developed in 1985 and used in the treatment of SHPT (Coyne et al. 2006). *In vitro* studies and experimental studies in rats indicate that paricalcitol can suppress PTH levels as effectively as $1,25(OH)_2D_3$, but does not induce as strong an effect on serum calcium and phosphorus levels (Martin et al. 1998). Lately, paricalcitol has been increasingly studied in combination with ACEI (Tan et al. 2009). It is well known that $1,25(OH)_2D_3$ functions as a negative endocrine regulator of the RAAS and suppresses renin biosynthesis (Li and Batuman 2009). As RAAS blockade generally causes reactive rise in PRA, combining a VDR activator with a RAAS inhibitor to suppress the renin increase may generate beneficial therapeutic effects and help ameliorate renal interstitial fibrosis and inflammation (Li and Batuman 2009).

5.2.2. Vascular calcification

Vascular calcification is a well-known risk factor for cardiovascular mortality even in the general population (Davies and Hruska 2001). Among patients with CKD, it is one of the principal causes of morbid cardiovascular events contributing to the excess mortality (Hruska et al. 2008). Two distinct sites of calcification have been described in CKD patients: arterial intimal and medial calcification (Shanahan 2013). Intimal calcification is

seen with advancing age, hypertension, dyslipidemia, and smoking, and takes the form of atherosclerotic vascular disease (Demer and Tintut 2008). It is a discontinuous and patchy process involving inflammatory macrophages and VSMCs in lipid-rich regions of the atherosclerotic plaque (Shroff et al. 2013). Medial calcification is more common in CKD, in which it involves sheet-like calcification of the tunica media with thickening of the vessel wall without the involvement of the intima. This phenomenon was originally assumed to be a degenerative age-related problem (Shanahan 2013). Arterial medial calcification is clinically pivotal, as it is the likely the most important factor in vascular stiffness and increased pulse pressure in CKD (Hruska et al. 2008).

Recent evidence has established that vascular calcification is a strictly regulated cell-mediated process that share many similarities with bone formation (Shroff et al. 2013). In bones and teeth where calcification is required, resident cells develop specific mechanisms to enable mineral nucleation and crystal growth in the ECM. Ectopic vascular calcification follows a very similar process. VSMCs are of mesenchymal origin and when facing stress can differentiate to several mesenchymal-derived cell types such as osteoblasts, chondrocytes, and adipocytes, leading to calcification, altered ECM production, and lipid accumulation. Before calcification, VSMCs undergo an osteochondrocytic differentiation and upregulate expression of regulatory proteins that are normally confined to bone and cartilage (Shanahan and Weissberg 1999). These regulators include a number of transcription factors, such as runt-related transcription factor 2 (Runx2), Osterix, Msx2, and Sox9 that together induce change of VSMCs to an osteochondrocytic phenotype (Tyson et al. 2003).

To create an environment permissive of calcification, specialized membrane-bound matrix vesicles serve as initiation sites for hydroxyapatite (Hsu and Camacho 1999). Under normal conditions, VSMC-derived vesicles do not calcify because they carry inhibitors of mineralization such as matrix Gla protein (MGP) and Fetuin-A (Reynolds et al. 2005). However, on exposure to high extracellular Ca^{2+} or with intracellular Ca^{2+} release, and when calcification inhibitor levels are low, VSMCs start to produce vesicles that already contain preformed hydroxyapatite (Shanahan 2013, Shroff et al. 2013). To enable crystal growth, vesicles contain alkaline phosphatase, which provides a source of phosphate by degrading pyrophosphate, a powerful inhibitor of hydroxyapatite growth. Matrix vesicles also contain annexins, Na-dependent phosphate transporters, and phospholipid components

such as phosphatidylserine (Genge et al. 2007). The deposition of these vesicles to the vascular wall stiffens the vessel. There is currently no direct therapy to counteract vascular calcification processes. Therefore, the prevention of mineral dysregulation and lowering of circulating phosphate, starting from the earliest stages of CKD, remains essential to the reduction of cardiovascular mortality in CKD patients (Shroff et al. 2013).

5.2.3. Phosphate binders

Hyperphosphatemia commonly leads to painful fractures, brown tumors, and generalized osteopenia in CKD patients (Tonelli et al. 2010). Dietary restriction of phosphate has long been the cornerstone of therapy, but this measure is usually not sufficient to control hyperphosphatemia. As a result, oral phosphate binders are used in over 90% of patients with late stage CKD, at an annual cost of approximately $750 million U.S. dollars worldwide (Tonelli et al. 2010).

Historically, treatment with oral phosphate binders was intended to prevent symptomatic SHPT. More recently, achieving tighter control of markers associated with abnormal mineral metabolism such as serum phosphate, calcium, and PTH levels, has become a specific therapeutic objective (Tonelli et al. 2010). Aluminium hydroxide was the first phosphorus binder available, and it was extensively used for many years (Cannata-Andia et al. 2010). It is the most potent phosphate binder, but also the most toxic one (Leung et al. 1983, Cannata-Andia and Fernandez-Martin 2002). For this reason, it was progressively replaced in the 1980's by calcium-containing binders. Their use also became widespread, but several disadvantages became apparent later on. It has been reported that the use of calcium salts, especially when exceeding doses of 1.5g daily, increases the risk of vascular calcification in ESRD patients (Cannata-Andia and Rodriguez-Garcia 2002), and can also lead to greater arterial stiffness (London et al. 2008). Magnesium-containing phosphate binders have also been used as an alternative, but they are generally less effective. The putative risk of cardiovascular and soft-tissue calcification has limited the clinical use of the calcium-containing binders and stimulated the synthesis of a new generation, including salts and polymers such as sevelamer and lanthanum carbonate (Cannata-Andia et al. 2010).

In experimental CRI, however, the increased intake of calcium carbonate has actually reduced kidney calcification, the probable mechanism being the lowering of plasma

phosphate (Cozzolino et al. 2002). Furthermore, most clinical and experimental studies concerning this complication have stated that high concurrent circulating levels of phosphate and calcium, or high Ca x Pi product, are risk factors for calcification, but have not given more information about the dietary calcium intake (Kimura and Nishio 1999, Raggi et al. 2002). Therefore, it seems that calcium-containing phosphate binders may only produce notable ectopic calcification if hyperphosphatemia is not in control (Chertow et al. 2004). Without doubt, the control of the hyperphosphatemia and the increased Ca x Pi product are important measures in the treatment of SHPT in CKD (Locatelli et al. 2002).

The ideal phosphate binder would efficiently bind dietary phosphate, have almost zero systemic absorption, no major side effects, low pill burden, and be inexpensive. Unfortunately, none of the currently available oral phosphate binders meet all these criteria (Tonelli et al. 2010). Sevelamer hydrochloride was the first non-aluminium, non-calcium phosphate binder commercially available (Cannata-Andia et al. 2010). Several studies have demonstrated that sevelamer is effective in lowering serum phosphate levels without increasing serum calcium, and may attenuate aortic calcification in comparison to calcium-based phosphate binders (Chertow et al. 2002). Despite the fact that sevelamer hydrochloride offers several advantages, gastrointestinal disturbances and metabolic acidosis have been the limiting factors for its widespread use. Lanthanum carbonate became available in 2005, and preclinical animal studies demonstrated that this non-aluminium, non-calcium binder had a binding capacity closer to that of aluminium with a better safety profile and a low systemic uptake (Cannata-Andia et al. 2010). As lanthanum can get enriched in bones, the long-term effects of this binder are questioned and more studies are needed to confirm its efficacy and safety. A number of new calcium-free phosphate binders are under currently study, but the high cost and safety concerns may keep the ideal phosphate binder still elusive (Tonelli et al. 2010).

AIMS OF THE STUDY

The principal aim of this series of studies was to understand the putative changes in RAAS component gene expression and the ensuing effects on the kidneys and vasculature, using dietary and pharmacological interventions in a well-established experimental animal model of CRI. The model used was 5/6 nephrectomy (NX) in the rat with dietary and pharmacological interventions including oxonic acid-induced hyperuricemia, paricalcitol treatment, and phosphate loading or binding with calcium carbonate.

The specific aims of the study were:

1. To investigate the effects of oxonic acid-induced hyperuricemia on the circulating RAAS and the renal components of the RAS, carotid artery tone, and antioxidant capacity in experimental renal insufficiency.

2. To find out whether delayed initiation of paricalcitol treatment in CRI could influence VDR-activation-induced suppression of RAS component gene expression in the kidney.

3. To test the hypothesis whether dietary modification of phosphate influences kidney and vascular RAS gene expression at both the mRNA and protein levels in CRI.

4. To examine the effects of dietary phosphate loading and binding with calcium carbonate on vascular function and NO metabolites in conduit-size arteries of NX rats.

The interventions were designed to mimic some of the most common complications of CKD patients during the progression of the disease. Even though the studies are experimental, our results may help in understanding the fundamental processes present in patients suffering from CKD. Combined together, these studies aim to provide further insight into the elaborate metabolic modulation pattern of RAAS and oxidative stress during stage 3 experimental CRI.

MATERIALS AND METHODS

1. ANIMALS AND EXPERIMENTAL DESIGN

The present series of studies is based on male Sprague-Dawley (SD) rats with free access to water and food pellets. Rats were housed 2-4 per cage in an animal laboratory with a temperature of 22°C and a controlled environmental 12h light-dark cycle.

Studies I and II

Study populations in studies I and II consisted of 48 and 40 rats, respectively (Figure 5). Rats underwent NX or sham-operation at the age of 8 weeks under ketamine/diazepam anesthesia (75 and 2.5 mg/kg intraperitoneally, respectively). NX was carried out by removal of upper and lower poles of the left kidney, and the whole right kidney (Jolma et al. 2003, Kööbi et al. 2003). The sham rats underwent decapsulation of both kidneys. Antibiotics (metronidazole 60 mg/kg and cefuroxim 225 mg/kg) were given postoperatively, and pain was relieved with buprenorphine (0.2 mg/kg subcutaneously, 3 times a day for 3 days).

Three weeks later, at rat age 11 weeks, the animals were divided into 4 groups so that mean systolic BP, body weights and urine volumes were similar in the two Sham (Sham and Sham+Oxo) and the two NX groups (NX and NX+Oxo), respectively. Systolic BP was measured at 28°C by the tail-cuff method as averages of five successful recordings in each rat (Model 129 Blood Pressure Meter; IITC Inc., Woodland Hills, CA, USA). In study I the size of each experimental group was 12 rats, whereas in study II it was 10 rats.

All groups were given standard laboratory chow (Lactamin R34, AnalyCen, Lindköping, Sweden). The chow contained 0.9% calcium, 0.8% phosphorus, 0.27% sodium, 0.2% magnesium, 0.6% potassium, 12550 kJ/kg energy, 16.5% protein, 4.0% fat, 58% nitrogen-free extract, 3.5% fibre, 6.0% ash, and 10% water. After the 3rd study week, oxonic acid (20 g/kg chow, Sigma-Aldrich Chemical Co., St. Louis, MO, USA) was supplemented in the food of the Sham+Oxo and NX+Oxo groups. These diets continued for 9 weeks, and hyperuricemia was confirmed by tail vein samples at study week 5. The 24-hour fluid consumption and urine output was measured and collected in metabolic cages at the end of the 2nd and 11th study weeks. At the end of the study, at study week 12, the rats were weighed and anesthetized (urethane 1.3 g/kg), while blood samples from cannulated

carotid artery were drawn into chilled tubes with EDTA and heparin as anticoagulants, as appropriate. In study I, blood samples were not obtained from one NX and three Sham rats due to cardiac arrest during anesthesia. The hearts and the kidneys were removed and weighed. A kidney half from each rat was snap-frozen in isopentane at -40°C and stored at -80°C, whereas the other half was fixed in 4% formaldehyde for 24 hours, and embedded in paraffin.

Study III

Study population consisted of 40 rats, which underwent the same NX (n=30) and Sham (n=10) procedures as described above with studies I and II (Figure 5). Standard laboratory chow Lactamin R34 was used as food pellets before treatment period. Fifteen weeks after the operations, the remaining NX rats were divided into two groups (NX and NX+Pari; n=13 per group; 4 rats were lost to surgery complications) with equal systolic BP, body weight, urine output, and plasma creatinine. During the next 12 weeks the NX+Pari rats were given intraperitoneal injections of VDR activator paricalcitol (Zemplar® intravenous injection solution, 5 µg/ml, vehicle containing 30% propylene glycol and 20% ethanol; Abbott Laboratories, Abbott Park, IL, USA) 200 ng/kg three times a week. Total vehicle volume was only about 10 µl, and thus no vehicle-treated group was included into study. As the calcium content in standard Lactamin R34 chow is rather high, all groups were fed a diet containing 0.3% calcium and 0.5% phosphate during the treatment period in order to aggravate the degree of SHPT and minimize the risk of hypercalcemia. Due to the high mortality present in all experimental CRI studies of this duration, the final animal numbers at the end of the 27-week experiment were 12, 7, and 8, in the Sham, NX, and NX+Pari groups, respectively.

Studies IV and V

Study populations consisted of 49 rats in each study, as the same rat cohort was used in both studies (Figure 5). At the age of 8 weeks, the NX and Sham rats underwent similar surgeries as described above with studies I and II. The rats were fed standard Lactamin R34 chow before commencing study diets.

Fifteen weeks after operations, at the age of 23 weeks, NX rats were divided into three groups with similar systolic BP, body weight, and plasma creatinine level. For the next 12 weeks, Sham and NX groups were put on 0.3% Ca, 0.5% Pi, NX+Ca group on 3.0% Ca, 0.5% Pi, and NX+Pi group on 0.3% Ca, 1.5% Pi diet. At the end of the study, 24-hour

urine excretion was collected in metabolic cages and water consumption measured. Tissue and blood collection was carried out as described above with studies I and II.

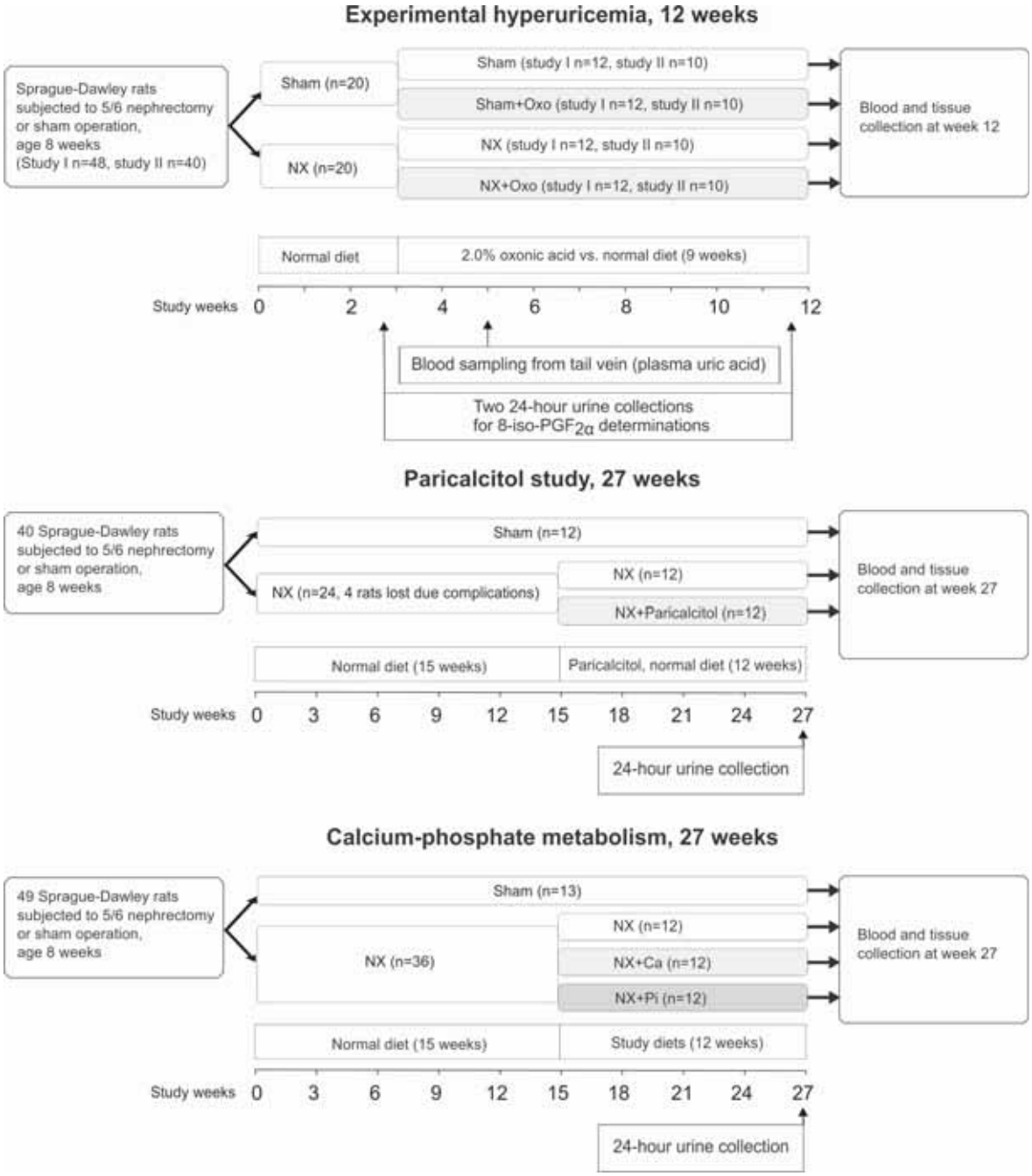

Figure 5. *Flow chart of study designs.* Three different study designs were developed. Studies I and II followed the same protocol, while studies IV and V featured the same rats (calcium-phosphate metabolism). Ca = Phosphate-binding diet (3.0% Ca, 0,5% Pi), Pi = Phosphate-loading diet (0,3% Ca, 1,5% Pi)

2. *IN VITRO* AUTORADIOGRAPHY

Studies I, IV, and V

Frozen 20 µm thick kidney **(I,IV)** and aortic **(V)** sections were cut on a cryostat at 17°C, thaw mounted onto Super Frost R Plus slides (Menzel-Gläser GmbH, Braunschweig, Germany), dried in a dessicator under reduced pressure at 4°C overnight, and stored at 80°C with silica gel until further processing (Bäcklund et al. 2001).

2.1. Angiotensin-converting enzyme autoradiography

A tyrosyl residue of lisinopril (MK351A, Merck, Sharp & Dohme Research Laboratories, West Point, PA, USA), was iodinated by chloramine T method, purified on SP-Sephadex C-25 column (Pharmacia, Piscataway, NJ, USA), and then a previously described technique was applied (Kohzuki et al. 1991, Bäcklund et al. 2001). Kidney or aortic sections were pre-incubated for 15 minutes at room temperature (RT) in 10 mM sodium phosphate buffer, pH 7.4, containing 150 mM NaCl and 0.2% bovine serum albumin (BSA), followed by incubation for 1 hour at RT in fresh volume of the same buffer containing 0.3 µCi/ml of ^{125}I-351A. Non-specific binding was determined in parallel incubations in the same buffer containing 1 mM Na_2-EDTA. After incubation, the sections were washed 4 times for 1 minute in ice-cold buffer without BSA and ^{125}I-351A to remove unbound radioligand, and dried under a stream of cool air. For quantification of ACE binding, the sections were placed on a Fuji Imaging Plate BAS-TP2025 (Tamro, Finland) for 3 hours. The optical densities were quantified by an image analysis system (AIDA 2D densitometry) coupled to FUJIFILM BAS-5000 phosphoimager (Tamro, Finland) from four kidney or aortic sections per rat, six representative areas per section, altogether 24 analyses per each kidney. Specific binding was calculated as total binding minus non-specific binding.

2.2. AT_{1R} and AT_{2R} autoradiography

In studies I and IV, Sar^1,Ile^8-Ang II (Sigma, St. Louis, MO, USA) was iodinated by chloramine T method and purified on a Sep-Pack C18 cartridge with methanolic gradient elution. Autoradiographic quantification of angiotensin receptors with [^{125}I]-Sar^1,Ile^8-Ang II was performed using a published modification (Stewen et al. 2003) of a previously described method (Zhuo et al. 1999). Kidney sections were pre-incubated for 15 minutes at

RT in 10 mM sodium phosphate buffer, pH 7.4, containing 150 mM NaCl, 5 mM Na_2-EDTA, and 0.2 % BSA, followed by a 1 hour incubation at 37ºC in fresh volume of the same buffer containing 0.2 µCi/ml of ^{125}I-[Sar^1,Ile^8]Ang II. Non-specific binding was determined in the presence of 1 µmol/l unlabeled Ang II (Sigma). The density of AT_{1R} was determined in presence of the AT_{2R} antagonist PD 123,313 (10 µM), and the density of AT_{2R} in presence of the AT_{1R} antagonist losartan (10 µM). After incubation, the sections were washed 4 times for 1 minute in ice-cold buffer without BSA and radioligand and dried under stream of cool air. The optical densities of angiotensin receptor binding from 10 kidney sections per rat was quantified as described above for ACE from six representative cortical and six medullary areas per each section: four sections were used for total specific binding, two sections for AT_{1R} binding, two sections for AT_{2R} binding, and two sections for non-specific binding.

The outcome in each group was related to the mean value of the Sham group, except for the medullary:cortical AT_{1R} density ratio, where the respective densities in each rat kidney were related to each other.

3. REAL-TIME QUANTITATIVE RT-PCR

Total RNA was isolated from rat kidney tissue using Trizol® reagent (Invitrogen, Carlsbad, CA, USA) and reverse transcription of RNA was performed using M-MLV reverse transcriptase (Invitrogen) according to the manufacturer's instructions.

Study I

The expressions of ACE, ACE2, AT_{1aR}, and AT_{2R} mRNAs were studied using real-time quantitative RT-PCR. PCR were performed either with SYBR Green chemistry (ACE and AT_{1aR}) or TaqMan chemistry (ACE2 and AT_{2R}) using ABI PRISM 7000 sequence detection system (Applied Biosystems, Foster City, CA, USA). PCR for ACE and AT_{1aR} were performed in duplicate in a 25 µl final volume containing 1X SYBR Green Master mix (Applied Biosystems) and 300 nM of primers (Table 2). PCR for ACE2 and AT_{2R} were performed in duplicate in a 25 µl final volume containing 1X TaqMan Master mix (Applied Biosystems), 300 nM of primers and 100 nM of ACE2, 150 nM of AT_{2R} TaqMan probe (Table 2). PCR cycling conditions were 10 min at 95ºC and 40 cycles of 20 seconds at 95ºC and 1 min at 60ºC. Data were analyzed using the absolute standard curve method and the amplification of a housekeeping gene 18S was used for normalizing the results.

The unnormalized expression of 18S mRNA did not differ between the experimental groups (data not shown) enabling its use as the control housekeeping gene in the present study. The intra- and inter-assay coefficients of variations for the studied mRNAs were ≤1.2% and ≤2.8%, respectively.

Table 2. Primer and probe sequences used in the real-time RT-PCR amplification.

Gene	Primer nucleotide sequence
ACE	Forward 5'-GGAGACGACTTACAGTGTAGCC-3' *
	Reverse 5'-CACACCCAAAGCAATTCTTC-3' *
AT_{1aR}	Forward 5'-GGCAGCCTCTGACTAAATGGC-3'
	Reverse 5'-ACGGCTTTGCTTGGTTACTCC-3'
ACE2	Forward 5'-ACCCTTCTTACATCAGCCCTACTG-3' †
	Reverse 5'-TGTCCAAAACCTACCCCACATAT-3' †
AT_{2R}	Forward 5'-TGTCTGTCCTCATTGCCAACA-3'
	Reverse 5'-TTCATTAAGGCAATCCCAGCA-3'
AT_{4R}	Forward 5'-TGACAAAGACCGAGCCAACCT-3'
	Reverse 5'-TCAAATCGAATGCCATCTGAAGA-3'
PRR	Forward 5'-AGCATCTCGCCAAGGATCAT-3'
	Reverse 5'-TCCATAACGCTTCCCAAGCT-3'
CTGF	Forward 5'-GTGTGTGATGAGCCCAAGGA-3'
	Reverse 5'-GCAGTTGGCTCGCATCATAG-3'
HO-1	Forward 5'-CACAAAGACCAGAGTCCCACACAG-3' ‡
	Reverse 5'-AAATTCCCACTGGCACGGT-3' ‡
Mas	Forward 5'-TCATGTGTATTGACAGCGGAGAA-3'
	Reverse 5'-CACTAACATGAGCGGAGTGAAGA-3'
GAPDH	Forward 5'-GCCAAGTATGATGACATCAAG-3'
	Reverse 5'-AAGGTGGAAGAATGGGAG-3'

Gene	Probe nucleotide sequence
ACE2	5'FAM-ATGCCTCCCTGCTCATTTGCTTGGT-TAMRA †
AT_{2R}	5'FAM-TCAGAACCATTGAATACTT-MGB
CTGF	5'FAM-CCAAATGTGTCTTCCAG-MGB

FAM = 6-carboxyfluorescein, TAMRA = tetramethylrhodamine, MGB = dihydro-cyclopyrroloindole tripeptide (minor groove binder); *(Harada et al. 2001), †(Tikellis et al. 2003), ‡(Essig et al. 1997)

Study III

RT-PCRs for AT_{1aR}, AT_{2R}, ACE, and ACE2 were carried out as described above with study I. PCRs for AT_{4R}, Mas, and PRR were performed in duplicate in 25 µl final volume containing 1X SYBR Green Master mix (Applied Biosystems) and 300 nM of primers (Table 2). PCRs for connective tissue growth factor (CTGF) were performed in duplicate in 25 µl final volume containing 1X TaqMan Master mix (Applied Biosystems), 300 nM of primers and 150 nM of AT_{2R} or 200 nM of CTGF TaqMan probe, respectively (Table 2). PCRs for 18S were performed in duplicate in 25 µl final volume containing 1X TaqMan Master mix (Applied Biosystems) and 1X 18S TaqMan Gene Expression Assay primer and probe mix (Hs999999_s1, Applied Biosystems).

Study IV

RT-PCRs were performed with SYBR Green or TaqMan chemistry using ABI PRISM 7000 sequence detection (Applied Biosystems). GAPDH and 18S were used as housekeeping genes.

PCRs for AT_{4R}, Mas, PRR, and CTGF were performed as above with study III. PCRs for AT_{1aR}, heme oxygenase-1 (HO-1), and GAPDH were performed in duplicate in 25 µl final volume containing 1X SYBR Green Master mix (Applied Biosystems) and 300 nM of primers (Table 2). PCRs for AT_{2R} were performed in duplicate in 25 µl final volume containing 1X TaqMan Master mix (Applied Biosystems), 300 nM of primers and 150 nM of AT_{2R} or 200 nM of CTGF TaqMan probe, respectively (Table 2). PCRs for 18S were performed in duplicate in 25 µl final volume containing 1X TaqMan Master mix (Applied Biosystems) and 1X 18S TaqMan Gene Expression Assay primer and probe mix (Hs999999_s1, Applied Biosystems).

PCR cycling conditions for GAPDH were 10 min at 95ºC and 40 cycles of 20 seconds at 95ºC and 1 min at 56ºC. PCR cycling conditions for other mRNAs were 10 min at 95ºC and 40 cycles of 20 seconds at 95ºC and 1 min at 60ºC. Data were analyzed using the absolute standard curve method (Lakkisto et al. 2002). The amplification of 18S was used for normalizing the results of AT_{4R}, Mas, and PRR mRNAs. The amplification of GAPDH was used for normalizing the results of AT_{1aR}, AT_{2R}, CTGF and HO-1 mRNAs. The unnormalized expressions of 18S and GAPDH did not differ in the groups, allowing their use as control genes.

4. WESTERN BLOTTING

Study IV

Frozen tissues (100 mg) were lysed in 1 ml of sodium dodecyl sulphate (SDS) buffer containing 10 mM Tris-HCl, pH 7.4, 2% SDS, and protein inhibitors (Complete™ Mini EDTA-free, Roche Diagnostics GmbH, Mannheim, Germany). Nuclear and other debris was removed by centrifugation (10.000g, 15 min), and protein concentrations were determined by Bio-Rad Protein Assay system (Bio-Rad Laboratories Inc., Richmond, CA, USA).

Aliquots of homogenate containing 50 µg of protein in loading buffer (10% glycerol, 2% SDS, 60 mM Tris-HCl, pH 6.8, 0.01% bromophenol blue, and 100 mM dithiothreitol) were boiled for 5 minutes before electrophoresis on 12% SDS-polyacrylamide gels. The proteins in the gel were electrophoretically transferred to Immun-Blot PVDF membrane (Bio-Rad Laboratories Inc.) in 25 mM Tris-HCl, pH 8.0, 192 mM glycine, and 20% methanol at 50 volts overnight. After washing in H_2O and TBS-T (20 mM Tris-HCl, pH 7.6, 136 mM NaCl, 0.3% Tween-20), membranes were blocked in 5% non-fat milk powder in TBS-T (RT, 1 hour), and incubated for 3 hours with goat polyclonal antibody against rat ACE (Santa Cruz Biotechnology Inc., Dallas, TX, USA) diluted 1:200 in 5% milk in TBS-T buffer. After extensive washing with 2.5% milk/TBS-T buffer, membranes were incubated with 1:2000 dilution of horseradish peroxidase-conjugated rabbit antigoat IgG for 1 hour (Sigma-Aldrich Co.). Antibody binding was detected by chemiluminescence (WB Chemiluminescent Reagent plus, NEN Inc., Boston, MA, USA), and the autoradiograph was analyzed with Image Gauge 3.3 software (Fuji Photo Film Company, Tokyo, Japan).

Study V

Frozen tissues were homogenized in 400µl distilled H_2O containing protease inhibitors (Complete™ Mini EDTA-free, Roche Diagnostics GmbH) by Ultra-Turrax T25 homogenizer (Janke & Kunkel GmbH & Co, IKA®-Labortechnik, Staufen, Germany). After removal of tissue debris in centrifugation (12,000g for 15min at 4°C), protein concentrations of the supernatants were determined using Coomassie Plus™ Protein Assay Kit (Pierce, Rockford, IL, USA). SDS-PAGE was run on 8% resolving gel and 4% stacking gel. Subsequently, proteins were transferred to a Hybond-ECL nitrocellulose membrane (Amersham Biosciences UK Limited, Buckinghamshire, UK). The primary antibodies used were: 1:2500 dilution of mouse eNOS antibodies (BD Biosciences

Pharmingen, CA, USA), 1:4000 dilution of rabbit NOS2 polyclonal antibodies (Santa Cruz Biotechnology) and 1:3333 dilution of mouse nitrotyrosine monoclonal antibody (Cayman Chemical, Ann Arbor, MI, USA). Antibody binding was detected by SuperSignal® West Pico chemiluminescent substrate (Pierce). The chemiluminescence signal was analyzed with FluorChem software version 3.1. (FluorChem 8800 imaging system, Alpha Innotech Corporation, San Leandro, CA, USA).

5. *IN VITRO* VASCULAR FUNCTION

5.1. Carotid artery responses *in vitro*

In study II, the carotid artery was chosen for closer inspection because of the controversial results concerning UA, central circulation and stroke (Lehto et al. 1998, Yu et al. 1998, Squadrito et al. 2000, Chamorro et al. 2002, Weir et al. 2003). In the rat carotid artery, the vasorelaxation to acetylcholine (Ach) is largely mediated via endothelium-derived NO (Arvola et al. 1999), which likely makes this vessel sensitive to changes in the antioxidant status *in vivo* (Vaziri et al. 2002). A two-millimeter-long standard section of left carotid artery from each animal was prepared, and suspended between hooks in an organ bath chamber in physiological salt solution (PSS; pH 7.4) containing (mM): NaCl 119.0, $NaHCO_3$ 25.0, glucose 11.1, $CaCl_2$ 1.6, KCl 4.7, KH_2PO_4 1.2, $MgSO_4$ 1.2. The PSS was aerated with 95% O_2 and 5% CO_2 and the ring was equilibrated for 1½ h at 37°C with a resting preload of 3.7 mN/mm to induce maximal contractile force generation in the carotid ring (Arvola et al. 1999), measured using isometric force-displacement transducers (FT 03, 7 E Polygraph, Grass Instrument Co., Quincy, MA, USA).

The rings were allowed 30 min at baseline tension in between each concentration-response challenge. Contractions to norepinephrine (NE) were cumulatively elicited, and relaxations to the NO donor nitroprusside and β-adrenoceptor agonist isoprenaline were examined in rings precontracted with 1 μM NE. The relaxations to Ach, in the absence and presence of the NO synthase inhibitor N^G-nitro-L-arginine methyl ester (L-NAME, 0.1 mM), were examined in rings precontracted with 1 μM NE.

5.2. Mesenteric artery responses *in vitro*

In study V, the main branch of the mesenteric artery was carefully cleaned from adjacent connective tissue. Three successive standard ring sections (3 mm in length) were cut, beginning 5 mm distally from the mesenteric artery-aorta junction. In two proximal rings the endothelium were left intact, and it was removed from the last piece (Arvola et al. 1992). The rings were placed between stainless steel hooks (diameter 0.3 mm) and suspended in organ bath chambers (20 ml) with physiological salt solution (PSS; pH 7.4) containing (mmol/L): NaCl 119.0, $NaHCO_3$ 25.0, glucose 11.1, $CaCl_2$ 1.6, KCl 4.7, KH_2PO_4 1.2, $MgSO_4$ 1.2, and aerated with 95% O_2 and 5% CO_2. All rings were initially equilibrated for about 2 hours at 37ºC with a resting preload of 4.905 mN/mm, and challenged with 125 mmol/L KCl several times. The force of contractions was measured with isometric force-displacement transducers and recorded on a polygraph (FT-03 transducer, Model 7E Polygraph; Grass Instrument Co.). The presence of intact endothelium was confirmed by a clear relaxation to 1 μmol/l Ach in 1 μmol/l NE-precontracted ring, and the absence of endothelium by the lack of this response.

6. RADIOIMMUNOASSAYS

In study I, PRA and plasma aldosterone concentration were determined using GammaCoat® PRA radioimmunoassay (RIA) kit and ALDOCTK-2 RIA kit (Diasorin S.p.A., Saluggia, Italy) according to the manufacturer's instructions. PRA was also measured in studies III and IV.

6.1. Aldosterone radioimmunoassay

For the measurement of aldosterone concentration, deep frozen (-80ºC) EDTA plasma samples were rapidly thawed to RT before assaying in duplicate. The assay is based on competition for a limited number of fixed antibody binding sites between the ^{125}I-labeled aldosterone and the aldosterone contained in calibrators or samples to be assayed. 200 μl per sample and 500 μl of ^{125}I-labeled aldosterone tracer were dispensed on the bottom of an anti-aldosterone antibody coated tube, then mixed thoroughly on vortex, and incubated overnight at RT. Zero and control calibrators were subjected to the same protocol as the measured samples. After the overnight incubation, all tubes were carefully aspirated so that no liquids were present during the actual measurement. Radioactivity measurements were

performed on a gamma counter (Wallac Wizard 1470, PerkinElmer Inc., Waltham, MA, USA), and the aldosterone concentrations were calculated using the obtained calibration curve. In this assay, the amount of ^{125}I-labeled aldosterone bound to the rabbit anti-aldosterone antibody on the tube walls is inversely related to the concentration of unlabeled aldosterone present in calibrators or samples, while the use of coated tubes gives the advantage of bound/free separation, as only the bound aldosterone is present after a complete aspiration of the incubation mixture.

6.2. Plasma renin activity radioimmunoassay

For the PRA measurement, deep frozen (-80ºC) EDTA plasma samples were rapidly thawed to RT before assaying in duplicate. The principle of this assay is that PRA is measured via its Ang I producing capability. Therefore, an incubation for Ang I generation was performed before the actual measurement. One ml of plasma per sample was dispensed in an uncoated plastic tube, marked accordingly, and mixed well with 10 µl phenylmethylsulfonyl fluoride solution and 100 µl maleate buffer (pH 6.0). All samples were then divided in two tubes (500 µl aliquots), after which one tube was placed in an ice bath (marked number 4) and the other in a 37ºC (marked number 37) water bath for 90 minutes of Ang I generation. After 90 minutes, the tubes in water bath were transferred to ice bath in order to stop Ang I generation for the beginning of the actual PRA assay. This part of the assay is based on competition for a limited number of fixed antibody binding sites between the ^{125}I-labeled Ang I and the Ang I contained in calibrators or samples. Rabbit anti-Ang I antibody coated tubes were used in this measurement. 100 µl of each sample and 1.0 ml of tracer were mixed thoroughly in a coated tube, and incubated for three hours in RT. All controls were subjected to the same protocol as the measured samples. After incubation, the liquid in all the tubes were aspirated completely, and the radioactivity in each tube was measured using a gamma counter (Wallac). PRA values for each sample were obtained by first deducting the measured value of each number 4 tube from the corresponding number 37 tube, and then calculating correct value using the calibration curve as reference.

6.3. 8-iso-$PGF_{2\alpha}$ radioimmunoassay

In study II, the urinary 8-iso-$PGF_{2\alpha}$ RIA was performed as previously described (Rossi et al. 2004). Urine samples were first vortexed and centrifuged at 3000g for 5 min. Three thousand disintegrations per minute of labeled 8-iso[^{3}H]-$PGF_{2\alpha}$ was added to 1 ml of supernatant (pH 3.0), and incubated overnight at 22ºC before extraction on a C2 silica cartridge (Applied Separation, Allentown, PA, USA). Rabbit polyclonal antibody was used at a dilution that was responsible for binding 30% of tracer. 8-iso[^{125}I]-$PGF_{2\alpha}$ methyl tyrosinate was diluted in 50mM phosphate buffer (pH 7.4) for the use as a tracer in RIA. A series of standards was diluted in 50mM phosphate buffer (pH 7.4) using non-labeled 8-iso-$PGF_{2\alpha}$ in the concentration range of 0-5 ng/ml (0-500 pg/tube). Dextran-coated charcoal suspension was prepared using 1% neutral activated charcoal in 10 mM phosphate buffer (pH 7.4) containing 0.5% Dextran T-70. RIA was carried out in polystyrene test tubes in 50 mM phosphate buffer (pH 7.4) containing 0.1% gelatine. The assay mixture contained 0.1 ml of antibody, 0.1 ml of 8-iso[^{125}I]-$PGF_{2\alpha}$ tracer, and 0.1 ml of 8-iso-$PGF_{2\alpha}$ standards or the measured samples. The final assay volume was adjusted to 0.4 ml by the addition of buffer. Measurements were performed in duplicate.

After incubation at 4ºC overnight, 0.5 ml of dextran-coated charcoal under continuous stirring was added to each assay tube except for the total count tubes to separate the bound from the free fraction. The tubes were vortexed and incubated for 10 min at 4ºC and centrifuged at 2000g for 10 min at the same temperature. 8-iso[^{125}I]-$PGF_{2\alpha}$ radioactivity was measured from supernatant aliquots of 0.6 ml in a gamma counter (Wallac). The 8-iso-$PGF_{2\alpha}$ concentrations were log-transformed before determination of the final values.

7. OTHER PLASMA AND URINE DETERMINATIONS

Study I

Plasma and urine creatinine was determined using Jaffe's colorimetric assay, and plasma urea using colorimetric enzymatic dry chemistry (Vitros 950 analyzer, Johnson & Johnson Clinical Diagnostics, Rochester, NY, USA). UA was measured by an enzymatic colorimetric method (Praetorius and Poulsen 1953).

Study II

Plasma and urine creatinine, plasma urea, and UA were measured as above in study I. Triglycerides, total and high-density lipoprotein (HDL) cholesterol concentrations were analyzed using Cobas Integra 800 automatic analyzer (Roche Diagnostics GmbH, Mannheim, Germany). Non-HDL cholesterol was calculated as total cholesterol minus HDL cholesterol.

Plasma TRAP was measured using luminol-enhanced chemiluminescence, based on peroxyl radical production by decomposition of 2,2-azo-bis(2-aminopropane) hydrochloride (ABAP; Polysciences, Warrington, PA, USA), as previously described (Alanko et al. 1999, Dugue et al. 2005). In the measurement, the tested compounds from 2 to 20 nmol per assay were subjected to peroxyl radicals produced at a known and constant rate by the thermal decomposition of ABAP at 37°C. The presence of free radicals in the reaction mixture was monitored by luminol-enhanced chemiluminescence. The composition of the reaction mixture in cuvette was: 475 ml of 100 mM phosphate buffer, pH 7.4 in saline; 50 ml of 400 mM ABAP and 50 ml of 10 mM luminol in 100 mM borate buffer, pH 10. The solvents used had themselves no radical-scavenging properties. The addition of an antioxidant dissolved in 20 ml of 100 mM phosphate buffer in saline, pH 7.4 to the reaction mixture extinguished the chemiluminescence. The duration of extinction had a linear correlation to the radical trapping capability of the tested compound. A water-soluble tocopherol, Trolox, which is known to trap two radicals per molecule (stoichiometric factor 2.0), was used as a standard. For each phenolic compound the plots of the extinction of chemiluminescence versus the concentration were drawn and stoichiometric factors were calculated.

Study IV

Creatinine, phosphate, and calcium measurements were carried out on Cobas Integra 800 Clinical Chemistry analyzer (Roche Diagnostics GmbH). Plasma phosphate was measured using a direct phosphomolybdate method according to Daly and Ertingshausen (Daly and Ertingshausen 1972). Plasma creatinine was measured by an enzymatic colorimetric method and Cobas Integra Creatinine plus (CREP2) reagents (Junge et al. 2004). Calcium levels were determined according to Schwarzenbach with o-cresolphthalein complexone (Schwarzenbach 1955).

Study V

Creatinine, phosphate, and calcium measurements were carried out on Cobas Integra 800 Clinical Chemistry analyzer (Roche Diagnostics GmbH) as described above with study IV. The NO metabolite (NOx) concentrations in plasma and urine were measured by conversion of nitrite and nitrate to NO, which was quantified by the ozone-chemiluminescense method (Kalliovalkama et al. 1999). The samples of plasma or urine were first treated with ethanol at 20°C for two hours to precipitate proteins. A 20 µl sample was then injected into solution of a cylinder containing saturated vanadium (III) chloride (VCl_3) in HCl (0.8 g VCl_3 / 100 ml of 1 mol/L HCl) at 95°C, and NO formed under these reducing conditions was measured by the NOA 280 analyzer (Sievers Instruments, Boulder, CO, USA) using sodium nitrate as the standard (Braman and Hendrix 1989).

8. IMMUNOSTAINING AND GRADING OF CALCIFICATIONS

Study II

For immunostaining determinations, five-µm-thick kidney sections were stained with hematoxylin-eosin and processed for light microscopic evaluation by an expert blinded to the treatments. The glomerulosclerosis score for each animal was derived as the mean of all sample glomeruli: 0 = normal, 1 = mesangial expansion or basement membrane thickening, 2 = segmental sclerosis <25% of the tuft, 3 = segmental sclerosis 25-50% of the tuft, 4 = diffuse sclerosis >50% of the tuft, 5 = diffuse glomerulosclerosis, total tuft obliteration and collapse (Pörsti et al. 2004).

Study V

Aortic calcifications were determined from von Kossa-stained aortic sections at 200X magnification. The total area of each aortic section and area of calcification was measured using a computerized interactive system (Scion Image Beta 4.02, Frederick, MD, USA). The index of calcification for each rat was expressed as percentage of the calcified area related to the total area of the aortic cross-section.

9. DRUGS AND DIETARY COMPOUNDS

The following drugs and chemicals were used: cefuroxim, diazepam (Orion Pharma Ltd., Espoo, Finland), ketamine (Parke-Davis Scandinavia AB, Solna, Sweden), metronidazole (B. Braun AG, Melsungen, Germany), buprenorphine (Reckitt & Colman, Hull, England),

acetylcholine chloride, isoprenaline hydrochloride, NG-nitro-L-arginine methyl ester, norepinephrine bitartrate, L-arginine, Ang II, oxonic acid (Sigma-Aldrich Chemical Co., St Louis, MO, USA), sodium nitroprusside (Fluka Chemie AG, Buchs SG, Switzerland), paricalcitol (Zemplar® intravenous injection solution, 5 µg/ml, vehicle containing 30% propylene glycol and 20% ethanol; Abbott Laboratories, Abbott Park, IL, USA). The stock solutions used in the *in vitro* studies were made by dissolving the compounds in distilled water. All solutions were freshly prepared before use and protected from light.

10. STATISTICAL METHODS

The statistical analysis was carried out using one-way and two-way analyses of variance (ANOVA) supported by the Bonferroni test when making pairwise comparisons between the test groups. Correlation analyses (r) were done using Spearman's Rho. The least significant difference test was used for post-hoc analyses. ANOVA for repeated measurements was applied for data consisting of repeated observations at successive observation points. If the distribution of the variables was skewed, the Kruskal-Wallis test was applied, and post-hoc analyses were performed with the Mann-Whitney U-test, the P values being corrected with the Bonferroni equation. Results were expressed as mean ± SEM, and differences were considered significant when $P<0.05$.

The contractile responses were expressed as wall tension (mN/mm). The EC50 for these contractions in each ring were calculated as a percentage of maximal response and presented as the negative logarithm (pD2), which values were also used in the statistical analysis. The relaxations in response to Ach, and nitroprusside were presented as a percentage of pre-existing contractile force. The areas under concentration response curve (AUC) analyses of Ach were used to present the change in AUC by L-NAME per group, and to show the contributions of NO in the endothelium-dependent relaxations. The areas under each individual curve of nitroprusside responses were determined and expressed in arbitrary units. The data in studies I-III were analyzed using SPSS 11.5 and data in studies IV-V using SPSS 17.0 (SPSS Inc., Chicago, IL, USA)

11. ETHICAL ASPECTS

The experimental design of these studies was approved by the Animal Experimentation Committee of the University of Tampere, and the Provincial Government of Western Finland Department of Social Affairs and Health, Finland. The investigations conform to the Guiding Principles for Research Involving Animals.

RESULTS

1. ANIMAL DATA

Blood pressure

In studies I and II, systolic BPs did not differ between the groups in the beginning of the oxonic acid feeding period (Table 3). However, at study week 9 of study I, the BP in the NX+Oxo group was higher than in the Sham group. No such difference was seen in study II, and no significant differences in BP were detected between the other groups. In study III, the systolic BPs were higher than Sham in both NX groups when measured at weeks 15 and 27. At the end of studies IV and V, the systolic BPs were higher in all NX groups than in Sham, whereas the NX+Ca group showed lower BP than the other NX groups.

Body weight, heart/body weight ratio, urine output, and rat count

In study I, the final body weight in the NX+Oxo group was slightly lower when compared with the NX group, and when analyzed using two-way ANOVA, a significant lowering influence on body weight was associated with oxonic acid feeding ($p=0.004$). In study II, the average body weight gain was comparable in all groups. The heart to body weight ratio and 24-hour urine output were higher in both NX groups when compared to Sham rats (Table 3).

In study III, due to the high mortality of all experimental CRI studies of this duration, the final animal numbers at the end of the 27-week experiment were 12, 7, and 8, in the Sham, NX, and NX+Pari groups, respectively (Table 3). The body weights at the end of the study did not differ between the groups, while heart weight/body weight ratio was lower in both NX groups when compared with Sham.

Studies IV and V were carried out using the same rats. The NX+Ca and NX+Pi rats had lower final body weights than Sham, whereas no difference was seen between the NX groups. The heart/body weight ratios were higher in all NX groups than in Sham rats. The initial animal count in all NX groups was 12-13. At the end of the study, lower rat count was observed in the NX (5 lost rats) and NX+Pi (6 lost rats) than Sham and NX+Ca (1 lost rat) groups (Table 3).

2. LABORATORY FINDINGS

2.1. Blood, plasma, and histological grading

In study I, the blood pH was slightly lower in the NX group than in Sham rats, while hemoglobin was decreased in the NX+Oxo group when compared with Sham (Table 4). The oxonic acid feeding elevated plasma UA by 80-90 μmol/l in both Sham and NX rats, as expected. Creatinine clearance was similarly reduced by approximately 60% in both NX groups, and also by about 25% in hyperuricemic Sham rats (Figure 7B). Plasma concentration of urea was over 2-fold higher in the NX group when compared to Sham rats, while no difference between the NX and NX+Oxo groups was observed (Table 4).

Hyperuricemia had a clear elevating effect on PRA (Figure 7A) and plasma aldosterone concentration (Figure 7C) in study I. In the Sham+Oxo group PRA increased 1.2-fold and plasma aldosterone 1.4-fold, while in the NX+Oxo group the increases were 2.5 and 2.3-fold, respectively. As 5/6 NX is a low-renin model of CRI, PRA was decreased in NX and NX+Pari groups when compared with Sham in study III (Table 5). In study I, the plasma aldosterone:renin ratios in the experimental groups were (mean±SEM) 12±2, 14±2, 360±208* and 213±110* in the Sham, Sham+Oxo, NX and NX+Oxo groups, respectively (*P<0.001 both NX groups vs. both Sham groups).

At the end of study II, the oxonic acid diet elevated plasma UA concentration 3.4-fold in the Sham+Oxo rats and 2.4-fold in the NX+Oxo rats, respectively (Table 4). Plasma creatinine and urea concentrations were approximately doubled in the NX rats when compared with Sham, and were not affected by oxonic acid diet. Creatinine clearance was reduced by approximately 60% in both NX groups, and also by 33% in hyperuricemic Sham rats. The plasma concentrations of TRAP were increased 1.5-fold in groups ingesting the oxonic acid diet (Table 4), and there was a linear correlation between plasma UA concentration and TRAP in all groups (Figure 7G).

Plasma total cholesterol, HDL cholesterol, and non-HDL cholesterol concentrations were elevated in NX rats of study II (Table 4). When analyzed using two-way ANOVA, an elevation of plasma triglycerides was also uncovered in NX rats when compared with Sham rats (P=0.006, two-way ANOVA). No differences in blood pH were detected. However, histological analysis revealed that the glomerular damage index was lower in the NX+Oxo than the NX group (1.1±0.4 vs. 1.8±0.2, p<0.05), whereas the Sham and

Sham+Oxo groups were completely devoid of glomerular changes (damage index was 0 in both groups).

Table 3. Experimental animal data.

Study I	Sham (n=9-12)	Sham+Oxo (n=12)	NX (n=11-12)	NX+Oxo (n=12)
Systolic BP at week 0 (mmHg)	120±4	121±5	127±5	125±5
Systolic BP at week 9 (mmHg)	134±7	136±5	142±6	152±4*
Body weight at week 0 (g)	339±6	338±7	333±8	332±7
Body weight at week 9 (g)	433±8	412±11	448±10	411±8†
Heart weight/body weight (g/kg)	3.97±0.05	4.12±0.09	4.95±0.27*	5.18±0.33*
Urine volume (ml/24h)	25.2±1.7	25.8±1.8	53.3±3.8*	49.3±3.9*
Study II	Sham (n=10)	Sham+Oxo (n=10)	NX (n=10)	NX+Oxo (n=10)
Systolic BP at week 3 (mmHg)	122±4	122±5	127±5	127±7
Systolic BP at week 12 (mmHg)	139±7	137±6	140±7	149±5
Heart weight/body weight (g/kg)	3.99±0.05	4.17±0.10	5.09±0.30*	5.25±0.39*
Body weight at week 3 (g)	333±5	334±6	327±8	330±7
Body weight at week 12 (g)	416±8	404±9	430±11	409±6
Study III	Sham (n=12)	NX (n=7)	NX+Pari (n=8)	
Rat count at week 27	12	7	8	
Systolic BP at week 15 (mmHg)	135±4	152±5*	155±3*	
Systolic BP at week 27 (mmHg)	130±2	171±4*	167±5*	
Body weight at week 27 (g)	565±8	507±41	503±32	
Heart weight/body weight (g/kg)	3.25±0.04	4.15±0.50*	4.55±0.30*	
Creatinine clearance (ml/min)	1.84±0.11	0.85±0.17*	0.71±0.15*	
Studies IV and V	Sham (n=11)	NX (n=7)	NX+Ca (n=12)	NX+Pi (n=7)
Systolic BP at week 27 (mmHg)	129±2	173±4*	145±3*†	161±4*†‡
Body weight at week 27 (g)	557±7	507±38	488±13*	431±35*
Heart weight/body weight (g/kg)	3.21±0.03	4.19±0.43*	4.03±0.13*	4.46±0.40*
Rat number at week 15	11	12	13	13
Rat number at week 27	11	7*	12†	7*‡
Creatinine clearance (ml/min)	1.84±0.10	0.85±0.15*	0.84±0.07*	0.69±0.17*

Values are mean ± SEM, *P<0.05 compared with the Sham group, $^{\dagger}P$<0.05 compared with the NX group, $^{\ddagger}P$<0.05 versus NX+Ca; BP = blood pressure.

Similarly to study III (Table 3), creatinine clearance was reduced in all NX groups in study IV (Table 4). Plasma ionized calcium did not differ from Sham in the NX group, but was increased in the NX+Ca, and decreased in the NX+Pi group. In comparison with Sham, plasma phosphate and calcium-phosphorus product were over doubled in the NX and three

to fivefold increased in the NX+Pi, but were decreased in the NX+Ca group. Plasma PTH and FGF23 were increased in the NX group and elevated 40 to 60-fold in the NX+Pi group when compared with Sham, while both were suppressed in the NX+Ca group. PRA, $25(OH)D_3$, and $1,25(OH)_2D_3$ levels were decreased in all NX groups. The indices of glomerulosclerosis (Figure 6A) and tubulointerstitial damage (Figure 6B) were increased in all NX groups. However, less tissue damage was seen in the NX+Ca than in the NX and NX+Pi groups. In study V, plasma NOx was increased in all NX groups when compared with Sham. The index of aortic calcification was increased in the NX and NX+Pi groups when compared with the NX+Ca and Sham groups (Figure 6C).

2.2. Urinary determinations

A clear K^+-loss/Na^+-retention -effect was observed in both hyperuricemic groups of study I. Subsequently, urine K^+ to Na^+ ratio was elevated 2-fold in the Sham+Oxo group and 1.6-fold in the NX+Oxo group (Figure 7D). The 24-hour urinary calcium excretion was 1.7-fold increased in the Sham+Oxo group, while no significant changes were observed in the NX groups (Table 4).

Before the oxonic acid diet was initiated in study II, no significant differences were found in the 24-hour urinary excretion of 8-iso-$PGF_{2\alpha}$, a marker of oxidative stress *in vivo* (Figure 7E). During the 9th week on the 2.0% oxonic acid diet, the 24-hour excretion of 8-iso-PGF2α was increased in the NX group, but was reduced by approximately 60% and 90% in the Sham+Oxo and NX+Oxo groups, respectively, when compared with their respective controls (Figure 7F). In study V, urinary NOx was increased in all NX groups when compared with Sham (Table 4).

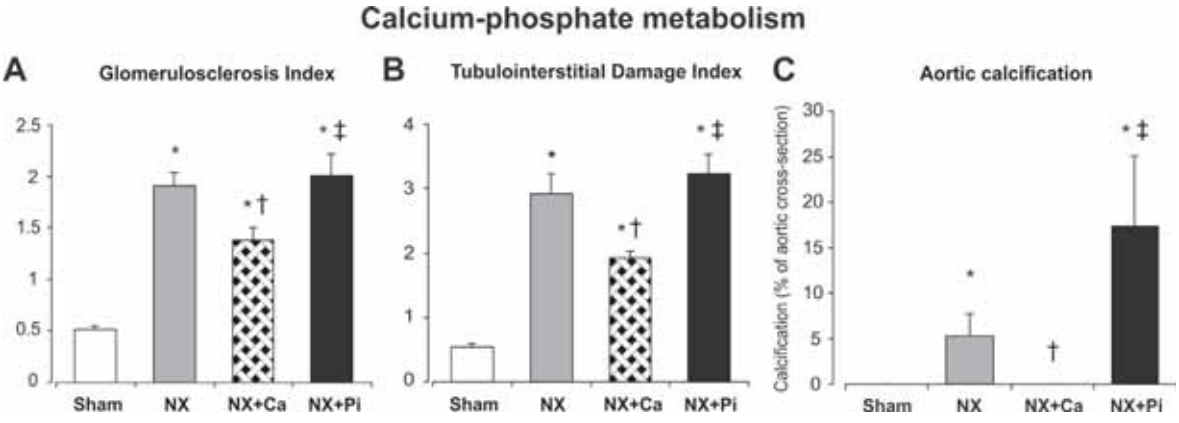

Figure 6. *Kidney glomerulosclerosis index, tubulointerstitial damage index, and aortic calcification.* **P*<0.05 compared with the Sham group, †*P*<0.05 compared with the NX group, ‡*P*<0.05 versus NX+Ca.

Table 4. Blood, plasma, and urine determinations in studies I, II, IV, and IV.

Study I	Sham (n=9-12)	Sham+Oxo (n=12)	NX (n=11-12)	NX+Oxo (n=12)
Blood and plasma determinations				
Uric acid (µmol/l)	36±11	117±21*	63±19	152±19*†
Urea (mmol/l)	6.62±0.34	8.33±0.42	13.54±0.87*	14.54±2.00*
pH	7.42±0.028	7.37±0.023	7.34±0.034*	7.37±0.023
Hemoglobin (g/l)	167.5±3.2	168.5±2.7	157.9±4.7	149.8±4.1*
Potassium (mmol/l)	4.12±0.13	3.79±0.08	4.28±0.19	4.42±0.18
Sodium (mmol/l)	136.5±0.5	137.3±0.6	136.7±0.9	137.0±0.5
Urine determinations				
Potassium (mmol/24h)	2.84±0.14	4.56±0.20*	2.93±0.09	3.73±0.21*†
Sodium (mmol/24h)	8.47±0.41	6.60±0.25*	7.62±0.25	6.44±0.65*
Calcium (µmol/24h)	28.65±4.47	47.45±5.47*	40.03±6.18	34.79±4.38
Study II	Sham (n=10)	Sham+Oxo (n=10)	NX (n=10)	NX+Oxo (n=10)
Blood and plasma determinations				
Uric acid at week 5 (µmol/l)	50.3±13.0	106.8±15.5*	49.1±10.2	86.6±9.6*
Uric acid at week 12 (µmol/l)	37.4±13.4	126.4±24.2*	65.9±23.2	156.6±22.7*†
Creatinine (µmol/l)	37.8±5.8	48.8±3.6	81.6±3.9*	84.1±9.8*
Creatinine clearance (ml/min)	3.0±0.4	2.0±0.2*	1.2±0.1*	1.2±0.1*
Urea (mmol/l)	6.8±0.4	8.6±0.5	13.7±1.0*	15.1±2.4*
TRAP (µmol/l)	422±52	611±70*	491±70	714±60*†
Cholesterol (mmol/l)	2.25±0.10	2.14±0.13	4.80±0.47*	5.09±0.65*
HDL (mmol/l)	1.64±0.09	1.62±0.10	3.55±0.37*	3.50±0.41*
Non-HDL (mmol/l)	0.61±0.03	0.51±0.04	1.25±0.21*	1.59±0.27*
Triglycerides (mmol/l)	1.16±0.11	0.96±0.08	1.46±0.09º	1.77±0.34º
Blood pH	7.44±0.04	7.39±0.03	7.37±0.04	7.41±0.03
Studies IV and V	Sham (n=11)	NX (n=7)	NX+Ca (n=12)	NX+Pi (n=7)
Plasma determinations				
Phosphate (mmol/l)	1.16±0.06	2.52±0.46*	0.81±0.08*†	5.47±1.12*†‡
PTH (pg/ml)	88±12	1172±343*	3.7±0.5*†	3620±236*†‡
Ionized calcium (mmol/l)	1.36±0.06	1.34±0.03	1.55±0.03*†	0.93±0.09*†‡
Calcium-phosphorus product	1.55±0.07	3.51±0.65*	1.11±0.09*†	4.41±0.53*†‡
$25(OH)D_3$ (nmol/l)	33.4±2.8	19.8±4.0*	13.8±0.9*	16.0±1.3*
$1,25(OH)_2D_3$ (pmol/l)	285±27	71±23*	106 ±22*	105±43*
logFGF23 (pg/ml)	2.32±0.05	2.96±0.06*	1.88±0.07*†	3.99±0.18*†‡
NOx (µmol/l)	8.9±0.4	11.4±0.9*	14.2±5.1*	18.4±5.1*
Urinary determinations				
NOx (µmol/24h)	0.03±0.01	1.36±0.66*	1.49±0.84*	0.80±0.36*

TRAP = total peroxyl radical-trapping antioxidant capacity; Values are mean ± SEM, **P*<0.05 compared with the Sham group, †*P*<0.05 versus the NX group, ‡*P*<0.05 versus NX+Ca, º*P*<0.05 NX groups compared with the Sham groups using two-way ANOVA.

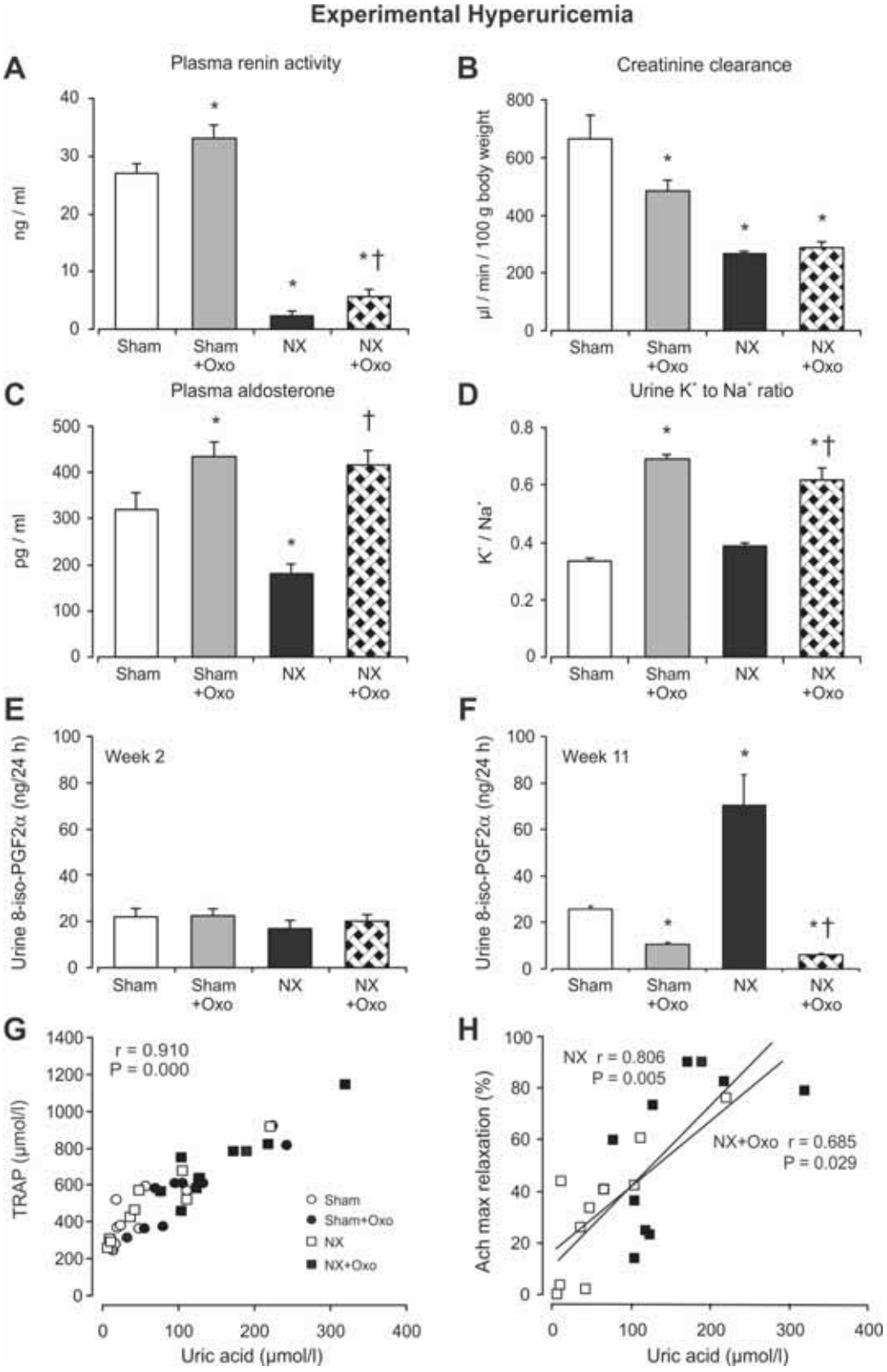

Figure 7. *Plasma and urinary determinations in experimental hyperuricemia.* PRA (I), plasma aldosterone (I), creatinine clearance (I), urinary K^+ to Na^+ ratio (I), urinary 8-iso-$PGF_{2\alpha}$ at weeks 2 and 11 (II), the correlation of plasma TRAP (II) versus plasma uric acid, as well as the correlation between maximum acetylcholine relaxation in carotid artery and plasma uric acid (II) were determined; **P*<0.05 compared with the Sham group, †*P*<0.05 compared with the NX group.

3. AUTORADIOGRAPHY, WESTERN BLOTTING, AND RT-PCR

3.1. Kidney angiotensin-converting enzymes

Protein measurements

When kidney tissue ACE content was analyzed in study I using quantitative *in vitro* autoradiography, which measures binding to the active site of ACE protein, no difference was observed in the NX groups when compared with the Sham rats (Figures 8C). Highest ACE signal was detected in a circular fashion in the inner cortex and outer medulla in the Sham-operated groups, whereas ACE was more widely distributed in the remnant kidneys of the NX groups (Figure 8A).

In study IV, the *in vitro* autoradiography revealed lower kidney ACE protein content in the NX+Ca group in comparison with NX, while ACE was highest in the NX+Pi group (Figure 8D). The distribution of renal ACE was also different between NX and Sham rats; similarly to study I, the highest ACE signal was detected in a circular fashion in the inner cortex and outer medulla in Sham rats, whereas ACE was more widely distributed throughout the remnant kidney in the NX and NX+Pi groups (Figure 8B). The outcome of Western blotting confirmed lower renal ACE protein in the NX+Ca than the NX group, and increased ACE protein in the NX and NX+Pi groups versus Sham (Figure 9E).

PCR measurements

In study I, when kidney ACE mRNA was determined using real-time quantitative RT-PCR both NX groups showed significantly lower levels than the respective Sham rats (Figure 9A). In addition, kidney tissue ACE2 mRNA levels were also lower in both NX groups than in the Sham rats (Figure 9B). In study III, the level of ACE mRNA was increased and ACE2 mRNA decreased in NX and NX+Pari rats versus Sham (Table 5).

RT-PCR analyses in study IV showed increased renal ACE mRNA content in the NX and NX+Pi groups, but not in NX+Ca rats, when compared with Sham. Highest values were seen in NX+Pi rats, as ACE mRNA was almost 2.5-fold higher than in NX+Ca and Sham rats (Figure 9C). The amount of ACE mRNA correlated well with ACE protein determined using autoradiography (Figure 9F; $r=0.830$; $P<0.001$) and Western blotting (0.787; $P<0.001$). Positive correlations ($P<0.001$) were also observed between ACE mRNA and calcium-phosphate product ($r=0.825$), phosphate ($r=0.771$), PTH ($r=0.766$),

FGF23 (r=0.670), and ionized calcium (r=0.659). Kidney ACE2 mRNA was decreased in all NX groups (Figure 9D).

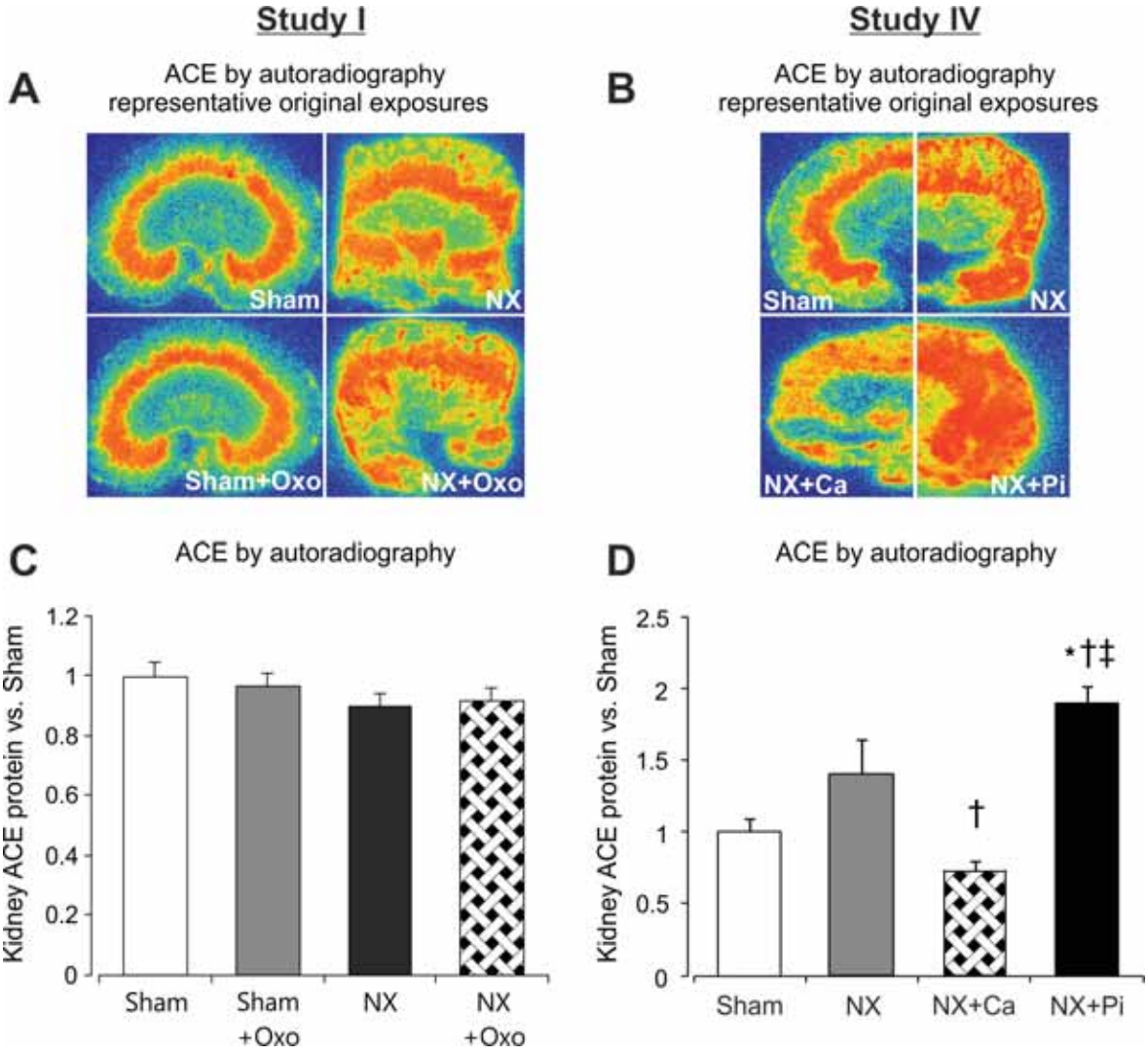

Figure 8. *Autoradiography measurement of kidney angiotensin-converting enzyme in vitro.* Kidney ACE autoradiography in studies I and IV. In panels A and B, ACE signal (red coloring) is located mainly in the inner cortex and outer medulla of kidney tissue; **P*<0.05 compared with the Sham group, †*P*<0.05 compared with the NX group, ‡*P*<0.05 versus NX+Ca.

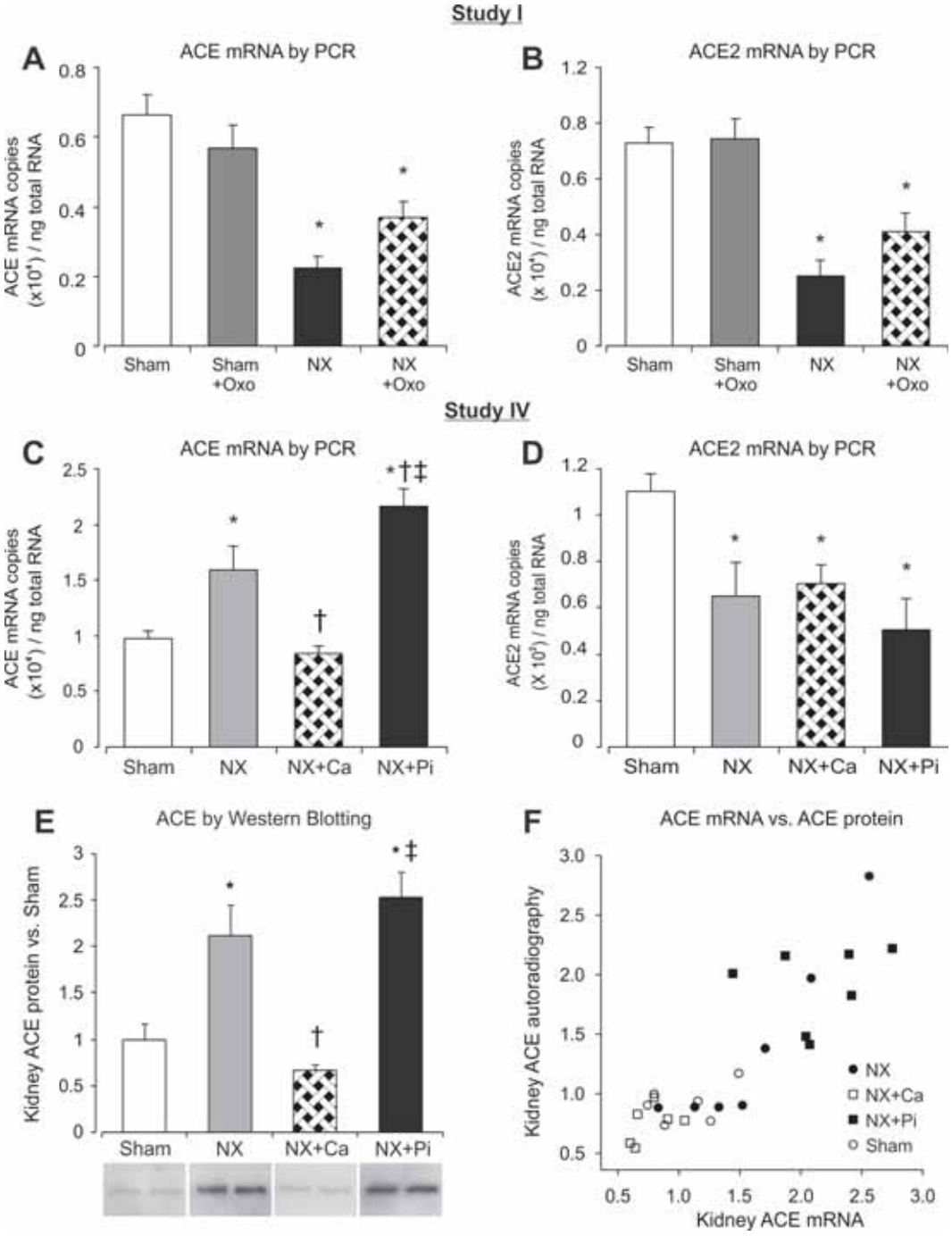

Figure 9. *Angiotensin-converting enzymes in studies I and IV.* Kidney ACE and ACE2 mRNA were determined using RT-PCR, and kidney ACE protein using Western blotting. Panel F shows the correlation between ACE mRNA and ACE protein by autoradiography in study IV; **P*<0.05 compared with the Sham group, †*P*<0.05 compared with the NX group, ‡*P*<0.05 versus NX+Ca.

3.2. Aortic and cardiac angiotensin-converting enzymes

In a 12-week pilot of study V, autoradiography results of randomly selected 8-10 rats in each group showed a decrease in aortic and cardiac ACE protein content after 8 weeks of

phosphate-binding diet (Figures 10A and 10B). In the 27-week study V, aortic ACE protein content was higher in the NX and NX+Pi groups than in Sham rats (Figures 10C and 10D). Notably, aortic ACE content was clearly lower in the NX+Ca group when compared with the NX and NX+Pi groups.

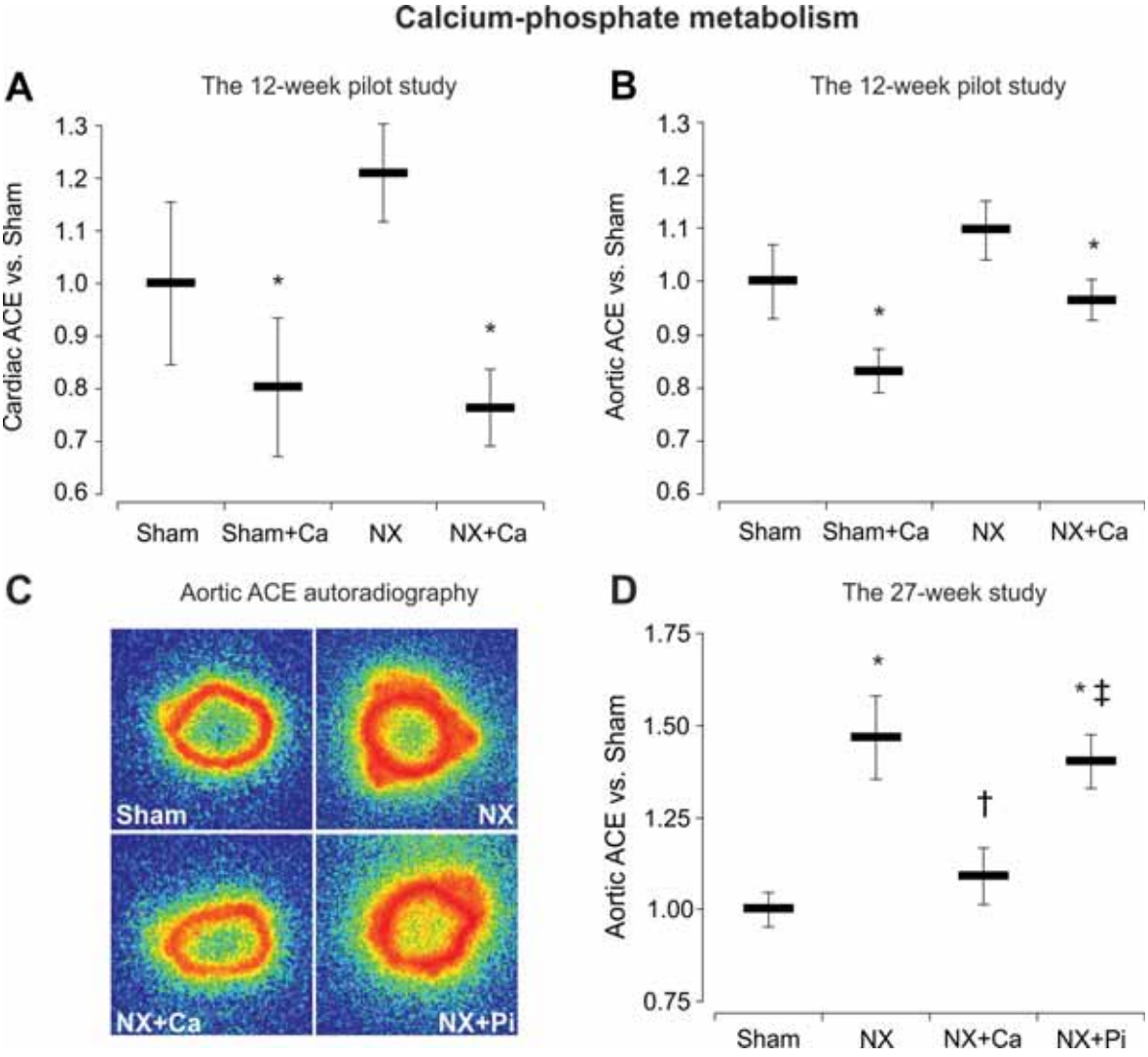

Figure 10. *Cardiac and aortic angiotensin-converting enzyme in study V.* Cardiac ACE was solely determined in the shorter 12-week pilot study. Aortic ACE was determined in both the 12-week and 27-week studies; **P*<0.05 compared with the Sham group, †*P*<0.05 compared with the NX group, ‡*P*<0.05 versus NX+Ca.

3.3. Renin-angiotensin system receptors

Protein measurements

When analyzed using autoradiography in study I, AT_{1R} densities in kidney cortex did not differ from Sham in the NX groups. However, cortical AT_{1R} density was approximately

25% higher in the NX+Oxo than NX rats (Figure 11A). In renal medulla, no difference in AT_{1R} density between the two NX groups was observed, while the density was about 43% higher in the NX+Oxo group when compared to Sham rats (Figure 11B). The Sham+Oxo rats featured no changes in renal AT_{1R} density. In all groups, AT_{1R} density in the kidney medulla was higher than in the cortex. In addition, the ratio of medullary to cortical AT_{1R} density was increased in both NX groups, the ratios being 2.27±0.08, 2.00±0.15, 3.25±0.34*, 3.04±0.24* in the Sham, Sham+Oxo, NX and NX+Oxo groups, respectively (*$P<0.02$ both NX groups vs. both Sham groups). AT_{2R} densities in cortex and medulla were similar in all study groups (not shown), and the AT_{2R} binding comprised only 1.2-2.1% of all Ang II receptor binding in the cortex, and 0.7-1.2% of all binding in the medulla.

In autoradiography analyses of study IV, AT_{1R} density in kidney cortex was lower in the NX+Ca and higher in the NX+Pi group versus Sham, while no significant differences in AT_{1R} density in the medulla were found (Table 5). In autoradiography analyses the proportion of AT_{2R} was low when compared with AT_{1R} (0.3-0.6% in cortex, 0.1-0.4% in medulla), and no significant differences in AT_{2R} density (not shown) were found between the groups.

PCR measurements

In study I, hyperuricemia had no effect on kidney tissue AT_{1aR} mRNA content, the levels of which were significantly lower in both NX groups than in Sham rats (Figure 11C). Kidney tissue AT_{2R} mRNA level was also lower in the NX group than in the Sham rats, and was not significantly affected by hyperuricemia (Figure 11D).

At the end of study III, the mRNA values of AT_{1aR}, AT_{2R}, and PRR were decreased in NX and NX+Pari groups when compared with sham-operated rats (Table 5). AT_{4R} mRNA was increased, while Mas mRNA was unaffected. However, no suppression of RAS genes between untreated and paricalcitol-treated NX rats was observed at the mRNA level. Due to high mortality, the final animal numbers at the end of the 27-week experiment were 10, 7, and 8, in the Sham, NX, and NX+Pari groups, respectively.

In study IV, kidney AT_{1aR} mRNA content was lower in the NX+Pi group versus Sham and NX+Ca groups, while no other differences were seen between the groups (Figure 11E). Kidney AT_{2R} mRNA content was decreased in the NX group in comparison with Sham (Figure 11F). Kidney AT_{4R} mRNA (Figure 12A) was increased and PRR mRNA

(Figure 12B) decreased in the NX and NX+Pi groups versus Sham, while the NX+Ca rats did not differ from Sham. Kidney Mas mRNA showed no significant differences between the groups (Table 5).

Table 5. The renin-angiotensin system determinations in studies III, IV, and V.

Study III	Sham (n=12)	NX (n=7)	NX+Pari (n=8)	
Kidney autoradiography				
Cortical AT_{1R} (vs. Sham)	1.00±0.06	1.18±0.05	1.05±0.08	
Medullary AT_{1R} (vs. Sham)	1.00±0.10	1.14±0.07	1.00±0.08	
Cortical AT_{2R} share (%)	0.27±0.16	0.37±0.30	0.40±0.18	
Medullary AT_{2R} share (%)	0.40±0.17	0.17±0.10	0.12±0.05	
ACE (vs. Sham)	1.00±0.09	1.39±0.26	1.68±0.17*	
CTGF	0.67±0.12	2.50±0.20*	1.89±0.29*	
Kidney mRNA				
AT_{1aR} ($x10^4$ / ng total RNA)	0.99±0.04	0.83±0.08*	0.80±0.05*	
AT_{2R} ($x10^2$ / ng total RNA)	0.76±0.15	0.32±0.06*	0.19±0.03*	
AT_4 ($x10^3$ / ng total RNA)	2.99±0.21	3.76±0.28*	3.90±0.24*	
PRR ($x10^4$ / ng total RNA)	2.31±0.15	1.77±0.11*	1.74±0.08*	
MAS ($x10^2$ / ng total RNA)	4.80±0.34	4.92±0.48	4.77±0.41	
ACE ($x10^4$ / ng total RNA)	0.98±0.68	1.72±0.21*	2.06±0.20*	
ACE2 ($x10^4$ / ng total RNA)	1.10±0.08	0.65±0.14*	0.49±0.09*	
CTGF ($x10^4$ / ng total RNA)	1.74±0.11	2.76±0.49*	2.84±0.19*	
Plasma renin activity	24.3±3.0	1.7±1.0*	1.4±0.7*	
Studies IV and V	Sham (n=11)	NX (n=7)	NX+Ca (n=12)	NX+Pi (n=7)
Plasma renin activity (ng of Ang I/ml/h)	22.0±2.9	1.7±1.0*	1.7±0.6*	1.8±0.6*
Kidney AT_{1R} autoradiography (vs. Sham)				
AT_{1R} in cortex	1.00±0.06	1.18±0.05*	0.78±0.03*†	1.21±0.10*‡
AT_{1R} in medulla	1.00±0.11	1.14±0.07	1.04±0.07	1.24±0.07
Mas mRNA (copies x 10^2 / ng total RNA)	4.80±0.34	4.92±0.48	5.06±0.68	5.13±0.32

Values are mean ± SEM, n=7-13 for all groups; *P<0.05 compared with the Sham group, $^{\dagger}P$<0.05 compared with the NX group, $^{\ddagger}P$<0.05 versus NX+Ca.

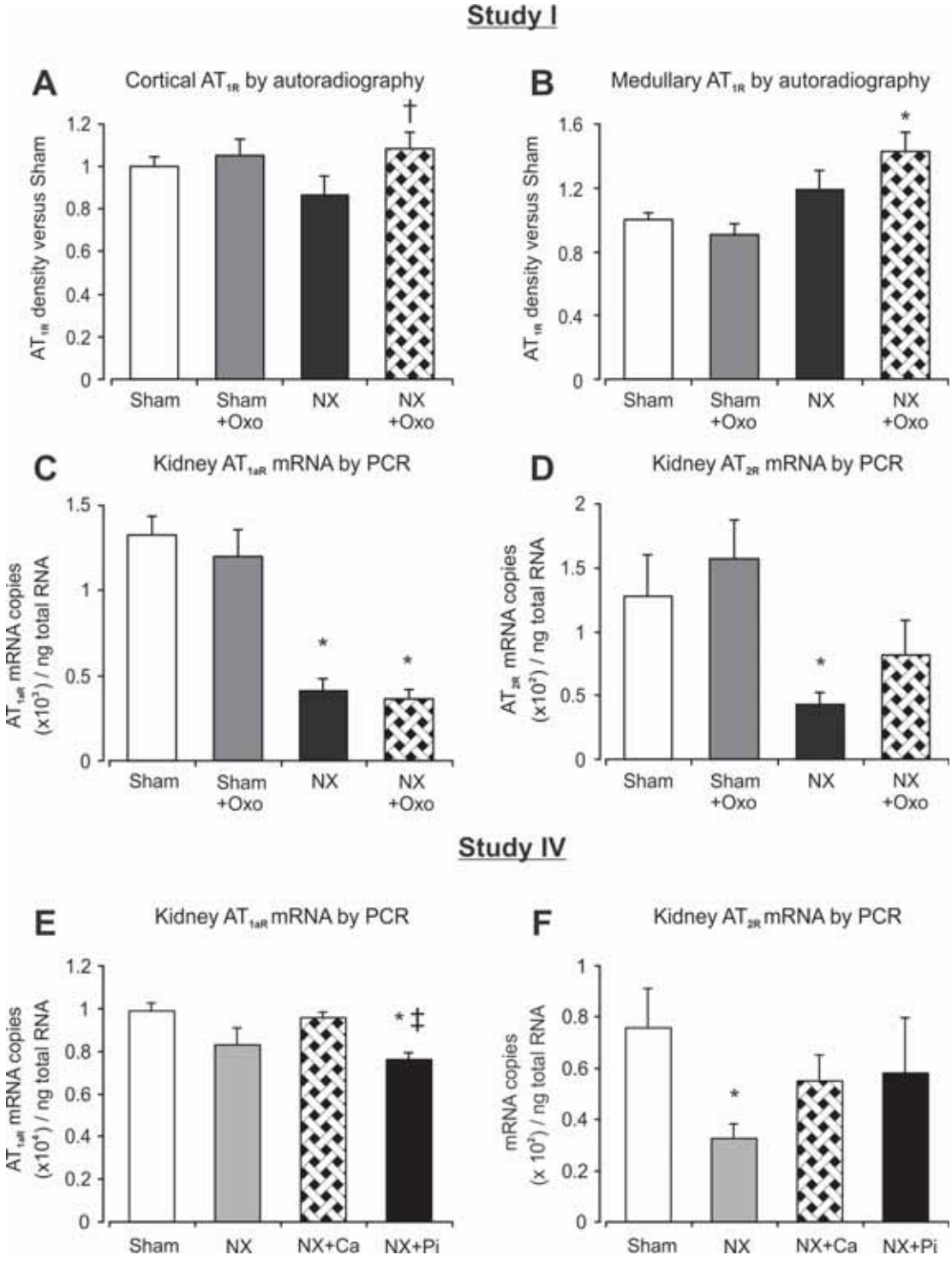

Figure 11. *Angiotensin II type 1 and type 2 receptor determinations.* AT_{1R} and AT_{2R} densities were determined from kidney cortex and medulla using *in vitro* autoradiography in study I. AT_{1aR} and AT_{2R} mRNA levels were determined by RT-PCR in studies I and IV; **P*<0.05 compared with the Sham group, †*P*<0.05 compared with the NX group, ‡*P*<0.05 versus NX+Ca.

3.4. Other measured proteins and mRNAs

In study III, renal CTGF mRNA was elevated in NX and NX+Pari rats versus sham-operated rats (Table 5). Similarly in study IV, renal CTGF mRNA was higher in NX and NX+Pi groups versus Sham rats, and also increased in NX+Pi rats versus NX+Ca rats (Figure 12C). Kidney HO-1 mRNA was up-regulated in all NX groups versus Sham (Figure 12D).

At the end of study V, aortic eNOS protein content, determined using Western blotting, was similarly decreased in all NX groups when compared with Sham rats (Figure 12E). However, no difference was detected in aortic iNOS protein (not shown) between the study groups, with average values ranging ±18% of the level observed in Sham rats. Aortic nitrated protein content, measured using Western blotting, was higher in the NX and NX+Pi groups versus Sham, but was lower in the NX+Ca than in NX and NX+Pi rats (Figure 12F).

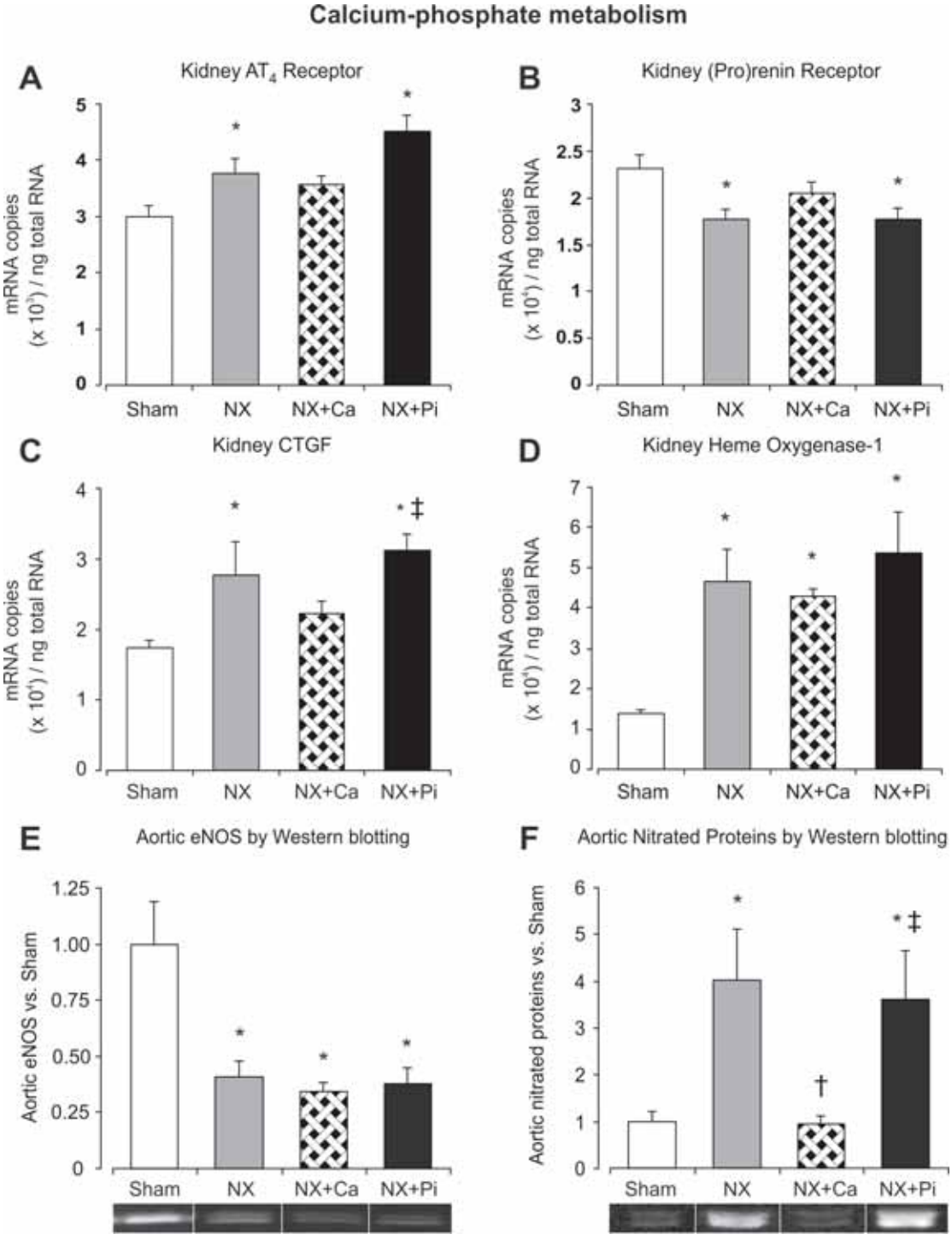

Figure 12. *Kidney AT_{4R}, (pro)renin receptor, CTGF, and heme oxygenase-1 mRNA by RT-PCR, and aortic eNOS and nitrated proteins by Western blotting.* Kidney AT_{4R}, (pro)renin receptor, CTGF, and heme oxygenase-1 mRNA were determined using RT-PCR in study IV. Aortic eNOS and nitrated protein content were determined using Western blotting in study V; **P*<0.05 compared with the Sham group, †*P*<0.05 compared with the NX group, ‡*P*<0.05 versus NX+Ca.

4. FUNCTIONAL RESPONSES OF ISOLATED ARTERIAL RINGS

4.1. Carotid artery responses *in vitro*

In study II, the carotid artery contractile responses to NE were similar between the study groups (Figure 13A and 13B). Thus, differences in vasoconstrictor sensitivity cannot explain the differences in vasorelaxations. The relaxations to Ach were reduced in NX rats when compared with Sham rats, while the maximal response to Ach was improved in the NX+Oxo group when compared with the NX group (Figure 12C; P=0.027). Hyperuricemia had no effect on the response to Ach in Sham rats. In both NX and NX+Oxo groups, plasma UA concentration correlated with the maximal relaxation to Ach (Figure 7H), while no correlation was observed between maximal Ach response and plasma levels of creatinine, urea, lipids or BP (not shown). Plasma TRAP also correlated with maximal Ach response in NX rats (r=0.73, P=0.026).

The NOS inhibitor L-NAME practically abolished the relaxation to Ach in all groups (Figure 13D), indicating that the response was mediated via NO. Vasorelaxation induced by isoprenaline was similar in all groups (Figure 13E). The relaxations to nitroprusside were reduced in both NX groups vs. Sham groups, while the reduction was less marked in the NX+Oxo group (Figure 13F). Higher relaxation to 10 nmol/l nitroprusside was detected in the NX+Oxo group when compared with the NX group (P=0.027).

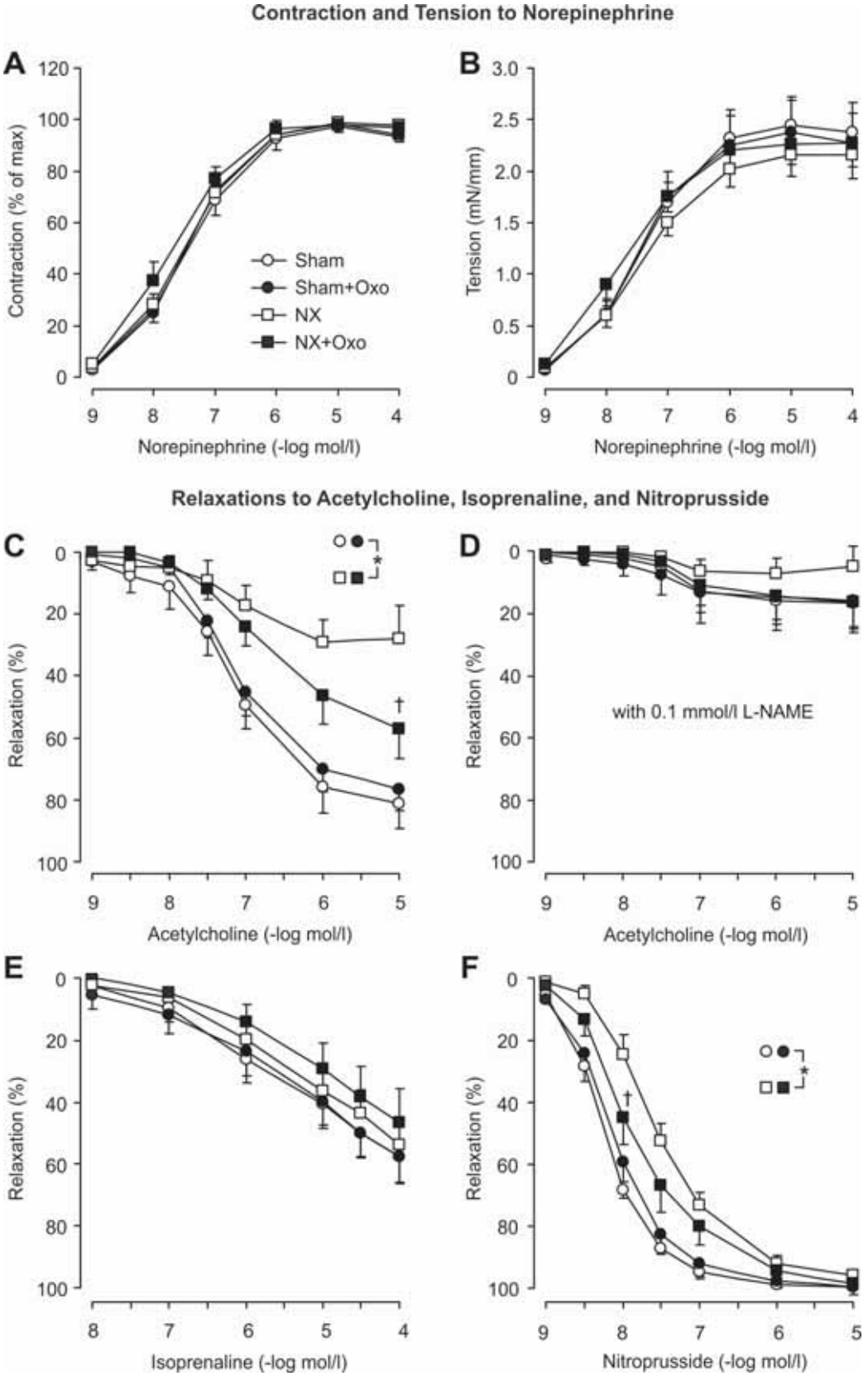

Figure 13. *Carotid artery in vitro.* Responses of carotid artery rings to norepinephrine (noradrenaline), acetylcholine (with and without L-NAME), isoprenaline, and nitroprusside were studied in study II; **P*<0.05, ANOVA for repeated measurements, †*P*<0.05 compared with the corresponding individual concentration in the NX group.

4.2. Mesenteric artery responses *in vitro*

In study V, vasorelaxation to the NO donor nitroprusside in endothelium-denuded rings was slightly decreased in the NX+Pi group when compared with Sham and NX+Ca rats, but did not differ between the Sham, NX and NX+Ca groups (Figure 14A). The relaxations induced by Ach in NE-precontracted endothelium-intact mesenteric artery rings were impaired in the NX and NX+Pi groups, but did not differ from Sham in the NX+Ca group (Figure 14B). The NOS inhibitor L-NAME reduced the relaxations to Ach in all study groups (Figure 14C), but the effect was more pronounced in the NX+Ca than the NX and NX+Pi groups, as the Ach response no more differed between the NX groups in the presence of L-NAME. The change in the AUC of the Ach-response induced by L-NAME suggested that the contribution of NO to the relaxation was reduced in the NX and NX+Pi groups, but did not differ from Sham in the NX+Ca group (Figure 14D). The addition of exogenous L-arginine (1 mmol/l) *in vitro* had no significant effects on the Ach-induced relaxations (data not shown).

Vasoconstrictor sensitivity and maximal responses of mesenteric arterial rings to NE did not differ between the Sham, NX and NX+Ca groups, while sensitivity to NE was slightly higher in the NX+Pi than Sham and NX+Ca groups, and maximal response was lower in the NX+Pi than Sham group (Table 6). The sensitivity and maximal responses to KCl did not significantly differ between the study groups. Vasoconstrictor sensitivity to Ang II was lower in the NX+Ca than Sham group, while maximal wall tension in response to Ang II was higher in the NX versus Sham group, and lower in the NX+Ca versus NX group.

Table 6. Contractile responses of isolated mesenteric arterial rings in study V.

Study V	Sham (n=11)	NX (n=7)	NX+Ca (n=12)	NX+Pi (n=7)
Norepinephrine (+E)				
pD_2 (-log mol/L)	6.45±0.11	6.73±0.11	6.44±0.07	6.98±0.20*‡
Maximal wall tension (mN/mm)	5.46±0.32	4.56±0.38	5.25±0.36	4.15±0.49*
Angiotensin II (+E)				
pD_2 (-log mol/L)	8.21±0.09	7.99±0.07	7.92±0.13*	8.12±0.10
Maximal wall tension (mN/mm)	0.50±0.12	0.97±0.18*	0.46±0.12†	0.63±0.11
Potassium Chloride (-E)				
pD_2 (-log mol/L)	1.54±0.01	1.55±0.02	1.55±0.02	1.58±0.02
Maximal wall tension (mN/mm)	4.89±0.37	4.79±0.42	5.42±0.48	3.70±0.59

Values are mean±SEM; +E and -E, endothelium-intact and -denuded arterial rings respectively; pD_2, negative logarithm of concentration of agonist producing 50% of maximal contractile force; *P<0.05 versus Sham, †P<0.05 versus NX, ‡P<0.05 versus NX+Ca.

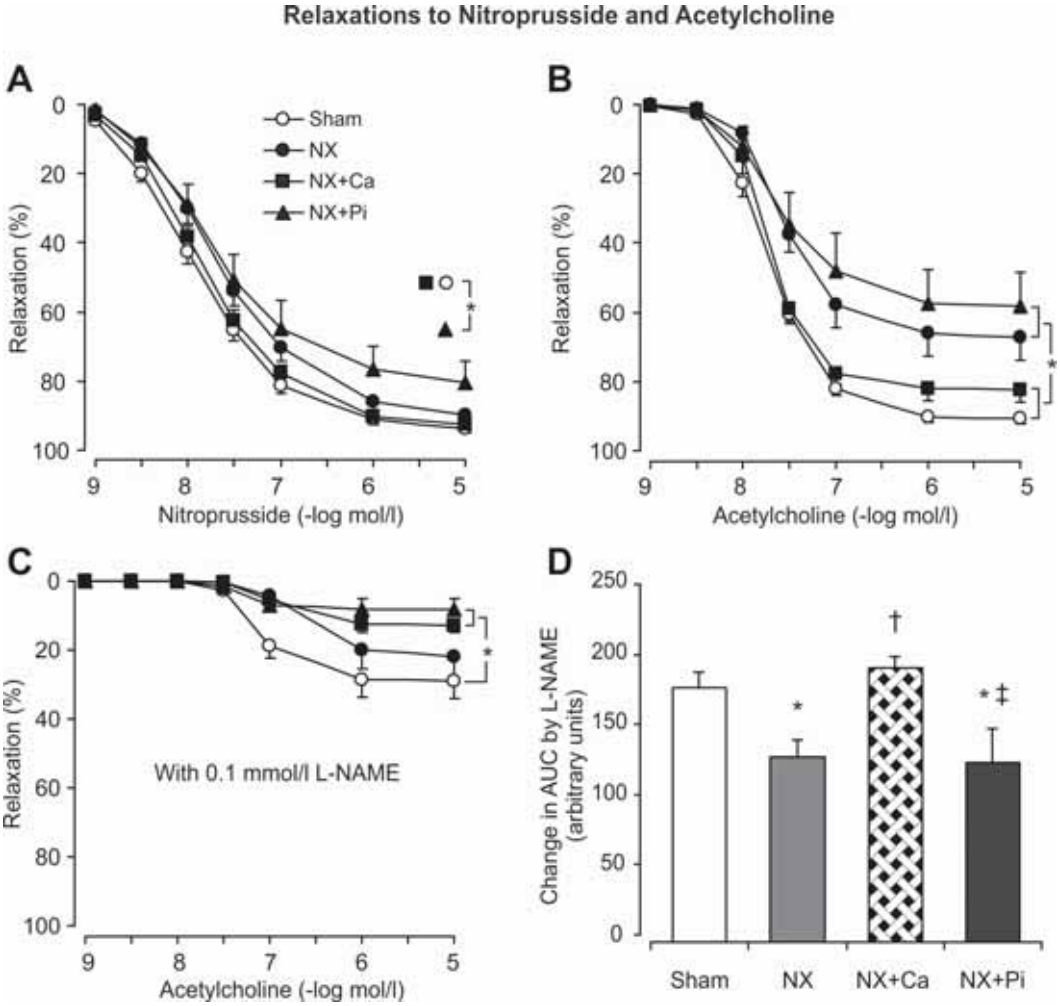

Figure 14. *Mesenteric artery in vitro.* Responses of mesenteric artery rings to nitroprusside and acetylcholine were studied in study V; *P<0.05, ANOVA for repeated measurements (A, B, C), *P<0.05 versus Sham, †P<0.05 versus NX, ‡P<0.05 versus NX+Ca (D).

DISCUSSION

1. STUDY DESIGN AND METHODS

In addition to the loss of renal function, CKD is linked to several disturbances of the normal homeostasis. Progressing kidney damage may alter cardiovascular physiology and lead to inflammation, arterial remodeling and elevated BP, as well as increase the damaging oxidative stress. This is the principal reason why CKD cannot simply be regarded as a disease of the kidney, but a syndrome that enacts on the whole body.

Experimental animal models provide a means to study disorders that cannot be otherwise investigated. The present series of studies featured a rat model of experimental CRI, the NX, which was induced by the removal of upper and lower poles of the left kidney, and the whole right kidney (Jolma et al. 2003, Kööbi et al. 2003). The sham rats underwent decapsulation of both kidneys. Animal models of CRI approximate the human disease and are essential to understanding its pathogenesis, as well as developing successful treatment strategies. While not perfect, the careful use of animal experiments offers the opportunity to examine individual mechanisms in an accelerated time frame (Becker and Hewitson 2013).

Dietary and pharmacological interventions in these studies included 2.0% oxonic acid-induced hyperuricemia **(I, II)**, paricalcitol treatment **(III)**, and phosphate loading or phosphate binding with 3.0% calcium carbonate **(IV, V)**. The studies were designed to mimic some of the most common complications associated with kidney disease.

1.1. Experimental models

Experimental chronic renal insufficiency

In all of the studies, characteristic findings of decreased renal function (Pörsti et al. 2004) were observed in the NX rats. As the best indicator of successful CRI, creatinine clearance of all NX rats was reduced (Figure 7, Tables 3 and 4). The shorter study duration, 12 weeks of CRI **(I, II)**, did not unearth a significant BP elevation in the NX rats on the normal diet, however, in all 27-week studies systolic BP was clearly elevated in these rats **(III-V)**. Longer study durations in previous studies have shown that after a follow-up of 20 weeks, the NX rats develop clear hypertension, so that systolic BP is elevated by 30 mmHg (Kööbi et al. 2006). The NX rats also develop polyuria, and here they exhibited a twofold

increase in 24-hour urine volume (Table 3) **(I)**. Increased volume diuresis and the subsequent kaliuresis (Gennari 1998) are the likely explanations for the absence of hyperkalemia in the NX. The observed increase in heart weight/body weight ratios of all NX rats is in agreement with the view that this model is characterized by volume overload (Kööbi et al. 2003) **(I-V)**.

Many experimental models of CRI are available and they all have their own specific characteristics (Becker and Hewitson 2013). The NX is characterized by low renin secretion from the remnant kidney. This inherently decreases PRA, which leads to effects in several other down-stream factors of regulation. One of the high-renin models of experimental CRI is unilateral ureteral obstruction, which is usually used for the studies on tubulointerstitial fibrosis (Yang et al. 2010). In comparison to the NX, unilateral ureteral obstruction is more easily reproduced without fatalities from surgery complications, progresses in a shorter time-course, and maintains the contralateral kidney as a control. However, the disadvantages include a normal serum creatinine level and the lack of proteinuria because the injured kidney is completely obstructed and therefore has no urine output. As a final point, the model does not induce hypertension (Yang et al. 2010).

The subtotal nephrectomy can also be induced by ligation in which branches of the renal artery in the rat are ligated after contralateral uninephrectomy. This model is typically associated with a more severe proteinuria and hypertension than the NX, and features a high level of PRA. The more severe hypertension with ligation is likely due to the notable up-regulation of the RAS near the infarcted tissue areas (Ma et al. 2005, Yang et al. 2010). For the present series of studies, the NX model proved to be appropriate and showed a reproducible loss of creatinine clearance and a steady progression of kidney disease **(I-V)**.

Oxonic acid-induced hyperuricemia

The oxonic acid diet induces hyperuricemia by inhibiting the hepatic uricase enzyme (Mazzali et al. 2001, Kang et al. 2002, Nakagawa et al. 2003, Sanchez-Lozada et al. 2005). Previous studies with 2.0% oxonic acid in rats have demonstrated a 1.3 to 2.8-fold rise in serum UA (Mazzali et al. 2001, Nakagawa et al. 2003, Sanchez-Lozada et al. 2005), which corresponds well to the 2.4 to 3.4-fold increase observed in these studies (Table 4) **(I, II)**. Treatment of hyperuricemia was not included in the present study protocol, as allopurinol and uricosuric agents have been repeatedly shown to prevent the pathological and pathophysiological changes induced by the oxonic acid feeding (Mazzali et al. 2001, Kang

et al. 2002, Mazzali et al. 2002, Sanchez-Lozada et al. 2002, Nakagawa et al. 2003, Sanchez-Lozada et al. 2005). Corresponding to previous findings showing preglomerular arterial disease after oxonic acid diet (Johnson et al. 2002), we found that hyperuricemia decreased creatinine clearance in the Sham rats (Figure 7, Table 4) **(I, II)**. It should be noted that hyperuricemia is also associated with decreased renal blood flow in man (Messerli et al. 1980). However, experimental hyperuricemia did not further reduce creatinine clearance in NX rats, suggesting that this form of hyperuricemia is not associated with reduced GFR in the present model of CKD **(I, II)**. An explanation may be the higher PRA values in Sham rats resulting in higher Ang II, which is the major modulator of glomerular blood flow and GFR. Experimental hyperuricemia did not influence 24-hour urine volume (Table 3), but increased urinary K^+ excretion (Table 4) **(I)**.

The NX+Oxo rats of study I presented with elevated BP after 9 weeks of diet, which probably resulted from the hyperuricemia-associated sodium retention. Such an effect was not observed in study II, however. Sodium sensitivity is considered a characteristic feature in hyperuricemia (Ward 1998). Hyperuricemia did not have an effect on heart weight **(I, II)**.

The present model of experimental hyperuricemia was effortless to produce via dietary intervention, and presented with successful hyperuricemia. Although the observed plasma UA values were lower than those generally observed in hyperuricemic patients, mainly due to dietary lack of excess purines and fructose (Johnson et al. 2013b), this model is a valuable tool in the effort to find evidence on the putative harmfulness of elevated UA.

Paricalcitol treatment

The treatment with paricalcitol (intraperitoneal injections, 200 ng/kg three times per week) was aimed to test its effects on the kidney RAS component genes **(III)**. Pharmacological treatment model is very similar to dietary interventions, however, the drug was injected, which produces extra stress to the animals when compared to dietary interventions. The advantage in this situation is the exact dosing, which may be more difficult to reproduce with similar precision using orally administered drug models in rats. In study III, paricalcitol did not influence the RAS component genes in the kidney, but there were no technical complications with this model in the present study that would render the outcome unreliable.

Calcium-phosphate metabolism

The dietary intervention to alter calcium-phosphate metabolism **(IV, V)** was carried out using phosphate loading with 1.5% dietary phosphate or phosphate binding with 3.0% calcium carbonate, both of which induced clear changes in all variables of the calcium-phosphate metabolism. Indeed, plasma phosphate, PTH, and FGF23 levels were different in all study groups (Table 4). The phosphate-loading and phosphate-binding diets had opposite influences on plasma calcium concentration. The observed changes in kidney tissue RAS components may have resulted from changes in all of the above variables. In general, when phosphate balance is altered this will always be reflected on calcium metabolism, and it is difficult to make the distinction which one of these two was the key player modulating renal tissue RAS components. However, the pathogenic influence of excess phosphate is increasingly recognized, and recent clinical evidence has linked high dietary phosphate intake to increased carotid intima-media thickness even in the general population (Itkonen et al. 2013). Dietary models are generally preferable to invasive approaches due to lower stress on the animals. Accordingly, this model was very easy to reproduce and functioned as expected.

1.2. Measurement methods

The measurement methods used in the present studies were found to be consistent and reproducible in the analysis of the underlying hypotheses. No significant problems were encountered during the experiments or laboratory determinations. The RIA determinations produced results that aligned well with the earlier observations in experimental hyperuricemia **(I, II)** (Ramsay et al. 1975, Mazzali et al. 2001). Taken together, the general reliability of the present results appears to be high, even though some alterations were observed between the determinations of the RAS components at the protein level versus the mRNA level. It is well known that wide-ranging post-transcriptional modulation may alter the ratios of mRNA to the final protein product (Gingold and Pilpel 2011), and thus knowledge of both levels is pivotal in determination of gene expression.

In vitro autoradiography

The *in vitro* autoradiography provides data on the localization and quantity of the assayed proteins in a histological sample. Generally, its shortcoming is the same as with any other histology-based assay, as the sample fixing procedure may sometimes cause interfering artefacts, which hamper the reliability of the obtained results. In this series of studies, no

artefact-causing fixatives were used, as the samples were cut frozen, thaw mounted, and then desiccated **(I, IV, V)**. It can be speculated how well the 20 µm thick sections of the kidney tissue represented the whole kidney. Nevertheless, altogether 24 analyses per each kidney were performed, and this approach certainly increased the dependability of the present autoradiography results.

Real-time quantitative RT-PCR

The real-time quantitative RT-PCR is a reliable method of determining gene transcription activity levels via amplification of the gene transcript. In regular real-time PCR the amount of product formed is monitored during the course of the reaction by monitoring the fluorescence of dyes or probes introduced into the reaction that is proportional to the amount of product formed, while the number of amplification cycles required to obtain a particular amount of DNA molecules is registered. When certain amplification efficiency is assumed, it is possible to calculate the number of DNA molecules of the amplified sequence that were initially present in the sample (Kubista et al. 2006). In the real-time RT-PCR, RNA is first isolated and reverse-transcribed using random hexamers as primers to form cDNA. The resulting cDNA is then assayed as in regular real-time PCR. While the real-time quantitative RT-PCR is not without limitations, it can provide unmatched sensitivity and speed for determining levels of specific transcripts when using proper controls, careful initial reaction characterization, and quality control (Wagner 2013). The quality analyses of RT-PCR measurements in this study were constant, and the intra-assay and inter-assay coefficients of variance were under 1.2% and 2.8%, respectively **(I, III, IV)**.

As the determination of the exact original macroscopic source of the extracted RNA in tissue samples is not possible, the obtained result is presumed to represent the mean transcriptional level of the whole cell population. However, in theory, a marginal number of cells with thousands of times higher or lower transcription levels may shift the result, and subsequently the outcome may indicate a higher or lower overall transcription level in the tissue. This makes RT-PCR determinations using tissue samples challenging, and therefore the method should optimally be used in combination with another method that provides information about the quantity and macroscopic localization of the gene product. Therefore, the combination of autoradiography and RT-PCR was able to reveal a better-focused snapshot of the gene expression activity.

Western blotting

Western blotting is commonly used to identify, quantify, and determine the molecular size of specific proteins. It evolved from Southern blotting, which is used to detect specific DNA sequences among DNA fragments separated by gel electrophoresis, and northern blotting, which is used to detect and quantify RNA and to determine its size (Jensen 2012). In this series of studies Western blotting was used to offer another means of protein quantification together with autoradiography **(IV, V)**. The quantification was semi-quantitative, as absolute quantification using only densitometric values is not achievable (Gassmann et al. 2009). Computerized image analysis was used to measure antibody binding, which provides higher sensitivity compared to earlier methods. The present Western blotting measurements were uncomplicated and reliable, however, the conditions need to be observed and well optimized to specifically suit the measured protein (MacPhee 2010).

In vitro vascular function

The *in vitro* vascular function measurements provide a technique to assay the contractile force of various vascular tissues. Optimally it produces highly reliable results, but care needs to be taken when preparing samples for measurement. Delicate handling ensures that the endothelial and smooth muscle layers remain intact and functional, while nonfunctional samples can be identified by hindered responses. In this series of studies, carotid **(II)** and mesenteric arteries **(V)** were measured. Both yielded consistent data for further analysis, while the differing effects of the used experimental treatments were also clearly noticeable in both vessels.

2. RESULTS AND FINDINGS

2.1. The renin-angiotensin-aldosterone system components

The circulating RAAS and the tissue-level RAS have generated a wealth of scientific interest in the recent years (Fyhrquist and Saijonmaa 2008, Nguyen Dinh Cat and Touyz 2011, Simoes e Silva and Flynn 2012, Simoes e Silva et al. 2013). This can well be understood, as they have traditionally been regarded as major regulators of various cardiovascular processes, while today these systems are known to regulate even the intracellular processes of diminutive systemic importance (Nguyen Dinh Cat and Touyz

2011). This virtually means that the effects of the RAAS and the various local RASs can be observed throughout the body.

As experimental hyperuricemia has been associated with increased number of renin-positive cells in the juxtaglomerular apparatus (Mazzali et al. 2001, Johnson et al. 2003), the circulating RAAS and renal components of RAS were investigated **(I)**. Immunohistochemical staining of renin-positive cells has been previously used as a marker of the tissue-level renin expression (Mazzali et al. 2001), but knowledge of circulating PRA in hyperuricemia has remained scarce. Experimental models of hyperuricemia are characterized by preglomerular arteriolar disease, leading to tubular ischemia and local vasoconstriction. As the severity of the arteriolar disease varies between nephrons, some nephrons will be underperfused and ischemic, whereas others may be overperfused. This leads to heterogeneity in renin expression and a failure to suppress renin release for the degree of sodium intake, resulting in sodium sensitivity (Sealey et al. 1988, Johnson et al. 2005b). Because of the putative nephron heterogeneity, we chose to measure PRA instead of renin staining to examine possible changes in the renin status during hyperuricemia **(I)**.

While the NX rat is a low renin CRI model (Pörsti et al. 2004), clear increases in PRA were observed in both Sham and NX rats after the oxonic acid diet (Figure 7) **(I)**. This corresponds well with the results of previous clinical studies suggesting a correlation between hyperuricemia and elevated PRA (Saito et al. 1978b, Gruskin 1985). The finding that plasma aldosterone/renin ratio was not affected by oxonic acid feeding suggests that increased PRA was the probable explanation for the observed increase of plasma aldosterone in NX rats. High circulating aldosterone concentration is acknowledged as a significant cardiovascular risk factor (Schmidt and Schmieder 2003, Schmidt et al. 2006), however, during hyperuricemia its role has received little attention. It should be noted that the present rats were not subjected to a metabolic balance study, and claims of a constant Na^+ retention and K^+ loss cannot be presented from these results. The possibility exists that the influence of plasma aldosterone on electrolyte balance became more evident in the unfamiliar environment of a metabolic cage. However, our results imply that increased plasma aldosterone may mediate the Na^+ retention associated with high serum UA.

Knowledge of the possible hyperuricemia-associated changes in renal tissue components of RAS is limited. Our aim was, therefore, to examine if some of the detrimental effects of elevated serum UA could be accounted for by alterations in renal RAS components. Kidney ACE, ACE2, AT_{1R}, and AT_{2R} were measured at protein and mRNA levels using

in vitro autoradiography and real-time quantitative RT-PCR, respectively **(I)**. The autoradiography analyses did not unearth any changes that could explain the hyperuricemia-induced alteration in Na^+-K^+ -balance (Figure 7). There were no differences in kidney ACE content between the study groups (Figure 8), while changes in cortical and medullary AT_{1R} densities were only observed in the NX+Oxo group: about 25% higher cortical AT_{1R} density than in the NX group, and 43% higher medullary AT_{1R} density than in the Sham group (Figure 11). Thus, hyperuricemia may be associated with increases in renal AT_{1R} density in CRI, but neither of these changes could explain the altered Na^+-K^+ -balance, as increased renal K^+ wasting was also observed in the Sham+Oxo group in the absence of alterations in renal AT_{1R} density.

When determined using RT-PCR, both NX groups showed significantly lower ACE and ACE2 mRNA levels than the respective Sham rats (Figure 9) **(I)**. Kidney AT_{1aR} and AT_{2R} mRNA contents were also lower in both NX groups than in Sham rats. Importantly, the oxonic acid diet did not influence ACE, ACE2, AT_{1aR} or AT_{2R} mRNA in kidney tissue of either Sham or NX rats. As the RT-PCR analyses were performed from kidney extracts, no macroscopic localization of the mRNA molecules could be obtained. In the case of AT receptors, the *in vitro* autoradiography provided information about distribution at the tissue level, i.e. localization in the cortex or medulla. Experimental CRI was also associated with an approximately 40% increase in the medullary/cortical ratio of AT_{1R} density, which was not influenced by 2.0% oxonic acid feeding. Moreover, highest ACE labeling was detected in the corticomedullary region in the sham-operated rats, but in the NX groups kidney ACE showed patchy and wider tissue distribution than in normal kidneys (Figure 8). Altogether, the investigated RAAS components showed no changes at the mRNA level that would explain the influence of hyperuricemia on Na^+-K^+ -balance **(I)**. Because the mRNA levels, but not the corresponding protein contents, were reduced in the two NX groups, the above RAAS components were probably subject to post-transcriptional modulation in experimental CRI. This may be related to the lower PRA and reduced circulating RAAS activity in this form of renal insufficiency.

Previously adrenal aldosterone production has been found to be increased 8 days after NX operation in rats despite a decrease of PRA. The putative stimulus for the adrenal aldosterone synthesis was suggested to be up-regulated adrenal renin synthesis (Endemann et al. 2004). In concert with these findings, subtotal nephrectomy was associated with a marked increase in plasma aldosterone/renin ratio in the present study **(I)**.

It has been previously shown that increased calcium intake reduces kidney ACE protein content in the NX rats (Pörsti et al. 2004), whereas the effects of calcium-phosphate balance on ACE mRNA and other kidney RAS components has remained largely uncharted. Translational efficiency depends on multiple determinants that can modulate protein synthesis (Gingold and Pilpel 2011), and awareness of both mRNA and protein levels is necessary for the assessment of gene function. In study IV, ACE mRNA and protein were elevated in NX rats, while phosphate loading induced a further increase in kidney ACE (Figures 8 and 9) **(IV)**. In contrast, the phosphate-lowering high calcium diet helped maintain both ACE mRNA and protein on a level comparable to that in Sham rats. The distribution of ACE protein was also altered in all NX groups so that the ACE signal was detected more widely throughout the remnant kidney (Figure 8). As ACE is one of the key targets of pharmacotherapy in kidney diseases, these findings stress the importance of effective plasma phosphate control in the treatment of CKD.

A clear decrease in kidney ACE2 mRNA levels in all NX groups was observed in study IV (Figure 9). ACE2 is considered a protective RAS component, since it degrades the vasoconstrictor Ang II and generates the vasodilator and natriuretic peptide Ang 1-7 (Ferrario 2006). Therefore, reduced ACE2 transcription shifts balance towards enhanced vasoconstrictive RAS activity (Fyhrquist and Saijonmaa 2008). The effects of Ang 1-7 are thought to be mediated via the recently identified receptor, Mas, which can also beneficially influence fibrogenesis in the kidney (Fyhrquist and Saijonmaa 2008, Pinheiro et al. 2009). In this study no differences were seen in Mas mRNA between the groups **(IV)**.

The main effector of the classic RAAS, Ang II, exerts its actions mainly through AT_{1R} and AT_{2R} (Fyhrquist and Saijonmaa 2008). AT_{1R} mediate the potentially harmful consequences, while AT_{2R} are thought to predominantly mediate vasodilatation and anti-proliferative effects (Fyhrquist and Saijonmaa 2008). However, the beneficial effects of AT_{2R} stimulation have been controversial and the clinical proof is lacking (Carey 2005). These results showed lower kidney AT_{2R} mRNA content in the NX group versus Sham (Figure 11) **(IV)**. Thus, lower Ang II action via the AT_{2R} may participate in the renal pathology and pathophysiology in the NX model of CRI.

The receptor for Ang IV peptide, AT_{4R}, is also known as IRAP (Fyhrquist and Saijonmaa 2008). Ang IV has regulatory functions in cognition, renal metabolism and cardiovascular damage, and the AT_{4R} mediated actions include renal vasodilatation, hypertrophy, and NF-κB activation. Ang IV is also involved in vascular inflammatory response (Fyhrquist

and Saijonmaa 2008). In study IV, increased levels of kidney AT_{4R} mRNA content was found in the NX and NX+Pi groups versus Sham (Figure 12). To our knowledge, this is the first time that increased AT_{4R} content has been reported in the NX model **(IV)**. Notably, phosphate-lowering high calcium diet was not associated with increased kidney AT_{4R} transcription, agreeing with the overall suppression of renal tissue RAS components achieved with improved plasma calcium-phosphate balance.

The PRR, which can bind both renin and prorenin, has been recently identified as a RAAS member (Nguyen 2007, Fyhrquist and Saijonmaa 2008). Experimental studies have suggested a potential role for this receptor in tissue fibrosis (Nguyen 2007). The PRR is highly expressed in podocytes, and it appears to be essential for normal podocyte function and survival (Riediger et al. 2011). In the present study **(II)**, kidney PRR mRNA was decreased in the NX and NX+Pi groups (Figure 12), but not in the NX+Ca group, when compared with Sham. In addition, PRR mRNA inversely correlated with glomerulosclerosis in the groups ($r=-0.50$, $p=0.002$). Thus, reduced PRR expression may have contributed to glomerular damage in the NX model. Interestingly, PRR mRNA was also modulated by alterations in calcium-phosphate balance, as phosphate binding suppressed the CRI-induced decrease of PRR mRNA level **(IV)**.

In study IV, calcium-phosphate balance was found to influence ACE content in kidney tissue, while the results of the preliminary 12-week pilot study of study V showed that the phosphate-binding diet also reduced the amount of ACE in the heart and aorta (Figure 10) **(V)**. In the 27-week study, aortic ACE protein was decreased after 12 weeks of oral calcium carbonate treatment (Figure 10) **(V)**. In study IV, the correlation between ACE protein and ACE mRNA content in kidney tissue was good ($r=0.83$), and this suggests that changes in tissue ACE are probably explained by alterations at the level of gene expression. In contrast to the results on kidney ACE in study IV, the content of ACE in the aorta was not increased after phosphate loading in NX rats **(V)**. This may be attributed to the abundant calcifications in the aortas of NX+Pi rats, as calcified tissue sections would not contain ACE to bind the iodinated autoradiography-tracer. Of note, the autoradiography tracings showed that aortic ACE protein was present throughout the vascular wall in all study groups and was not limited to the endothelium (Figure 10) **(V)**.

2.2. Vascular function, nitric oxide, plasma lipids, and oxidative stress

In study II, the principal focus was on the putative changes in NO-mediated vasorelaxation, and therefore the functional responses in the carotid artery were studied. In many vessels the vasorelaxation to Ach is mediated via NO, prostacyclin and endothelium-derived hyperpolarization (Roman 2002), but in the rat carotid artery the vasorelaxation is largely mediated via endothelium-derived NO (Arvola et al. 1999). Carotid vasorelaxation via both endothelial NO (Ach) and exogenous NO (nitroprusside) was found to be impaired in experimental CRI **(II)**. Unexpectedly, hyperuricemia improved vasorelaxation in response to NO in NX rats, and the plasma concentration of UA correlated positively with maximal Ach-mediated relaxation. In contrast, the vasorelaxation via cyclic AMP (isoprenaline) was not affected by hyperuricemia. Thus, the differences in carotid artery vasorelaxation were related to alterations in NO-mediated responses **(II)**.

The present results of study II appear to contradict with previous findings *in vitro* suggesting that UA inhibits NO production in cultured aortic endothelial cells (Khosla et al. 2005), and that UA induces oxidative stress through stimulation of RAS in cultured VSMCs (Corry et al. 2008). In addition, experimental studies have suggested that UA is a mediator of CVD and CKD (Mazzali et al. 2001, Kang et al. 2002, Nakagawa et al. 2003, Khosla et al. 2005, Sanchez-Lozada et al. 2005). Altogether, the antioxidant properties of UA may mitigate the harmful influences of RAAS stimulation associated with increased UA concentration. In addition, some of the differences between the results of the studies on oxonic acid-induced hyperuricemia may be related to the fact that 2.0% oxonic acid diet was used in some (Mazzali et al. 2001, Kang et al. 2002, Nakagawa et al. 2003), while administration of oxonic acid by gastric gavage (750 mg/kg/day) was used in others (Sanchez-Lozada et al. 2005, Sanchez-Lozada et al. 2007, Sanchez-Lozada et al. 2008). It seems likely that the effects of oxonic acid administration by gavage on the kinetics of plasma UA differ from those following 2.0% oxonic acid dietary intake.

Although hyperuricemia has in general been considered a cardiovascular risk factor (Patetsios et al. 2001, Johnson et al. 2003), conflicting data also exists. UA serves as a scavenger of various free radicals (Davies et al. 1986, Becker et al. 1991, Squadrito et al. 2000). Intravenous UA infusion increases serum free-radical scavenging capacity in healthy volunteers (Waring et al. 2001), and improves endothelial function in the forearm vascular bed of smokers and patients with type 1 diabetes mellitus (Waring et al. 2006).

Higher UA concentration is also associated with increased serum antioxidant capacity and reduced oxidative stress during acute physical exercise (Waring et al. 2003). However, the antioxidant role of UA is complicated by the generation of superoxide anion as a by-product in the reaction of xanthine with XO to produce UA (Johnson et al. 2003). Furthermore, the reaction of superoxide with NO leads to the formation of highly toxic peroxynitrite with possible further formation of secondary free radicals (Squadrito et al. 2000). Yet, UA can indirectly protect against the harmful effects of peroxynitrite by scavenging these secondary radicals (Squadrito et al. 2000).

Increased oxidative stress is a characteristic feature of CRI (Vaziri et al. 2002). Indeed, a marked increase was observed in the urinary 8-iso-$PGF_{2\alpha}$ excretion after 11 weeks of CRI in the present study (Figure 7), a finding that has not been reported previously in NX rats **(II)**. Interestingly, 8-iso-$PGF_{2\alpha}$ excretion was not increased during the third week after subtotal nephrectomy, indicating that increased oxidative stress is not a straightforward result of renal mass reduction but develops later in the course of chronically impaired renal function.

The levels of UA are higher in humans than in most other mammals (Johnson et al. 2003). Moreover, the relation of the UA levels with CVD in humans has been suggested to show a J-shaped curve with the nadir of risk being in the second quartile (Fang and Alderman 2000, Johnson et al. 2003, Hsu et al. 2004). The increased risk for the lowest quartile may reflect the decreased plasma antioxidant activity, whereas the increased risk at the higher levels may reflect the role of UA in inducing CVD, leaving the antioxidant role of UA insignificant. In the 2.0% oxonic acid rat model of hyperuricemia, the levels of plasma UA are still rather low when compared with humans (Table 4), and higher levels may be required to induce vascular damage in rats **(I, II)**.

CRI is also associated with unfavorable changes in plasma lipids (Vaziri et al. 2001). The impaired vasorelaxation may result from the increased level of LDL cholesterol, which inhibits endothelium-dependent vasodilatation (Mougenot et al. 1997), while the underlying mechanisms are impaired vascular NO production and increased superoxide anion generation that inactivates NO (Vaziri et al. 2002). In line with these findings, plasma lipid values were increased by 2 to 3-fold in the NX rats in the present study (Table 4) **(II)**. Higher UA level may also provide antioxidant protection against the detrimental effects of LDL cholesterol on NO-mediated vasorelaxation.

Deficient endothelium-mediated vasodilatation is a common finding in CRI (Joannides et al. 1997, Rabelink and Koomans 1997, van Guldener et al. 1997, Kööbi et al. 2006). Previously, we observed that the correction of abnormal calcium, phosphate and PTH levels in NX rats improved endothelium-mediated vasorelaxation via K^+-channels in small 3rd order mesenteric arterial branches (Jolma et al. 2003), and enhanced vasorelaxation via NO and K^+ channels in slightly larger 2nd order mesenteric arterial rings (Kööbi et al. 2006). In the present study V, we examined arterial tone in a conduit-size artery due to the greater contribution of endothelium-derived NO to vasodilatation in larger vessels (Garland et al. 1995, Boegehold 1998), and found that phosphate binding reversed the impaired relaxation to Ach in the main branch of the mesenteric artery (Figure 14) **(V)**. As the improved vasorelaxation was entirely inhibited by the NOS inhibitor L-NAME, and the change in AUC induced by L-NAME was more pronounced in the NX+Ca than NX and NX+Pi groups, the beneficial effect may be attributed to enhanced NO-mediated component in the Ach response. Dietary phosphate loading did not decrease the relaxation to Ach, and the contribution of endothelium-derived NO to the vasorelaxation was corresponding in the NX and NX+Pi groups, as judged by the change in AUC induced by L-NAME (Figure 14). Of note, enhanced vasorelaxation after calcium carbonate was not explained by changes in NO sensitivity in arterial smooth muscle, as the endothelium-independent response to nitroprusside did not differ between the Sham, NX and NX+Ca groups. Moreover, vasorelaxation via exogenous NO was slightly impaired in the NX+Pi group **(V)**.

Many previous studies have examined the effect of CRI on L-arginine metabolism and functional role of the NOS enzymes with somewhat contradictory results (Aiello et al. 1997, Vaziri et al. 1998, Thuraisingham et al. 2002, Thuraisingham and Yaqoob 2003). In study V, eNOS content in the abdominal aorta was found to be equally reduced in all NX groups (Figure 12) **(V)**. Thus, the enhanced endothelium-mediated vasorelaxation in the NX+Ca group was not explained by changes in the amount of eNOS, as the modulation of calcium-phosphate balance was without effect on the quantity of eNOS protein.

The major effector-peptide of the classic RAAS, Ang II, can reduce NO bioactivity through increased production of superoxide radicals, which rapidly inactivate NO and thus prevent its dilatory actions in vascular smooth muscle (Enseleit et al. 2001, Chabrashvili et al. 2003). At the molecular level Ang II, generated predominantly via the action of ACE, up-regulates and activates NADPH oxidases in the vascular wall, resulting in increased

superoxide release (Förstermann 2010). Vascular oxidative stress is considered one of the culprits leading to the loss of NO-mediated vasodilatation (Förstermann 2010). Furthermore, when superoxide radicals react with NO, the highly reactive radical peroxynitrite is formed, at a reaction rate that is several-fold faster than the scavenging of superoxide by SOD (Beckman and Koppenol 1996, Bouloumie et al. 1997, Thuraisingham and Yaqoob 2003). Peroxynitrite, in turn, can modify tyrosine-residues in proteins to create nitrotyrosine, thus leaving a detectable footprint of oxidative stress in tissues (Beckman and Koppenol 1996). Here we determined aortic nitrated proteins using Western blotting, and found that the levels were increased in the NX and NX+Pi group, but were significantly reduced in the NX+Ca group (Figure 12) **(V)**. Therefore, phosphate binding with calcium carbonate reduced oxidative stress in vascular tissue. One mechanism leading to reduced local Ang II and superoxide generation may be the reduced amount of arterial tissue ACE (Figure 10). Furthermore, reduced superoxide generation in the vascular wall would result in increased bioactivity of endothelium-derived NO, and this mechanism may explain the enhanced Ach response in the NX+Ca when compared with the NX group.

NO has a short half-life, and thereby NOx determination as the stable end-product of NO metabolism was used to evaluate NO production *in vivo* **(V)**. Plasma NOx concentration was increased in all NX rats after 27 weeks of CRI (Table 5), in agreement with previous results in experimental and clinical CRI (Aiello et al. 1997, Thuraisingham and Yaqoob 2003). Urine NOx was also increased in all NX groups. The elevated NOx is considered to reflect oxidative stress and inflammation in CRI (Thuraisingham et al. 2002, Thuraisingham and Yaqoob 2003). The source of NOx remains unknown from the present results, as reduced eNOS and no differences in abdominal aortic iNOS content were detected after 27 weeks of CRI. Previously, studies examining NO release have shown increased production, whereas those examining NO bioactivity have shown attenuated responses in CRI, and even endothelial cells cultured with uremic plasma *in vitro* have shown increased NO release (Thuraisingham and Yaqoob 2003). Thus, elevated plasma NOx could result from the effects of uremic milieu on NOS activity *in vivo*, while reduced NO bioactivity in uremia has been strongly related to excess NO consumption due to oxidative stress (Thuraisingham and Yaqoob 2003). Of note, elevated NOx could also result from the increased oxidative stress in CRI, as peroxynitrite can break down to form NOx (Moncada and Higgs 1991, Thuraisingham et al. 2002).

The arterial contractions were examined in study V to uncover possible differences in vasoconstrictor sensitivity that would interfere with the interpretation of the relaxation experiments (Table 6). No differences were found in responses elicited by membrane depolarisation with KCl, and contractions elicited by NE were also corresponding in the Sham, NX and NX+Ca groups **(V)**. Therefore, alterations in vasoconstrictor sensitivity did not explain enhanced vasorelaxation in NX+Ca rats when compared with NX rats. The NX+Pi group exhibited lower maximal response but higher sensitivity to NE when compared with Sham rats (Table 6), and increased vasoconstrictor sensitivity to NE may thus partially explain impaired vasodilator response to exogenous NO after phosphate loading. Finally, mesenteric arterial rings in the NX group exhibited increased maximal wall tension induced by Ang II, while the response in the NX+Ca group did not differ from Sham rats, and contractile sensitivity to Ang II was even lower in NX+Ca than Sham rats. This implies that phosphate binding with oral calcium carbonate reduced Ang II-mediated responses in arterial tissue even at the level of the AT_{1R} or its signal transduction cascade.

2.3. Other findings

Increased expression of CTGF, a key mediator of fibrosis, has been reported in both clinical and experimental kidney disease (Gupta et al. 2000). In injured kidneys, CTGF expression correlates with cellular proliferation and ECM accumulation (Gupta et al. 2000), and is up-regulated by Ang II (Ruperez et al. 2003). Our measurements in study IV showed up-regulated kidney CTGF mRNA versus Sham rats in the NX and NX+Pi groups, but not in the NX+Ca group (Figure 12) **(IV)**. This suggests that phosphate lowering can decrease fibrosis signaling, which also translated to kidney histology: glomerulosclerosis and tubulointerstitial damage indices were increased in all NX groups, but the phosphate-lowering high calcium diet helped to decelerate tissue damage in comparison with the NX and NX+Pi groups (Figure 6) **(IV)**. It is also of note that the beneficial influences of hyperuricemia were not limited to carotid vasorelaxation, as glomerulosclerosis was additionally alleviated by the oxonic acid-induced hyperuricemia in NX rats **(II)**.

HO provides the rate-limiting step in the catabolism of heme with two isoenzymes, the inducible HO-1 and the constitutive HO-2 (Abraham and Kappas 2008). HO-1 is induced by several agents that cause oxidative stress and is thought to offer cellular protection after injury (Abraham and Kappas 2008). In study IV, the transcription of kidney HO-1 was elevated in all NX groups compared to Sham rats, which was likely triggered to counter the

elevated oxidative stress after partial nephrectomy (Figure 12) **(IV)**. Abnormal calcium, phosphate, and PTH metabolism are known causes for increased cardiovascular calcification in CRI (Marco et al. 2003, Tyralla and Amann 2003), and in the present study V phosphate binding with calcium carbonate reduced aortic calcifications in NX rats, as expected (Pörsti et al. 2004) (Figure 6) **(V)**.

3. STUDY IMPLICATIONS

The effects of hyperuricemia are currently researched intensely due to the influence of sugar-sweetened foods and drinks, mainly fructose, on UA levels (Johnson et al. 2013a, Johnson et al. 2013b, Kanbay et al. 2013). It seems that the harmful effects are brought forward with relentless force, whereas the disorders associated with low UA levels are mainly swept aside. However, the J-shaped curve hypothesis (Fang and Alderman 2000, Johnson et al. 2003, Hsu et al. 2004) still holds firm, and we should not forget that UA is indeed a significant antioxidant with pivotal function in vitamin C recycling (Lopez-Torres et al. 1993, Johnson et al. 2008b). Oxidative stress is a constant menace to each and every cell and tissue of our bodies, while antioxidants offer a means to combat this threat. In study II, elevated UA reduced oxidative stress and increased antioxidant capacity *in vivo*. In parallel, hyperuricemia enhanced vasorelaxation via NO in the carotid artery in the NX, independently of the level of BP and renal function **(II)**. If the optimal level of UA could be found, it would be much easier to form a consensus on the need for UA lowering treatment versus recommendations on UA promoting food and drink. Today, no such consensus exists, but the work towards it continues.

Nonetheless, the potentially harmful effects of hyperuricemia are factual. In this series of studies, experimental hyperuricemia induced by 2.0% oxonic acid diet activated the circulating RAAS **(I)**, as evidenced by increased PRA and aldosterone in both Sham and NX rats. This finding clearly highlights the role of aldosterone in the hyperuricemia-induced sodium retention and BP elevation. As this series of investigations comprise experimental findings, no direct implications to human CKD should be made. However, these results may open up new ideas for further research in clinical settings. The RAAS is already a key target for pharmacotherapy of many disorders, while these findings may provide another view point to consider.

Without doubt, the NX operation produces a shock that alters gene expression in the remnant kidney and the cardiovascular system. Therefore it seems highly unlikely that these processes should stabilize in only four days. In the well-known study by Freundlich et al., the NX rats were put on paricalcitol (100 ng/kg or 300 ng/kg) already four days after surgery (Freundlich et al. 2008). In our experiment with paricalcitol **(III)**, the treatment started 15 weeks after surgery in a well-established stage of CRI. This situation more closely resembles the clinical CKD, and may be the reason behind the discrepancy of observations with paricalcitol treatment. Paricalcitol treatment therefore does not always suppress RAS components in the kidney, and the timing of the treatment may be pivotal in determining its efficacy. This implies that the early diagnosis and initiation might correspondingly be major factors in clinical treatment of SHPT. Importantly, in their response, Freundlich et al. (Freundlich et al. 2009) later admitted that their unpublished observations also indicated that delaying paricalcitol treatment for 8 weeks after nephrectomy essentially abrogated the functional and histological improvement of VDR activator treatment in the renal ablation model.

Disturbances of calcium-phosphate metabolism are ubiquitous in later stage CKD. In our studies on calcium-phosphate metabolism **(IV, V)**, dietary phosphate loading was associated with elevated kidney, cardiac, and vascular ACE expression, increased kidney tissue damage, as well as increased aortic calcification in the NX rats. Phosphate binding had opposite effects on ACE and kidney damage, as well as reduced nitrated proteins in the aorta and enhanced vasorelaxation via increased bioactivity of endothelium-derived NO. Hypertension in the NX model was also associated with impaired NO-mediated vasorelaxation in the mesenteric artery, decreased eNOS, increased ACE and nitrated proteins in the aorta, as well as elevated levels of plasma and urine NO metabolites. These findings strongly underline the importance of effective phosphate management together with successful BP treatment in CKD. In addition, control of the above harmful factors may beneficially influence the expression of RAS components in both kidneys and vasculature.

SUMMARY AND CONCLUSIONS

The present series of studies was designed to investigate several different interventions in the experimental NX rat model of CRI. In the first two 12-week studies, hyperuricemia was induced by feeding 2.0% oxonic acid diet, which effectively inhibits the uricase enzyme responsible for breakdown of uric acid into allantoin. The effect of VDR activator paricalcitol, 200 ng/kg three times weekly, was studied in a 27-week study, which assessed the levels of RAS component gene transcription. The final two 27-week studies involved analysis of altered calcium-phosphate metabolism induced by phosphate loading with 1.5% phosphate diet or phosphate binding with 3.0% calcium carbonate.

The major findings and conclusions are:

1. Hyperuricemia induced by 2.0% oxonic acid diet did not induce changes in the local components of the RAS in renal tissue, but activated the circulating RAAS, reflected as increased PRA and aldosterone in both Sham and NX rats. The role of aldosterone is emphasized in the hyperuricemia-induced sodium retention and subsequent BP elevation.

2. Experimental hyperuricemia reduced oxidative stress and increased antioxidant capacity *in vivo*, as evidenced by the reduced 24-hour urinary 8-iso-$PGF_{2\alpha}$ excretion and increased plasma TRAP, respectively. Hyperuricemia also enhanced vasorelaxation via NO in the carotid artery, independently of the level of BP and renal function. These findings show that increased uric acid level is not solely harmful on the cardiovascular system, but can also provide beneficial effects as a powerful antioxidant.

3. Delayed initiation of paricalcitol treatment decreases treatment efficacy, as exhibited by the reduced suppression of kidney RAS component gene transcription. An earlier study reported major suppression of RAS gene expression in the NX model when the treatment was initiated only four days after the NX operation. In the present study, the commencement of treatment was delayed for 15 weeks and no suppression of RAS transcription was observed. In order to maximize the possible benefits on the RAS, the early initiation of paricalcitol treatment seems vital.

4. Dietary phosphate loading was associated with elevated kidney ACE expression, increased tissue damage, and lower AT_{1a} transcription in the NX rats. Phosphate binding with 3.0% calcium carbonate had opposite effects on kidney ACE and kidney damage. According to these findings, effective phosphate control in CKD may beneficially influence the expression of RAS components in kidney tissue.

5. In the 27-week study, elevated BP was associated with impaired vasorelaxation via endothelium-derived NO in the mesenteric artery. Elevated BP also involved decreased eNOS content, increased aortic ACE, and increased nitrated proteins in the aorta, as well as elevated levels of plasma and urine NO metabolites. Phosphate binding with 3.0% calcium carbonate reduced ACE and nitrated proteins in the aorta, and enhanced vasorelaxation via increased bioactivity of endothelium-derived NO. Therefore, correction of the disturbances of calcium-phosphate metabolism seems to beneficially influence vascular pathophysiology in CKD also via influences on arterial wall ACE and NO bioactivity.

ACKNOWLEDGEMENTS

The main work of this thesis involving the actual animal experiments, *in vitro* vascular function studies, and radioimmunoassays, was carried out at the School of Medicine, University of Tampere. Decisively important laboratory analyses were also performed at the Minerva Institute for Medical Research, University of Helsinki, and at the Department of Laboratory Medicine, Seinäjoki University Hospital.

First and foremost, I wish to thank my ever-supportive and inspiringly enthusiastic supervisor, Professor Ilkka Pörsti. His experienced guidance kept me on track when my own focus was faltering. His generous support and advice during crucial times was vital for the completion of this thesis. Above it all, however, I see Ilkka as a friend who always has time to talk about the truly important aspects of life – the family, kids, sports, as well as many other interests we share. Ilkka's thorough knowledge of medicine made it easy for me to interpret my findings and grasp the big picture.

I also wish to express my genuine gratitude to Professor Jukka Mustonen, who has been a major factor in all my published work. His warm personality and brilliant questions have helped me find many correct answers.

I sincerely thank the reviewers of this thesis, Docent Risto Kerkelä and Docent Risto Tertti for their tireless effort in combing through these pages and offering constructive comments.

I offer my heartfelt thanks to Professors Ilkka Tikkanen, Onni Niemelä, and Eeva Moilanen, as well as Päivi Lakkisto, M.D. for providing their collaboration, facilities, expertise and reagents to this study. Without them the completion of this thesis would have been impossible. I also wish to thank the other co-authors of the original publications, Pasi Jolma, M.D., Jarkko Kalliovalkama, M.D., Meng Fan, M.D., Juhani Myllymäki, M.D., Jyrki Parkkinen, M.D., and Asko Riutta, M.Sc. for their invaluable contributions.

My appreciation and thanks also belong to Professor Mika Kähönen for his encouraging words and warm personality, Peeter Kööbi, M.D. for his helpful guidance and truly awe inspiring surgical skills, Tuija Vehmas, M.Sc. for our friendship along with her tremendous help in getting me up to speed in laboratory, and finally Terhi Suvanto for her priceless technical assistance during the radioimmunoassay determinations.

I am deeply thankful to our top-of-the-line research group without which this project would have been a long and lonely endeavor. I thank each and everyone of you! Especially I want to thank my co-authors Venla Kurra, M.D., Anna Tahvanainen, M.D., and Jenni Koskela, M.D. for their excellent research efforts and encouraging support. I also want to thank Antti Haring, M.D., Miia Leskinen, M.D., Suvi Törmänen, M.D., Jarkko Kuusinen, M.D., and Sirpa Walker for our long and fruitful conversations and true mutual friendship. I am glad to express my appreciation to Antti Tikkakoski, M.D., Jani Viitala, M.Sc. (Tech.), Pauliina Kangas, M.D., Elina Hautaniemi, M.Sc., Jyrki Taurio, M.D., and Matias Wilenius, M.D. for their support and warm camaraderie. Last, but definitely not the least, I want to thank our great research nurses Reeta Kulmala and Paula Erkkilä who have brought laughter and happiness to our group. Their efforts in our clinical research cannot be appreciated enough.

It would have been impossible to carry out this work without the support of my friends and family. I wish to thank my sisters and their families for valuable support during these years. I also wish to thank all my friends – you know who you are. I want to give my deepest thanks to my parents Maija and Jouko Eräranta, who have done their all to provide me this opportunity in life. I know I haven't always been the easiest son, but you have prevailed!

Finally, I would like to express my wholehearted and loving gratitude to my wife Sonja, my son Aaro, and my daughter Elsa. You fill my world with joy and gratitude every single day. Thank you for all the beautiful things you continuously provide my life with!

This work has been supported by the grants from Pirkanmaa Regional Fund of the Finnish Cultural Foundation, Emil Aaltonen Foundation, Finnish Kidney Foundation, Competitive Research Funding of the Pirkanmaa Hospital District, and Finnish Foundation for Cardiovascular Research.

REFERENCES

(2012). The Finnish Registry for Kidney Diseases. Report 2011.

Abraham NG and Kappas A (2008). Pharmacological and clinical aspects of heme oxygenase. Pharmacol Rev 60: 79-127.

Achard V, Boullu-Ciocca S, Desbriere R, Nguyen G and Grino M (2007). Renin receptor expression in human adipose tissue. Am J Physiol Regul Integr Comp Physiol 292: R274-282.

Aiello S, Noris M, Todeschini M, Zappella S, Foglieni C, Benigni A, Corna D, Zoja C, Cavallotti D and Remuzzi G (1997). Renal and systemic nitric oxide synthesis in rats with renal mass reduction. Kidney Int 52: 171-181.

Alanko J, Riutta A, Holm P, Mucha I, Vapaatalo H and Metsä-Ketelä T (1999). Modulation of arachidonic acid metabolism by phenols: relation to their structure and antioxidant/prooxidant properties. Free Radic Biol Med 26: 193-201.

Albiston AL, Peck GR, Yeatman HR, Fernando R, Ye S and Chai SY (2007). Therapeutic targeting of insulin-regulated aminopeptidase: heads and tails? Pharmacol Ther 116: 417-427.

Amann K, Wolf B, Nichols C, Törnig J, Schwarz U, Zeier M, Mall G and Ritz E (1997). Aortic changes in experimental renal failure: hyperplasia or hypertrophy of smooth muscle cells? Hypertension 29: 770-775.

Amann K, Simonaviciene A, Medwedewa T, Koch A, Orth S, Gross ML, Haas C, Kuhlmann A, Linz W, Schölkens B and Ritz E (2001). Blood pressure-independent additive effects of pharmacologic blockade of the renin-angiotensin and endothelin systems on progression in a low-renin model of renal damage. J Am Soc Nephrol 12: 2572-2584.

Ames BN, Cathcart R, Schwiers E and Hochstein P (1981). Uric acid provides an antioxidant defense in humans against oxidant- and radical-caused aging and cancer: a hypothesis. Proc Natl Acad Sci U S A 78: 6858-6862.

Annuk M, Zilmer M and Fellström B (2003). Endothelium-dependent vasodilation and oxidative stress in chronic renal failure: impact on cardiovascular disease. Kidney Int Suppl: S50-53.

Anzai N, Kanai Y and Endou H (2007). New insights into renal transport of urate. Curr Opin Rheumatol 19: 151-157.

Arvola P, Pörsti I, Vuorinen P, Pekki A and Vapaatalo H (1992). Contractions induced by potassium-free solution and potassium relaxation in vascular smooth muscle of hypertensive and normotensive rats. Br J Pharmacol 106: 157-165.

Arvola P, Wu X, Kähönen M, Mäkynen H, Riutta A, Mucha I, Solakivi T, Kainulainen H and Pörsti I (1999). Exercise enhances vasorelaxation in experimental obesity associated hypertension. Cardiovasc Res 43: 992-1002.

Bader M (2010). Tissue renin-angiotensin-aldosterone systems: Targets for pharmacological therapy. Annu Rev Pharmacol Toxicol 50: 439-465.

Barsony J and McKoy W (1992). Molybdate increases intracellular 3',5'-guanosine cyclic monophosphate and stabilizes vitamin D receptor association with tubulin-containing filaments. J Biol Chem 267: 24457-24465.

Basso N and Terragno NA (2001). History about the discovery of the renin-angiotensin system. Hypertension 38: 1246-1249.

Becker BF, Reinholz N, Leipert B, Raschke P, Permanetter B and Gerlach E (1991). Role of uric acid as an endogenous radical scavenger and antioxidant. Chest 100: 176S-181S.

Becker GJ and Hewitson TD (2013). Animal models of chronic kidney disease: useful but not perfect. Nephrol Dial Transplant 28: 2432-2438.

Beckman JS and Koppenol WH (1996). Nitric oxide, superoxide, and peroxynitrite: the good, the bad, and ugly. Am J Physiol 271: C1424-1437.

Begun DR (2003). Planet of the apes. Sci Am 289: 74-83.

Behrendt D and Ganz P (2002). Endothelial function. From vascular biology to clinical applications. Am J Cardiol 90: 40L-48L.

Benetos A, Rudnichi A, Thomas F, Safar M and Guize L (1999). Influence of heart rate on mortality in a French population: role of age, gender, and blood pressure. Hypertension 33: 44-52.

Bernstein KE (2006). Views of the renin-angiotensin system: brilling, mimsy, and slithy tove. Hypertension 47: 509-514.

Blacher J, Guerin AP, Pannier B, Marchais SJ, Safar ME and London GM (1999). Impact of aortic stiffness on survival in end-stage renal disease. Circulation 99: 2434-2439.

Block GA, Klassen PS, Lazarus JM, Ofsthun N, Lowrie EG and Chertow GM (2004). Mineral metabolism, mortality, and morbidity in maintenance hemodialysis. J Am Soc Nephrol 15: 2208-2218.

Blumsohn A (2004). What have we learnt about the regulation of phosphate metabolism? Curr Opin Nephrol Hypertens 13: 397-401.

Boegehold MA (1998). Heterogeneity of endothelial function within the circulation. Curr Opin Nephrol Hypertens 7: 71-78.

Boehm M and Nabel EG (2002). Angiotensin-converting enzyme 2 - a new cardiac regulator. N Engl J Med 347: 1795-1797.

Bohle A, Wehrmann M, Bogenschutz O, Batz C, Vogl W, Schmitt H, Muller CA and Muller GA (1992). The long-term prognosis of the primary glomerulonephritides. A morphological and clinical analysis of 1747 cases. Pathol Res Pract 188: 908-924.

Bouloumie A, Bauersachs J, Linz W, Scholkens BA, Wiemer G, Fleming I and Busse R (1997). Endothelial dysfunction coincides with an enhanced nitric oxide synthase expression and superoxide anion production. Hypertension 30: 934-941.

Braman RS and Hendrix SA (1989). Nanogram nitrite and nitrate determination in environmental and biological materials by vanadium (III) reduction with chemiluminescence detection. Anal Chem 61: 2715-2718.

Brasier AR and Li J (1996). Mechanisms for inducible control of angiotensinogen gene transcription. Hypertension 27: 465-475.

Brown EM (2000). Calcium receptor and regulation of parathyroid hormone secretion. Rev Endocr Metab Disord 1: 307-315.

Brown NJ and Vaughan DE (1998). Angiotensin-converting enzyme inhibitors. Circulation 97: 1411-1420.

Bäcklund T, Palojoki E, Grönholm T, Eriksson A, Vuolteenaho O, Laine M and Tikkanen I (2001). Dual inhibition of angiotensin converting enzyme and neutral endopeptidase by omapatrilat in rat in vivo. Pharmacol Res 44: 411-418.

Cachofeiro V, Miana M, de Las Heras N, Martin-Fernandez B, Ballesteros S, Fernandez-Tresguerres J and Lahera V (2008). Aldosterone and the vascular system. J Steroid Biochem Mol Biol.

Cannata-Andia JB and Fernandez-Martin JL (2002). The clinical impact of aluminium overload in renal failure. Nephrol Dial Transplant 17 Suppl 2: 9-12.

Cannata-Andia JB and Rodriguez-Garcia M (2002). Hyperphosphataemia as a cardiovascular risk factor - how to manage the problem. Nephrol Dial Transplant 17 Suppl 11: 16-19.

Cannata-Andia JB, Rodriguez-Garcia M, Roman-Garcia P, Tunon-le Poultel D, Lopez-Hernandez F and Rodriguez-Puyol D (2010). New therapies: calcimimetics, phosphate binders and vitamin D receptor activators. Pediatr Nephrol 25: 609-616.

Cappuccio FP, Strazzullo P, Farinaro E and Trevisan M (1993). Uric acid metabolism and tubular sodium handling. Results from a population-based study. JAMA 270: 354-359.

Carey RM (2005). Update on the role of the AT_2 receptor. Curr Opin Nephrol Hypertens 14: 67-71.

Carney SL (1997). Calcitonin and human renal calcium and electrolyte transport. Miner Electrolyte Metab 23: 43-47.

Chabrashvili T, Kitiyakara C, Blau J, Karber A, Aslam S, Welch WJ and Wilcox CS (2003). Effects of ANG II type 1 and 2 receptors on oxidative stress, renal NADPH oxidase, and SOD expression. Am J Physiol Regul Integr Comp Physiol 285: R117-124.

Chai SY, Fernando R, Peck G, Ye SY, Mendelsohn FA, Jenkins TA and Albiston AL (2004). The angiotensin IV/AT_4 receptor. Cell Mol Life Sci 61: 2728-2737.

Chamorro A, Obach V, Cervera A, Revilla M, Deulofeu R and Aponte JH (2002). Prognostic significance of uric acid serum concentration in patients with acute ischemic stroke. Stroke 33: 1048-1052.

Chen X, Touyz RM, Park JB and Schiffrin EL (2001). Antioxidant effects of vitamins C and E are associated with altered activation of vascular NADPH oxidase and superoxide dismutase in stroke-prone SHR. Hypertension 38: 606-611.

Chertow GM, Burke SK and Raggi P (2002). Sevelamer attenuates the progression of coronary and aortic calcification in hemodialysis patients. Kidney Int 62: 245-252.

Chertow GM, Raggi P, Chasan-Taber S, Bommer J, Holzer H and Burke SK (2004). Determinants of progressive vascular calcification in haemodialysis patients. Nephrol Dial Transplant 19: 1489-1496.

Cockcroft DW and Gault MH (1976). Prediction of creatinine clearance from serum creatinine. Nephron 16: 31-41.

Converse RL, Jr., Jacobsen TN, Toto RD, Jost CM, Cosentino F, Fouad-Tarazi F and Victor RG (1992). Sympathetic overactivity in patients with chronic renal failure. N Engl J Med 327: 1912-1918.

Corry DB, Eslami P, Yamamoto K, Nyby MD, Makino H and Tuck ML (2008). Uric acid stimulates vascular smooth muscle cell proliferation and oxidative stress via the vascular renin-angiotensin system. J Hypertens 26: 269-275.

Coyne D, Acharya M, Qiu P, Abboud H, Batlle D, Rosansky S, Fadem S, Levine B, Williams L, Andress DL and Sprague SM (2006). Paricalcitol capsule for the treatment of secondary hyperparathyroidism in stages 3 and 4 CKD. Am J Kidney Dis 47: 263-276.

Cozzolino M, Dusso AS, Liapis H, Finch J, Lu Y, Burke SK and Slatopolsky E (2002). The effects of sevelamer hydrochloride and calcium carbonate on kidney calcification in uremic rats. J Am Soc Nephrol 13: 2299-2308.

Crowley SD, Gurley SB, Oliverio MI, Pazmino AK, Griffiths R, Flannery PJ, Spurney RF, Kim HS, Smithies O, Le TH and Coffman TM (2005). Distinct roles for the kidney and systemic tissues in blood pressure regulation by the renin-angiotensin system. J Clin Invest 115: 1092-1099.

Curtis JJ, Luke RG, Dustan HP, Kashgarian M, Whelchel JD, Jones P and Diethelm AG (1983). Remission of essential hypertension after renal transplantation. N Engl J Med 309: 1009-1015.

Dahl LK and Heine M (1975). Primary role of renal homografts in setting chronic blood pressure levels in rats. Circ Res 36: 692-696.

Daly JA and Ertingshausen G (1972). Direct method for determining inorganic phosphate in serum with the "CentrifiChem". Clin Chem 18: 263-265.

Danser AH (2003). Local renin-angiotensin systems: the unanswered questions. Int J Biochem Cell Biol 35: 759-768.

Danser AJ and Nguyen G (2008). The Renin Academy Summit: advancing the understanding of renin science. J Renin Angiotensin Aldosterone Syst 9: 119-123.

Davies KJ, Sevanian A, Muakkassah-Kelly SF and Hochstein P (1986). Uric acid-iron ion complexes. A new aspect of the antioxidant functions of uric acid. Biochem J 235: 747-754.

Davies MR and Hruska KA (2001). Pathophysiological mechanisms of vascular calcification in end-stage renal disease. Kidney Int 60: 472-479.

Dawson J and Walters M (2006). Uric acid and xanthine oxidase: future therapeutic targets in the prevention of cardiovascular disease? Br J Clin Pharmacol.

de Jong PE, van der Velde M, Gansevoort RT and Zoccali C (2008). Screening for chronic kidney disease: where does Europe go? Clin J Am Soc Nephrol 3: 616-623.

Delanaye P, Cavalier E, Mariat C, Krzesinski JM and Rule AD (2011a). Estimating glomerular filtration rate in Asian subjects: where do we stand? Kidney Int 80: 439-440.

Delanaye P, Mariat C, Maillard N, Krzesinski JM and Cavalier E (2011b). Are the creatinine-based equations accurate to estimate glomerular filtration rate in African American populations? Clin J Am Soc Nephrol 6: 906-912.

Delanaye P, Pottel H, Botev R, Inker LA and Levey AS (2013). Con: Should we abandon the use of the MDRD equation in favour of the CKD-EPI equation? Nephrol Dial Transplant 28: 1396-1403; discussion 1403.

Demer LL and Tintut Y (2008). Vascular calcification: pathobiology of a multifaceted disease. Circulation 117: 2938-2948.

Demuth K, Blacher J, Guerin AP, Benoit MO, Moatti N, Safar ME and London GM (1998). Endothelin and cardiovascular remodelling in end-stage renal disease. Nephrol Dial Transplant 13: 375-383.

Doehner W and Anker SD (2005). Uric acid in chronic heart failure. Semin Nephrol 25: 61-66.

Donoghue M, Hsieh F, Baronas E, Godbout K, Gosselin M, Stagliano N, Donovan M, Woolf B, Robison K, Jeyaseelan R, Breitbart RE and Acton S (2000). A novel angiotensin-converting enzyme-related carboxypeptidase (ACE2) converts angiotensin I to angiotensin 1-9. Circ Res 87: E1-9.

Drüeke TB (2001). The place of calcium and calcimimetics in the treatment of secondary hyperparathyroidism. Nephrol Dial Transplant 16 Suppl 6: 15-17.

Drüeke TB (2013). Anemia treatment in patients with chronic kidney disease. N Engl J Med 368: 387-389.

Dugue B, Smolander J, Westerlund T, Oksa J, Nieminen R, Moilanen E and Mikkelsson M (2005). Acute and long-term effects of winter swimming and whole-body cryotherapy on plasma antioxidative capacity in healthy women. Scand J Clin Lab Invest 65: 395-402.

Dusso AS, Brown AJ and Slatopolsky E (2005). Vitamin D. Am J Physiol Renal Physiol 289: F8-28.
Eaton SB and Konner M (1985). Paleolithic nutrition. A consideration of its nature and current implications. N Engl J Med 312: 283-289.

Ellman MH and Becker MA (2006). Crystal-induced arthropathies: recent investigative advances. Curr Opin Rheumatol 18: 249-255.

Endemann DH, Wolf K, Boeger CA, Riegger GA and Kramer BK (2004). Adrenal aldosterone biosynthesis is elevated in a model of chronic renal failure - role of local adrenal renin-angiotensin system. Nephron Physiol 97: p37-44.

Enseleit F, Hurlimann D and Luscher TF (2001). Vascular protective effects of angiotensin converting enzyme inhibitors and their relation to clinical events. J Cardiovasc Pharmacol 37 Suppl 1: S21-30.

Esler MD, Krum H, Sobotka PA, Schlaich MP, Schmieder RE and Bohm M (2010). Renal sympathetic denervation in patients with treatment-resistant hypertension (The Symplicity HTN-2 Trial): a randomised controlled trial. Lancet 376: 1903-1909.

Essig DA, Borger DR and Jackson DA (1997). Induction of heme oxygenase-1 (HSP32) mRNA in skeletal muscle following contractions. Am J Physiol 272: C59-67.

Esteban V, Heringer-Walther S, Sterner-Kock A, de Bruin R, van den Engel S, Wang Y, Mezzano S, Egido J, Schultheiss HP, Ruiz-Ortega M and Walther T (2009). Angiotensin-(1-7) and the g protein-coupled receptor MAS are key players in renal inflammation. PLoS One 4: e5406.

Fang J and Alderman MH (2000). Serum uric acid and cardiovascular mortality the NHANES I epidemiologic follow-up study, 1971-1992. National Health and Nutrition Examination Survey. JAMA 283: 2404-2410.

Feig DI and Johnson RJ (2003). Hyperuricemia in childhood primary hypertension. Hypertension 42: 247-252.

Feig DI, Nakagawa T, Karumanchi SA, Oliver WJ, Kang DH, Finch J and Johnson RJ (2004). Hypothesis: Uric acid, nephron number, and the pathogenesis of essential hypertension. Kidney Int 66: 281-287.

Feig DI and Johnson RJ (2007). The role of uric acid in pediatric hypertension. J Ren Nutr 17: 79-83.

Ferrario CM (2006). Angiotensin-converting enzyme 2 and angiotensin-(1-7): an evolving story in cardiovascular regulation. Hypertension 47: 515-521.

Fogo AB (2007). Mechanisms of progression of chronic kidney disease. Pediatr Nephrol 22: 2011-2022.

Foley RN, Parfrey PS and Sarnak MJ (1998). Clinical epidemiology of cardiovascular disease in chronic renal disease. Am J Kidney Dis 32 Suppl 3: S112-119.

Fraser DR and Kodicek E (1970). Unique biosynthesis by kidney of a biological active vitamin D metabolite. Nature 228: 764-766.

Freundlich M, Quiroz Y, Zhang Z, Zhang Y, Bravo Y, Weisinger JR, Li YC and Rodriguez-Iturbe B (2008). Suppression of renin-angiotensin gene expression in the kidney by paricalcitol. Kidney Int 74: 1394-1402.

Freundlich M, Li YC and Rodriguez-Iturbe B (2009). Response to 'Paricalcitol and renin-angiotensin components in remnant kidneys'. Kidney Int 75: 340-340.

Fuller PJ and Young MJ (2005). Mechanisms of mineralocorticoid action. Hypertension 46: 1227-1235.

Fyhrquist F and Saijonmaa O (2008). Renin-angiotensin system revisited. J Intern Med 264: 224-236.

Förstermann U (2010). Nitric oxide and oxidative stress in vascular disease. Pflugers Arch 459: 923-939.

Garland CJ, Plane F, Kemp BK and Cocks TM (1995). Endothelium-dependent hyperpolarization: a role in the control of vascular tone. Trends Pharmacol Sci 16: 23-30.

Gassmann M, Grenacher B, Rohde B and Vogel J (2009). Quantifying Western blots: pitfalls of densitometry. Electrophoresis 30: 1845-1855.

Geiger M, Stone A, Mason SN, Oldham KT and Guice KS (1997). Differential nitric oxide production by microvascular and macrovascular endothelial cells. Am J Physiol 273: L275-281.

Genge BR, Wu LN and Wuthier RE (2007). In vitro modeling of matrix vesicle nucleation: synergistic stimulation of mineral formation by annexin A5 and phosphatidylserine. J Biol Chem 282: 26035-26045.

Gennari FJ (1998). Hypokalemia. N Engl J Med 339: 451-458.

Gingold H and Pilpel Y (2011). Determinants of translation efficiency and accuracy. Mol Syst Biol 7: 481.

GISEN-group (1997). Randomised placebo-controlled trial of effect of ramipril on decline in glomerular filtration rate and risk of terminal renal failure in proteinuric, non-diabetic nephropathy. The GISEN Group (Gruppo Italiano di Studi Epidemiologici in Nefrologia). Lancet 349: 1857-1863.

Go AS, Mozaffarian D, Roger VL, Benjamin EJ, Berry JD, Blaha MJ, Dai S, Ford ES, Fox CS, Franco S, Fullerton HJ, Gillespie C, Hailpern SM, Heit JA, Howard VJ, Huffman MD, Judd SE, Kissela BM, Kittner SJ, Lackland DT, Lichtman JH, Lisabeth LD, Mackey RH, Magid DJ, Marcus GM, Marelli A, Matchar DB, McGuire DK, Mohler ER, 3rd, Moy CS, Mussolino ME, Neumar RW, Nichol G, Pandey DK, Paynter NP, Reeves MJ, Sorlie PD, Stein J, Towfighi A, Turan TN, Virani SS, Wong ND, Woo D and Turner MB (2014). Executive summary: heart disease and stroke statistics--2014 update: a report from the american heart association. Circulation 129: 399-410.

Griendling KK, Murphy TJ and Alexander RW (1993). Molecular biology of the renin-angiotensin system. Circulation 87: 1816-1828.

Gruskin AB (1985). The adolescent with essential hypertension. Am J Kidney Dis 6: 86-90.

Gupta S, Clarkson MR, Duggan J and Brady HR (2000). Connective tissue growth factor: potential role in glomerulosclerosis and tubulointerstitial fibrosis. Kidney Int 58: 1389-1399.

Hackenthal E, Paul M, Ganten D and Taugner R (1990). Morphology, physiology, and molecular biology of renin secretion. Physiol Rev 70: 1067-1116.

Harada E, Yoshimura M, Yasue H, Nakagawa O, Nakagawa M, Harada M, Mizuno Y, Nakayama M, Shimasaki Y, Ito T, Nakamura S, Kuwahara K, Saito Y, Nakao K and Ogawa H (2001). Aldosterone induces angiotensin-converting-enzyme gene expression in cultured neonatal rat cardiocytes. Circulation 104: 137-139.

Harrison-Bernard LM, El-Dahr SS, O'Leary DF and Navar LG (1999). Regulation of angiotensin II type 1 receptor mRNA and protein in angiotensin II-induced hypertension. Hypertension 33: 340-346.

Harrison R (1997). Human xanthine oxidoreductase: in search of a function. Biochem Soc Trans 25: 786-791.

He J, Xu Y, Koya D and Kanasaki K (2013). Role of the endothelial-to-mesenchymal transition in renal fibrosis of chronic kidney disease. Clin Exp Nephrol 17: 488-497.

Herrington JD and Dinh BC (2014). Fixed, low-dose rasburicase for the treatment or prevention of hyperuricemia in adult oncology patients. J Oncol Pharm Pract.

Higuchi S, Ohtsu H, Suzuki H, Shirai H, Frank GD and Eguchi S (2007). Angiotensin II signal transduction through the AT1 receptor: novel insights into mechanisms and pathophysiology. Clin Sci (Lond) 112: 417-428.

Hitom H, Liu G and Nishiyama A (2010). Role of (pro)renin receptor in cardiovascular cells from the aspect of signaling. Front Biosci (Elite Ed) 2: 1246-1249.

Holick MF (1981). The cutaneous photosynthesis of previtamin D3: a unique photoendocrine system. J Invest Dermatol 77: 51-58.

Holick MF (2000). Calcium and vitamin D. Diagnostics and therapeutics. Clin Lab Med 20: 569-590.

Holick MF (2013). Vitamin D, sunlight and cancer connection. Anticancer Agents Med Chem 13: 70-82.

Hostetter TH, Olson JL, Rennke HG, Venkatachalam MA and Brenner BM (1981). Hyperfiltration in remnant nephrons: a potentially adverse response to renal ablation. Am J Physiol 241: F85-93.

Hruska KA, Mathew S, Lund R, Qiu P and Pratt R (2008). Hyperphosphatemia of chronic kidney disease. Kidney Int 74: 148-157.

Hsu HH and Camacho NP (1999). Isolation of calcifiable vesicles from human atherosclerotic aortas. Atherosclerosis 143: 353-362.

Hsu S, Pai M, Peng Y, Chiang C, Ho T and Hung K (2004). Serum uric acid levels show a J-shaped association with all-cause mortality in haemodialysis patients. Nephrol Dial Transplant 19: 457-462.

Hu DE, Moore AM, Thomsen LL and Brindle KM (2004). Uric acid promotes tumor immune rejection. Cancer Res 64: 5059-5062.

Hu MC, Shi M, Zhang J, Quinones H, Griffith C, Kuro-o M and Moe OW (2011). Klotho deficiency causes vascular calcification in chronic kidney disease. J Am Soc Nephrol 22: 124-136.

Ichihara A, Kobori H, Nishiyama A and Navar LG (2004). Renal renin-angiotensin system. Contrib Nephrol 143: 117-130.

Inker LA and Levey AS (2013). Pro: Estimating GFR using the chronic kidney disease epidemiology collaboration (CKD-EPI) 2009 creatinine equation: the time for change is now. Nephrol Dial Transplant 28: 1390-1396.

Itkonen ST, Karp HJ, Kemi VE, Kokkonen EM, Saarnio EM, Pekkinen MH, Kärkkäinen MU, Laitinen EK, Turanlahti MI and Lamberg-Allardt CJ (2013). Associations among total and food additive phosphorus intake and carotid intima-media thickness - a cross-sectional study in a middle-aged population in Southern Finland. Nutr J 12: 94.

Ito M, Oliverio MI, Mannon PJ, Best CF, Maeda N, Smithies O and Coffman TM (1995). Regulation of blood pressure by the type 1A angiotensin II receptor gene. Proc Natl Acad Sci U S A 92: 3521-3525.

Jensen EC (2012). The basics of western blotting. Anat Rec (Hoboken) 295: 369-371.

Jin XH, Siragy HM and Carey RM (2001). Renal interstitial cGMP mediates natriuresis by direct tubule mechanism. Hypertension 38: 309-316.

Joannides R, Bakkali EH, Le Roy F, Rivault O, Godin M, Moore N, Fillastre JP and Thuillez C (1997). Altered flow-dependent vasodilatation of conduit arteries in maintenance haemodialysis. Nephrol Dial Transplant 12: 2623-2628.

Johnson RJ (1994). The glomerular response to injury: progression or resolution? Kidney Int 45: 1769-1782.

Johnson RJ, Herrera-Acosta J, Schreiner GF and Rodriguez-Iturbe B (2002). Subtle acquired renal injury as a mechanism of salt-sensitive hypertension. N Engl J Med 346: 913-923.

Johnson RJ, Kang DH, Feig D, Kivlighn S, Kanellis J, Watanabe S, Tuttle KR, Rodriguez-Iturbe B, Herrera-Acosta J and Mazzali M (2003). Is there a pathogenetic role for uric acid in hypertension and cardiovascular and renal disease? Hypertension 41: 1183-1190.

Johnson RJ and Rideout BA (2004). Uric acid and diet - insights into the epidemic of cardiovascular disease. N Engl J Med 350: 1071-1073.

Johnson RJ, Feig DI, Herrera-Acosta J and Kang DH (2005a). Resurrection of uric acid as a causal risk factor in essential hypertension. Hypertension 45: 18-20.

Johnson RJ, Rodriguez-Iturbe B, Nakagawa T, Kang DH, Feig DI and Herrera-Acosta J (2005b). Subtle renal injury is likely a common mechanism for salt-sensitive essential hypertension. Hypertension 45: 326-330.

Johnson RJ, Segal MS, Srinivas T, Ejaz A, Mu W, Roncal C, Sanchez-Lozada LG, Gersch M, Rodriguez-Iturbe B, Kang DH and Acosta JH (2005c). Essential hypertension, progressive renal disease, and uric acid: a pathogenetic link? J Am Soc Nephrol 16: 1909-1919.

Johnson RJ, Titte S, Cade JR, Rideout BA and Oliver WJ (2005d). Uric acid, evolution and primitive cultures. Semin Nephrol 25: 3-8.

Johnson RJ, Feig DI, Nakagawa T, Sanchez-Lozada LG and Rodriguez-Iturbe B (2008a). Pathogenesis of essential hypertension: historical paradigms and modern insights. J Hypertens 26: 381-391.

Johnson RJ, Gaucher EA, Sautin YY, Henderson GN, Angerhofer AJ and Benner SA (2008b). The planetary biology of ascorbate and uric acid and their relationship with the epidemic of obesity and cardiovascular disease. Med Hypotheses.

Johnson RJ, Nakagawa T, Jalal D, Sanchez-Lozada LG, Kang DH and Ritz E (2013a). Uric acid and chronic kidney disease: which is chasing which? Nephrol Dial Transplant 28: 2221-2228.

Johnson RJ, Nakagawa T, Sanchez-Lozada LG, Shafiu M, Sundaram S, Le M, Ishimoto T, Sautin YY and Lanaspa MA (2013b). Sugar, uric acid, and the etiology of diabetes and obesity. Diabetes 62: 3307-3315.

Johnston CI (1994). Tissue angiotensin converting enzyme in cardiac and vascular hypertrophy, repair, and remodeling. Hypertension 23: 258-268.

Jolma P, Kööbi P, Kalliovalkama J, Saha H, Fan M, Jokihaara J, Moilanen E, Tikkanen I and Pörsti I (2003). Treatment of secondary hyperparathyroidism by high calcium diet is associated with enhanced resistance artery relaxation in experimental renal failure. Nephrol Dial Transplant 18: 2560-2569.

Julius S, Palatini P, Kjeldsen SE, Zanchetti A, Weber MA, McInnes GT, Brunner HR, Mancia G, Schork MA, Hua TA, Holzhauer B, Zappe D, Majahalme S, Jamerson K and Koylan N (2012). Usefulness of heart rate to predict cardiac events in treated patients with high-risk systemic hypertension. Am J Cardiol 109: 685-692.

Junge W, Wilke B, Halabi A and Klein G (2004). Determination of reference intervals for serum creatinine, creatinine excretion and creatinine clearance with an enzymatic and a modified Jaffe method. Clin Chim Acta 344: 137-148.

K/DOQI (2002). K/DOQI clinical practice guidelines for chronic kidney disease: evaluation, classification, and stratification. Am J Kidney Dis 39: S1-266.

Kalliovalkama J, Jolma P, Tolvanen JP, Kähönen M, Hutri-Kähönen N, Saha H, Tuorila S, Moilanen E and Pörsti I (1999). Potassium channel-mediated vasorelaxation is impaired in experimental renal failure. Am J Physiol 277: H1622-1629.

Kanbay M, Segal M, Afsar B, Kang DH, Rodriguez-Iturbe B and Johnson RJ (2013). The role of uric acid in the pathogenesis of human cardiovascular disease. Heart.

Kang DH, Nakagawa T, Feng L, Watanabe S, Han L, Mazzali M, Truong L, Harris R and Johnson RJ (2002). A role for uric acid in the progression of renal disease. J Am Soc Nephrol 13: 2888-2897.

KDIGO (2013). KDIGO clinical practice guideline for the evaluation and management of chronic kidney disease. Kidney Int Suppl 3: 1-150.

Keith DS, Nichols GA, Gullion CM, Brown JB and Smith DH (2004). Longitudinal follow-up and outcomes among a population with chronic kidney disease in a large managed care organization. Arch Intern Med 164: 659-663.

Kemperman FA, Krediet RT and Arisz L (2002). Formula-derived prediction of the glomerular filtration rate from plasma creatinine concentration. Nephron 91: 547-558.

Khosla UM, Zharikov S, Finch JL, Nakagawa T, Roncal C, Mu W, Krotova K, Block ER, Prabhakar S and Johnson RJ (2005). Hyperuricemia induces endothelial dysfunction. Kidney Int 67: 1739-1742.

Khwaja A, El Kossi M, Floege J and El Nahas M (2007). The management of CKD: a look into the future. Kidney Int 72: 1316-1323.

Kimura K and Nishio I (1999). Impaired endothelium-dependent relaxation in mesenteric arteries of reduced renal mass hypertensive rats. Scand J Clin Lab Invest 59: 199-204.

Klahr S, Levey AS, Beck GJ, Caggiula AW, Hunsicker L, Kusek JW and Striker G (1994). The effects of dietary protein restriction and blood-pressure control on the progression of chronic renal disease. Modification of Diet in Renal Disease Study Group. N Engl J Med 330: 877-884.

Kobori H, Nangaku M, Navar LG and Nishiyama A (2007a). The intrarenal renin-angiotensin system: from physiology to the pathobiology of hypertension and kidney disease. Pharmacol Rev 59: 251-287.

Kobori H, Ozawa Y, Satou R, Katsurada A, Miyata K, Ohashi N, Hase N, Suzaki Y, Sigmund CD and Navar LG (2007b). Kidney-specific enhancement of ANG II stimulates endogenous intrarenal angiotensinogen in gene-targeted mice. Am J Physiol Renal Physiol 293: F938-945.

Kohzuki M, Johnston CI, Chai SY, Jackson B, Perich R, Paxton D and Mendelsohn FA (1991). Measurement of angiotensin converting enzyme induction and inhibition using quantitative in vitro autoradiography: tissue selective induction after chronic lisinopril treatment. J Hypertens 9: 579-587.

Komlosi P, Fuson AL, Fintha A, Peti-Peterdi J, Rosivall L, Warnock DG and Bell PD (2003). Angiotensin I conversion to angiotensin II stimulates cortical collecting duct sodium transport. Hypertension 42: 195-199.

Korkor AB (1987). Reduced binding of [^{3}H]1,25-dihydroxyvitamin D_3 in the parathyroid glands of patients with renal failure. N Engl J Med 316: 1573-1577.

Kovesdy CP and Quarles LD (2013). Fibroblast growth factor-23: what we know, what we don't know, and what we need to know. Nephrol Dial Transplant 28: 2228-2236.

Kriz W, Gretz N and Lemley KV (1998). Progression of glomerular diseases: is the podocyte the culprit? Kidney Int 54: 687-697.

Kubista M, Andrade JM, Bengtsson M, Forootan A, Jonak J, Lind K, Sindelka R, Sjöbäck R, Sjögreen B, Strömbom L, Ståhlberg A and Zoric N (2006). The real-time polymerase chain reaction. Mol Aspects Med 27: 95-125.

Kuro-o OM (2006). Klotho as a regulator of fibroblast growth factor signaling and phosphate/calcium metabolism. Curr Opin Nephrol Hypertens 15: 437-441.

Kuro-o OM (2011). Phosphate and Klotho. Kidney Int Suppl: S20-23.

Kurosu H and Kuro-o OM (2008). The Klotho gene family and the endocrine fibroblast growth factors. Curr Opin Nephrol Hypertens 17: 368-372.

Kutzing MK and Firestein BL (2008). Altered uric acid levels and disease states. J Pharmacol Exp Ther 324: 1-7.

Kuzkaya N, Weissmann N, Harrison DG and Dikalov S (2003). Interactions of peroxynitrite, tetrahydrobiopterin, ascorbic acid, and thiols: implications for uncoupling endothelial nitric-oxide synthase. J Biol Chem 278: 22546-22554.

Kvist S and Mulvany MJ (2003). Contrasting regression of blood pressure and cardiovascular structure in declipped renovascular hypertensive rats. Hypertension 41: 540-545.

Kööbi P, Kalliovalkama J, Jolma P, Rysä J, Ruskoaho H, Vuolteenaho O, Kähönen M, Tikkanen I, Fan M, Ylitalo P and Pörsti I (2003). AT_1 receptor blockade improves vasorelaxation in experimental renal failure. Hypertension 41: 1364-1371.

Kööbi P, Vehmas TI, Jolma P, Kalliovalkama J, Fan M, Niemelä O, Saha H, Kähönen M, Ylitalo P, Rysä J, Ruskoaho H and Pörsti I (2006). High-calcium vs high-phosphate intake and small artery tone in advanced experimental renal insufficiency. Nephrol Dial Transplant 21: 2754-2761.

Lakkisto P, Palojoki E, Bäcklund T, Saraste A, Tikkanen I, Voipio-Pulkki LM and Pulkki K (2002). Expression of heme oxygenase-1 in response to myocardial infarction in rats. J Mol Cell Cardiol 34: 1357-1365.

Lameire N, Jager K, Van Biesen W, de Bacquer D and Vanholder R (2005). Chronic kidney disease: a European perspective. Kidney Int Suppl: S30-38.

Lantelme P, Rohrwasser A, Gociman B, Hillas E, Cheng T, Petty G, Thomas J, Xiao S, Ishigami T, Herrmann T, Terreros DA, Ward K and Lalouel JM (2002). Effects of dietary sodium and genetic background on angiotensinogen and renin in mouse. Hypertension 39: 1007-1014.

Largo R, Gomez-Garre D, Soto K, Marron B, Blanco J, Gazapo RM, Plaza JJ and Egido J (1999). Angiotensin-converting enzyme is upregulated in the proximal tubules of rats with intense proteinuria. Hypertension 33: 732-739.

Lee SJ, Terkeltaub RA and Kavanaugh A (2006). Recent developments in diet and gout. Curr Opin Rheumatol 18: 193-198.

Lehto S, Niskanen L, Rönnemaa T and Laakso M (1998). Serum uric acid is a strong predictor of stroke in patients with non-insulin-dependent diabetes mellitus. Stroke 29: 635-639.

Lemley KV (2012). Protecting podocytes: how good do we need to be? Kidney Int 81: 9-11.

Leung AC, Henderson IS, Halls DJ and Dobbie JW (1983). Aluminium hydroxide versus sucralfate as a phosphate binder in uraemia. Br Med J (Clin Res Ed) 286: 1379-1381.

Levey AS, Bosch JP, Lewis JB, Greene T, Rogers N and Roth D (1999). A more accurate method to estimate glomerular filtration rate from serum creatinine: a new prediction equation. Modification of Diet in Renal Disease Study Group. Ann Intern Med 130: 461-470.

Levey AS, Eckardt KU, Tsukamoto Y, Levin A, Coresh J, Rossert J, De Zeeuw D, Hostetter TH, Lameire N and Eknoyan G (2005). Definition and classification of chronic kidney disease: a position statement from Kidney Disease: Improving Global Outcomes (KDIGO). Kidney Int 67: 2089-2100.

Levey AS, Andreoli SP, DuBose T, Provenzano R and Collins AJ (2007a). Chronic kidney disease: common, harmful, and treatable--World Kidney Day 2007. Clin J Am Soc Nephrol 2: 401-405.

Levey AS, Atkins R, Coresh J, Cohen EP, Collins AJ, Eckardt KU, Nahas ME, Jaber BL, Jadoul M, Levin A, Powe NR, Rossert J, Wheeler DC, Lameire N and Eknoyan G (2007b). Chronic kidney disease as a global public health problem: approaches and initiatives - a position statement from Kidney Disease Improving Global Outcomes. Kidney Int 72: 247-259.

Levey AS, Stevens LA, Schmid CH, Zhang YL, Castro AF, 3rd, Feldman HI, Kusek JW, Eggers P, Van Lente F, Greene T and Coresh J (2009). A new equation to estimate glomerular filtration rate. Ann Intern Med 150: 604-612.

Levin A, Bakris GL, Molitch M, Smulders M, Tian J, Williams LA and Andress DL (2007). Prevalence of abnormal serum vitamin D, PTH, calcium, and phosphorus in patients with chronic kidney disease: results of the study to evaluate early kidney disease. Kidney Int 71: 31-38.

Li M and Batuman V (2009). Vitamin D: a new hope for chronic kidney disease? Kidney Int 76: 1219-1221.

Liu S and Quarles LD (2007). How fibroblast growth factor 23 works. J Am Soc Nephrol 18: 1637-1647.

Locatelli F, Cannata-Andia JB, Drueke TB, Horl WH, Fouque D, Heimburger O and Ritz E (2002). Management of disturbances of calcium and phosphate metabolism in chronic renal insufficiency, with emphasis on the control of hyperphosphataemia. Nephrol Dial Transplant 17: 723-731.

London GM, Pannier B, Agharazii M, Guerin AP, Verbeke FH and Marchais SJ (2004). Forearm reactive hyperemia and mortality in end-stage renal disease. Kidney Int 65: 700-704.

London GM, Marchais SJ, Guerin AP, Boutouyrie P, Metivier F and de Vernejoul MC (2008). Association of bone activity, calcium load, aortic stiffness, and calcifications in ESRD. J Am Soc Nephrol 19: 1827-1835.

Lopez-Torres M, Perez-Campo R, Rojas C, Cadenas S and Barja G (1993). Maximum life span in vertebrates: relationship with liver antioxidant enzymes, glutathione system, ascorbate, urate, sensitivity to peroxidation, true malondialdehyde, in vivo H_2O_2, and basal and maximum aerobic capacity. Mech Ageing Dev 70: 177-199.

Lopez-Vargas PA, Tong A, Sureshkumar P, Johnson DW and Craig JC (2013). Prevention, detection and management of early chronic kidney disease: a systematic review of clinical practice guidelines. Nephrology (Carlton) 18: 592-604.

Luke RG (1998). Chronic renal failure - a vasculopathic state. N Engl J Med 339: 841-843.

Ma LJ, Nakamura S, Aldigier JC, Rossini M, Yang H, Liang X, Nakamura I, Marcantoni C and Fogo AB (2005). Regression of glomerulosclerosis with high-dose angiotensin inhibition is linked to decreased plasminogen activator inhibitor-1. J Am Soc Nephrol 16: 966-976.

Macdougall IC (2012). New anemia therapies: translating novel strategies from bench to bedside. Am J Kidney Dis 59: 444-451.

MacKinnon M, Shurraw S, Akbari A, Knoll GA, Jaffey J and Clark HD (2006). Combination therapy with an angiotensin receptor blocker and an ACE inhibitor in proteinuric renal disease: a systematic review of the efficacy and safety data. Am J Kidney Dis 48: 8-20.

MacPhee DJ (2010). Methodological considerations for improving Western blot analysis. J Pharmacol Toxicol Methods 61: 171-177.

Magwood JS, Lebby A, Chen B, Kessler S, Norris L and Bennett CL (2013). Emerging drugs for treatment of anemia of chronic kidney disease. Expert Opin Emerg Drugs.

Mancia G, Fagard R, Narkiewicz K, Redon J, Zanchetti A, Bohm M, Christiaens T, Cifkova R, De Backer G, Dominiczak A, Galderisi M, Grobbee DE, Jaarsma T, Kirchhof P, Kjeldsen SE, Laurent S, Manolis AJ, Nilsson PM, Ruilope LM, Schmieder RE, Sirnes PA, Sleight P, Viigimaa M, Waeber B and Zannad F (2013). 2013 ESH/ESC Guidelines for the management of arterial hypertension: the Task Force for the management of arterial hypertension of the European Society of Hypertension (ESH) and of the European Society of Cardiology (ESC). J Hypertens 31: 1281-1357.

Marco MP, Craver L, Betriu A, Belart M, Fibla J and Fernandez E (2003). Higher impact of mineral metabolism on cardiovascular mortality in a European hemodialysis population. Kidney Int Suppl: S111-114.

Martin KJ, Gonzalez EA, Gellens M, Hamm LL, Abboud H and Lindberg J (1998). 19-Nor-1-alpha-25-dihydroxyvitamin D_2 (Paricalcitol) safely and effectively reduces the levels of intact parathyroid hormone in patients on hemodialysis. J Am Soc Nephrol 9: 1427-1432.

Mazzali M, Hughes J, Kim YG, Jefferson JA, Kang DH, Gordon KL, Lan HY, Kivlighn S and Johnson RJ (2001). Elevated uric acid increases blood pressure in the rat by a novel crystal-independent mechanism. Hypertension 38: 1101-1106.

Mazzali M, Kanellis J, Han L, Feng L, Xia YY, Chen Q, Kang DH, Gordon KL, Watanabe S, Nakagawa T, Lan HY and Johnson RJ (2002). Hyperuricemia induces a primary renal arteriolopathy in rats by a blood pressure-independent mechanism. Am J Physiol Renal Physiol 282: F991-997.

McBride A, Lathon SC, Boehmer L, Augustin KM, Butler SK and Westervelt P (2013). Comparative evaluation of single fixed dosing and weight-based dosing of rasburicase for tumor lysis syndrome. Pharmacotherapy 33: 295-303.

Mendis S, Lindholm LH, Anderson SG, Alwan A, Koju R, Onwubere BJ, Kayani AM, Abeysinghe N, Duneas A, Tabagari S, Fan W, Sarraf-Zadegan N, Nordet P, Whitworth J and Heagerty A (2011). Total cardiovascular risk approach to improve efficiency of cardiovascular prevention in resource constrain settings. J Clin Epidemiol 64: 1451-1462.

Merke J, Hugel U, Zlotkowski A, Szabo A, Bommer J, Mall G and Ritz E (1987). Diminished parathyroid $1,25(OH)_2D_3$ receptors in experimental uremia. Kidney Int 32: 350-353.

Messerli FH, Frohlich ED, Dreslinski GR, Suarez DH and Aristimuno GG (1980). Serum uric acid in essential hypertension: an indicator of renal vascular involvement. Ann Intern Med 93: 817-821.

Mezzano S, Droguett A, Burgos ME, Ardiles LG, Flores CA, Aros CA, Caorsi I, Vio CP, Ruiz-Ortega M and Egido J (2003). Renin-angiotensin system activation and interstitial inflammation in human diabetic nephropathy. Kidney Int Suppl: S64-70.

Mihai R and Farndon JR (2000). Parathyroid disease and calcium metabolism. Br J Anaesth 85: 29-43.

Miyata N, Park F, Li XF and Cowley AW, Jr. (1999). Distribution of angiotensin AT_1 and AT_2 receptor subtypes in the rat kidney. Am J Physiol 277: F437-446.

Miyazaki M and Takai S (2006). Tissue angiotensin II generating system by angiotensin-converting enzyme and chymase. J Pharmacol Sci 100: 391-397.

Mizobuchi M, Hatamura I, Ogata H, Saji F, Uda S, Shiizaki K, Sakaguchi T, Negi S, Kinugasa E, Koshikawa S and Akizawa T (2004). Calcimimetic compound upregulates decreased calcium-sensing receptor expression level in parathyroid glands of rats with chronic renal insufficiency. J Am Soc Nephrol 15: 2579-2587.

Moncada S and Higgs EA (1991). Endogenous nitric oxide: physiology, pathology and clinical relevance. Eur J Clin Invest 21: 361-374.

Moncada S and Higgs A (1993). The L-arginine-nitric oxide pathway. N Engl J Med 329: 2002-2012.

Morishita Y and Kusano E (2013). Direct Renin inhibitor: aliskiren in chronic kidney disease. Nephrourol Mon 5: 668-672.

Morris ST, McMurray JJ, Spiers A and Jardine AG (2001). Impaired endothelial function in isolated human uremic resistance arteries. Kidney Int 60: 1077-1082.

Morrison AB (1962). Experimentally induced chronic renal insufficiency in the rat. Lab Invest 11: 321-332.

Morrison AB and Howard RM (1966). The functional capacity of hypertrophied nephrons. Effect of partial nephrectomy on the clearance of inulin and PAH in the rat. J Exp Med 123: 829-844.

Mougenot N, Lesnik P, Ramirez-Gil JF, Nataf P, Diczfalusy U, Chapman MJ and Lechat P (1997). Effect of the oxidation state of LDL on the modulation of arterial vasomotor response in vitro. Atherosclerosis 133: 183-192.

Muntner P, Anderson A, Charleston J, Chen Z, Ford V, Makos G, O'Connor A, Perumal K, Rahman M, Steigerwalt S, Teal V, Townsend R, Weir M and Wright JT, Jr. (2010). Hypertension awareness, treatment, and control in adults with CKD: results from the Chronic Renal Insufficiency Cohort (CRIC) Study. Am J Kidney Dis 55: 441-451.

Muscelli E, Natali A, Bianchi S, Bigazzi R, Galvan AQ, Sironi AM, Frascerra S, Ciociaro D and Ferrannini E (1996). Effect of insulin on renal sodium and uric acid handling in essential hypertension. Am J Hypertens 9: 746-752.

Nagase M and Fujita T (2008). Aldosterone and glomerular podocyte injury. Clin Exp Nephrol 12: 233-242.

Nakagawa T, Mazzali M, Kang DH, Kanellis J, Watanabe S, Sanchez-Lozada LG, Rodriguez-Iturbe B, Herrera-Acosta J and Johnson RJ (2003). Hyperuricemia causes glomerular hypertrophy in the rat. Am J Nephrol 23: 2-7.

Nakagawa T, Hu H, Zharikov S, Tuttle KR, Short RA, Glushakova O, Ouyang X, Feig DI, Block ER, Herrera-Acosta J, Patel JM and Johnson RJ (2006). A causal role for uric acid in fructose-induced metabolic syndrome. Am J Physiol Renal Physiol 290: F625-631.

Nakagawa T, Cirillo P, Sato W, Gersch M, Sautin Y, Roncal C, Mu W, Sanchez-Lozada LG and Johnson RJ (2008). The conundrum of hyperuricemia, metabolic syndrome, and renal disease. Intern Emerg Med 3: 313-318.

Nanes MS (2013). Phosphate wasting and fibroblast growth factor-23. Curr Opin Endocrinol Diabetes Obes 20: 523-531.

Navar LG, Von Thun AM, Zou L, el-Dahr SS and Mitchell KD (1995). Enhancement of intrarenal angiotensin II levels in 2 kidney 1 clip and angiotensin II induced hypertension. Blood Press Suppl 2: 88-92.

Navar LG (1997). The kidney in blood pressure regulation and development of hypertension. Med Clin North Am 81: 1165-1198.

Navar LG and Nishiyama A (2001). Intrarenal formation of angiotensin II. Contrib Nephrol: 1-15.

Navar LG, Harrison-Bernard LM, Nishiyama A and Kobori H (2002). Regulation of intrarenal angiotensin II in hypertension. Hypertension 39: 316-322.

Naveh-Many T, Marx R, Keshet E, Pike JW and Silver J (1990). Regulation of 1,25-dihydroxyvitamin D_3 receptor gene expression by 1,25-dihydroxyvitamin D_3 in the parathyroid in vivo. J Clin Invest 86: 1968-1975.

Naveh-Many T, Rahamimov R, Livni N and Silver J (1995). Parathyroid cell proliferation in normal and chronic renal failure rats. The effects of calcium, phosphate, and vitamin D. J Clin Invest 96: 1786-1793.

Nguyen Dinh Cat A and Touyz RM (2011). A new look at the renin-angiotensin system - Focusing on the vascular system. Peptides 32: 2141-2150.

Nguyen G, Delarue F, Burckle C, Bouzhir L, Giller T and Sraer JD (2002). Pivotal role of the renin/prorenin receptor in angiotensin II production and cellular responses to renin. J Clin Invest 109: 1417-1427.

Nguyen G (2007). The (pro)renin receptor: pathophysiological roles in cardiovascular and renal pathology. Curr Opin Nephrol Hypertens 16: 129-133.

Nichols M, Townsend N, Scarborough P and Rayner M (2013). Cardiovascular disease in Europe: epidemiological update. Eur Heart J 34: 3028-3034.

Novick AC, Gephardt G, Guz B, Steinmuller D and Tubbs RR (1991). Long-term follow-up after partial removal of a solitary kidney. N Engl J Med 325: 1058-1062.

Oda M, Satta Y, Takenaka O and Takahata N (2002). Loss of urate oxidase activity in hominoids and its evolutionary implications. Mol Biol Evol 19: 640-653.

Ohara Y, Peterson TE and Harrison DG (1993). Hypercholesterolemia increases endothelial superoxide anion production. J Clin Invest 91: 2546-2551.

Okamoto K, Eger BT, Nishino T, Kondo S, Pai EF and Nishino T (2003). An extremely potent inhibitor of xanthine oxidoreductase. Crystal structure of the enzyme-inhibitor complex and mechanism of inhibition. J Biol Chem 278: 1848-1855.

Okamura DM, Bahrami NM, Ren S, Pasichnyk K, Williams JM, Gangoiti JA, Lopez-Guisa JM, Yamaguchi I, Barshop BA, Duffield JS and Eddy AA (2013). Cysteamine Modulates Oxidative Stress and Blocks Myofibroblast Activity in CKD. J Am Soc Nephrol.

Olauson H and Larsson TE (2013). FGF23 and Klotho in chronic kidney disease. Curr Opin Nephrol Hypertens 22: 397-404.

Olson JL and Heptinstall RH (1988). Nonimmunologic mechanisms of glomerular injury. Lab Invest 59: 564-578.

Pascual E and Sivera F (2007). Therapeutic advances in gout. Curr Opin Rheumatol 19: 122-127.

Patetsios P, Song M, Shutze WP, Pappas C, Rodino W, Ramirez JA and Panetta TF (2001). Identification of uric acid and xanthine oxidase in atherosclerotic plaque. Am J Cardiol 88: 188-191, A186.

Paul M, Poyan Mehr A and Kreutz R (2006). Physiology of local renin-angiotensin systems. Physiol Rev 86: 747-803.

Pinheiro SV, Ferreira AJ, Kitten GT, da Silveira KD, da Silva DA, Santos SH, Gava E, Castro CH, Magalhaes JA, da Mota RK, Botelho-Santos GA, Bader M, Alenina N, Santos RA and Simoes e Silva AC (2009). Genetic deletion of the angiotensin-(1-7) receptor Mas leads to glomerular hyperfiltration and microalbuminuria. Kidney Int 75: 1184-1193.

Praetorius E and Poulsen H (1953). Enzymatic determination of uric acid; with detailed directions. Scand J Clin Lab Invest 5: 273-280.

Prescott G, Silversides DW and Reudelhuber TL (2002). Tissue activity of circulating prorenin. Am J Hypertens 15: 280-285.

Puca AA, Carrizzo A, Villa F, Ferrario A, Casaburo M, Maciag A and Vecchione C (2013). Vascular ageing: the role of oxidative stress. Int J Biochem Cell Biol 45: 556-559.

Purkerson ML, Hoffsten PE and Klahr S (1976). Pathogenesis of the glomerulopathy associated with renal infarction in rats. Kidney Int 9: 407-417.

Pörsti I, Bara AT, Busse R and Hecker M (1994). Release of nitric oxide by angiotensin-(1-7) from porcine coronary endothelium: implications for a novel angiotensin receptor. Br J Pharmacol 111: 652-654.

Pörsti I, Fan M, Kööbi P, Jolma P, Kalliovalkama J, Vehmas TI, Helin H, Holthöfer H, Mervaala E, Nyman T and Tikkanen I (2004). High calcium diet down-regulates kidney angiotensin-converting enzyme in experimental renal failure. Kidney Int 66: 2155-2166.

Quarles LD (2012). Role of FGF23 in vitamin D and phosphate metabolism: implications in chronic kidney disease. Exp Cell Res 318: 1040-1048.

Rabelink TJ and Koomans HA (1997). Endothelial function and the kidney. An emerging target for cardiovascular therapy. Drugs 53 Suppl 1: 11-19.

Raggi P, Boulay A, Chasan-Taber S, Amin N, Dillon M, Burke SK and Chertow GM (2002). Cardiac calcification in adult hemodialysis patients. A link between end-stage renal disease and cardiovascular disease? J Am Coll Cardiol 39: 695-701.

Raij L (2001). Workshop: hypertension and cardiovascular risk factors: role of the angiotensin II-nitric oxide interaction. Hypertension 37: 767-773.

Ramsay LE, Auty RM, Horth CE, Levine D, Shelton JR and Branch RA (1975). Plasma uric acid concentration related to the urinary excretion of aldosterone and of electrolytes in normal subjects. Clin Sci Mol Med 49: 613-616.

Remuzzi G, Perico N, Macia M and Ruggenenti P (2005). The role of renin-angiotensin-aldosterone system in the progression of chronic kidney disease. Kidney Int Suppl: S57-65.

Renkema KY, Alexander RT, Bindels RJ and Hoenderop JG (2008). Calcium and phosphate homeostasis: concerted interplay of new regulators. Ann Med 40: 82-91.

Rettig R, Folberth C, Kopf D, Stauss H and Unger T (1990). Role of the kidney in the pathogenesis of primary hypertension. Clin Exp Hypertens A 12: 957-1002.

Reynolds JL, Skepper JN, McNair R, Kasama T, Gupta K, Weissberg PL, Jahnen-Dechent W and Shanahan CM (2005). Multifunctional roles for serum protein fetuin-a in inhibition of human vascular smooth muscle cell calcification. J Am Soc Nephrol 16: 2920-2930.

Ridao N, Luno J, Garcia de Vinuesa S, Gomez F, Tejedor A and Valderrabano F (2001). Prevalence of hypertension in renal disease. Nephrol Dial Transplant 16 Suppl 1: 70-73.

Riediger F, Quack I, Qadri F, Hartleben B, Park JK, Potthoff SA, Sohn D, Sihn G, Rousselle A, Fokuhl V, Maschke U, Purfurst B, Schneider W, Rump LC, Luft FC, Dechend R, Bader M, Huber TB, Nguyen G and Muller DN (2011). Prorenin receptor is essential for podocyte autophagy and survival. J Am Soc Nephrol 22: 2193-2202.

Rivard C, Thomas J, Lanaspa MA and Johnson RJ (2013). Sack and sugar, and the aetiology of gout in England between 1650 and 1900. Rheumatology (Oxford) 52: 421-426.

Rodriguez ME, Almaden Y, Canadillas S, Canalejo A, Siendones E, Lopez I, Aguilera-Tejero E, Martin D and Rodriguez M (2007). The calcimimetic R-568 increases vitamin D receptor expression in rat parathyroid glands. Am J Physiol Renal Physiol 292: F1390-1395.

Roman RJ (2002). P-450 metabolites of arachidonic acid in the control of cardiovascular function. Physiol Rev 82: 131-185.

Rosamond W, Flegal K, Furie K, Go A, Greenlund K, Haase N, Hailpern SM, Ho M, Howard V, Kissela B, Kittner S, Lloyd-Jones D, McDermott M, Meigs J, Moy C, Nichol G, O'Donnell C, Roger V, Sorlie P, Steinberger J, Thom T, Wilson M and Hong Y (2008). Heart disease and stroke statistics - 2008 update: a report from the American Heart Association Statistics Committee and Stroke Statistics Subcommittee. Circulation 117: e25-146.

Rossi P, Riutta A, Kuukasjärvi P, Vehmas T, Mucha I and Salenius JP (2004). Revascularization decreases 8-isoprostaglandin F_2alpha excretion in chronic lower limb ischemia. Prostaglandins Leukot Essent Fatty Acids 71: 97-101.

Rostand SG and Drüeke TB (1999). Parathyroid hormone, vitamin D, and cardiovascular disease in chronic renal failure. Kidney Int 56: 383-392.

Rule AD, Rodeheffer RJ, Larson TS, Burnett JC, Jr., Cosio FG, Turner ST and Jacobsen SJ (2006). Limitations of estimating glomerular filtration rate from serum creatinine in the general population. Mayo Clin Proc 81: 1427-1434.

Ruperez M, Lorenzo O, Blanco-Colio LM, Esteban V, Egido J and Ruiz-Ortega M (2003). Connective tissue growth factor is a mediator of angiotensin II-induced fibrosis. Circulation 108: 1499-1505.

Saito I, Saruta T, Eguchi T, Kondo K, Nakamura R and Matsuki S (1978a). Role of angiotensin III in the regulation of blood pressure, plasma aldosterone and plasma renin activity in rabbit. Acta Endocrinol (Copenh) 89: 132-141.

Saito I, Saruta T, Kondo K, Nakamura R, Oguro T, Yamagami K, Ozawa Y and Kato E (1978b). Serum uric acid and the renin-angiotensin system in hypertension. J Am Geriatr Soc 26: 241-247.

Salonen T, Reina T, Oksa H, Rissanen P and Pasternack A (2007). Alternative strategies to evaluate the cost-effectiveness of peritoneal dialysis and hemodialysis. Int Urol Nephrol 39: 289-298.

Sanchez-Lozada LG, Tapia E, Avila-Casado C, Soto V, Franco M, Santamaria J, Nakagawa T, Rodriguez-Iturbe B, Johnson RJ and Herrera-Acosta J (2002). Mild hyperuricemia induces glomerular hypertension in normal rats. Am J Physiol Renal Physiol 283: F1105-1110.

Sanchez-Lozada LG, Tapia E, Santamaria J, Avila-Casado C, Soto V, Nepomuceno T, Rodriguez-Iturbe B, Johnson RJ and Herrera-Acosta J (2005). Mild hyperuricemia induces vasoconstriction and maintains glomerular hypertension in normal and remnant kidney rats. Kidney Int 67: 237-247.

Sanchez-Lozada LG, Tapia E, Jimenez A, Bautista P, Cristobal M, Nepomuceno T, Soto V, Avila-Casado C, Nakagawa T, Johnson RJ, Herrera-Acosta J and Franco M (2007). Fructose-induced metabolic syndrome is associated with glomerular hypertension and renal microvascular damage in rats. Am J Physiol Renal Physiol 292: F423-429.

Sanchez-Lozada LG, Tapia E, Soto V, Avila-Casado C, Franco M, Zhao L and Johnson RJ (2008). Treatment with the xanthine oxidase inhibitor febuxostat lowers uric acid and alleviates systemic and glomerular hypertension in experimental hyperuricaemia. Nephrol Dial Transplant 23: 1179-1185.

Santos CX, Anjos EI and Augusto O (1999). Uric acid oxidation by peroxynitrite: multiple reactions, free radical formation, and amplification of lipid oxidation. Arch Biochem Biophys 372: 285-294.

Santos RA, Simoes e Silva AC, Maric C, Silva DM, Machado RP, de Buhr I, Heringer-Walther S, Pinheiro SV, Lopes MT, Bader M, Mendes EP, Lemos VS, Campagnole-Santos MJ, Schultheiss HP, Speth R and Walther T (2003). Angiotensin-(1-7) is an endogenous ligand for the G protein-coupled receptor Mas. Proc Natl Acad Sci U S A 100: 8258-8263.

Sasser JM (2013). The emerging role of relaxin as a novel therapeutic pathway in the treatment of chronic kidney disease. Am J Physiol Regul Integr Comp Physiol 305: R559-565.

Sautin YY, Nakagawa T, Zharikov S and Johnson RJ (2007). Adverse effects of the classic antioxidant uric acid in adipocytes: NADPH oxidase-mediated oxidative/nitrosative stress. Am J Physiol Cell Physiol 293: C584-596.

Schainuck LI, Striker GE, Cutler RE and Benditt EP (1970). Structural-functional correlations in renal disease. II. The correlations. Hum Pathol 1: 631-641.

Schiffl H, Fricke H and Sitter T (1993). Hypertension secondary to early-stage kidney disease: the pathogenetic role of altered cytosolic calcium (Ca2+) homeostasis of vascular smooth muscle cells. Am J Kidney Dis 21: 51-57.

Schmidt BM and Schmieder RE (2003). Aldosterone-induced cardiac damage: focus on blood pressure independent effects. Am J Hypertens 16: 80-86.

Schmidt BM, Sammer U, Fleischmann I, Schlaich M, Delles C and Schmieder RE (2006). Rapid nongenomic effects of aldosterone on the renal vasculature in humans. Hypertension 47: 650-655.

Schwarzenbach G (1955). The complexones and their analytical application. Analyst 80: 713-729.

Sealey JE, Glorioso N, Itskovitz J and Laragh JH (1986). Prorenin as a reproductive hormone. New form of the renin system. Am J Med 81: 1041-1046.

Sealey JE, Blumenfeld JD, Bell GM, Pecker MS, Sommers SC and Laragh JH (1988). On the renal basis for essential hypertension: nephron heterogeneity with discordant renin secretion and sodium excretion causing a hypertensive vasoconstriction-volume relationship. J Hypertens 6: 763-777.

Shanahan CM and Weissberg PL (1999). Smooth muscle cell phenotypes in atherosclerotic lesions. Curr Opin Lipidol 10: 507-513.

Shanahan CM (2013). Mechanisms of vascular calcification in CKD - evidence for premature ageing? Nat Rev Nephrol 9: 661-670.

Sherman RA (2007). Dietary phosphate restriction and protein intake in dialysis patients: a misdirected focus. Semin Dial 20: 16-18.

Shi Y, Evans JE and Rock KL (2003). Molecular identification of a danger signal that alerts the immune system to dying cells. Nature 425: 516-521.

Shimamura T and Morrison AB (1975). A progressive glomerulosclerosis occurring in partial five-sixths nephrectomized rats. Am J Pathol 79: 95-106.

Shroff R, Long DA and Shanahan C (2013). Mechanistic insights into vascular calcification in CKD. J Am Soc Nephrol 24: 179-189.

Shultz PJ (1992). An emerging role for endothelin in renal disease. J Lab Clin Med 119: 448-449.

Silver J, Kilav R and Naveh-Many T (2002). Mechanisms of secondary hyperparathyroidism. Am J Physiol Renal Physiol 283: F367-376.

Silver J and Naveh-Many T (2009). Phosphate and the parathyroid. Kidney Int 75: 898-905.

Simoes e Silva AC and Flynn JT (2012). The renin-angiotensin-aldosterone system in 2011: role in hypertension and chronic kidney disease. Pediatr Nephrol 27: 1835-1845.

Simoes e Silva AC, Silveira KD, Ferreira AJ and Teixeira MM (2013). ACE2, angiotensin-(1-7) and Mas receptor axis in inflammation and fibrosis. Br J Pharmacol 169: 477-492.

Siragy HM and Carey RM (1999). Protective role of the angiotensin AT_2 receptor in a renal wrap hypertension model. Hypertension 33: 1237-1242.

Sivera F, Andres M, Carmona L, Kydd AS, Moi J, Seth R, Sriranganathan M, van Durme C, van Echteld I, Vinik O, Wechalekar MD, Aletaha D, Bombardier C, Buchbinder R, Edwards CJ, Landewe RB, Bijlsma JW, Branco JC, Burgos-Vargas R, Catrina AI, Elewaut D, Ferrari AJ, Kiely P, Leeb BF, Montecucco C, Muller-Ladner U, Ostergaard M, Zochling J, Falzon L and van der Heijde DM (2014). Multinational evidence-based recommendations for the diagnosis and management of gout: integrating systematic literature review and expert opinion of a broad panel of rheumatologists in the 3e initiative. Ann Rheum Dis 73: 328-335.

Slatopolsky E, Dusso A and Brown AJ (1999). The role of phosphorus in the development of secondary hyperparathyroidism and parathyroid cell proliferation in chronic renal failure. Am J Med Sci 317: 370-376.

Slatopolsky E, Brown A and Dusso A (2001). Role of phosphorus in the pathogenesis of secondary hyperparathyroidism. Am J Kidney Dis 37: S54-57.

Slatopolsky E (2011). The intact nephron hypothesis: the concept and its implications for phosphate management in CKD-related mineral and bone disorder. Kidney Int Suppl: S3-8.

Smith HW (1951). The kidney: structure and function in health and disease. New York, Oxford University Press.

Souza-Barbosa LA, Ferreira-Melo SE, Ubaid-Girioli S, Arantes Nogueira E, Yugar-Toledo JC and Moreno H, Jr. (2006). Endothelial vascular function in hypertensive patients after renin-angiotensin system blockade. J Clin Hypertens (Greenwich) 8: 803-809.

Spitsin S and Koprowski H (2008). Role of uric acid in multiple sclerosis. Curr Top Microbiol Immunol 318: 325-342.

Squadrito GL, Cueto R, Splenser AE, Valavanidis A, Zhang H, Uppu RM and Pryor WA (2000). Reaction of uric acid with peroxynitrite and implications for the mechanism of neuroprotection by uric acid. Arch Biochem Biophys 376: 333-337.

Stavreus-Evers A, Parini P, Freyschuss B, Elger W, Reddersen G, Sahlin L and Eriksson H (2001). Estrogenic influence on the regulation of hepatic estrogen receptor-alpha and serum level of angiotensinogen in female rats. J Steroid Biochem Mol Biol 78: 83-88.

Stewen P, Mervaala E, Karppanen H, Nyman T, Saijonmaa O, Tikkanen I and Fyhrquist F (2003). Sodium load increases renal angiotensin type 1 receptors and decreases bradykinin type 2 receptors. Hypertens Res 26: 583-589.

Stevens PE and Levin A (2013). Evaluation and management of chronic kidney disease: synopsis of the kidney disease: improving global outcomes 2012 clinical practice guideline. Ann Intern Med 158: 825-830.

Sundstrom J, Sullivan L, D'Agostino RB, Levy D, Kannel WB and Vasan RS (2005). Relations of serum uric acid to longitudinal blood pressure tracking and hypertension incidence. Hypertension 45: 28-33.

Takano Y, Hase-Aoki K, Horiuchi H, Zhao L, Kasahara Y, Kondo S and Becker MA (2005). Selectivity of febuxostat, a novel non-purine inhibitor of xanthine oxidase/xanthine dehydrogenase. Life Sci 76: 1835-1847.

Takeda E, Yamamoto H, Nashiki K, Sato T, Arai H and Taketani Y (2004). Inorganic phosphate homeostasis and the role of dietary phosphorus. J Cell Mol Med 8: 191-200.

Takeda Y, Yoneda T, Demura M, Miyamori I and Mabuchi H (2000). Cardiac aldosterone production in genetically hypertensive rats. Hypertension 36: 495-500.

Talreja H, Ruzicka M and McCormick BB (2013). Pharmacologic treatment of hypertension in patients with chronic kidney disease. Am J Cardiovasc Drugs 13: 177-188.

Tan X, He W and Liu Y (2009). Combination therapy with paricalcitol and trandolapril reduces renal fibrosis in obstructive nephropathy. Kidney Int 76: 1248-1257.

Tejwani V and Qian Q (2013). Calcium regulation and bone mineral metabolism in elderly patients with chronic kidney disease. Nutrients 5: 1913-1936.

Terada LS, Guidot DM, Leff JA, Willingham IR, Hanley ME, Piermattei D and Repine JE (1992). Hypoxia injures endothelial cells by increasing endogenous xanthine oxidase activity. Proc Natl Acad Sci U S A 89: 3362-3366.

Terkeltaub R (2006). Gout in 2006: the perfect storm. Bull NYU Hosp Jt Dis 64: 82-86.

Thuraisingham RC, Roberts NB, Wilkes M, New DI, Mendes-Ribeiro AC, Dodd SM and Yaqoob MM (2002). Altered L-arginine metabolism results in increased nitric oxide release from uraemic endothelial cells. Clin Sci (Lond) 103: 31-41.

Thuraisingham RC and Yaqoob MM (2003). Oxidative consumption of nitric oxide: a potential mediator of uremic vascular disease. Kidney Int Suppl: S29-32.

Tikellis C, Johnston CI, Forbes JM, Burns WC, Burrell LM, Risvanis J and Cooper ME (2003). Characterization of renal angiotensin-converting enzyme 2 in diabetic nephropathy. Hypertension 41: 392-397.

Tonelli M, Pannu N and Manns B (2010). Oral phosphate binders in patients with kidney failure. N Engl J Med 362: 1312-1324.

Tonelli M (2013). Serum phosphorus in people with chronic kidney disease: you are what you eat. Kidney Int 84: 871-873.

Tsuji K, Maeda T, Kawane T, Matsunuma A and Horiuchi N (2010). Leptin stimulates fibroblast growth factor 23 expression in bone and suppresses renal 1alpha,25-dihydroxyvitamin D_3 synthesis in leptin-deficient mice. J Bone Miner Res 25: 1711-1723.

Tufro-McReddie A and Gomez RA (1993). Ontogeny of the renin-angiotensin system. Semin Nephrol 13: 519-530.

Tyralla K and Amann K (2003). Morphology of the heart and arteries in renal failure. Kidney Int Suppl: S80-83.

Tyson KL, Reynolds JL, McNair R, Zhang Q, Weissberg PL and Shanahan CM (2003). Osteo/chondrocytic transcription factors and their target genes exhibit distinct patterns of expression in human arterial calcification. Arterioscler Thromb Vasc Biol 23: 489-494.

Wagner EM (2013). Monitoring gene expression: quantitative real-time rt-PCR. Methods Mol Biol 1027: 19-45.

van Guldener C, Lambert J, Janssen MJ, Donker AJ and Stehouwer CD (1997). Endothelium-dependent vasodilatation and distensibility of large arteries in chronic haemodialysis patients. Nephrol Dial Transplant 12 Suppl 2: 14-18.

Wang HX, Zhang QF, Zeng XJ, Wang W, Tang CS and Zhang LK (2010). Effects of angiotensin III on protein, DNA, and collagen synthesis of neonatal cardiomyocytes and cardiac fibroblasts in vitro. J Cardiovasc Pharmacol Ther 15: 393-402.

Wang SN and Hirschberg R (2000). Growth factor ultrafiltration in experimental diabetic nephropathy contributes to interstitial fibrosis. Am J Physiol Renal Physiol 278: F554-560.

Wang SN, LaPage J and Hirschberg R (2000). Role of glomerular ultrafiltration of growth factors in progressive interstitial fibrosis in diabetic nephropathy. Kidney Int 57: 1002-1014.

Ward HJ (1998). Uric acid as an independent risk factor in the treatment of hypertension. Lancet 352: 670-671.

Waring WS, Webb DJ and Maxwell SR (2000). Uric acid as a risk factor for cardiovascular disease. Qjm 93: 707-713.

Waring WS, Webb DJ and Maxwell SR (2001). Systemic uric acid administration increases serum antioxidant capacity in healthy volunteers. J Cardiovasc Pharmacol 38: 365-371.

Waring WS, Convery A, Mishra V, Shenkin A, Webb DJ and Maxwell SR (2003). Uric acid reduces exercise-induced oxidative stress in healthy adults. Clin Sci (Lond) 105: 425-430.

Waring WS, McKnight JA, Webb DJ and Maxwell SR (2006). Uric acid restores endothelial function in patients with type 1 diabetes and regular smokers. Diabetes 55: 3127-3132.

Watanabe S, Kang DH, Feng L, Nakagawa T, Kanellis J, Lan H, Mazzali M and Johnson RJ (2002). Uric acid, hominoid evolution, and the pathogenesis of salt-sensitivity. Hypertension 40: 355-360.

Watson AJ (1989). Adverse effects of therapy for the correction of anemia in hemodialysis patients. Semin Nephrol 9: 30-34.

Vaziri ND, Ni Z, Wang XQ, Oveisi F and Zhou XJ (1998). Downregulation of nitric oxide synthase in chronic renal insufficiency: role of excess PTH. Am J Physiol 274: F642-649.

Vaziri ND, Liang K and Parks JS (2001). Down-regulation of hepatic lecithin: cholesterol acyltransferase gene expression in chronic renal failure. Kidney Int 59: 2192-2196.

Vaziri ND, Ni Z, Oveisi F, Liang K and Pandian R (2002). Enhanced nitric oxide inactivation and protein nitration by reactive oxygen species in renal insufficiency. Hypertension 39: 135-141.

Weber MA, Black H, Bakris G, Krum H, Linas S, Weiss R, Linseman JV, Wiens BL, Warren MS and Lindholm LH (2009). A selective endothelin-receptor antagonist to reduce blood pressure in patients with treatment-resistant hypertension: a randomised, double-blind, placebo-controlled trial. Lancet 374: 1423-1431.

Weir CJ, Muir SW, Walters MR and Lees KR (2003). Serum urate as an independent predictor of poor outcome and future vascular events after acute stroke. Stroke 34: 1951-1956.

Williams JD and Coles GA (1994). Proteinuria--a direct cause of renal morbidity? Kidney Int 45: 443-450.

Wu XW, Lee CC, Muzny DM and Caskey CT (1989). Urate oxidase: primary structure and evolutionary implications. Proc Natl Acad Sci U S A 86: 9412-9416.

Wu XW, Muzny DM, Lee CC and Caskey CT (1992). Two independent mutational events in the loss of urate oxidase during hominoid evolution. J Mol Evol 34: 78-84.

Xiao L and Liu Y (2013). Chronic kidney disease: Fibrosis and anaemia in CKD--two beasts, one ancestor. Nat Rev Nephrol 9: 563-565.

Xiong M, Gong J, Liu Y, Xiang R and Tan X (2012). Loss of vitamin D receptor in chronic kidney disease: a potential mechanism linking inflammation to epithelial-to-mesenchymal transition. Am J Physiol Renal Physiol 303: F1107-1115.

Yang HC, Zuo Y and Fogo AB (2010). Models of chronic kidney disease. Drug Discov Today Dis Models 7: 13-19.

Ye P, Yang S, Zhang W, Lv Q, Cheng Q, Mei M, Luo T, Liu L, Chen S and Li Q (2013). Efficacy and tolerability of febuxostat in hyperuricemic patients with or without gout: a systematic review and meta-analysis. Clin Ther 35: 180-189.

Yu ZF, Bruce-Keller AJ, Goodman Y and Mattson MP (1998). Uric acid protects neurons against excitotoxic and metabolic insults in cell culture, and against focal ischemic brain injury in vivo. J Neurosci Res 53: 613-625.

Zhuo J, Ohishi M and Mendelsohn FA (1999). Roles of AT1 and AT2 receptors in the hypertensive Ren-2 gene transgenic rat kidney. Hypertension 33: 347-353.

Zoccali C (2008). Endothelial dysfunction in CKD: a new player in town? Nephrol Dial Transplant 23: 783-785.

Oxonic acid-induced hyperuricemia elevates plasma aldosterone in experimental renal insufficiency

Arttu Eräranta[a,b], Venla Kurra[c], Anna M. Tahvanainen[b], Tuija I. Vehmas[b,d], Peeter Kööbi[d,e], Päivi Lakkisto[f,g], Ilkka Tikkanen[f,h], Onni J. Niemelä[i], Jukka T. Mustonen[b,j] and Ilkka H. Pörsti[b,j]

Background **Hyperuricemia is associated with renal insufficiency and may predispose to Na^+ retention and hypertension. Whether hyperuricemia plays a causal role in the pathogenesis of cardiovascular disease remains controversial.**

Objective **We examined the effects of hyperuricemia on circulating and renal components of the renin–angiotensin–aldosterone system in experimental renal insufficiency.**

Methods **Three weeks after 5/6 nephrectomy or sham-operation, rats were put on 2.0% oxonic acid diet for 9 weeks. Blood pressure was monitored using tail-cuff, and blood, urine, and kidney samples were taken, as appropriate. Kidney angiotensin-converting enzyme , angiotensin-converting enzyme 2 and angiotensin II receptors (AT_{1R}, AT_{2R}) were examined using real-time reverse transcriptase-PCR and autoradiography.**

Results **Oxonic acid diet increased plasma uric acid by 80–90 μmol/l, while blood pressure was elevated only in hyperuricemic 5/6 nephrectomy rats (18 mmHg). Creatinine clearance was reduced by 60% in both 5/6 nephrectomy groups and by 25% in hyperuricemic Sham rats. The 5/6 nephrectomy group showed over 90% suppression of plasma renin activity, whereas the Sham + oxonic acid diet group showed 1.2 and 1.4-fold, and 5/6 nephrectomy + oxonic acid diet group 2.5 and 2.3-fold increases in plasma renin activity and plasma aldosterone, respectively. Hyperuricemia increased K^+ and decreased Na^+ excretion in Sham and 5/6 nephrectomy rats, leading to a more than 1.6-fold increase in urine K^+ to Na^+ ratio. No changes in kidney angiotensin-converting enzyme, angiotensin-converting enzyme 2, AT_{1R} or AT_{2R} were detected that could explain the hyperuricemia-induced alteration in Na^+–K^+ balance.**

Conclusion **As oxonic acid diet increased plasma renin activity, plasma aldosterone, and urine K^+ to Na^+ ratio, these changes may play a significant role in the harmful cardiovascular actions of hyperuricemia. *J Hypertens* 26:1661–1668 © 2008 Wolters Kluwer Health | Lippincott Williams & Wilkins.**

Journal of Hypertension 2008, **26**:1661–1668

Keywords: chronic renal insufficiency, renin–angiotensin–aldosterone system, uric acid

Abbreviations: ACE, angiotensin-converting enzyme; ACE2, angiotensin-converting enzyme 2; Ang II, angiotensin II; AT_{1aR}, angiotensin II type 1A receptor; AT_{1R}, angiotensin II type 1 receptor; AT_{2R}, angiotensin II type 2 receptor; CRI, chronic renal insufficiency; NX, 5/6 nephrectomy; Oxo, oxonic acid; PRA, plasma renin activity; RAS, the renin-angiotensin system

[a]Institute of Medical Technology, [b]Department of Internal Medicine, [c]Medical School, [d]Department of Pharmacological Sciences, [e]Department of Ophtalmology, University of Tampere, Tampere, [f]Minerva Institute for Medical Research, [g]Department of Clinical Chemistry, [h]Department of Medicine, Helsinki University Central Hospital, Helsinki, [i]Department of Laboratory Medicine, Seinäjoki Central Hospital and University of Tampere and [j]Department of Internal Medicine, Tampere University Hospital, Tampere, Finland

Correspondence to Ilkka Pörsti, MD, Medical School, Department of Internal Medicine, FIN-33014 University of Tampere, Tampere, Finland
Tel: +358 3 3116 6010; fax: +358 3 3116 6164; e-mail: ilkka.porsti@uta.fi

Received 8 October 2007 **Revised** 31 March 2008
Accepted 3 April 2008

Introduction

Hyperuricemia is a typical finding in patients with hypertension, metabolic syndrome and renal disease [1,2]. Uric acid is generated during purine metabolism and, in most mammals, is further metabolized to allantoin by uricase (urate oxidase). In humans, the uricase gene was rendered nonfunctional during evolution, causing significant increases in serum uric acid [3]. This may have helped to maintain blood pressure (BP) under low-sodium intake, as high serum uric acid levels are associated with increased proximal tubular sodium reabsorption in men [4]. However, the relatively recent switch to high-salt intake coupled with high serum uric acid may be a culprit in the current epidemic of hypertension [5]. Elevated uric acid correlates with increased cardiovascular mortality [6], but the contribution of uric acid to the pathogenesis of cardiovascular disease remains controversial [1].

Experimental studies [7–12], in which rats were made hyperuricemic by the ingestion of uricase inhibitor oxonic acid (2.0% in diet for 4–7 weeks), have suggested that high uric acid may play a causal role in the development of hypertension. The oxonic acid model of hyperuricemia

0263-6352 © 2008 Wolters Kluwer Health | Lippincott Williams & Wilkins

has been shown to induce preglomerular arteriolar disease leading to tubular ischemia, interstitial infiltration of lymphocytes and macrophages, oxidant generation, and local vasoconstriction. These changes are associated with a decreased glomerular filtration rate and thus sodium filtration and increased sodium reabsorption, thus resulting in salt sensitivity [13]. Additionally, ischemia may increase uric acid synthesis, whereas release of lactate can block uric acid secretion in the proximal tubule [1]. As the renal microvascular disease progresses, hypertension may switch to a salt-sensitive form independent of uric acid levels and is driven by the kidney [5,14].

The initial increase in BP in hyperuricemic rats is associated with an increased number of renin-positive cells in the juxtaglomerular apparatus [14], and a direct correlation of serum uric acid with the percentage of renin-positive juxtaglomerular cells has been reported [8]. A close correlation between plasma renin activity (PRA) and serum uric acid has also been found in patients with essential hypertension [15] and PRA has been found to be higher in hyperuricemic than normouricemic children [16]. Plasma uric acid has also been reported to correlate positively with aldosterone excretion to the urine in healthy men [17].

The detrimental effects of uric acid may be mediated via enhanced renin release and, in experimental models, the renal vasculopathy and hypertension can be prevented by the blockade of the renin–angiotensin system (RAS) [8,9,12]. However, information about the circulating PRA and aldosterone concentration in the oxonic acid model is lacking. Therefore, the present study aimed to examine the effects of oxonic acid-induced hyperuricemia on components of the RAS in the circulation and in renal tissue, with a special interest in putative changes of plasma aldosterone concentration.

Methods

Animals and treatment

Male Sprague–Dawley rats were used ($n = 48$) with free access to water and food pellets (Lactamin R34, Analy-Cen, Lindköping, Sweden). The chow contained 0.9% calcium, 0.8% phosphorus, 0.27% sodium, 0.2% magnesium, 0.6% potassium, 12550 kJ/kg energy, 16.5% protein, 4.0% fat, 58% nitrogen-free extract, 3.5% fiber, 6.0% ash, and 10% water. Surgery was performed at 8 weeks of age: 5/6 nephrectomy (NX) was carried out by removal of upper and lower poles of the left kidney and the whole right kidney [18,19], while sham-operation was performed by kidney decapsulation. Anesthesia, antibiotics, postoperative pain relief, and measurement of systolic BP by tail-cuff were as previously reported [18,19].

Three weeks after NX (rat age 11 weeks), the animals were divided into four groups so that systolic BPs and body weights in the Sham, Sham + oxonic acid diet (Oxo), and NX and NX + Oxo groups, respectively, ($n = 12$ in each) were similar. After division, the Sham + Oxo and NX + Oxo rats were switched to chow containing additional 2.0% oxonic acid.

These diets continued for 9 weeks, and 24-h fluid consumption and urine output were measured during the last study week. The rats were anesthetized (urethane 1.3 g/kg) and blood samples from cannulated carotid artery were drawn with EDTA and heparin as anticoagulants, as appropriate. Blood samples were not obtained from one NX and three Sham rats due to cardiac arrest during anesthesia. The hearts and the kidneys were removed and weighed. A kidney half from each rat was snap-frozen in isopentane at −40°C and stored at −80°C. The experimental design of the study was approved by the Animal Experimentation Committee of the University of Tampere and the Provincial Government of Western Finland Department of Social Affairs and Health, Finland. The investigation conforms to the Guiding Principles for Research Involving Animals.

In-vitro autoradiography

Frozen kidney sections (20 μm thick) were cut on a cryostat at −17°C, thaw mounted onto Super Frost R Plus slides (Menzel-Gläser, Braunschweig, Germany), dried in a desiccator under reduced pressure at 4°C overnight, and stored at −80°C with silica gel until further processing [20].

Angiotensin-converting enzyme autoradiography

A tyrosyl residue of lisinopril (MK351A, Merck, Sharp & Dohme Research Laboratories, West Point, Pennsylvania, USA) was iodinated by chloramine T method, purified on SP-Sephadex C-25 column (Pharmacia, Piscataway, New Jersey, USA), and then a previously described technique was applied [20,21]. Kidney sections were preincubated for 15 min at room temperature (RT) in 10 mmol/l sodium phosphate buffer, pH 7.4, containing 150 mmol/l NaCl and 0.2% bovine serum albumin (BSA), followed by incubation for 1 h at RT in fresh volume of the same buffer containing 0.3 μCi/ml of ^{125}I-351A. Nonspecific binding was determined in parallel incubations in the same buffer containing 1 mmol/l Na_2-EDTA. After incubation, the sections were washed four times for 1 min in ice-cold buffer without BSA and ^{125}I-351A to remove unbound radioligand and dried under a stream of cool air. For quantification of ACE binding, the sections were placed on a Fuji Imaging Plate BAS-TP2025 (Tamro, Finland) for 3 h. The optical densities were quantified by an image analysis system (AIDA 2D densitometry) coupled to FUJIFILM BAS-5000 phosphoimager (Tamro, Finland) from four kidney sections per rat, six representative areas per section, altogether 24 analyses per each kidney. Specific binding was calculated as total binding minus nonspecific binding.

Table 1 Primers and probes used in real-time reverse transcriptase-PCR amplification

Gene	Primer nucleotide sequence	Probe sequence
ACE	Forward 5′-GGAGACGACTTACAGTGTAGCC-3′ [24] Reverse 5′-CACACCCAAAGCAATTCTTC-3′ [24]	
AT_{1aR}	Forward 5′-GGCAGCCTCTGACTAAATGGC-3′ Reverse 5′-ACGGCTTTGCTTGGTTACTCC-3′	
ACE2	Forward 5′-ACCCTTCTTACATCAGCCCTACTG-3′ [25] Reverse 5′-TGTCCAAAACCTACCCCACATAT-3′ [25]	5′FAM-ATGCCTCCCTGCTCATTTGCTTGGT-TAMRA [25]
AT_{2R}	Forward 5′-TGTCTGTCCTCATTGCCAACA-3′ Reverse 5′-TTCATTAAGGCAATCCCAGCA-3′	5′FAM-TCAGAACCATTGAATACTT-MGB

ACE, angiotensin-converting enzyme.

AT_{1R} and AT_{2R} autoradiography

Sar^1,Ile^8-angiotensin II (Ang II) (Sigma, St Louis, Missouri, USA) was iodinated by chloramine T method and purified on a Sep-Pack C18 cartridge with methanolic gradient elution. Autoradiographic quantification of angiotensin receptors with [^{125}I]-Sar^1,Ile^8-Ang II was performed using a modification [22] of a previously described method [23]. Kidney sections were preincubated for 15 min at RT in 10 mmol/l sodium phosphate buffer, pH 7.4, containing 150 mmol/l NaCl, 5 mmol/l Na_2-EDTA, and 0.2% BSA, followed by a 1 h incubation at 37°C in fresh volume of the same buffer containing 0.2 μCi/ml of ^{125}I-[Sar^1,Ile^8]Ang II. Nonspecific binding was determined in the presence of 1 μmol/l unlabelled Ang II (Sigma). The density of AT_{1R} was determined in presence of the AT_{2R} antagonist PD 123 313 (10 μmol/l) and the density of AT_{2R} in presence of the AT_{1R} antagonist losartan (10 μmol/l). After incubation, the sections were washed four times for 1 min in ice-cold buffer without BSA and radioligand and dried under stream of cool air. The optical densities of angiotensin receptor binding from 10 kidney sections per rat were quantified as described above for ACE from six representative cortical and six medullary areas per each section: four sections were used for total specific binding, two sections for AT_{1R} binding, two sections for AT_{2R} binding, and two sections for nonspecific binding.

The outcome in each group was related to the mean value of the Sham group, except for the medullary:cortical AT_{1R} density ratio, in which the respective densities in each rat kidney were related to each other.

Real-time quantitative reverse transcriptase-PCR

Total RNA was isolated from rat kidney tissue using Trizol reagent (Invitrogen, Carlsbad, California, USA) and reverse transcription of RNA was performed using M-MLV reverse transcriptase (Invitrogen) according to the manufacturer's instructions.

The expression of ACE, ACE2, AT_{1aR}, and AT_{2R} mRNAs was studied using real-time quantitative reverse transcriptase-PCR. PCR was performed either with SYBR Green chemistry (ACE and AT_{1aR}) or TaqMan chemistry (ACE2 and AT_{2R}) using an ABI PRISM 7000 sequence detection system (Applied Biosystems, Foster City, California, USA). PCRs for ACE and AT_{1aR} were performed in duplicate in a 25 μl final volume containing 1X SYBR Green Master mix (Applied Biosystems) and 300 nmol/l of primers (Table 1) [24,25]. PCRs for ACE2 and AT_{2R} were performed in duplicate in a 25 μl final volume containing 1X TaqMan Master mix (Applied Biosystems), 300 nmol/l of primers and 100 nmol/l of ACE2, 150 nmol/l of AT_{2R} TaqMan probe (Table 1). PCR cycling conditions were 10 min at 95°C and 40 cycles of 20 s at 95°C and 1 min at 60°C. Data were analyzed using the absolute standard curve method, and the amplification of a housekeeping gene 18S was used for normalizing the results. The unnormalized expression of 18S mRNA did not differ between the experimental groups (data not shown), enabling its use as the control housekeeping gene in the present study. The intra-assay and inter-assay coefficients of variations for the studied mRNAs were 1.2 and 2.8% or less, respectively.

Plasma renin activity, aldosterone, electrolytes, urea nitrogen, protein, hemoglobin, and creatinine clearance

PRA and plasma aldosterone concentrations were determined using radioimmunoassays (GammaCoat PRA RIA kit and ALDOCTK-2 RIA kit, Diasorin SpA Saluggia, Italy) according to the manufacturer's instructions. All other determinations were carried out as previously described [18,19].

Data presentation and analysis of results

The amounts of ACE and AT_{1R} in renal tissue were depicted in relation to the mean value of the Sham group. Statistics were by one-way and two-way analyses of variance (ANOVA), and the least significant difference test was used for posthoc analyses (SPSS 11.5, SPSS Inc., Chicago, Illinois, USA). If the distribution of the variables was skewed, the Kruskal–Wallis test was applied, and posthoc analyses were performed with the Mann–Whitney *U*-test, the *P*-values being corrected with the Bonferroni equation. Results were expressed as mean ± SEM, and differences were considered significant when $P < 0.05$.

Results

Animal data

Systolic BPs at the beginning of the oxonic acid feeding period did not differ between the groups, while, at study week 9, BP in the NX + Oxo group was higher than that in the Sham group (Table 2). No significant difference in

Table 2 Experimental group data and laboratory findings

	Sham ($n=9-12$)	Sham + Oxo ($n=12$)	NX ($n=11-12$)	NX + Oxo ($n=12$)
Systolic BP at week 0 (mmHg)	120 ± 4	121 ± 5	127 ± 5	125 ± 5
Systolic BP at week 9 (mmHg)	134 ± 7	136 ± 5	142 ± 6	152 ± 4*
Body weight at week 0 (g)	339 ± 6	338 ± 7	333 ± 8	332 ± 7
Body weight at week 9 (g)	433 ± 8	412 ± 11	448 ± 10	411 ± 8†
Heart weight/body weight (g/kg)	3.97 ± 0.05	4.12 ± 0.09	4.95 ± 0.27*	5.18 ± 0.33*
Urine volume (ml/24 h)	25.2 ± 1.7	25.8 ± 1.8	53.3 ± 3.8*	49.3 ± 3.9*
Blood and plasma determinations				
Uric acid (μmol/l)	36 ± 11	117 ± 21*	63 ± 19	152 ± 19*,†
Urea (mmol/l)	6.62 ± 0.34	8.33 ± 0.42	13.54 ± 0.87*	14.54 ± 2.00*
pH	7.42 ± 0.028	7.37 ± 0.023	7.34 ± 0.034*	7.37 ± 0.023
Hemoglobin (g/l)	167.5 ± 3.2	168.5 ± 2.7	157.9 ± 4.7	149.8 ± 4.1*
Potassium (mmol/l)	4.12 ± 0.13	3.79 ± 0.08	4.28 ± 0.19	4.42 ± 0.18
Sodium (mmol/l)	136.5 ± 0.5	137.3 ± 0.6	136.7 ± 0.9	137.0 ± 0.5
Urine determinations				
Potassium (mmol/24 h)	2.84 ± 0.14	4.56 ± 0.20*	2.93 ± 0.09	3.73 ± 0.21*,†
Sodium (mmol/24 h)	8.47 ± 0.41	6.60 ± 0.25*	7.62 ± 0.25	6.44 ± 0.65*
Calcium (μmol/24 h)	28.65 ± 4.47	47.45 ± 5.47*	40.03 ± 6.18	34.79 ± 4.38

Values are mean ± SEM. NX, 5/6 nephrectomy; Oxo, oxonic acid diet. *$P<0.05$ compared with the Sham group, †$P<0.05$ compared with the NX group.

BP was detected between the other groups. Final body weight in the NX + Oxo group was slightly lower when compared with the NX group and, when analyzed using two-way ANOVA, a significant lowering influence on body weight was associated with oxonic acid feeding ($P=0.004$). The heart to body weight ratio and 24-h urine output were higher in both NX groups when compared with Sham rats (Table 2).

Laboratory findings

The oxonic acid feeding elevated plasma uric acid by 80–90 μmol/l in both Sham and NX rats, as expected (Table 2). Creatinine clearance was similarly reduced by approximately 60% in both NX groups and also by about 25% in hyperuricemic Sham rats (Fig. 1a). Plasma concentration of urea was over two-fold higher in the NX group when compared with Sham rats, whereas no

Fig. 1

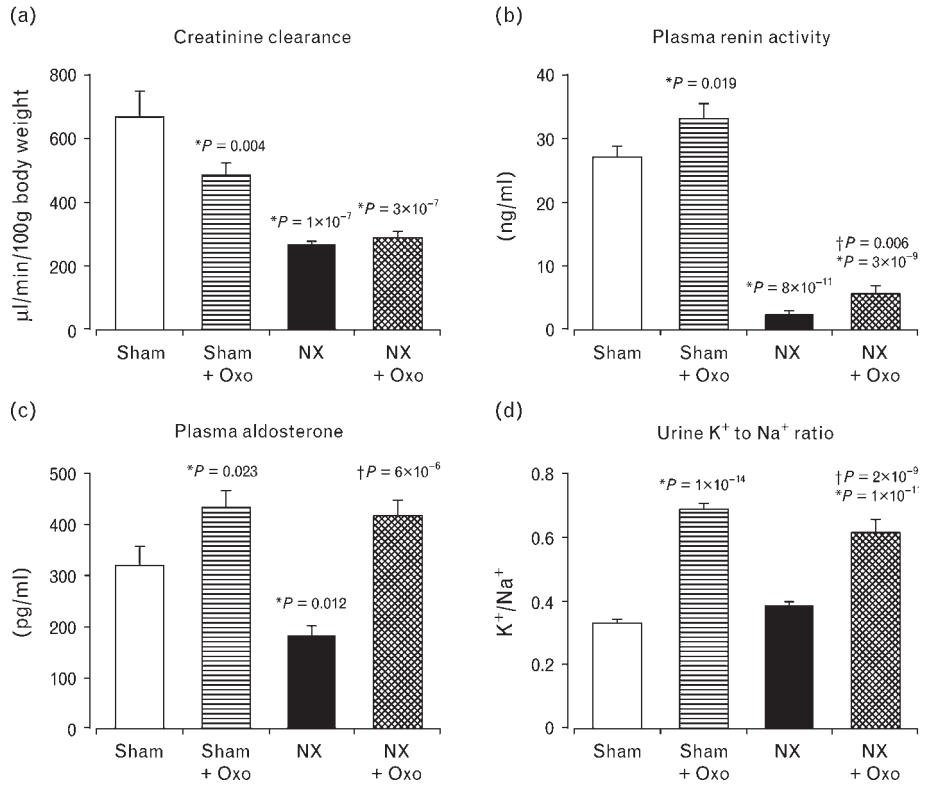

Bar graphs show creatinine clearance (a, $n=9-12$ in each group), plasma renin activity (b, $n=8-12$), plasma aldosterone (c, $n=8-12$), and urine K to Na ratio (d, $n=12$) in sham-operated (Sham) and 5/6 nephrectomized (NX) rats, ingesting either normal or 2.0% oxonic acid diet (Oxo); mean ± SEM; *$P<0.05$ vs. Sham, †$P<0.05$ vs. 5/6 nephrectomy.

difference between the NX and NX + Oxo groups was observed (Table 2). Blood pH was slightly lower in the NX group than in Sham rats, while hemoglobin was decreased in the NX + Oxo group when compared with Sham rats.

Hyperuricemia had a clear elevating effect on PRA and plasma aldosterone concentration (Fig. 1b,c). In the Sham + Oxo group, PRA increased 1.2-fold and plasma aldosterone 1.4-fold, whereas in the NX + Oxo group the increases were 2.5-fold and 2.3-fold, respectively. The plasma aldosterone : renin ratios in the experimental groups were (mean ± SEM) 12 ± 2, 14 ± 2, $360 \pm 208^{*}$ and $213 \pm 110^{*}$ in the Sham, Sham + Oxo, NX and NX + Oxo groups, respectively ($P < 0.001$ both NX groups vs. both Sham groups). A clear K^+ loss/Na^+ retention-effect was observed in both hyperuricemic groups (Table 2). Subsequently, urine K^+ to Na^+ ratio was elevated two-fold in the Sham + Oxo group and 1.6-fold in the NX + Oxo group (Fig. 1d). The 24-h urinary calcium excretion was 1.7-fold increased in the Sham + Oxo group, whereas no significant changes were observed in the NX groups (Table 2).

Autoradiography and real-time quantitative reverse transcriptase-PCR

When kidney tissue ACE content was analyzed using quantitative in-vitro autoradiography, which measures binding to the active site of ACE protein [26], no difference was observed in the NX groups when compared with Sham rats (Fig. 2a,b). Highest ACE signal was detected in a circular fashion in the inner cortex and outer medulla in the Sham-operated groups, whereas ACE was more widely distributed in the remnant kidneys of the NX groups (Fig. 2a). However, when determined using real-time quantitative reverse transcriptase-PCR, both NX groups showed significantly lower ACE mRNA levels than the respective Sham rats (Fig. 2c). In addition, kidney tissue ACE2 mRNA levels were also lower in both NX groups than in the Sham rats (Fig. 2d).

When analyzed using autoradiography, AT_{1R} densities in kidney cortex did not differ from Sham in the NX groups. However, cortical AT_{1R} density was approximately 25% higher in NX + Oxo than NX rats (Fig. 3a). In renal medulla, no difference in AT_{1R} density between the two NX groups was observed, whereas the density was

Fig. 2

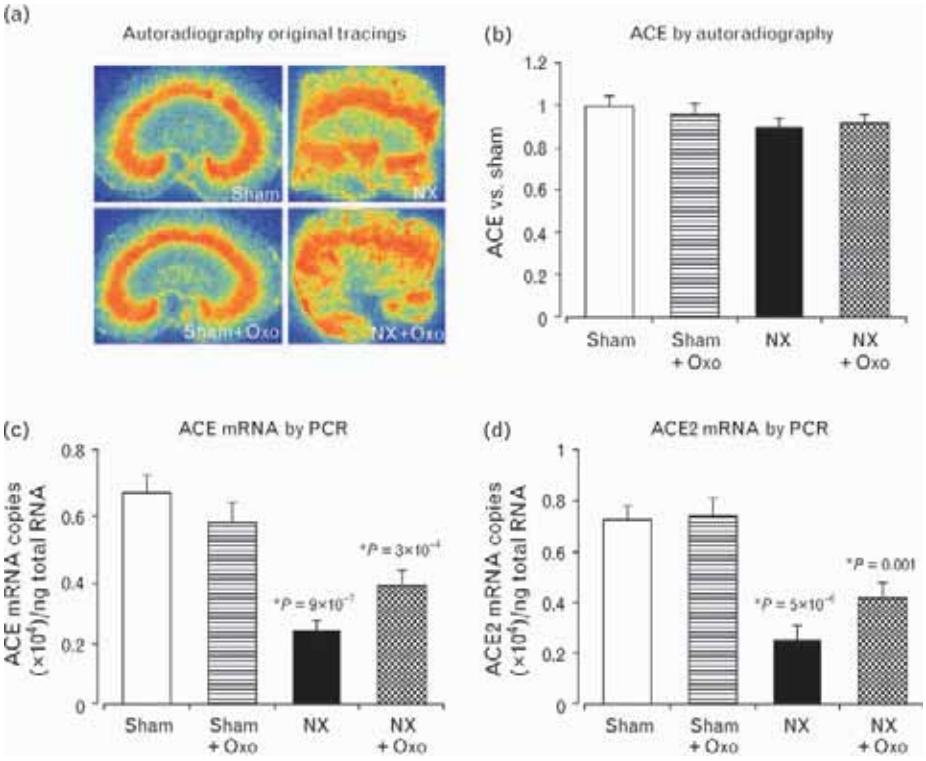

Representative original tracings [a, intensity of red coloring reflects active binding to angiotensin-converting enzyme (ACE)] and bar graphs show ACE determined using autoradiography (b, values related to the mean value of the Sham group); and bar graphs show ACE mRNA (c) and ACE2 mRNA (d) determined using PCR; groups as in Fig. 1, $n = 11-12$, mean ± SEM; $^{*}P < 0.05$ vs. Sham. NX, 5/6 nephrectomy; Oxo, oxonic acid diet.

Fig. 3

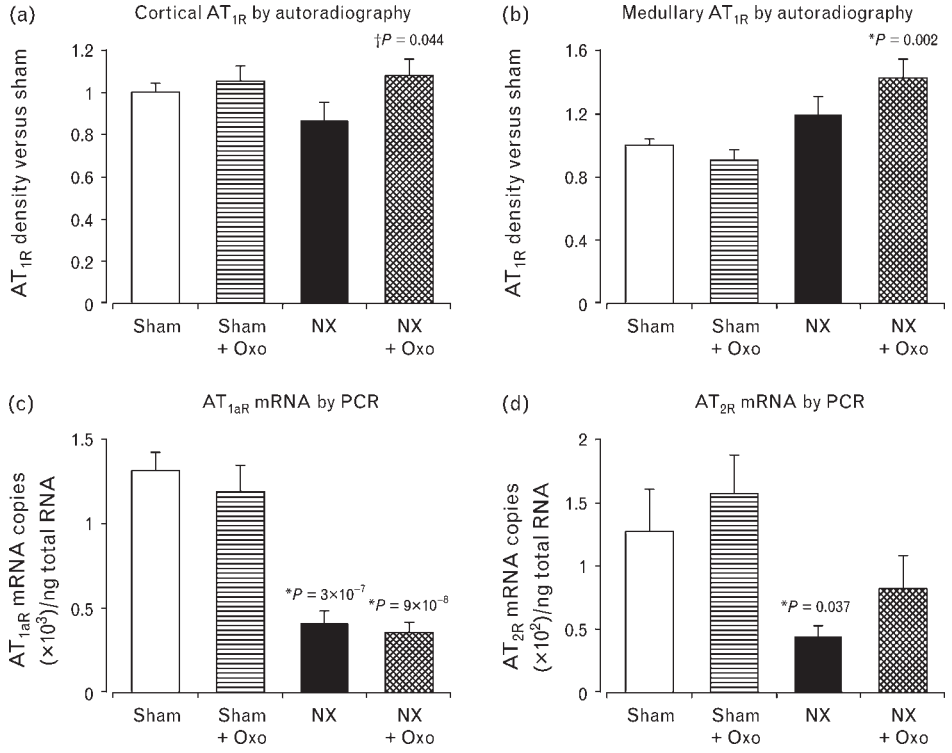

Bar graphs show AT_{1R} densities in kidney cortex (a) and medulla (b) determined using autoradiography, and AT_{1aR} (c) and AT_{2R} (d) mRNA determined using PCR; groups as in Fig. 1, $n = 11-12$, mean ± SEM; $^*P < 0.05$ vs. Sham, $^\dagger P < 0.05$ vs. 5/6 nephrectomy (NX). Oxo, oxonic acid diet.

about 43% higher in the NX + Oxo group when compared with Sham rats (Fig. 3b). The Sham + Oxo rats featured no changes in renal AT_{1R} density. In all groups, AT_{1R} density in the kidney medulla was higher than that in the cortex (data not shown). In addition, the ratio of medullary to cortical AT_{1R} density was increased in both NX groups, the ratios being 2.27 ± 0.08, 2.00 ± 0.15, 3.25 ± 0.34*, 3.04 ± 0.24* in the Sham, Sham + Oxo, NX and NX + Oxo groups, respectively ($^*P < 0.02$ both NX groups vs. both Sham groups).

Hyperuricemia had no effect on kidney tissue AT_{1aR} mRNA content, the levels of which were significantly lower in both NX groups than in Sham rats (Fig. 3c). AT_{2R} densities in cortex and medulla were similar in all study groups (not shown), and the AT_{2R} binding comprised only 1.2–2.1% of all AT receptor binding in the cortex and 0.7–1.2% of all binding in the medulla. Kidney tissue AT_{2R} mRNA level was also lower in the NX + Oxo group than in the Sham rats and was not significantly affected by hyperuricemia (Fig. 3d).

Discussion

The present study demonstrated that hyperuricemia, induced by 2.0% oxonic acid diet for 9 weeks, was associated with increased PRA and plasma aldosterone concentrations. Hyperuricemia also increased K^+ excretion and reduced Na^+ excretion, leading to an elevated K^+ to Na^+ ratio in the urine. This may be largely explained by the elevation in plasma aldosterone levels and the subsequent increase in Na^+ reabsorption in the distal nephron.

As expected, the 2.0% oxonic acid diet was successful in raising plasma uric acid values in both oxonic acid-treated groups [7,9,11]. Treatment of hyperuricemia was not included in the present study protocol, as allopurinol and uricosuric agents have been repeatedly shown to prevent the pathological and pathophysiological changes induced by oxonic acid feeding [7–12]. Renal insufficiency was induced by surgical 5/6 nephrectomy, and the NX rats showed several characteristic findings of chronic renal insufficiency (CRI) (Table 2). Creatinine clearance was reduced, and blood urea was increased in both NX groups. Corresponding to previous findings showing preglomerular arterial disease after oxonic acid diet [13], we found that hyperuricemia decreased creatinine clearance in Sham rats. It should be noted that hyperuricemia is also associated with decreased renal blood flow in humans [27]. However, the present hyperuricemia did not reduce

creatinine clearance in NX rats. An explanation for this may be the higher PRA values in Sham rats resulting in higher Ang II, which is the major modulator of glomerular blood flow and filtration rate. Both NX groups developed polyuria and exhibited two-fold increases in 24-h urine volume. Increased volume diuresis and the subsequent kaliuresis [28] is a likely explanation for the absence of hyperkalemia in the NX groups.

The 12 weeks of CRI in this study did not reveal a significant BP elevation in the NX rats on the normal diet. Our previous studies have shown that, after an additional 8 weeks (total follow-up of 20 weeks), the NX rats developed clear hypertension, so that systolic BP was elevated by 30 mmHg [29]. However, the NX + Oxo rats presented with elevated BP after 9 weeks of diet, which probably resulted from the hyperuricemia-associated sodium retention. Sodium sensitivity is considered a characteristic feature in hyperuricemia [30]. Both NX and NX + Oxo groups exhibited increased heart to body weight ratios, an apparent result of the increased volume load in CRI [29].

As experimental hyperuricemia has been associated with an increased number of renin-positive cells in the juxtaglomerular apparatus [1,8], we scrutinized the circulating and renal components of RAS. Immunohistochemical staining of renin-positive cells has been used previously as a marker of the tissue-level renin expression [8], but knowledge about circulating renin activity in hyperuricemia is scarce. Experimental models of hyperuricemia are characterized by preglomerular arteriolar disease, leading to tubular ischemia and local vasoconstriction. As the severity of the arteriolar disease varies between nephrons, some nephrons will be underperfused and ischemic, whereas others may be overperfused. This leads to heterogeneity in renin expression and a failure to suppress renin release for the degree of sodium intake, resulting in sodium sensitivity [14,31]. Because of the putative nephron heterogeneity, we chose to measure PRA instead of renin staining to examine possible changes in the renin status during hyperuricemia.

The 5/6 nephrectomy rat is a low renin CRI model [32], but clear increases in PRA were observed in both Sham and NX rats after the oxonic acid diet. This corresponds well with the results of previous clinical studies [15,16], suggesting a correlation between hyperuricemia and elevated PRA. Previously, adrenal aldosterone production has been found to be increased 8 days after 5/6 nephrectomy in rats despite a decrease in plasma renin activity, the putative stimulus for the aldosterone synthesis being upregulated adrenal renin synthesis [33]. In concert with these findings, subtotal nephrectomy was associated with a marked increase in plasma aldosterone : renin ratio in the present study. However, this ratio was not affected by oxonic acid feeding, which suggests that increased plasma renin activity was the probable explanation for the observed increase in plasma aldosterone. High circulating aldosterone concentration is acknowledged as a significant cardiovascular risk factor [34,35] but, during hyperuricemia, its role has received little attention. It should be noted that the present rats were not subjected to a metabolic balance study, and claims of a constant Na^+ retention and K^+ loss cannot be presented from these results. The possibility exists that the influence of plasma aldosterone on electrolyte balance became more evident in the unfamiliar environment of a metabolic cage. However, our results imply that increased plasma aldosterone may mediate the Na^+ retention associated with high serum uric acid.

The knowledge of the possible hyperuricemia-associated changes in renal tissue components of RAS is limited. Our aim was, therefore, to determine whether some of the detrimental effects of elevated serum uric acid could be accounted for by alterations in renal RAS components. Kidney ACE, ACE2, AT_{1R}, and AT_{2R} were measured at protein and mRNA levels using in-vitro autoradiography and real-time quantitative reverse transcriptase-PCR, respectively. The autoradiography analyses did not reveal any changes that could explain the hyperuricemia-induced alteration in Na^+–K^+ balance. There were no differences in kidney ACE content between the study groups, whereas changes in cortical and medullary AT_{1R} densities were only observed in the NX + Oxo group: about 25% higher cortical AT_{1R} density than in the NX group, and 43% higher medullary AT_{1R} density than in the Sham group. Thus, hyperuricemia may be associated with increases in renal AT_{1R} density in CRI, but neither of these changes could explain the altered Na^+–K^+ balance, as increased renal K^+ wasting was also observed in the Sham + Oxo group in the absence of alterations in renal AT_{1R} density.

When determined using reverse transcriptase-PCR, both NX groups showed significantly lower ACE and ACE2 mRNA levels than the respective Sham rats. Kidney AT_{1aR} and AT_{2R} mRNA contents were also lower in both NX groups than in Sham rats. Importantly, the oxonic acid diet did not influence ACE, ACE2, AT_{1aR} or AT_{2R} mRNA in kidney tissue of either Sham or NX rats. As the reverse transcriptase-PCR analyses were performed from kidney extracts, no macroscopic localization of the mRNA molecules could be obtained. In the case of AT receptors, the in-vitro autoradiography provided information about distribution at the tissue level (i.e. localization in the cortex or medulla). Experimental renal insufficiency was also associated with an approximately 40% increase in the medullary : cortical ratio of AT_{1R} density, which was not influenced by 2.0% oxonic acid feeding. Moreover, highest ACE labeling was detected in the corticomedullary region in the sham-operated rats but, in the 5/6 nephrectomized rats, kidney

ACE showed patchy and wider tissue distribution than in normal kidneys [32]. Altogether, the RAS components investigated showed no changes at the mRNA level that would explain the influence of hyperuricemia on Na^+–K^+ balance. As the mRNA levels, but not the corresponding protein contents, were reduced in the two NX groups, the above RAS components were probably subject to post-transcriptional modulation in experimental CRI. This may be related to the lower PRA and reduced circulating RAS activity in this form of renal insufficiency.

In conclusion, hyperuricemia induced by 2.0% oxonic acid diet did not induce changes in the local components of RAS in renal tissue, but activated the circulating RAS, reflected as increased PRA and aldosterone in both Sham and NX rats. The present results emphasize the role of aldosterone in the hyperuricemia-induced sodium retention and BP elevation.

Acknowledgements

The excellent technical assistance of Terhi Suvanto, Riina Hatakka, Riikka Kosonen, and Jarkko Lakkisto is greatly appreciated. This study was supported by the Medical Research Funds of Tampere and Helsinki University Hospitals, Finnish Kidney Foundation, the Finnish Foundation for Cardiovascular Research, the Pirkanmaa Regional Fund of Finnish Cultural Foundation, and the Sigrid Jusélius Foundation.

There are no conflicts of interest.

References

1 Johnson RJ, Kang DH, Feig D, Kivlighn S, Kanellis J, Watanabe S, *et al.* Is there a pathogenetic role for uric acid in hypertension and cardiovascular and renal disease? *Hypertension* 2003; **41**:1183–1190.
2 Fam AG. Gout, diet, and the insulin resistance syndrome. *J Rheumatol* 2002; **29**:1350–1355.
3 Wu XW, Muzny DM, Lee CC, Caskey CT. Two independent mutational events in the loss of urate oxidase during hominoid evolution. *J Mol Evol* 1992; **34**:78–84.
4 Cappuccio FP, Strazzullo P, Farinaro E, Trevisan M. Uric acid metabolism and tubular sodium handling. Results from a population-based study. *JAMA* 1993; **270**:354–359.
5 Watanabe S, Kang DH, Feng L, Nakagawa T, Kanellis J, Lan H, *et al.* Uric acid, hominoid evolution, and the pathogenesis of salt-sensitivity. *Hypertension* 2002; **40**:355–360.
6 Fang J, Alderman MH. Serum uric acid and cardiovascular mortality the NHANES I epidemiologic follow-up study, 1971–1992. National Health and Nutrition Examination Survey. *JAMA* 2000; **283**:2404–2410.
7 Kang DH, Nakagawa T, Feng L, Watanabe S, Han L, Mazzali M, *et al.* A role for uric acid in the progression of renal disease. *J Am Soc Nephrol* 2002; **13**:2888–2897.
8 Mazzali M, Hughes J, Kim YG, Jefferson JA, Kang DH, Gordon KL, *et al.* Elevated uric acid increases blood pressure in the rat by a novel crystal-independent mechanism. *Hypertension* 2001; **38**:1101–1106.
9 Mazzali M, Kanellis J, Han L, Feng L, Xia YY, Chen Q, *et al.* Hyperuricemia induces a primary renal arteriolopathy in rats by a blood pressure-independent mechanism. *Am J Physiol Renal Physiol* 2002; **282**:F991–F997.
10 Sanchez-Lozada LG, Tapia E, Avila-Casado C, Soto V, Franco M, Santamaria J, *et al.* Mild hyperuricemia induces glomerular hypertension in normal rats. *Am J Physiol Renal Physiol* 2002; **283**:F1105–1110.
11 Sanchez-Lozada LG, Tapia E, Santamaria J, Avila-Casado C, Soto V, Nepomuceno T, *et al.* Mild hyperuricemia induces vasoconstriction and maintains glomerular hypertension in normal and remnant kidney rats. *Kidney Int* 2005; **67**:237–247.
12 Nakagawa T, Mazzali M, Kang DH, Kanellis J, Watanabe S, Sanchez-Lozada LG, *et al.* Hyperuricemia causes glomerular hypertrophy in the rat. *Am J Nephrol* 2003; **23**:2–7.
13 Johnson RJ, Herrera-Acosta J, Schreiner GF, Rodriguez-Iturbe B. Subtle acquired renal injury as a mechanism of salt-sensitive hypertension. *N Engl J Med* 2002; **346**:913–923.
14 Johnson RJ, Rodriguez-Iturbe B, Nakagawa T, Kang DH, Feig DI, Herrera-Acosta J. Subtle renal injury is likely a common mechanism for salt-sensitive essential hypertension. *Hypertension* 2005; **45**:326–330.
15 Saito I, Saruta T, Kondo K, Nakamura R, Oguro T, Yamagami K, *et al.* Serum uric acid and the renin–angiotensin system in hypertension. *J Am Geriatr Soc* 1978; **26**:241–247.
16 Gruskin AB. The adolescent with essential hypertension. *Am J Kidney Dis* 1985; **6**:86–90.
17 Ramsay LE, Auty RM, Horth CE, Levine D, Shelton JR, Branch RA. Plasma uric acid concentration related to the urinary excretion of aldosterone and of electrolytes in normal subjects. *Clin Sci Mol Med* 1975; **49**: 613–616.
18 Jolma P, Kööbi P, Kalliovalkama J, Saha H, Fan M, Jokihaara J, *et al.* Treatment of secondary hyperparathyroidism by high calcium diet is associated with enhanced resistance artery relaxation in experimental renal failure. *Nephrol Dial Transplant* 2003; **18**:2560–2569.
19 Kööbi P, Kalliovalkama J, Jolma P, Rysä J, Ruskoaho H, Vuolteenaho O, *et al.* AT1 receptor blockade improves vasorelaxation in experimental renal failure. *Hypertension* 2003; **41**:1364–1371.
20 Bäcklund T, Palojoki E, Grönholm T, Eriksson A, Vuolteenaho O, Laine M, *et al.* Dual inhibition of angiotensin converting enzyme and neutral endopeptidase by omapatrilat in rat in vivo. *Pharmacol Res* 2001; **44**: 411–418.
21 Kohzuki M, Johnston CI, Chai SY, Jackson B, Perich R, Paxton D, *et al.* Measurement of angiotensin converting enzyme induction and inhibition using quantitative in vitro autoradiography: tissue selective induction after chronic lisinopril treatment. *J Hypertens* 1991; **9**:579–587.
22 Stewen P, Mervaala E, Karppanen H, Nyman T, Saijonmaa O, Tikkanen I, *et al.* Sodium load increases renal angiotensin type 1 receptors and decreases bradykinin type 2 receptors. *Hypertens Res* 2003; **26**:583–589.
23 Zhuo J, Ohishi M, Mendelsohn FA. Roles of AT1 and AT2 receptors in the hypertensive Ren-2 gene transgenic rat kidney. *Hypertension* 1999; **33**:347–353.
24 Harada E, Yoshimura M, Yasue H, Nakagawa O, Nakagawa M, Harada M, *et al.* Aldosterone induces angiotensin-converting-enzyme gene expression in cultured neonatal rat cardiocytes. *Circulation* 2001; **104**: 137–139.
25 Tikellis C, Johnston CI, Forbes JM, Burns WC, Burrell LM, Risvanis J, *et al.* Characterization of renal angiotensin-converting enzyme 2 in diabetic nephropathy. *Hypertension* 2003; **41**:392–397.
26 Zhuo JL, Froomes P, Casley D, Liu JJ, Murone C, Chai SY, *et al.* Perindopril chronically inhibits angiotensin-converting enzyme in both the endothelium and adventitia of the internal mammary artery in patients with ischemic heart disease. *Circulation* 1997; **96**:174–182.
27 Messerli FH, Frohlich ED, Dreslinski GR, Suarez DH, Aristimuno GG. Serum uric acid in essential hypertension: an indicator of renal vascular involvement. *Ann Intern Med* 1980; **93**:817–821.
28 Gennari FJ. Hypokalemia. *N Engl J Med* 1998; **339**:451–458.
29 Kööbi P, Vehmas TI, Jolma P, Kalliovalkama J, Fan M, Niemelä O, *et al.* High-calcium vs high-phosphate intake and small artery tone in advanced experimental renal insufficiency. *Nephrol Dial Transplant* 2006; **21**:2754–2761.
30 Ward HJ. Uric acid as an independent risk factor in the treatment of hypertension. *Lancet* 1998; **352**:670–671.
31 Sealey JE, Blumenfeld JD, Bell GM, Pecker MS, Sommers SC, Laragh JH. On the renal basis for essential hypertension: nephron heterogeneity with discordant renin secretion and sodium excretion causing a hypertensive vasoconstriction-volume relationship. *J Hypertens* 1988; **6**:763–777.
32 Pörsti I, Fan M, Kööbi P, Jolma P, Kalliovalkama J, Vehmas TI, *et al.* High calcium diet down-regulates kidney angiotensin-converting enzyme in experimental renal failure. *Kidney Int* 2004; **66**:2155–2166.
33 Endemann DH, Wolf K, Boeger CA, Riegger GA, Kramer BK. Adrenal aldosterone biosynthesis is elevated in a model of chronic renal failure–role of local adrenal renin–angiotensin system. *Nephron Physiol* 2004; **97**:37–44.
34 Schmidt BM, Sammer U, Fleischmann I, Schlaich M, Delles C, Schmieder RE. Rapid nongenomic effects of aldosterone on the renal vasculature in humans. *Hypertension* 2006; **47**:650–655.
35 Schmidt BM, Schmieder RE. Aldosterone-induced cardiac damage: focus on blood pressure independent effects. *Am J Hypertens* 2003; **16**:80–86.

Manuscript to *American Journal of Hypertension*

Hyperuricemia, Oxidative Stress, and Carotid Artery Tone in Experimental Renal Insufficiency

Venla Kurra[1]; Arttu Eräranta[1];Pasi Jolma[1,2]; Tuija I. Vehmas[1]; Asko Riutta[1]; Eeva Moilanen[1]; Anna Tahvanainen[1]; Jarkko Kalliovalkama[3]; Onni Niemelä[4]; Juhani Myllymäki[1,5]; Jukka Mustonen[1,5] & Ilkka Pörsti[1,5]

[1]Medical School, University of Tampere, Tampere; Departments of [2]Neurology, and [5]Internal Medicine, Tampere University Hospital, Tampere;
[3]Coxa Hospital for Joint Replacement, Tampere; and [4]Etelä-Pohjanmaa Central Hospital Laboratory, Department of Clinical Chemistry, Seinäjoki, Finland

Correspondence and requests for reprints:
Ilkka Pörsti, M.D.
Medical School, Internal Medicine
FIN-33014 University of Tampere
Finland
Tel. +358 3 3551 6890
Fax. +358 3 3551 6164
E-mail ilkka.porsti@uta.fi

Sources of funding: This study was supported by the Medical Research Fund of Tampere University Hospital (grant number 9F061), the Finnish Foundation for Cardiovascular Research, the Finnish Kidney Foundation, the Paavo Nurmi Foundation, and the Pirkanmaa Regional Fund of the Finnish Cultural Foundation.

Short title: Hyperuricemia and vasorelaxation

Word count: 2999 words; abstract 244 words; 40 references, 4 figures, and 2 tables.

Conflicts of Interest: The authors report no conflicts of interest.

This is a pre-copy-editing, author-produced PDF of an article accepted for publication in American Journal of Hypertension following peer review. The definitive publisher-authenticated version Am J Hypertens (2009) 22 (9): 964-970. doi: 10.1038/ajh.2009.109 is available online at: http://ajh.oxfordjournals.org/content/22/9/964.abstract?sid=5fbc66a1-7217-4421-9619-9866e23300b7.

Abstract

Background. Hyperuricemia may play a role in the pathogenesis of cardiovascular disease, but uric acid is also a significant antioxidant. We investigated the effects of oxonic acid-induced hyperuricemia on carotid artery tone in experimental renal insufficiency.

Methods. Three weeks after 5/6 nephrectomy (NX) or sham operation, male Sprague-Dawley rats were allocated to 2.0% oxonic acid or control diet for 9 weeks. Blood pressure was monitored using tail-cuff, isolated arterial rings were examined using myographs, and blood and urine samples were taken, as appropriate. Oxidative stress and antioxidant status were evaluated by measuring urinary 8-isoprostaglandin $F_{2\alpha}$ excretion and plasma total peroxyl radical-trapping capacity, respectively.

Results. Plasma creatinine was elevated 2-fold in NX rats, but neither NX nor oxonic acid diet influenced blood pressure. Urinary 8-isoprostaglandin $F_{2\alpha}$ excretion was increased over 2.5-fold in NX rats on control diet. Oxonic acid diet increased plasma uric acid 2 to 3-fold, total peroxyl radical-trapping capacity 1.5-fold, and reduced urinary 8-isoprostaglandin $F_{2\alpha}$ excretion by 60-90%. Carotid vasorelaxation to acetylcholine *in vitro*, which could be abolished by nitric oxide synthase inhibition, was reduced following NX, while maximal response to acetylcholine was augmented in hyperuricemic NX rats. Vasorelaxation to nitroprusside was impaired in NX rats, while oxonic acid diet increased sensitivity also to nitroprusside in NX rats.

Conclusions. Oxonic acid-induced hyperuricemia reduced oxidative stress *in vivo*, as evaluated using urinary 8-isoprostaglandin $F_{2\alpha}$ excretion, increased plasma total peroxyl radical-trapping capacity, and improved nitric oxide-mediated vasorelaxation in the carotid artery in experimental renal insufficiency.

Keywords: arterial smooth muscle; chronic renal insufficiency; endothelium; nitric oxide; uric acid

1. Introduction

Hyperuricemia is a typical finding in subjects with metabolic syndrome and renal disease.[1,2] Elevated uric acid correlates with increased cardiovascular mortality,[3] but the contribution of uric acid to the pathogenesis of cardiovascular disease remains controversial.[1] However, hyperuricemia may predispose to hypertension by increasing renal sodium reabsorption.[4,5]

Experimental studies, where rats were made hyperuricemic by the uricase inhibitor oxonic acid, have suggested that high uric acid may play a causal role in the development cardiovascular disease.[6-9] Oxonic acid diet has resulted in renal injury consisting of afferent arteriolopathy and renal cortical vasoconstriction, glomerulosclerosis and increased fibrosis.[6,8,9] The hyperuricemia-induced renal vasculopathy could be prevented by blockade of the renin-angiotensin system (RAS), stimulation of nitric oxide (NO) synthesis with dietary L-arginine, or administration of the superoxide scavenger, tempol.[7,10,11] Increased uric acid concentration has also been suggested to impair NO production in cultured endothelial cells *in vitro,* and hyperuricemic rats have shown decreased NO concentration in serum.[12] Collectively these findings suggest that the detrimental effects of uric acid may be mediated via impaired NO-mediated responses or enhanced RAS activity.

High uric acid concentration is a risk factor for atherosclerosis,[13] while hyperuricemia is a predictor of stroke in patients with type II diabetes.[14] Increased amounts of uric acid have been found in atherosclerotic plaques, suggesting a role for uric acid in the aetiology of atherosclerosis.[15] Yet, uric acid is an antioxidant, as its soluble form urate can scavenge various radicals.[16,17] Uric acid provides protection against oxidative stress induced by peroxynitrite, a toxic product formed in the reaction between superoxide anion and NO.[17] Uric acid also prevents the degradation of extracellular superoxide dismutase (SOD), an enzyme maintaining

normal NO levels and endothelial function.[18] The antioxidant properties of uric acid are in conflict with the concept that hyperuricemia *per se* induces vascular damage.

Despite the several vascular associations and actions of uric acid, the effects of hyperuricemia on arterial tone have only been examined in the glomerular afferent arteriole.[8] Here we tested the hypothesis whether oxonic acid-induced hyperuricemia influences arterial tone in experimental chronic renal insufficiency (CRI), and subjected 5/6 nephrectomized and sham-operated rats to 2.0% oxonic acid diet. This model of CRI is characterized by increased oxidative stress,[19] impaired endothelial function, but only a modest increase in blood pressure 12 weeks after subtotal nephrectomy.[20-22] The present results show that carotid artery relaxation via NO was impaired in CRI, while oxonic acid diet improved vasorelaxation, possibly because of the antioxidant properties of uric acid.

2. Methods

2.1. Animals and experimental design

Male Sprague-Dawley rats were subjected to 5/6 nephrectomy (NX) or sham-operation at the age of 8 weeks under ketamine/diazepam anaesthesia (75 and 2.5 mg/kg intraperitoneally, respectively). In NX rats the upper and lower poles of the left kidney were cut off, and the right kidney was removed.[20,21] In the sham groups both kidneys were decapsulated. Antibiotics (metronidazole 60 and cefuroxim 225 mg/kg) were given postoperatively, and pain was relieved with buprenorphine (0.2 mg/kg subcutaneously, 3 times a day, 3 days). Three weeks later the rats were divided into 4 groups (n=10 in each) so that mean systolic blood pressures, body weights and urine volumes were similar in the two Sham (Sham, Sham+Oxo) and the two NX groups (NX, NX+Oxo), respectively. Systolic blood pressures were measured at +28°C by the tail-cuff method as averages of five recordings in each rat (Model 129 Blood Pressure Meter; IITC Inc., Woodland Hills, Ca., USA) (flow chart in Figure 1).

All groups were given standard chow (Lactamin R34, AnalyCen, Lindköping, Sweden). After the 3rd study week, oxonic acid (20 g/kg chow, Sigma-Aldrich Chemical Co, St Louis, Mo., USA) was supplemented in the food of the Sham+Oxo and NX+Oxo groups. Hyperuricemia was confirmed by tail vein samples at study week 5, and 24-hour urine was collected in metabolic cages at the end of the 2nd and 11th study weeks (Figure 1).

After 9 diet weeks the rats were weighed and anaesthetized (urethane 1.3 g/kg), and blood samples from carotid artery for plasma creatinine, urea, uric acid, lipids and total peroxyl radical-trapping capacity (TRAP) measurements were drawn into chilled tubes with heparin or EDTA as anticoagulants. The hearts and kidneys were removed and weighed, and the kidneys fixed in 4% formaldehyde for 24 hours, and embedded in paraffin. The experiments were approved by the Animal Experimentation Committee of the University of Tampere, Finland, and the Provincial Government of Western Finland Department of Social Affairs and Health, Finland. The investigation conforms to the Guide for the Care and Use of Laboratory Animals published by the US National Institutes of Health (NIH Publication No. 85-23, revised 1996).

2.2. Carotid artery responses in vitro

The carotid artery was chosen for the studies because of the controversial results concerning uric acid, central circulation and stroke.[14,17,23-25] In the rat carotid artery the vasorelaxation to acetylcholine (Ach) is largely mediated via endothelium-derived NO,[26] which probably makes this vessel sensitive to changes in the antioxidant status *in vivo*.[19] A two-millimeter-long standard section of left carotid artery from each animal was prepared, and suspended between hooks in an organ bath chamber in physiological salt solution (PSS; pH 7.4) containing (mM): NaCl 119.0, $NaHCO_3$ 25.0, glucose 11.1, $CaCl_2$ 1.6, KCl 4.7, KH_2PO_4 1.2, $MgSO_4$ 1.2. The PSS was aerated with 95% O_2 and 5% CO_2 and the ring was equilibrated for 1½ h at +37°C with a resting preload of 3.7 mN/mm to induce maximal contractile force

generation in the carotid ring,[26] measured using isometric force-displacement transducers (FT 03, 7 E Polygraph, Grass Instrument Co., Quincy, Ma., USA).

The rings were allowed 30 min at baseline tension in between each concentration-response challenge. Contractions to NA were cumulatively elicited, and relaxations to the NO donor nitroprusside and β-adrenoceptor agonist isoprenaline were examined in rings precontracted with 1 μM NA. The relaxations to Ach, in the absence and presence of the NO synthase (NOS) inhibitor N^G-nitro-L-arginine methyl ester (L-NAME, 0.1 mM), were examined in rings precontracted with 1 μM NA.

2.3. Plasma creatinine, urea, uric acid, and TRAP, urine 8-isoprostaglandin $F_{2\alpha}$ (8-iso-$PGF_{2\alpha}$) excretion, and glomerular histology

Plasma and urine creatinine was determined using Jaffe's colorimetric assay, and plasma urea using colorimetric enzymatic dry chemistry (Vitros 950 analyzer, Johnson & Johnson Clinical Diagnostics, Rochester, NY, USA). Uric acid was measured by an enzymatic colorimetric method,[27] and triglycerides, total and high density lipoprotein (HDL) cholesterol concentrations were analyzed using Cobas Integra 800 automatic analyzer (Hoffman-La Roche Ltd, Basel, Switzerland). Non-HDL cholesterol was calculated as total cholesterol minus HDL cholesterol.

Plasma TRAP was measured using luminol-enhanced chemiluminescence, based on peroxyl radical production by decomposition of 2,2-azo-bis(2-aminopropane) hydrochloride (ABAP; Polysciences, Warrington, Pa., USA), as previously described.[28,29] The 8-iso-$PGF_{2\alpha}$ assay was also performed as previously described.[30] Briefly, urine was extracted on a C_2 silica cartridge (Applied Separation, Allentown, Pa., USA) and 8-iso-$PGF_{2\alpha}$ was determined using 8-iso[^{125}I]-$PGF_{2\alpha}$ radioimmunoassay.

Five-µm-thick kidney sections were stained with hematoxylin-eosin and processed for light microscopic evaluation by an expert blinded to the treatments. The glomerulosclerosis score for each animal was derived as the mean of all sample glomeruli: 0=normal, 1=mesangial expansion or basement membrane thickening, 2=segmental sclerosis <25% of the tuft, 3=segmental sclerosis 25-50% of the tuft, 4=diffuse sclerosis >50% of the tuft, 5=diffuse glomerulosclerosis, total tuft obliteration and collapse.[22]

2.4. Data presentation and analysis of results

The contractile responses were expressed as wall tension (mN/mm) and as percentage of maximum. The vasorelaxations were presented as a percentage of pre-existing contractile force. Statistical analyses were by one-way and two-way analyses of variance (ANOVA), as appropriate, and the least significant difference test was used for post-hoc analyses (SPSS 11.5, SPSS Inc., Chicago, Il., USA). ANOVA for repeated measurements was applied for data consisting of repeated observations at successive observation points. Spearman's two-tailed correlation coefficient (r) was used, and the results were expressed as means and standard errors of the mean (SEM). $P<0.05$ was considered significant. Unless otherwise indicated the P values in the text refer to one-way ANOVA.

2.5. Drugs

Ketamine (Parke-Davis Scandinavia AB, Solna, Sweden), cefuroxim, diazepam (Orion Pharma Ltd., Espoo, Finland), metronidazole (B. Braun AG, Melsungen, Germany), buprenorphine (Reckitt & Colman, Hull, England), acetylcholine chloride, isoprenaline hydrochloride, N^G-nitro-L-arginine methyl ester, noradrenaline bitartrate (Sigma-Aldrich Chemical Co, St Louis, Mo., USA) and sodium nitroprusside (Fluka Chemie AG, Buchs SG, Switzerland).

3. Results

3.1. Blood pressure, heart and body weights, and glomerulosclerosis

Systolic blood pressure was not significantly influenced by the oxonic acid diet or NX (Table 1). However, heart weight to body weight ratio was higher in the NX and NX+Oxo groups when compared with Sham rats (P=0.004 and 0.001, respectively). Average body weight gain was comparable in all groups (Table 1). Histological analysis revealed that the glomerular damage index was lower in the NX+Oxo than the NX group (1.1±0.4 vs. 1.8±0.2, $p<0.05$), whereas the Sham and Sham+Oxo groups were completely devoid of glomerular changes (damage index was 0 in both groups).

3.2. Laboratory findings

At the end of the study, the oxonic acid diet elevated plasma uric acid concentration 3.4-fold in the Sham+Oxo rats and 2.4-fold in the NX+Oxo rats, respectively (Table 2). Plasma creatinine and urea concentrations were approximately two-fold higher in the NX rats when compared with Sham, and were not affected by oxonic acid diet. Creatinine clearance was reduced by approximately 60% in both NX groups, and also by 33% in hyperuricemic Sham rats.

Before the oxonic acid diet was started, no significant differences were found in the 24-hour urinary excretion of 8-iso-$PGF_{2\alpha}$, a marker of oxidative stress *in vivo* (Figures 1 and 2A).[31] During the 9th week on the 2.0% oxonic acid diet the 24-hour excretion of 8-iso-$PGF_{2\alpha}$ was increased in the NX group, but was reduced by approximately 60% and 90% in the Sham+Oxo and NX+Oxo groups, respectively, when compared with their respective controls (Figures 1 and 2B).

At the end of the study, the plasma concentrations of TRAP were increased 1.5-fold in groups ingesting the oxonic acid diet (Table 2), and there was a linear correlation between

plasma uric acid concentration and TRAP in all groups (Figure 2C). Plasma total cholesterol, HDL cholesterol, and non-HDL cholesterol concentrations were elevated in NX rats (Table 2). When analysed using two-way ANOVA, an elevation of plasma triglycerides was also uncovered in NX rats when compared with Sham rats (P=0.006, two-way ANOVA). No differences in blood pH were detected (Table 2).

3.3. Functional responses of isolated carotid arterial rings

Contractile responses to NA were similar between the study groups (Figures 3A and 3B). Thus, differences in vasoconstrictor sensitivity cannot explain the differences in vasorelaxations.

The relaxations to Ach were reduced in NX rats when compared with Sham rats, while the maximal response to Ach was improved in the NX+Oxo group when compared with the NX group (P=0.027; Figure 4A). Hyperuricemia had no effect on the response to Ach in Sham rats. In both NX and NX+Oxo groups, plasma uric acid concentration correlated with the maximal relaxation to Ach (Figure 2D), while no correlation was observed between maximal Ach response and plasma levels of creatinine, urea, lipids or blood pressure (not shown). Plasma TRAP also correlated with maximal Ach response in NX rats (r=0.73, P=0.026).

The NOS inhibitor L-NAME abolished the relaxation to Ach in all groups (Figure 4B), indicating that the response was mediated via NO. The relaxations to nitroprusside were also reduced in both NX groups vs. Sham groups, while the reduction was less marked in the NX+Oxo group (Figure 4C). Higher relaxation to 10 nmol/l nitroprusside was detected in the NX+Oxo group when compared with the NX group (P=0.027). Vasorelaxation induced by isoprenaline was similar in all groups (Figure 4D).

4. Discussion

Here we demonstrated for the first time that oxonic acid-induced hyperuricemia reduced oxidative stress and increased total peroxyl radical-trapping capacity *in vivo* in the rat, as evaluated by urinary 8-iso-$PGF_{2\alpha}$ excretion and plasma TRAP, respectively. Higher uric acid concentration paralleled with improved carotid artery vasorelaxation via NO in NX rats, the improvement of which correlated significantly with plasma concentration of uric acid. These findings suggest that by counterbalancing the oxidative stress associated with CRI,[19] uric acid improved NO-mediated vasorelaxation independently of the level of blood pressure.

The oxonic acid diet induces hyperuricemia by inhibiting the hepatic uricase.[6-9] Previous studies with 2.0% oxonic acid in rats have demonstrated a 1.3 to 2.8-fold rise in serum uric acid,[7-9] corresponding to the present 2.4 to 3.4-fold increase. Since allopurinol and uricosuric agents have been shown to prevent the pathological and pathophysiological changes induced by 2.0% oxonic acid feeding in several studies, treatment of hyperuricemia was not included in the present study.[6-9] The NX rats showed several characteristic findings of moderate renal insufficiency,[5,21,22] while the observed increase in heart weight is in agreement with the view that this model is characterized by volume overload.[21]

As our principal focus was on putative changes in NO-mediated vasorelaxation, we studied the functional responses in the carotid artery. In many vessels the vasorelaxation to Ach is mediated via NO, prostacyclin and endothelium-derived hyperpolarization,[32] but in the rat carotid artery the vasorelaxation is largely mediated via endothelium-derived NO.[26] We found that carotid vasorelaxation via both endothelial NO (Ach) and exogenous NO (nitroprusside) was impaired in CRI. Unexpectedly, oxonic acid diet improved vasorelaxation in response to NO in NX rats, and the plasma concentration of uric acid correlated positively with maximal Ach-mediated relaxation. In contrast, the vasorelaxation via cyclic AMP (isoprenaline) was not

affected by oxonic acid feeding. Thus, the differences in carotid artery vasorelaxation were related to alterations in NO-mediated responses.

The present results appear to contradict with previous findings *in vitro* suggesting that uric acid inhibits NO production in cultured aortic endothelial cells,[12] and that uric acid induces oxidative stress through stimulation of RAS in cultured vascular smooth muscle cells.[33] In addition, experimental studies have suggested that uric acid is a mediator of cardiovascular and renal disease.[6-9,12] We recently found that experimental hyperuricemia elevated plasma aldosterone with a deleterious influence on sodium:potassium balance in rats with CRI. In that study the Sham+Oxo rats also showed reduced creatinine clearance when compared with Sham rats, but no such reduction was observed in the NX+Oxo rats when compared with the NX group.[5] A similar finding was observed in this study, suggesting that this form of hyperuricemia is not associated with reduced glomerular filtration rate in NX rats. Altogether, the antioxidant properties of urate may mitigate the harmful influences of RAS stimulation associated with increased uric acid concentration. In addition, some of the differences between the results of the studies on oxonic acid-induced hyperuricemia may be related to the fact that 2.0% oxonic acid diet was used in some,[5-7,9] while administration of oxonic acid by gastric gavage (750 mg/kg/day) was used in others.[8,10,11] It seems likely that the effects of oxonic acid administration by gavage on the kinetics of plasma uric acid differ from those following 2.0% oxonic acid dietary intake.

Although hyperuricemia has in general been considered a cardiovascular risk factor,[1,15] conflicting data also exists. Uric acid serves as a scavenger of various free radicals.[16,17,34] Intravenous uric acid infusion increases serum free-radical scavenging capacity in healthy volunteers,[35] and improves endothelial function in the forearm vascular bed of smokers and patients with type 1 diabetes.[36] Higher uric acid concentration is also associated with increased serum antioxidant capacity and reduced oxidative stress during acute physical exercise.[37]

However, the antioxidant role of uric acid is complicated by the generation of superoxide anion as a by-product in the reaction of xanthine with xanthine oxidase to produce uric acid.[1] Furthermore, the reaction of superoxide with NO leads to the formation of the highly toxic peroxynitrite, with possible further formation of secondary free radicals.[17] Yet, uric acid can indirectly protect against the harmful effects of peroxynitrite by scavenging these secondary radicals.[17]

Increased oxidative stress is a characteristic feature of CRI.[19] Indeed, we observed a marked increase in the urinary 8-iso-$PGF_{2\alpha}$ excretion after 11 weeks of renal insufficiency in the present study, a finding that has not been reported previously in NX rats. Interestingly, 8-iso-$PGF_{2\alpha}$ excretion was not increased during the third week after subtotal nephrectomy, indicating that increased oxidative stress is not a straightforward result of renal mass reduction but develops later in the course of chronically impaired renal function. It is of note that the beneficial influences were not limited to carotid vasorelaxation, as glomerulosclerosis was also alleviated by the oxonic acid-induced hyperuricemia in NX rats.

The levels of uric acid are higher in humans than in most other mammals.[1] Moreover, the relation of the uric acid levels with cardiovascular disease in humans has been suggested to show a J-shaped curve with the nadir of risk being in the second quartile.[1,3,38] The increased risk for the lowest quartile may reflect the decreased plasma antioxidant activity, whereas the increased risk at the higher levels may reflect the role of uric acid in inducing cardiovascular disease, leaving the antioxidant role of uric acid insignificant. In the 2.0% oxonic acid rat model of hyperuricemia, the levels of plasma uric acid are still rather low when compared with humans, and higher levels may be required to induce vascular damage in rats.

CRI is also associated with unfavourable changes in plasma lipids,[39] and impaired vasorelaxation could result from the increased level of LDL cholesterol, which inhibits endothelium-dependent vasodilatation.[40] The underlying mechanisms are impaired vascular NO

production and increased superoxide anion generation that inactivates NO.[19] In line with these findings, plasma lipid values were increased by 2 to 3-fold in the NX rats in the present study. Higher uric acid level may also provide antioxidant protection against the detrimental effects of LDL cholesterol on NO-mediated vasorelaxation.

In conclusion, we found that 2.0% oxonic acid diet which increased plasma uric acid, also reduced oxidative stress and increased peroxyl radical-trapping capacity *in vivo*, as evidenced by reduced 24-hour urinary 8-iso-$PGF_{2\alpha}$ excretion and increased plasma TRAP, respectively. In parallel, oxonic acid diet enhanced vasorelaxation via NO in the carotid artery in experimental CRI, independently of the level of blood pressure and renal function. Therefore, this form of experimental hyperuricemia is not always associated with a deleterious influence on the cardiovascular system.

Acknowledgements

This study was supported by the Medical Research Fund of Tampere University Hospital (grant number 9F061), the Finnish Foundation for Cardiovascular Research, the Finnish Kidney Foundation, the Paavo Nurmi Foundation, and the Pirkanmaa Regional Fund of the Finnish Cultural Foundation.

Disclosure

The authors declare no conflicts of interest.

References

1. Johnson RJ, Kang DH, Feig D, Kivlighn S, Kanellis J, Watanabe S, Tuttle KR, Rodriguez-Iturbe B, Herrera-Acosta J, Mazzali M. Is there a pathogenetic role for uric acid in hypertension and cardiovascular and renal disease? *Hypertension* 2003; 41:1183-1190.
2. Fam AG. Gout, diet, and the insulin resistance syndrome. *J Rheumatol* 2002; 29:1350-1355.
3. Fang J, Alderman MH. Serum uric acid and cardiovascular mortality the NHANES I epidemiologic follow-up study, 1971-1992. National Health and Nutrition Examination Survey. *JAMA* 2000; 283:2404-2410.
4. Cappuccio FP, Strazzullo P, Farinaro E, Trevisan M. Uric acid metabolism and tubular sodium handling. Results from a population-based study. *JAMA* 1993; 270:354-359.
5. Eräranta A, Kurra V, Tahvanainen AM, Vehmas TI, Kööbi P, Lakkisto P, Tikkanen I, Niemelä OJ, Mustonen JT, Pörsti IH. Oxonic acid-induced hyperuricemia elevates plasma aldosterone in experimental renal insufficiency. *J Hypertens* 2008; 26:1661-1668.
6. Kang DH, Nakagawa T, Feng L, Watanabe S, Han L, Mazzali M, Truong L, Harris R, Johnson RJ. A role for uric acid in the progression of renal disease. *J Am Soc Nephrol* 2002; 13:2888-2897.
7. Mazzali M, Hughes J, Kim YG, Jefferson JA, Kang DH, Gordon KL, Lan HY, Kivlighn S, Johnson RJ. Elevated uric acid increases blood pressure in the rat by a novel crystal-independent mechanism. *Hypertension* 2001; 38:1101-1106.
8. Sanchez-Lozada LG, Tapia E, Santamaria J, Avila-Casado C, Soto V, Nepomuceno T, Rodriguez-Iturbe B, Johnson RJ, Herrera-Acosta J. Mild hyperuricemia induces vasoconstriction and maintains glomerular hypertension in normal and remnant kidney rats. *Kidney Int* 2005; 67:237-247.

9. Nakagawa T, Mazzali M, Kang DH, Kanellis J, Watanabe S, Sanchez-Lozada LG, Rodriguez-Iturbe B, Herrera-Acosta J, Johnson RJ. Hyperuricemia causes glomerular hypertrophy in the rat. *Am J Nephrol* 2003; 23:2-7.
10. Sanchez-Lozada LG, Tapia E, Lopez-Molina R, Nepomuceno T, Soto V, Avila-Casado C, Nakagawa T, Johnson RJ, Herrera-Acosta J, Franco M. Effects of acute and chronic L-arginine treatment in experimental hyperuricemia. *Am J Physiol Renal Physiol* 2007; 292:F1238-1244.
11. Sanchez-Lozada LG, Soto V, Tapia E, Avila-Casado C, Sautin YY, Nakagawa T, Franco M, Rodriguez-Iturbe B, Johnson RJ. Role of oxidative stress in the renal abnormalities induced by experimental hyperuricemia. *Am J Physiol Renal Physiol* 2008; 295:F1134-1141.
12. Khosla UM, Zharikov S, Finch JL, Nakagawa T, Roncal C, Mu W, Krotova K, Block ER, Prabhakar S, Johnson RJ. Hyperuricemia induces endothelial dysfunction. *Kidney Int* 2005; 67:1739-1742.
13. Vigna GB, Bolzan M, Romagnoni F, Valerio G, Vitale E, Zuliani G, Fellin R. Lipids and other risk factors selected by discriminant analysis in symptomatic patients with supra-aortic and peripheral atherosclerosis. *Circulation* 1992; 85:2205-2211.
14. Lehto S, Niskanen L, Rönnemaa T, Laakso M. Serum uric acid is a strong predictor of stroke in patients with non-insulin-dependent diabetes mellitus. *Stroke* 1998; 29:635-639.
15. Patetsios P, Song M, Shutze WP, Pappas C, Rodino W, Ramirez JA, Panetta TF. Identification of uric acid and xanthine oxidase in atherosclerotic plaque. *Am J Cardiol* 2001; 88:188-191, A186.
16. Davies KJ, Sevanian A, Muakkassah-Kelly SF, Hochstein P. Uric acid-iron ion complexes. A new aspect of the antioxidant functions of uric acid. *Biochem J* 1986; 235:747-754.

17. Squadrito GL, Cueto R, Splenser AE, Valavanidis A, Zhang H, Uppu RM, Pryor WA. Reaction of uric acid with peroxynitrite and implications for the mechanism of neuroprotection by uric acid. *Arch Biochem Biophys* 2000; 376:333-337.

18. Hink HU, Santanam N, Dikalov S, McCann L, Nguyen AD, Parthasarathy S, Harrison DG, Fukai T. Peroxidase properties of extracellular superoxide dismutase: role of uric acid in modulating in vivo activity. *Arterioscler Thromb Vasc Biol* 2002; 22:1402-1408.

19. Vaziri ND, Ni Z, Oveisi F, Liang K, Pandian R. Enhanced nitric oxide inactivation and protein nitration by reactive oxygen species in renal insufficiency. *Hypertension* 2002; 39:135-141.

20. Jolma P, Kööbi P, Kalliovalkama J, Saha H, Fan M, Jokihaara J, Moilanen E, Tikkanen I, Pörsti I. Treatment of secondary hyperparathyroidism by high calcium diet is associated with enhanced resistance artery relaxation in experimental renal failure. *Nephrol Dial Transplant* 2003; 18:2560-2569.

21. Kööbi P, Kalliovalkama J, Jolma P, Rysä J, Ruskoaho H, Vuolteenaho O, Kähönen M, Tikkanen I, Fan M, Ylitalo P, Pörsti I. AT1 receptor blockade improves vasorelaxation in experimental renal failure. *Hypertension* 2003; 41:1364-1371.

22. Pörsti I, Fan M, Koobi P, Jolma P, Kalliovalkama J, Vehmas TI, Helin H, Holthöfer H, Mervaala E, Nyman T, Tikkanen I. High calcium diet down-regulates kidney angiotensin-converting enzyme in experimental renal failure. *Kidney Int* 2004; 66:2155-2166.

23. Yu ZF, Bruce-Keller AJ, Goodman Y, Mattson MP. Uric acid protects neurons against excitotoxic and metabolic insults in cell culture, and against focal ischemic brain injury in vivo. *J Neurosci Res* 1998; 53:613-625.

24. Weir CJ, Muir SW, Walters MR, Lees KR. Serum urate as an independent predictor of poor outcome and future vascular events after acute stroke. *Stroke* 2003; 34:1951-1956.

25. Chamorro A, Obach V, Cervera A, Revilla M, Deulofeu R, Aponte JH. Prognostic significance of uric acid serum concentration in patients with acute ischemic stroke. *Stroke* 2002; 33:1048-1052.

26. Arvola P, Wu X, Kähönen M, Mäkynen H, Riutta A, Mucha I, Solakivi T, Kainulainen H, Pörsti I. Exercise enhances vasorelaxation in experimental obesity associated hypertension. *Cardiovasc Res* 1999; 43:992-1002.

27. Praetorius E, Poulsen H. Enzymatic determination of uric acid; with detailed directions. *Scand J Clin Lab Invest* 1953; 5:273-280.

28. Alanko J, Riutta A, Holm P, Mucha I, Vapaatalo H, Metsä-Ketelä T. Modulation of arachidonic acid metabolism by phenols: relation to their structure and antioxidant/prooxidant properties. *Free Radic Biol Med* 1999; 26:193-201.

29. Dugue B, Smolander J, Westerlund T, Oksa J, Nieminen R, Moilanen E, Mikkelsson M. Acute and long-term effects of winter swimming and whole-body cryotherapy on plasma antioxidative capacity in healthy women. *Scand J Clin Lab Invest* 2005; 65:395-402.

30. Rossi P, Riutta A, Kuukasjärvi P, Vehmas T, Mucha I, Salenius JP. Revascularization decreases 8-isoprostaglandin F2alpha excretion in chronic lower limb ischemia. *Prostaglandins Leukot Essent Fatty Acids* 2004; 71:97-101.

31. Roberts LJ, Morrow JD. Measurement of F_2-isoprostanes as an index of oxidative stress in vivo. *Free Radic Biol Med* 2000; 28:505-513.

32. Roman RJ. P-450 metabolites of arachidonic acid in the control of cardiovascular function. *Physiol Rev* 2002; 82:131-185.

33. Corry DB, Eslami P, Yamamoto K, Nyby MD, Makino H, Tuck ML. Uric acid stimulates vascular smooth muscle cell proliferation and oxidative stress via the vascular renin-angiotensin system. *J Hypertens* 2008; 26:269-275.

34. Becker BF, Reinholz N, Leipert B, Raschke P, Permanetter B, Gerlach E. Role of uric acid as an endogenous radical scavenger and antioxidant. *Chest* 1991; 100:176S-181S.

35. Waring WS, Webb DJ, Maxwell SR. Systemic uric acid administration increases serum antioxidant capacity in healthy volunteers. *J Cardiovasc Pharmacol* 2001; 38:365-371.

36. Waring WS, McKnight JA, Webb DJ, Maxwell SR. Uric acid restores endothelial function in patients with type 1 diabetes and regular smokers. *Diabetes* 2006; 55:3127-3132.

37. Waring WS, Convery A, Mishra V, Shenkin A, Webb DJ, Maxwell SR. Uric acid reduces exercise-induced oxidative stress in healthy adults. *Clin Sci (Lond)* 2003; 105:425-430.

38. Hsu SP, Pai MF, Peng YS, Chiang CK, Ho TI, Hung KY. Serum uric acid levels show a 'J-shaped' association with all-cause mortality in haemodialysis patients. *Nephrol Dial Transplant* 2004; 19:457-462.

39. Vaziri ND, Liang K, Parks JS. Down-regulation of hepatic lecithin:cholesterol acyltransferase gene expression in chronic renal failure. *Kidney Int* 2001; 59:2192-2196.

40. Mougenot N, Lesnik P, Ramirez-Gil JF, Nataf P, Diczfalusy U, Chapman MJ, Lechat P. Effect of the oxidation state of LDL on the modulation of arterial vasomotor response in vitro. *Atherosclerosis* 1997; 133:183-192.

Figure legends

Figure 1. Flow chart of the study; NX = 5/6 nephrectomized rat, Sham = sham-operated rat, Oxo = 2.0% oxonic acid diet, 8-iso-$PGF_{2\alpha}$ = 8-isoprostaglandin $F_{2\alpha,}$ TRAP = total peroxyl radical-trapping capacity.

Figure 2. Bar graphs show 24-hour urinary excretion of 8-isoprostaglandin $F_{2\alpha}$ before the 2.0% oxonic acid feeding period at the end of study week 2 (A), and during the 2.0% oxonic acid diet at the end of study week 11 (B). Scatter plots show plasma uric acid and total peroxyl radical-trapping capacity (TRAP) (C), and plasma uric acid and maximal relaxation induced by Ach (D) after 12 study weeks in the experimental groups; group codes as in Figure 1; $^{*}P<0.05$ vs. the Sham group, $^{\dagger}P<0.05$ vs. the NX group.

Figure 3. Line graphs show contractile responses induced by noradrenaline as developed tension (A) and percent of maximum (B) in the experimental groups; group codes as in Figure 1.

Figure 4. Line graphs show relaxations induced by acetylcholine in the absence (A) and presence (B) of 0.1 mmol/l L-NAME, and relaxations elicited by nitroprusside (C) and isoprenaline (D) in the experimental groups; $^{*}P<0.05$, ANOVA for repeated measurements; $^{\dagger}P<0.05$ compared with the corresponding individual concentration in the NX group; group codes as in Figure 1.

Figure 1.

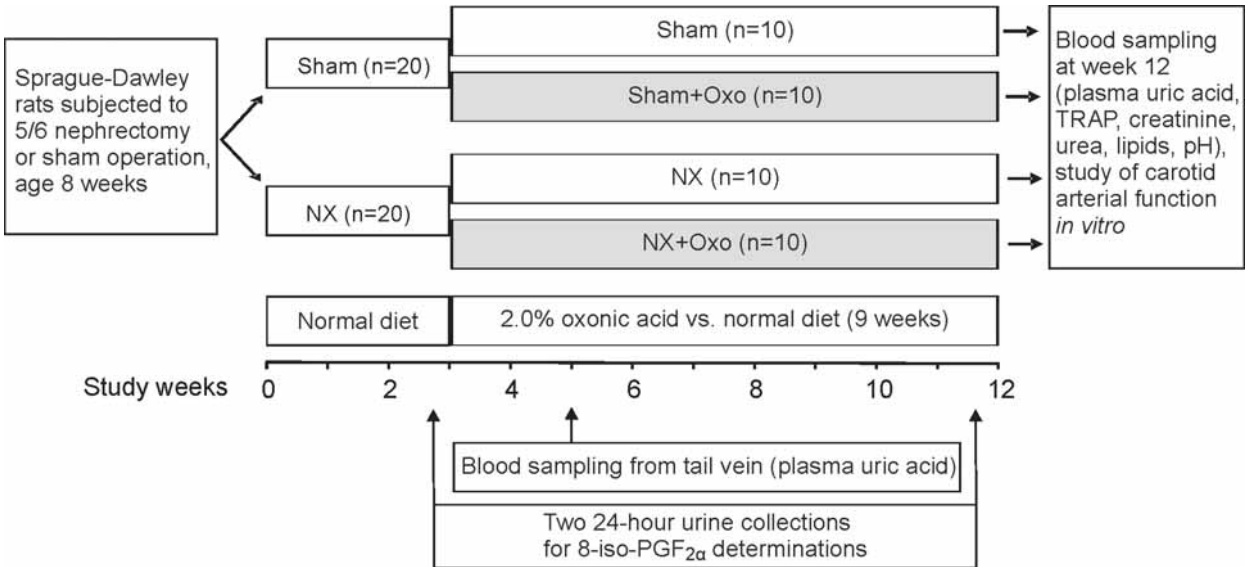
Sprague-Dawley rats subjected to 5/6 nephrectomy or sham operation, age 8 weeks
Sham (n=20)
NX (n=20)
Sham (n=10)
Sham+Oxo (n=10)
NX (n=10)
NX+Oxo (n=10)
Blood sampling at week 12 (plasma uric acid, TRAP, creatinine, urea, lipids, pH), study of carotid arterial function *in vitro*
Normal diet
2.0% oxonic acid vs. normal diet (9 weeks)
Study weeks
0
2
4
6
8
10
12
Blood sampling from tail vein (plasma uric acid)
Two 24-hour urine collections for 8-iso-$PGF_{2\alpha}$ determinations

Figure 2.

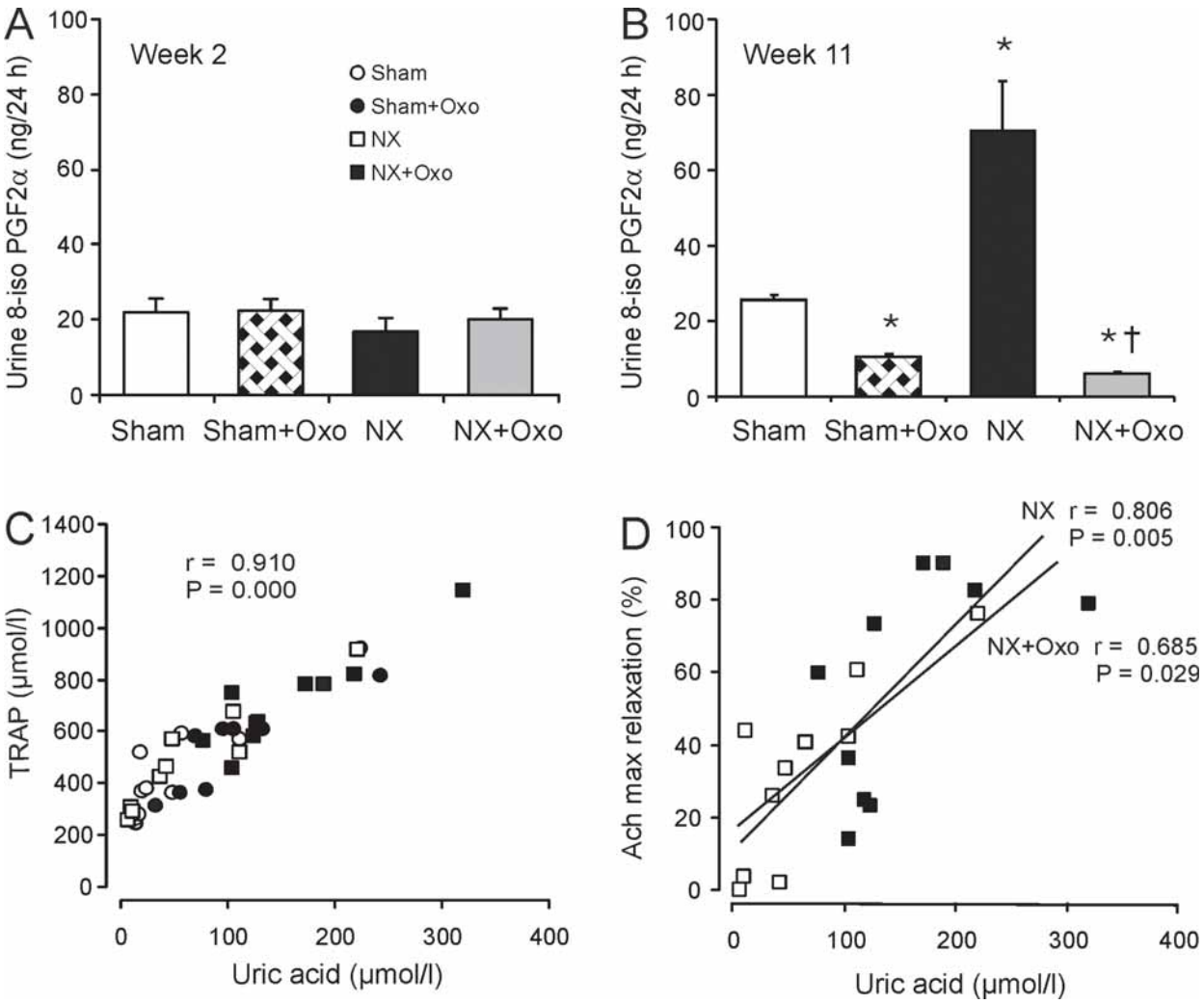
A
Week 2
Sham
Sham+Oxo
NX
NX+Oxo
Urine 8-iso PGF2α (ng/24 h)
Sham Sham+Oxo NX NX+Oxo
B
Week 11
*
*
*†
C
r = 0.910
P = 0.000
TRAP (µmol/l)
Uric acid (µmol/l)
D
NX r = 0.806
P = 0.005
NX+Oxo r = 0.685
P = 0.029
Ach max relaxation (%)
Uric acid (µmol/l)

Figure 3.

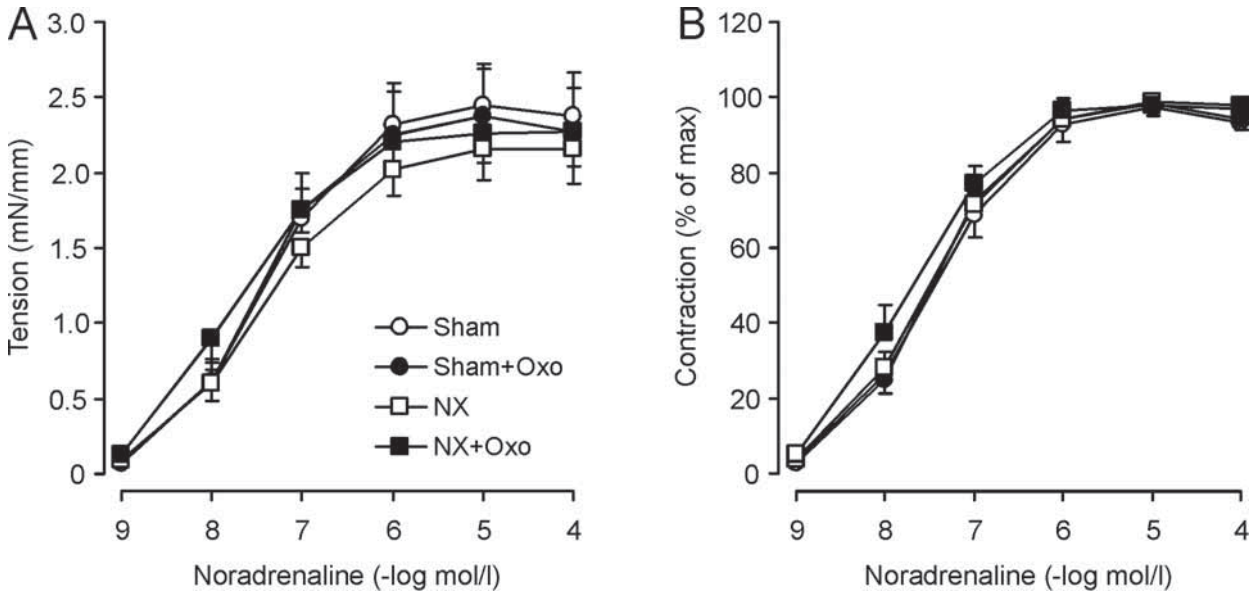
A
Tension (mN/mm)
3.0
2.5
2.0
1.5
1.0
0.5
0
Sham
Sham+Oxo
NX
NX+Oxo
9
8
7
6
5
4
Noradrenaline (-log mol/l)
B
Contraction (% of max)
120
100
80
60
40
20
0
9
8
7
6
5
4
Noradrenaline (-log mol/l)

Figure 4.

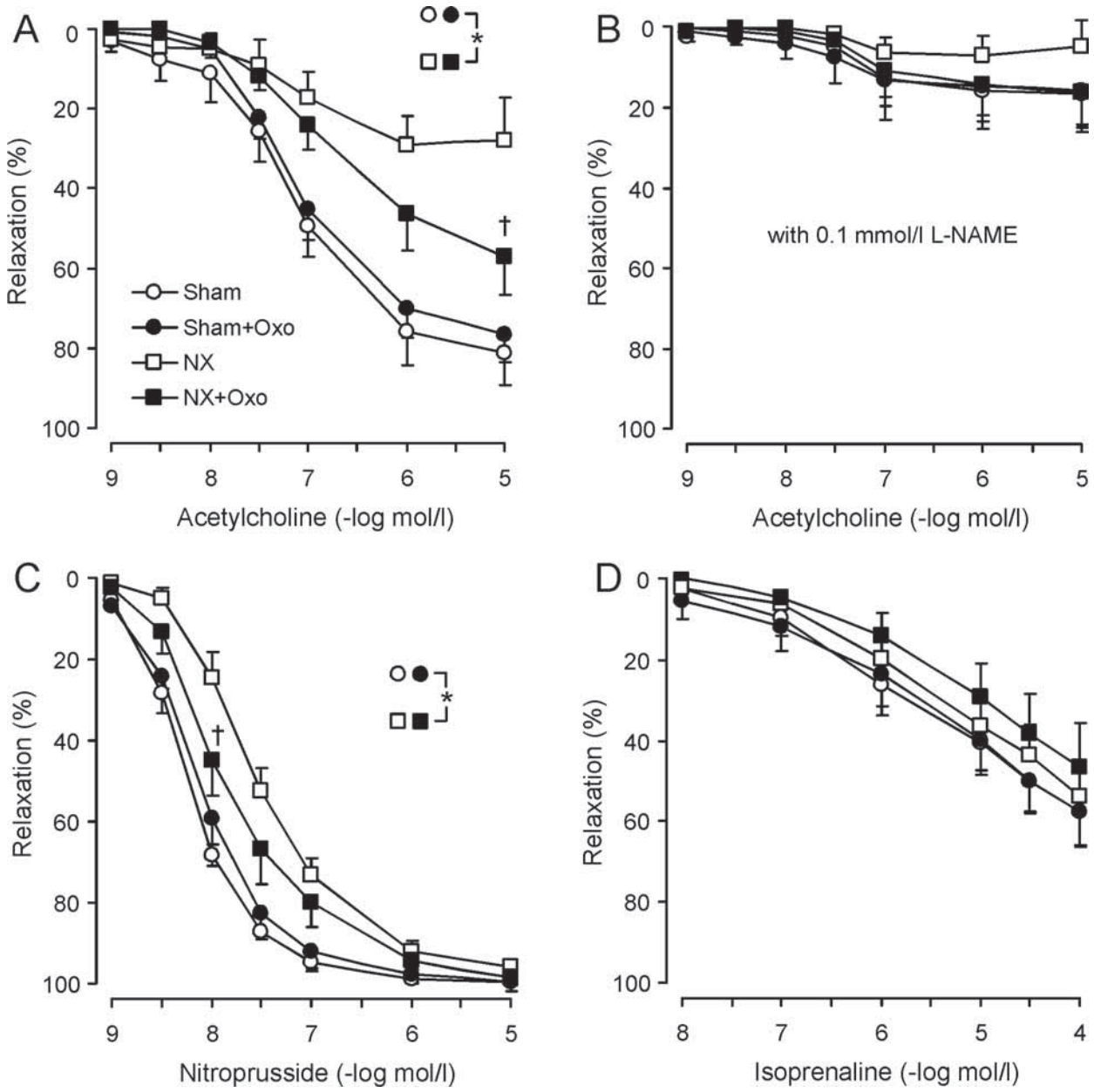
A
B
C
D
Relaxation (%)
Acetylcholine (-log mol/l)
Nitroprusside (-log mol/l)
Isoprenaline (-log mol/l)
with 0.1 mmol/l L-NAME
Sham
Sham+Oxo
NX
NX+Oxo
*
†

Table 1. Experimental group gross data (oxonic acid feeding period from week 3 to 12).

	Sham	Sham+Oxo	NX	NX+Oxo
Systolic blood pressure (mmHg)				
Week 3	122±4	122±5	127±5	127±7
Week 12	139±7	137±6	140±7	149±5
Heart / body weight (g/kg)	3.99±0.05	4.17±0.10	5.09±0.30*	5.25±0.39*
Body weight (g)				
Week 3	333±5	334±6	327±8	330±7
Week 12	416±8	404±9	430±11	409±6

Values are mean±SEM, n=10 for all groups.

*P<0.05 compared with the Sham group, $^{\dagger}P$<0.05 compared with the NX group

Table 2. Plasma uric acid after 2 and 9 weeks of the oxonic acid diet (study weeks 5 and 12), and plasma chemistry and blood pH after the 12-week study in the experimental groups.

	Sham	Sham+Oxo	NX	NX+Oxo
Uric acid (µmol/l)				
Week 5	50.3±13.0	106.8±15.5*	49.1±10.2	86.6±9.6*
Week 12	37.4±13.4	126.4±24.2*	65.9±23.2	156.6±22.7*†
Creatinine (µmol/l)	37.8±5.8	48.8±3.6	81.6±3.9*	84.1±9.8*
Creatinine clearance (ml/min)	3.0±0.4	2.0±0.2*	1.2±0.1*	1.2±0.1*
Urea (mmol/l)	6.8±0.4	8.6±0.5	13.7±1.0*	15.1±2.4*
TRAP (µmol/l)	422±52	611±70*	491±70	714±60*†
Cholesterol (mmol/l)	2.25±0.10	2.14±0.13	4.80±0.47*	5.09±0.65*
HDL (mmol/l)	1.64±0.09	1.62±0.10	3.55±0.37*	3.50±0.41*
Non-HDL (mmol/l)	0.61±0.03	0.51±0.04	1.25±0.21*	1.59±0.27*
Triglycerides (mmol/l)	1.16±0.11	0.96±0.08	1.46±0.09‡	1.77±0.34‡
Blood pH	7.44±0.04	7.39±0.03	7.37±0.04	7.41±0.03

TRAP = total peroxyl radical trapping antioxidant capacity; values are mean±SEM, n=10 for all groups. *P<0.05 compared with the Sham group, †P<0.05 compared with the NX group, ‡P<0.05 NX groups compared with the Sham groups using two-way ANOVA.

Kidney International (2009) 75, 339–340; doi:10.1038/ki.2008.593

Paricalcitol and renin-angiotensin components in remnant kidneys

Arttu Eräranta[a], Päivi Lakkisto[b,c], Ilkka Tikkanen[b,d], Jukka Mustonen[a,e] and Ilkka Pörsti[a,e]

[a]Medical School, University of Tampere, Tampere;
[b]Minerva Institute for Medical Research, Helsinki;
[c]Department of Clinical Chemistry, Helsinki University Central Hospital, Helsinki;
[d]Department of Medicine, Helsinki University Central Hospital, Helsinki;
[e]Department of Internal Medicine, Tampere University Hospital, Tampere, Finland

Correspondence:
Ilkka Pörsti, MD
Medical School
Department of Internal Medicine
FIN-33014 University of Tampere
Finland
Tel. +358 3 3116 6010
Fax. +358 3 3116 6164
E-mail ilkka.porsti@uta.fi

Running head: Paricalcitol and RAS

Keywords: paricalcitol, renin-angiotensin system, renal insufficiency

Word count: 236 words (1500 characters including spaces)

Dear Sir,

A recent article demonstrated that 8-week paricalcitol treatment of 5/6 nephrectomized rats suppressed expression of several genes of the renin-angiotensin system (RAS) in the kidney at the mRNA level (1). We recently performed a similar study (2), and have now determined the RAS components from the kidneys with very different results.

In our experiment, rats were put on a 12-week paricalcitol (200 ng/kg) treatment period 15 weeks after 5/6 nephrectomy (NX). After 27 weeks of renal insufficiency, the mRNA values of almost all RAS components and CTGF were different from sham-operated rats. However, no suppression of RAS genes between untreated and paricalcitol-treated NX rats were observed at the mRNA level (table). In the study by Freundlich et al., the NX rats were put on paricalcitol (100 ng/kg or 300 ng/kg) already 4 days after surgery (1). The subtotal nephrectomy produces a shock that undoubtedly alters gene expression in the remnant kidney, and it seems likely that these processes have not yet stabilized in 4 days. In our experiment, the treatment started 15 weeks after surgery in established chronic renal insufficiency. This situation more resembles the clinical renal disease, and may explain the differences in the observed results.

We conclude that paricalcitol treatment does not always suppress RAS components in the kidney, and suggest that the observed effects of paricalcitol on RAS gene expression in remnant kidneys may depend on the timing of the treatment.

References

1. Freundlich M, Quiroz Y, Zhang Z, *et al.*: Suppression of renin-angiotensin gene expression in the kidney by paricalcitol. *Kidney Int* 2008.
2. Karavalakis E, Eraranta A, Vehmas TI, *et al.*: Paricalcitol treatment and arterial tone in experimental renal insufficiency. *Nephron Exp Nephrol* 2008; **109**: e84-93.

Conflict of interest

The authors report no conflicts of interest

Sources of funding

The Medical Research Fund of Tampere University Hospital, the Finnish Kidney Foundation, the Finnish Foundation for Cardiovascular Research, the Pirkanmaa Regional Fund of Finnish Cultural Foundation, the Paavo Nurmi Foundation, and the Medical Research Fund of Helsinki University Hospital.

Table. No differences in RAS components between untreated and paricalcitol-treated NX rats (200 ng/kg thrice weekly); 5/6 nephrectomy at the age of 8 weeks (study week 0), disease progression period 0-15 weeks, treatment period 15-27 weeks (12 weeks).

	Sham (n=12)	NX (n=7)	NX+Paricalcitol (n=8)
Kidney mRNA using RT-PCR			
AT_{1a} receptor ($x10^4$ / ng total RNA)	0.99 ± 0.04	0.83 ± 0.08*	0.80 ± 0.05*
AT_2 receptor ($x10^2$ / ng total RNA)	0.76 ± 0.15	0.32 ± 0.06*	0.19 ± 0.03*
AT_4 receptor ($x10^3$ / ng total RNA)	2.99 ± 0.21	3.76 ± 0.28*	3.90 ± 0.24*
Renin receptor ($x10^4$ / ng total RNA)	2.31 ± 0.15	1.77 ± 0.11*	1.74 ± 0.08*
MAS oncogene ($x10^2$ / ng total RNA)	4.80 ± 0.34	4.92 ± 0.48	4.77 ± 0.41
ACE ($x10^4$ / ng total RNA)	0.98 ± 0.68	1.72 ± 0.21*	2.06 ± 0.20*
ACE2 ($x10^4$ / ng total RNA)	1.10 ± 0.08	0.65 ± 0.14*	0.49 ± 0.09*
CTGF ($x10^4$ / ng total RNA)	1.74 ± 0.11	2.76 ± 0.49*	2.84 ± 0.19*
Plasma renin activity (ng/ml/h)	24.3 ± 3.0	1.7 ± 1.0*	1.4 ± 0.7*

Mean ± SEM, *P<0.05 compared with the Sham group; NX, 5/6 nephrectomy; ACE, angiotensin converting enzyme; CTGF, connective tissue growth factor.

Kidney International (2009) 75, 340; doi:10.1038/ki.2008.595

Response to 'Paricalcitol and renin-angiotensin components in remnant kidneys'

Michael Freundlich[1], Yan C. Li[2] and Bernardo Rodriguez-Iturbe[3]

[1]Department of Pediatric Nephrology, University of Miami, Miami, Florida, USA;

[2]Department of Medicine, The University of Chicago, Chicago, Illinois, USA and

[3]Hospital Universitario de Maracaibo, Maracaibo, Zulia, Venezuela

Correspondence:

Michael Freundlich,

Department of Pediatric Nephrology,

University of Miami, P.O. Box 1696 M-719, Miami, Florida 33101, USA.

E-mail: mfmefex@pol.net

Dear Sir,

The comments by Karavalakis et al. refer to their experiments in which paricalcitol administration was delayed for 15 weeks following 5/6 nephrectomy and maintained for 12 weeks.(1) In the supplementary table provided in their above letter, reverse transcription–PCR determinations of various renin-angiotensin system (RAS) components were not modified by paricalcitol treatment and they suggest that the suppression of the RAS components in our experiments is related to a nonspecific postsurgical reduction of gene expression and/or the timing of the therapeutic intervention.

To be noted, in their work reverse transcription–PCR determinations of several RAS components display inconsistent directional variability with either up- or downregulated levels in kidney tissues of both treated and untreated nephrectomized animals compared to sham. Their findings of simultaneous downregulation of AT1R and AT2R as well as that of the renin receptor in the remnant kidney are in contrast with the results of others (2,3) as well as ours.(4) If what they observed is confirmed, then the question is whether the ability of paricalcitol to suppress an already downregulated genetic system in kidneys with advanced chronic kidney disease is detectable. Unfortunately, neither renin nor additional RAS genes mRNA or their protein expressions are shown, and no indication about effects of functional or histopathological changes in the remnant kidney by the delayed paricalcitol treatment is given.

It is not clear what the authors mean by the shock produced by the nephrectomy and its effects on gene expression, because this is a well-established experimental model employed to evaluate the effects of early therapeutic intervention on multiple molecular markers linked to progressive chronic renal insufficiency.(3) Furthermore, in our own experiments,(4) there was not a universal suppression of the renal mRNAs of the RAS but a specific reduction in only some components, which argues against a postsurgical nonspecific inhibition.

We agree with Karavalakis et al. that as we started paricalcitol 4 days after nephrectomy and they started 15 weeks later, the experiments are not strictly comparable and the timing of the therapeutic intervention could be the reason for the differences between our results and theirs. Unpublished observations in our laboratories indicate that delaying paricalcitol treatment for 8 weeks after nephrectomy essentially abrogates the functional and histological improvement of vitamin D analogues in the renal ablation model.

References

1. Karavalakis E, Eräranta A, Vehmas TI et al. Paricalcitol treatment and arterial tone in experimental renal insufficiency. Nephron Exp Nephrol 2008; 109: e84–e93.

2. Cao Z, Bonnet F, Candido R et al. Angiotensin type 2 receptor antagonism confers renal protection in a rat model of progressive renal injury. J Am Soc Nephrol 2002; 13: 1773–1787.

3. Vaziri ND, Bai Y, Ni Z et al. Intra-renal angiotensin II/AT1 receptor, oxidative stress, inflammation, and progressive injury in renal mass reduction. J Pharmacol Exp Ther 2007; 323: 85–93.

4. Freundlich M, Quiroz Y, Zhang Z et al. Suppression of renin-angiotensin gene expression in the kidney by paricalcitol. Kidney Int 2008.

Original Report: Laboratory Investigation

American Journal of Nephrology

Am J Nephrol 2012;35:401–408
DOI: 10.1159/000337942

Received: July 8, 2011
Accepted: February 25, 2012
Published online: April 19, 2012

Dietary Phosphate Binding and Loading Alter Kidney Angiotensin-Converting Enzyme mRNA and Protein Content in 5/6 Nephrectomized Rats

Arttu Eräranta[a] Asko Riutta[a] Meng Fan[a] Jenni Koskela[a] Ilkka Tikkanen[d] Päivi Lakkisto[d] Onni Niemelä[e] Jyrki Parkkinen[b] Jukka Mustonen[a, c] Ilkka Pörsti[a, c]

[a]School of Medicine, University of Tampere, and Departments of [b]Pathology and [c]Internal Medicine, Tampere University Hospital, Tampere, [d]Minerva Institute for Medical Research, and Helsinki University Central Hospital, Helsinki, and [e]Department of Clinical Chemistry, Etelä-Pohjanmaa Central Hospital Laboratory, Seinäjoki, Finland

Key Words
Angiotensin-converting enzyme · Calcium · Chronic renal insufficiency · Phosphate · Renin-angiotensin system

Abstract
Background: Vitamin D receptor activation with paricalcitol can modulate the transcription of renin-angiotensin system components in the surgical 5/6 nephrectomy rat model (5/6 NX) of chronic renal insufficiency. We tested the hypothesis whether dietary modification of phosphate influences kidney renin-angiotensin system gene expression at the mRNA level in 5/6 NX rats. ***Methods:*** Fifteen weeks after surgery, rats were given control diet (0.3% calcium, 0.5% phosphate), phosphate-lowering diet (3% calcium as carbonate) or high-phosphate diet (1.5%) for 12 weeks. Sham-operated rats were on control diet. ***Results:*** Blood pressure, plasma phosphate, parathyroid hormone, glomerulosclerosis, tubulointerstitial damage, and FGF-23 were increased in remnant kidney rats, whereas creatinine clearance was decreased. Phosphate, parathyroid hormone, glomerulosclerosis, tubulointerstitial damage, and FGF-23 were further elevated by the high-phosphate diet, but were reduced by the phosphate-lowering diet. Plasma calcium was increased with the phosphate-lowering diet and decreased with the high-phosphate diet. Remnant kidney rats on control diet showed upregulated kidney angiotensin-converting enzyme (ACE) and angiotensin (Ang) IV receptor (AT_4) transcription, while ACE2, Ang II type 2 receptor and renin receptor transcription were downregulated in comparison with sham rats. Phosphate-lowering diet reduced whereas high-phosphate diet increased kidney ACE, and these effects were observed at both mRNA and protein levels. Dietary phosphate loading also resulted in lower AT_{1a} gene transcription. ***Conclusion:*** Dietary phosphate loading was associated with elevated kidney ACE expression, increased tissue damage and lower AT_{1a} transcription in 5/6 NX rats. Phosphate binding with 3% calcium carbonate had opposite effects on ACE and kidney damage.

Introduction

Disturbed calcium-phosphorus balance is associated with an accelerated decline in residual kidney function and ectopic calcification [1]. Elevated serum phosphate is an independent risk factor of increased mortality in patients with chronic kidney disease (CKD) [2]. However, even in healthy adults, higher serum phosphate levels

KARGER
Fax +41 61 306 12 34
E-Mail karger@karger.ch
www.karger.com

0250–8095/12/0355–0401$38.00/0

Accessible online at:
www.karger.com/ajn

Ilkka Pörsti, MD
School of Medicine
Department of Internal Medicine
FI–33014 University of Tampere (Finland)
Tel. +358 3 247 6010, E-Mail ilkka.porsti@uta.fi

correlate with elevated coronary artery calcium [3]. Phosphate retention, hypocalcemia and reduced vitamin D levels lead to the development of secondary hyperparathyroidism already at stage 2–3 of chronic renal insufficiency (CRI) [4].

Dietary phosphate restriction can suppress the development of secondary hyperparathyroidism [4] and retard CRI progression [1]. Oral phosphate binders, including low doses of calcium salts, are commonly needed to manage hyperphosphatemia and secondary hyperparathyroidism in CRI [5]. In patients with stage 5 CKD, a high intake of calcium salts may predispose to soft tissue calcification [6]. However, lowering of plasma phosphate using increased intake of calcium carbonate may reduce kidney calcification in experimental CRI [7].

The renin-angiotensin system (RAS) is an important regulator of blood pressure (BP), sodium retention and renal function. The complexity of RAS has recently increased with new peptides such as angiotensin (Ang) 1–7, receptors such as Mas, renin receptor and Ang IV receptor (AT_{4R}), and enzymes including ACE2 [8]. The kidney contains all components of RAS, and intrarenal formation of Ang II not only controls glomerular hemodynamics and tubule sodium transport, but also activates inflammatory and fibrotic pathways [9]. We have previously found that increased calcium intake reduces kidney ACE protein in rats with CRI [10]. Here, we explored whether phosphorus binding and loading can influence renal expression of RAS components in advanced experimental CRI. We subjected rats to 5/6 nephrectomy (NX), followed them for 15 weeks and then divided them into three groups given either control, phosphate-lowering or high-phosphate diet for 12 weeks.

Methods

Animals and Experimental Design

Male Sprague-Dawley rats (n = 51) were housed 2 to a cage with free access to water and food (Lactamin R34, AnalyCen, Lindköping, Sweden). NX was performed by surgical resection of the upper and lower poles (2/3) of the left kidney, followed by contralateral NX [10, 11]. Sham operation was kidney decapsulation. Anesthesia, antibiotics, postoperative pain relief and measurement of systolic BP by tail cuff were performed as previously reported [10, 11].

Fifteen weeks after operations, at the age of 23 weeks, NX rats were divided into three groups with similar systolic BPs, body weights and plasma creatinine levels. Then, for 12 weeks, sham and NX groups continued on 0.3% Ca + 0.5% Pi, the NX+Ca group on 3.0% Ca + 0.5% Pi, and the NX+Pi group on 0.3% Ca + 1.5% Pi diet. At the end of the study, 24-hour urine excretion was collected in metabolic cages.

After 27 study weeks, the rats were anesthetized (intraperitoneal urethane 1.3 g/kg). Blood samples from the cannulated carotid artery were drawn with EDTA and heparin as anticoagulants, as appropriate. The kidneys were removed, weighed and sagittally split into two halves. One half was fixed in 4% formaldehyde for 24 h and embedded in paraffin. The other half was snap-frozen in isopentane at –40°C and stored at –80°C for RAS component measurements. The experimental design was approved by the Animal Experimentation Committee of the University of Tampere and the Provincial Government of Western Finland, Department of Social Affairs and Health, Finland. The investigation conforms to the Guiding Principles for Research Involving Animals.

Real-Time Quantitative RT-PCR

Total RNA was isolated from kidney tissue using Trizol reagent (Invitrogen, Carlsbad, Calif., USA), and reverse transcription of RNA was performed using M-MLV reverse transcriptase (Invitrogen). GAPDH and 18S were used as housekeeping genes. PCRs were performed with SYBR Green or TaqMan chemistry using ABI Prism 7000 sequence detection (Applied Biosystems, Foster City, Calif., USA).

PCRs for AT_{1aR}, AT_{4R}, heme oxygenase-1 (HO-1), GAPDH, Mas and renin receptor were performed in duplicate in 25-μl final volume containing 1× SYBR Green Master mix (Applied Biosystems) and 300 nM of primers (online supplementary table 1, see www.karger.com/doi/10.1159/000337942). PCRs for AT_{2R} and connective tissue growth factor (CTGF) were performed in duplicate in 25-μl final volume containing 1× TaqMan Master mix (Applied Biosystems), 300 nM of primers and 150 nM of AT_{2R} or 200 nM of CTGF TaqMan probe, respectively. PCRs for 18S were performed in duplicate in 25-μl final volume containing 1× TaqMan Master mix (Applied Biosystems) and 1× 18S TaqMan Gene Expression Assay primer and probe mix (Hs999999_s1, Applied Biosystems).

PCR cycling conditions for GAPDH were 10 min at +95°C and 40 cycles of 20 s at +95°C and 1 min at +56°C. PCR cycling conditions for other mRNAs were 10 min at +95°C and 40 cycles of 20 s at +95°C and 1 min at +60°C. Data were analyzed using the absolute standard curve method [12]. The amplification of 18S was used for normalizing the results of AT_{4R}, Mas and renin receptor mRNAs. The amplification of GAPDH was used for normalizing the results of AT_{1aR}, AT_{2R}, CTGF and HO-1 mRNAs. The unnormalized expressions of 18S and GAPDH did not differ in the groups, allowing their use as control genes.

In vitro Autoradiography of ACE and Ang II Receptors

Frozen kidney sections (20 μm thick) were cut on a cryostat at –17°C, thaw mounted onto Super Frost R Plus slides (Menzel-Gläser, Germany), dried in a desiccator under reduced pressure at 4°C overnight and stored at –80°C with silica gel until further processing [13]. Quantitative in vitro autoradiography of ACE and Ang II receptors was performed on 20-μm kidney tissue sections with the radioligands [^{125}I]-MK351A (lisinopril) and [^{125}I]-Sar1, Ile8-Ang II, respectively [10, 13, 14]. For quantifications, kidney sections were placed on Fuji Imaging Plate BAS-TP2025 (Tamro, Finland) for 3 h. AT_{1R} density was determined in the presence of AT_{2R} antagonist PD 123,313 (10 μM) and AT_{2R} density in the presence of AT_{1R} antagonist losartan (10 μM). The optical densities were quantified by an image analysis system (AIDA 2D densitom-

Table 1. Experimental group data and laboratory findings

	Sham	NX	NX+Ca	NX+Pi
Animal data				
Systolic blood pressure at week 27, mm Hg	129 ± 2	173 ± 4*	145 ± 3*, †	161 ± 4*, †, ‡
Body weight at week 27, g	557 ± 7	507 ± 38	488 ± 13*	431 ± 35*
Heart weight/body weight, g/kg	3.21 ± 0.03	4.19 ± 0.43*	4.03 ± 0.13*	4.46 ± 0.40*
Number of rats at week 15	11	14	13	13
Number of rats at week 27	11	7*	12†	7*, ‡
Creatinine clearance, ml/min	1.84 ± 0.10	0.85 ± 0.15*	0.84 ± 0.07*	0.69 ± 0.17*
Plasma				
Phosphate, mmol/l	1.16 ± 0.06	2.52 ± 0.46*	0.81 ± 0.08*, †	5.47 ± 1.12*, †, ‡
Ionized calcium, mmol/l	1.36 ± 0.06	1.34 ± 0.03	1.55 ± 0.03*, †	0.93 ± 0.09*, †, ‡
Calcium-phosphorus product	1.55 ± 0.07	3.31 ± 0.65*	1.11 ± 0.09*, †	4.41 ± 0.53*, †, ‡
PTH, pmol/l	9.7 ± 1.3	129.0 ± 37.7*	0.4 ± 0.1*, †	398.2 ± 26.0*, †, ‡
25OH-D_3, nmol/l	33.4 ± 2.8	19.8 ± 4.0*	13.8 ± 0.9*	16.0 ± 1.3*
1,25$(OH)_2D_3$, pmol/l	285 ± 27	71 ± 23*	106 ± 22*	105 ± 43*
log FGF-23, pg/ml	2.32 ± 0.05	2.96 ± 0.06*	1.88 ± 0.07*, †	3.99 ± 0.18*, †, ‡
RAS components				
Plasma renin activity, ng of Ang I/ml/h	22.0 ± 2.9	1.7 ± 1.0*	1.7 ± 0.6*	1.8 ± 0.6*
Kidney ACE by autoradiography (vs. sham)	1.00 ± 0.09	1.39 ± 0.26	0.73 ± 0.06†	1.90 ± 0.12*, †, ‡
Kidney AT_{1R} by autoradiography (vs. sham)				
AT_{1R} in cortex	1.00 ± 0.06	1.18 ± 0.05	0.78 ± 0.03*, †	1.21 ± 0.10*, ‡
AT_{1R} in medulla	1.00 ± 0.11	1.14 ± 0.07	1.04 ± 0.07	1.24 ± 0.07
Mas mRNA, copies × 10^2/ng total RNA	4.80 ± 0.34	4.92 ± 0.48	5.06 ± 0.68	5.13 ± 0.32

Values are means ± SEM (n = 7–14). * $p < 0.05$ versus sham; † $p < 0.05$ versus NX; ‡ $p < 0.05$ versus NX+Ca.

etry) coupled to Fujifilm BAS-5000 phosphoimager (Tamro, Finland), with 24 analyses for each kidney section. Specific binding was calculated as total binding minus non-specific binding.

Western Blotting

Frozen tissues (100 mg) were lysed in 1 ml buffer containing 10 mM Tris-HCl, pH 7.4, 2% sodium dodecyl sulfate, with protein inhibitors (CompleteP Mini EDTA-free, Roche Diagnostics, Mannheim, Germany). Western blotting was then performed as previously reported [10]. Antibody binding to ACE was detected by chemiluminescence (WB Chemiluminescent Reagent plus, NEN Inc., Boston, Mass., USA), and the autoradiograph was analyzed with Image Gauge 3.3 software (Fuji Photo Film Co., Tokyo, Japan).

Plasma and Urine Determinations

Plasma and urine creatinine were determined by colorimetric assay according to Jaffe, phosphate by colorimetric dry chemistry (Vitros 950 analyzer, Johnson & Johnson, Rochester, N.Y., USA), calcium by ion-selective electrode (634 Ca^{2+}/pH Analyzer, Ciba Corning, Sudbury, UK), parathyroid hormone (PTH) by immunoradiometric assay for intact rat PTH (Immutopics, San Clemente, Calif., USA), and 1,25$(OH)_2D_3$ and 25OH-D_3 using kits (IDS Ltd., Boldon, UK). Plasma FGF-23 was determined by Human FGF-23 ELISA kit (Kinos Inc., Tokyo, Japan) applicable for analyses in rats [15] and plasma renin activity using radioimmunoassay (GammaCoat® PRA RIA kit, Diasorin S.p.A., Italy).

Kidney Histology

Paraffin kidney sections (5 μm) were stained with hematoxylin-eosin or periodic acid Schiff. Glomerulosclerosis and tubulointerstitial damage were semi-quantitatively scored by light microscopy in a blinded manner [10].

Data Presentation and Analysis of Results

Statistical analysis was done by one-way analysis of variance and the least-significant difference test (post-hoc). If variable distribution was skewed, the Kruskal-Wallis test and the Mann-Whitney U test were applied, and p values were corrected with the Bonferroni equation. Due to large variability and non-normal distribution, the FGF-23 values were log transformed. Correlation analyses (r) were performed by Spearman's ρ; results are means ± SEM, and $p < 0.05$ was considered significant.

Results

Animal Data

At the close of the study, BP was higher in all NX groups than in sham rats (table 1), while the NX+Ca group showed lower BP than the other NX groups. The NX+Ca and NX+Pi rats had lower final body weights

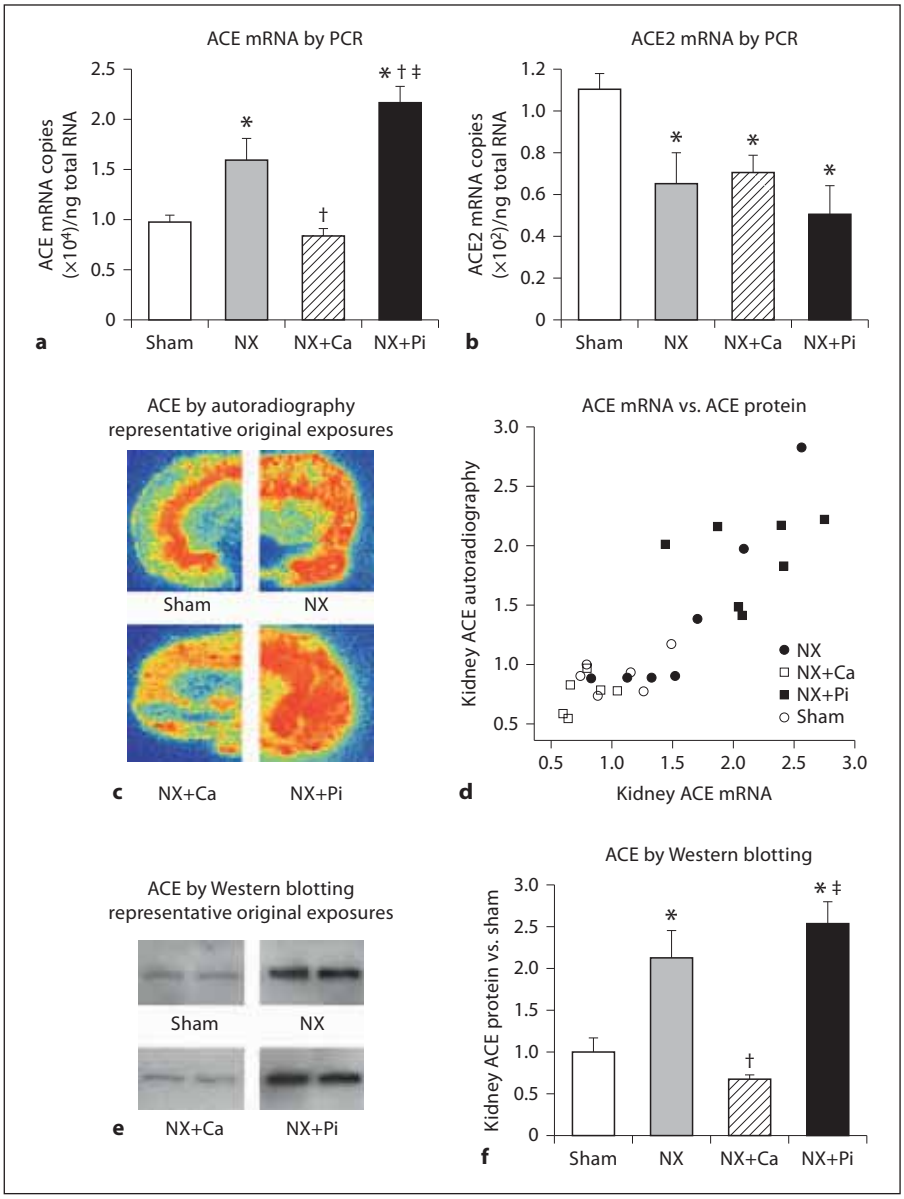

Fig. 1. Bar graphs show ACE mRNA (**a**) and ACE2 mRNA (**b**) determined using RT-PCR. Representative original exposures (**c**; intensity of red coloring reflects active binding to ACE) show ACE protein determined using in vitro autoradiography. Scatter blot shows relationship between ACE mRNA and ACE protein (**d**) determined using RT-PCR and autoradiography. Representative original exposures (**e**; intensity of the band reflects antibody binding to ACE) and bar graph (**f**) show ACE protein determined using Western blotting in sham and 5/6 NX rats ingesting either normal (NX), phosphate-lowering (NX+Ca) or high-phosphate diet (NX+Pi). Data are means ± SEM (n = 7–12). * $p < 0.05$ versus sham; † $p < 0.05$ versus NX; ‡ $p < 0.05$ versus NX+Ca.

than the sham rats, whereas no difference was seen between the NX groups. The heart/body weight ratios were increased in all NX groups. At the end of the study, lower rat count was observed in the NX and NX+Pi compared with the NX+Ca and sham groups (7, 6, 1 and 0 lost rats, respectively).

Laboratory Findings

Creatinine clearance was reduced in all NX groups (table 1). Plasma ionized calcium did not differ from sham rats in the NX group, but was increased in the NX+Ca group and decreased in the NX+Pi group. Plasma phosphate and the calcium-phosphorus product were over 2-fold increased in the NX and 3- to 5-fold increased in the NX+Pi versus the sham rats, but were decreased in the NX+Ca group. Plasma PTH and FGF-23 were increased in the NX and NX+Pi groups when compared with sham rats, while both were suppressed in the NX+Ca group. Plasma renin activity, 25OH-D_3 and 1,25$(OH)_2D_3$ levels were decreased in all NX groups.

Kidney ACE and ACE2

Renal ACE mRNA content was increased in the NX and NX+Pi groups, but not in the NX+Ca rats, when com-

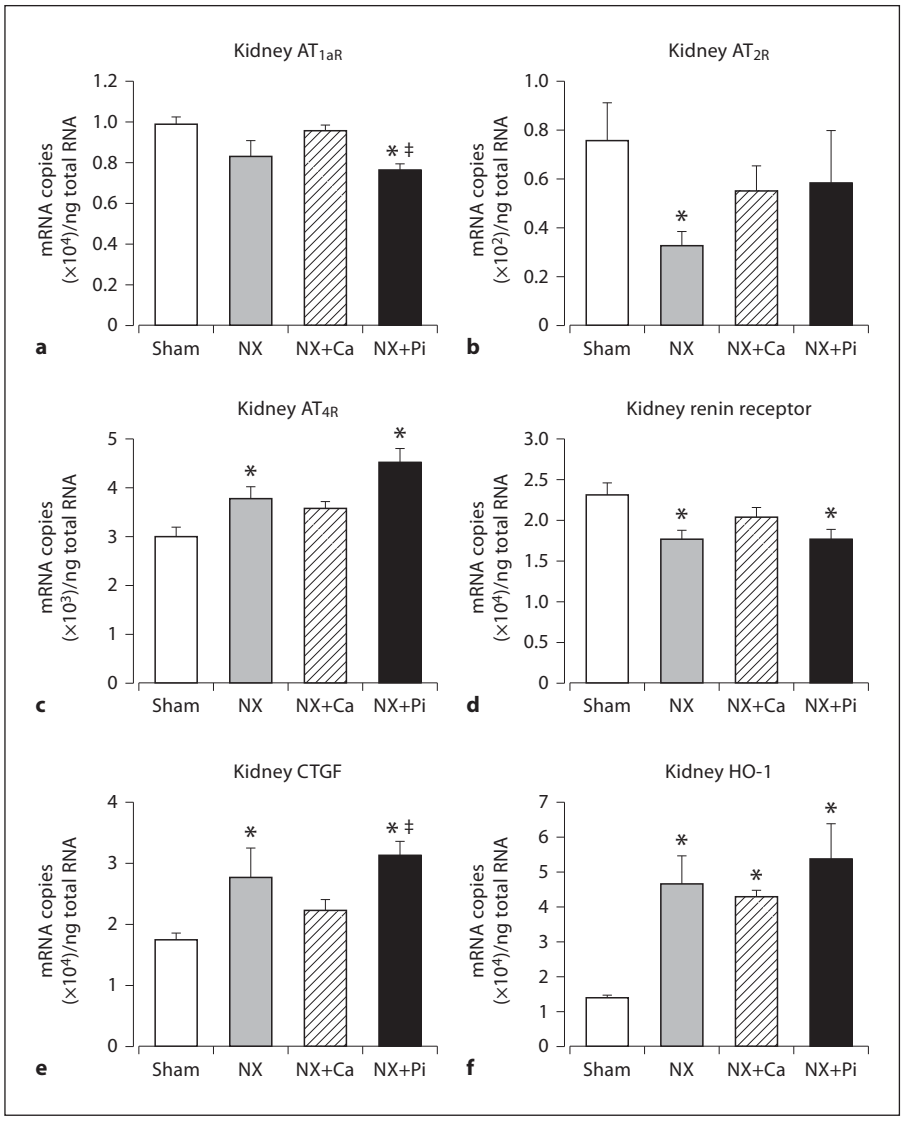

Fig. 2. Bar graphs show kidney AT_{1aR} mRNA (**a**), kidney AT_{2R} mRNA (**b**), kidney AT_{4R} mRNA (**c**), kidney renin receptor mRNA (**d**), kidney CTGF mRNA (**e**), and kidney HO-1 mRNA (**f**) determined using RT-PCR; groups as in figure 1. Data are means ± SEM (n = 7–12). * $p < 0.05$ versus sham; ‡ $p < 0.05$ versus NX+Ca.

pared with sham rats (fig. 1a). Highest values were seen in NX+Pi rats, as ACE mRNA was almost 2.5-fold higher than in NX+Ca and sham rats. Kidney ACE mRNA correlated well with ACE protein determined using autoradiography (fig. 1d; r = 0.830; $p < 0.001$) and Western blotting (r = 0.787; $p < 0.001$). Positive correlations ($p < 0.001$) were also observed between ACE mRNA and calcium-phosphate product (r = 0.825), phosphate (r = 0.771), PTH (r = 0.766), FGF-23 (r = 0.670) and ionized calcium (r = 0.659). Kidney ACE2 mRNA was decreased in all NX groups (fig. 1b).

In vitro autoradiography revealed lower kidney ACE protein content in the NX+Ca rats than in the NX rats, while ACE was highest in the NX+Pi group (table 1). The distribution of renal ACE was also different between NX and sham rats: the highest ACE signal was detected in a circular fashion in the inner cortex and outer medulla in sham rats, whereas ACE was more widely distributed throughout the remnant kidney in the NX and NX+Pi groups (fig. 1c). Western blotting analyses confirmed lower renal ACE protein in NX+Ca than in NX rats, and increased ACE protein in the NX and NX+Pi groups versus sham rats (fig. 1e, f).

Renal RAS Receptors, HO-1 and CTGF

Kidney AT_{1aR} mRNA content was lower in the NX+Pi versus the sham and NX+Ca groups, while no other differences were seen between the groups (fig. 2a). In auto-

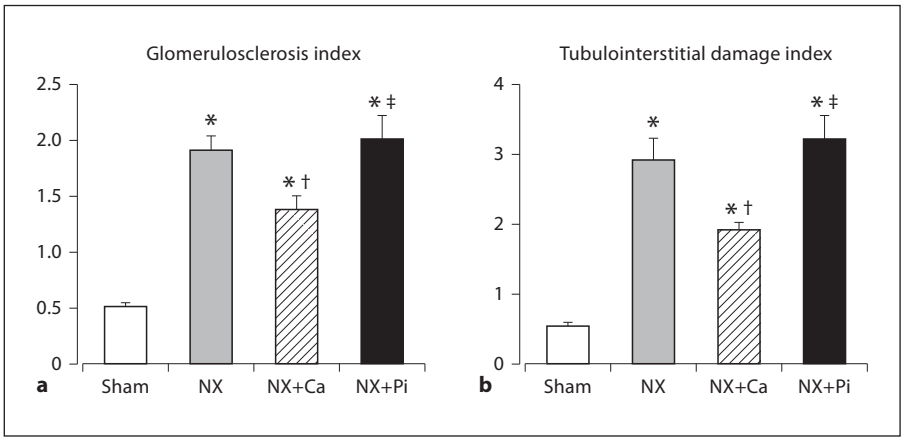

Fig. 3. Bar graphs show glomerulosclerosis index (**a**) and tubulointerstitial damage index (**b**); groups as in figure 1. Data are means ± SEM (n = 7–12). * $p < 0.05$ versus sham; † $p < 0.05$ versus NX; ‡ $p < 0.05$ versus NX+Ca.

radiography analyses, AT_{1R} density in the kidney cortex was lower in the NX+Ca and higher in the NX+Pi group versus the sham group, while no significant differences in AT_{1R} density in the medulla were found (table 1).

Kidney AT_{2R} mRNA content was decreased in the NX group in comparison with sham rats (fig. 2b). In autoradiography analyses, the proportion of AT_{2R} was low when compared with AT_{1R} (0.3–0.6% in the cortex, 0.1–0.4% in the medulla), and no significant differences in AT_{2R} density were found between the groups (data not shown). Kidney AT_{4R} mRNA (fig. 2c) was increased and renin receptor mRNA (fig. 2d) decreased in the NX and NX+Pi groups versus the sham group, while the NX+Ca rats did not differ from sham rats. Kidney Mas mRNA showed no significant differences between the groups (table 1).

Renal CTGF mRNA was higher in NX and NX+Pi rats than in sham rats and in NX+Pi rats compared with NX+Ca rats (fig. 2e). Kidney HO-1 mRNA was upregulated in all NX groups versus sham rats (fig. 2f).

Kidney Histology

Glomerulosclerosis (fig. 3a) and tubulointerstitial (fig. 3b) damage were increased in all NX groups. However, less tissue damage was seen in the NX+Ca group than in the NX and NX+Pi groups.

Discussion

This study investigated the effects of dietary phosphate loading and binding with calcium carbonate on renal tissue RAS components in experimental CRI. After 27 study weeks, elevated BP, suppressed plasma renin activity and decreased creatinine clearance were seen in all NX groups. The higher heart weight in NX rats can be attributed to the increased pressure and volume load [10]. The elevation of BP in NX rats was not affected by phosphate diet, but was reduced by phosphate-lowering diet. Several rats were lost from the NX and NX+Pi groups, probably because they were so uremic. Only one rat was lost from the NX+Ca group, which can possibly be explained by the lower plasma phosphate, reduced blood pressure and reduced kidney RAS component expression in these animals. Previously, the blood pressure-lowering influence of high-calcium diet has been repeatedly observed in experimental studies; possible mechanisms including increased natriuresis reduced sympathetic activity and enhanced vasodilatation [10, 16]. Since kidney RAS components were influenced by the present diets, possible parallel influences on vascular RAS components should be examined in the future.

We have previously found that increased calcium intake reduces the kidney ACE protein content in NX rats [10], whereas effects of phosphate-calcium balance on ACE mRNA and other kidney RAS components remain largely uncharted. As multiple determinants can modulate protein synthesis [17], knowledge about both mRNA and protein levels is necessary for the assessment of gene function. In this study, ACE mRNA and protein were elevated in NX rats, phosphate loading further increased kidney ACE, while a phosphate-lowering high-calcium diet maintained ACE mRNA and protein on a level comparable to that in sham rats. As ACE is a key target of pharmacotherapy in kidney diseases, these findings stress the importance of effective plasma phosphate control in the treatment of CKD.

We found a clear decrease in kidney ACE2 mRNA levels in all NX groups. ACE2 is considered a protective RAS

component, since it degrades the vasoconstrictor Ang II and generates the vasodilator and natriuretic peptide Ang 1–7 [18]. Therefore, reduced ACE2 transcription shifts balance towards enhanced vasoconstrictive RAS activity [8]. The effects of Ang 1–7 are thought to be mediated via the recently identified receptor Mas, which can also beneficially influence fibrogenesis in the kidney [8, 19]. In this study, no differences were seen in Mas mRNA between the groups.

The main effector of RAS, Ang II, exerts its actions mainly through AT_{1R} and AT_{2R} [8]. AT_{1R} mediate the potentially harmful consequences, while AT_{2R} are thought to mediate vasodilatation and antiproliferative effects [8]. However, the beneficial effects of AT_{2R} stimulation have been controversial and clinical proof is lacking [20]. Our results showed lower kidney AT_{2R} mRNA content in the NX group versus the sham group. Thus, lower Ang II action via AT_{2R} may participate in the renal pathology and pathophysiology in this model of CRI.

The receptor for Ang IV peptide, AT_{4R}, is also known as insulin-regulated aminopeptidase [8]. Ang IV has regulatory functions in cognition, renal metabolism and cardiovascular damage, and the AT_{4R}-mediated actions include renal vasodilatation, hypertrophy and nuclear factor-κB activation [8]. We found increased levels of kidney AT_{4R} mRNA in the NX and NX+Pi groups versus sham rats. To our knowledge, this is the first time that increased AT_{4R} content has been reported in the NX model. Notably, a high-calcium diet was not associated with increased kidney AT_{4R} transcription, agreeing with the overall suppression of renal tissue RAS components with improved plasma phosphate-calcium balance.

The renin receptor, which can bind both renin and prorenin, may play a role in tissue fibrosis [21]. The renin receptor is highly expressed in podocytes and appears to be essential for normal podocyte function and survival [22]. In the present study, kidney renin receptor mRNA was decreased in the NX and NX+Pi groups, but not in the NX+Ca group, when compared with the sham group. Renin receptor mRNA also inversely correlated with glomerulosclerosis in these groups ($r = -0.50$; $p = 0.002$). Thus, reduced renin receptor expression may have contributed to glomerular damage in this model of CRI. Interestingly, renin receptor mRNA was also modulated by alterations in calcium-phosphorus balance.

Increased expression of the fibrosis mediator CTGF has been reported in clinical and experimental kidney disease [23]. CTGF expression correlates with cellular proliferation and extracellular matrix accumulation [23] and is upregulated by Ang II [24]. Our measurements showed higher kidney CTGF mRNA versus sham rats in the NX and NX+Pi groups, but not in the NX+Ca group. This suggests that phosphate lowering decreased fibrosis signaling, which was also translated to kidney histology: glomerulosclerosis and tubulointerstitial damage were increased in all NX groups, but the high-calcium diet was associated with lower tissue damage.

HO provides the rate-limiting step in the catabolism of heme with two isoenzymes, the inducible HO-1 and the constitutive HO-2 [25]. HO-1 is induced by several agents that cause oxidative stress and is thought to offer cellular protection after injury [25]. In this study, the transcription of kidney HO-1 was elevated in all NX groups compared to sham rats, which was likely triggered to counter the elevated oxidative stress after partial NX.

The present intervention using high-phosphorus and high-calcium diets induced clear changes in all variables of the calcium-phosphorus metabolism: plasma phosphate, PTH and FGF-23 levels were different in all study groups. The changes in kidney tissue RAS components may have resulted from alterations in all of the above variables. In general, when phosphate balance is altered, this is reflected on calcium metabolism, and it is difficult to make the distinction which one of these two was the key player modulating renal tissue RAS components. However, high phosphate concentration can influence gene expression in tissues. Elevated phosphate can change the phenotype of vascular smooth muscle cell to an osteoblast-like cell via the induction of transcription factors (Msx2, osterix, runx2) [26]. An increase in phosphate concentration from 0.9 to 2.06 mmol/l can modulate the effect on vitamin D receptor-mediated gene expression induced by paricalcitol in human vascular smooth muscle cells in vitro [27]. Altogether, 325 target genes were affected by paricalcitol at 0.9 mmol/l phosphate, but the number of genes affected by paricalcitol at 2.06 mmol/l Pi decreased to 86. This may have resulted from high phosphate-induced alterations in the cytosolic versus the nuclear distribution of nuclear factor-κB and nuclear receptor co-repressor 1 [27]. The present data suggest that lowering of plasma phosphate can reduce RAS component expression and alleviate tissue damage in the kidney.

In conclusion, dietary phosphate loading was associated with elevated kidney ACE expression, increased tissue damage and lower AT_{1a} transcription in 5/6 NX rats. Phosphate binding had opposite effects on ACE and kidney damage. Our present findings stress the importance of effective phosphate control in CKD, as this may also beneficially influence the expression of RAS components in kidney tissue.

Acknowledgements

The excellent technical assistance of Marja-Leena Koskinen, Riina Hatakka and Jarkko Lakkisto are sincerely acknowledged. This study was supported by the Finnish Kidney Foundation, the Competitive Research Funding of the Pirkanmaa Hospital District, the Paavo Nurmi Foundation, the Emil Aaltonen Foundation, the Pirkanmaa Regional Fund of the Finnish Cultural Foundation, the Sigrid Jusélius Foundation, and the Competitive Research Funding of the Hospital District of Helsinki and Uusimaa.

Disclosure Statement

The authors declare no conflicts of interest.

References

1 Koizumi T, Murakami K, Nakayama H, Kuwahara T, Yoshinari O: Role of dietary phosphorus in the progression of renal failure. Biochem Biophys Res Commun 2002;295:917–921.
2 Kestenbaum B, Sampson JN, Rudser KD, Patterson DJ, Seliger SL, Young B, Sherrard DJ, Andress DL: Serum phosphate levels and mortality risk among people with chronic kidney disease. J Am Soc Nephrol 2005;16:520–528.
3 Foley RN, Collins AJ, Herzog CA, Ishani A, Kalra PA: Serum phosphorus levels associate with coronary atherosclerosis in young adults. J Am Soc Nephrol 2009;20:397–404.
4 Slatopolsky E, Brown A, Dusso A: Role of phosphorus in the pathogenesis of secondary hyperparathyroidism. Am J Kidney Dis 2001;37:S54–S57.
5 Nolan CR, Qunibi WY: Treatment of hyperphosphatemia in patients with chronic kidney disease on maintenance hemodialysis. Kidney Int Suppl 2005;S13–S20.
6 Cannata-Andia JB, Rodriguez-Garcia M: Hyperphosphataemia as a cardiovascular risk factor – how to manage the problem. Nephrol Dial Transplant 2002;17(suppl 11):16–19.
7 Cozzolino M, Dusso AS, Liapis H, Finch J, Lu Y, Burke SK, Slatopolsky E: The effects of sevelamer hydrochloride and calcium carbonate on kidney calcification in uremic rats. J Am Soc Nephrol 2002;13:2299–2308.
8 Fyhrquist F, Saijonmaa O: Renin-angiotensin system revisited. J Intern Med 2008;264:224–236.
9 Siragy HM, Carey RM: Role of the intrarenal renin-angiotensin-aldosterone system in chronic kidney disease. Am J Nephrol 2010;31:541–550.
10 Porsti I, Fan M, Koobi P, Jolma P, Kalliovalkama J, Vehmas TI, Helin H, Holthofer H, Mervaala E, Nyman T, Tikkanen I: High calcium diet down-regulates kidney angiotensin-converting enzyme in experimental renal failure. Kidney Int 2004;66:2155–2166.
11 Koobi P, Kalliovalkama J, Jolma P, Rysa J, Ruskoaho H, Vuolteenaho O, Kahonen M, Tikkanen I, Fan M, Ylitalo P, Porsti I: AT1 receptor blockade improves vasorelaxation in experimental renal failure. Hypertension 2003;41:1364–1371.
12 Lakkisto P, Palojoki E, Backlund T, Saraste A, Tikkanen I, Voipio-Pulkki LM, Pulkki K: Expression of heme oxygenase-1 in response to myocardial infarction in rats. J Mol Cell Cardiol 2002;34:1357–1365.
13 Bäcklund T, Palojoki E, Grönholm T, Eriksson A, Vuolteenaho O, Laine M, Tikkanen I: Dual inhibition of angiotensin converting enzyme and neutral endopeptidase by omapatrilat in rat in vivo. Pharmacol Res 2001;44:411–418.
14 Zhuo J, Ohishi M, Mendelsohn FA: Roles of AT1 and AT2 receptors in the hypertensive Ren-2 gene transgenic rat kidney. Hypertension 1999;33:347–353.
15 Saito H, Maeda A, Ohtomo S, Hirata M, Kusano K, Kato S, Ogata E, Segawa H, Miyamoto K, Fukushima N: Circulating FGF-23 is regulated by 1alpha,25-dihydroxyvitamin D_3 and phosphorus in vivo. J Biol Chem 2005;280:2543–2549.
16 Hatton DC, McCarron DA: Dietary calcium and blood pressure in experimental models of hypertension. A review. Hypertension 1994;23:513–530.
17 Gingold H, Pilpel Y: Determinants of translation efficiency and accuracy. Mol Syst Biol 2011;7:481.
18 Ferrario CM: Angiotensin-converting enzyme 2 and angiotensin-(1–7): an evolving story in cardiovascular regulation. Hypertension 2006;47:515–521.
19 Pinheiro SV, Ferreira AJ, Kitten GT, da Silveira KD, da Silva DA, Santos SH, Gava E, Castro CH, Magalhaes JA, da Mota RK, Botelho-Santos GA, Bader M, Alenina N, Santos RA, Simoes e Silva AC: Genetic deletion of the angiotensin-(1–7) receptor Mas leads to glomerular hyperfiltration and microalbuminuria. Kidney Int 2009;75:1184–1193.
20 Carey RM: Update on the role of the AT2 receptor. Curr Opin Nephrol Hypertens 2005;14:67–71.
21 Nguyen G: The (pro)renin receptor: pathophysiological roles in cardiovascular and renal pathology. Curr Opin Nephrol Hypertens 2007;16:129–133.
22 Riediger F, Quack I, Qadri F, Hartleben B, Park JK, Potthoff SA, Sohn D, Sihn G, Rousselle A, Fokuhl V, Maschke U, Purfurst B, Schneider W, Rump LC, Luft FC, Dechend R, Bader M, Huber TB, Nguyen G, Muller DN: Prorenin receptor is essential for podocyte autophagy and survival. J Am Soc Nephrol 2011;22:2193–2202.
23 Gupta S, Clarkson MR, Duggan J, Brady HR: Connective tissue growth factor: potential role in glomerulosclerosis and tubulointerstitial fibrosis. Kidney Int 2000;58:1389–1399.
24 Ruperez M, Ruiz-Ortega M, Esteban V, Lorenzo O, Mezzano S, Plaza JJ, Egido J: Angiotensin II increases connective tissue growth factor in the kidney. Am J Pathol 2003;163:1937–1947.
25 Abraham NG, Kappas A: Pharmacological and clinical aspects of heme oxygenase. Pharmacol Rev 2008;60:79–127.
26 Mizobuchi M, Towler D, Slatopolsky E: Vascular calcification: the killer of patients with chronic kidney disease. J Am Soc Nephrol 2009;20:1453–1464.
27 Wu-Wong JR, Nakane M, Ma J, Ruan X, Kroeger PE: Elevated phosphorus modulates vitamin D receptor-mediated gene expression in human vascular smooth muscle cells. Am J Physiol Renal Physiol 2007;293:F1592–F1604.

Manuscript to *American Journal of Nephrology*

Phosphate Binding with Calcium Carbonate Reduces Aortic Angiotensin Converting Enzyme and Enhances Bioactivity of Endothelium-derived Nitric Oxide in Experimental Renal Insufficiency

Arttu Eräranta[a], Suvi Törmänen[a], Peeter Kööbi[a,b], Tuija I. Vehmas[a], Päivi Lakkisto[c,d], Ilkka Tikkanen[c,e], Eeva Moilanen[a], Onni Niemelä[f], Jukka Mustonen[a,g], and Ilkka Pörsti[a,g]

[a]School of Medicine, University of Tampere, Tampere;
[b]Department of Ophthalmology, Tampere University Hospital, Tampere;
[c]Minerva Institute for Medical Research, Helsinki;
[d]Department of Clinical Chemistry, University of Helsinki, Helsinki;
[e]Department of Medicine, Helsinki University Central Hospital, Helsinki, Finland;
[f]Department of Clinical Chemistry, Etelä-Pohjanmaa Central Hospital Laboratory, Seinäjoki, Finland;
[g]Department of Internal Medicine, Tampere University Hospital, Tampere, Finland

Correspondence:
Ilkka Pörsti, MD
School of Medicine / Internal Medicine
FIN-33014 University of Tampere
Finland
Tel. +358 3 3551 6890
Fax. +358 3 3641 472
E-mail ilkka.porsti@uta.fi

Running head: Phosphate, aortic ACE, and NO in renal failure

Word count: 4997 words incl. references, legends to the figures, and tables

Conflicts of interest: None declared

Keywords: angiotensin-converting enzyme, calcium, chronic renal insufficiency, nitric oxide, phosphate, renin-angiotensin system

Abstract

Background: Disturbed calcium-phosphorus metabolism is associated with increased kidney angiotensin-converting enzyme (ACE) in experimental chronic renal insufficiency (CRI). However, information about the effects of phosphate binding and loading on vascular ACE is lacking.

Methods: Fifteen weeks after 5/6 nephrectomy (NX), rats were placed on phosphate-binding (NX+Ca, 3.0% Ca), phosphate-loading (NX+Pi, 1.5% Pi) or control diet for 12 weeks (NX and Sham).

Results: Aortic ACE, blood pressure, plasma phosphate, and parathyroid hormone were increased in the NX and NX+Pi groups, but were reduced with phosphate binding. Endothelium-mediated relaxations of isolated mesenteric conduit artery rings to acetylcholine were impaired in the NX and NX+Pi groups, but did not differ from Sham in NX+Ca rats. Experiments with nitric oxide (NO) synthase inhibition *in vitro* suggested that the NO-mediated component of acetylcholine response was lower in the NX and NX+Pi groups, but did not differ from Sham in NX+Ca rats. In all NX groups, aortic endothelial NO synthase (eNOS) was reduced, while plasma and urine concentrations of NO metabolites were increased. Aortic nitrated proteins and calcification were increased in the NX and NX+Pi groups when compared with the NX+Ca and Sham groups.

Conclusion: Hypertension in the 5/6 nephrectomy model of CRI was associated with reduced vasorelaxation, decreased eNOS, and increased ACE and nitrated proteins in the aorta. Phosphate binding with calcium carbonate enhanced vasorelaxation via endogenous NO and suppressed elevation of ACE and nitrated proteins, suggesting reduced vascular oxidative stress. Our findings support the view that correction of calcium-phosphorus balance prevents CRI-induced vascular pathophysiology.

Introduction

In chronic kidney disease (CKD), cardiovascular complications pose a major clinical problem [1]. These complications are commonly aggravated by increased serum phosphate and parathyroid hormone (PTH) concentrations [2]. Reduced renal function is independently associated with stiffening of large arteries and morphological vascular disorders including increased intima-media thickness, smooth muscle hyperplasia, and medial calcification [1,3]. In addition, changes in the function and structure of resistance arteries have been described in both clinical [1] and experimental forms of chronic renal insufficiency (CRI) [4]. Phosphate retention, hypocalcaemia, and reduced vitamin D levels lead to the development of secondary hyperparathyroidism already at stage 2-3 of CRI [5], while all of these factors also influence remodelling in the vascular wall [6]. In order to manage CRI-induced hyperphosphatemia and secondary hyperparathyroidism [7], oral phosphate binders are frequently needed.

The endothelial cells continuously synthesize nitric oxide (NO) from L-arginine by the constitutive endothelial NO synthase (eNOS) [8]. When compared with small vessels, the contribution of eNOS to vasomotion seems to be greater in conduit-size arteries, as the NO-mediated relaxation is more pronounced in large arteries [9,10]. The interaction between activation of vascular renin-angiotensin system (RAS) and bioavailability of endothelium-derived NO has been suggested to be an important regulator of vascular tone [11].

A key target for the pharmacological inhibition of RAS is angiotensin-converting enzyme (ACE) [12], which catalyzes the conversion of angiotensin I to angiotensin II (Ang II), and also degrades kinins [13]. We recently found that dietary phosphate loading was associated with elevated kidney ACE expression and increased tissue damage in the 5/6 nephrectomy (NX) rat model of CRI [14]. In contrast, phosphate binding with 3.0% calcium carbonate reduced kidney ACE protein [15], ACE mRNA, and kidney damage [14].

The present study explored whether phosphate binding and loading can influence ACE content in the abdominal aorta, and NO-mediated endothelium-dependent vasodilatation in the main branch of the mesenteric artery. In order to evaluate oxidative stress, nitrated protein and eNOS contents in the abdominal aorta, and NO metabolites (NOx) in plasma and urine were determined. Rats were subjected to NX, followed for 15 weeks, and then divided into groups given either control, phosphate-lowering or high-phosphate diet for another 12 weeks.

Methods

Animals and experimental design

In order to reduce the use of experimental animals, we utilized samples from rats that had been previously used for reports elucidating resistance artery function [4] and kidney tissue ACE [14] in experimental CRI. The NX groups underwent removal of right kidney and surgical resection of the upper and lower poles (2/3) of the left kidney, whereas sham operation was kidney decapsulation [4,14-16]. Diets, anaesthesia, antibiotics, postoperative pain relief, and measurement of systolic BP by tail-cuff were as previously [4,15,16].

Preliminary 12-week study examined whether phosphate binding with calcium carbonate influences aortic or cardiac ACE. Four weeks after NX (rat age 12 weeks), 4 groups with corresponding systolic BPs and body weights in Sham vs. Sham+Ca groups, and NX vs. NX+Ca groups, respectively, were formed (n=10-11 in each) [4]. Then for 8 weeks, Sham and NX rats ingested 0.3% calcium, while Sham+Ca and NX+Ca rats ingested 3% calcium chow (carbonate supplement, AnalyCen, Sweden) [4]. Aortic and cardiac samples were harvested after 12 study weeks.

The 27-week study. Fifteen weeks after NX, three groups (n=13-14) of remnant kidney rats, having equal mean systolic BP, body weight, and plasma creatinine level, and Sham rats (n=11) of equal age, were put on chow containing 0.3% Ca and 0.5% Pi (NX and Sham),

3.0% Ca and 0.5% Pi (NX+Ca) and 0.3% Ca and 1.5% Pi (NX+Pi) (AnalyCen) [14]. We have previously found clear differences in calcium-phosphate metabolism after 0.3% versus 3.0% calcium intake in experimental CRI, in the absence adverse effects that would indicate calcium deficiency or excess [4,14,15]. Then for 12 weeks, body weight and systolic BP were monitored fortnightly. The 24-hour water intake and urine output were measured in metabolic cages. Urine samples were stored at -80°C for creatinine and NO metabolite determinations. From the NX, NX+Pi and NX+Ca groups, 7, 6, and 1 rats were lost, and the final numbers of animals in these groups were 7, 7 and 12, respectively [14].

At close of the study, rats were anaesthetized (intraperitoneal urethane 1.3 g/kg), carotid artery was cannulated, and blood samples were drawn with EDTA and heparin as anticoagulants, as appropriate. Main branches of the mesenteric arteries were excised, and the hearts were removed and weighed. Cardiac and abdominal aortic tissue for the measurement of ACE, eNOS, and nitrated proteins were frozen in isopentane at -40ºC and stored at -80ºC. Aortic samples were fixed in 4% formaldehyde for 24 hours and embedded in paraffin for calcification determinations. The experimental design was approved by the Animal Experimentation Committee of the University of Tampere, and the Provincial Government of Western Finland, Department of Social Affairs and Health, Finland. The investigation conforms to the Guiding Principles for Research Involving Animals.

Mesenteric arterial responses in vitro

The mesenteric artery was cleaned of adjacent tissue, and three successive 3 mm-long ring sections were cut, beginning 5 mm distally from the mesenteric artery-aorta junction. In two proximal rings the endothelium was left intact, while endothelium was denuded from the distal sample [17]. The rings were suspended between hooks in organ bath chambers (20 ml) with physiological salt solution (PSS; pH 7.4) containing (mmol/L): NaCl 119, $NaHCO_3$ 25, glucose 11.1, $CaCl_2$ 1.6, KCl 4.7, KH_2PO_4 1.2, $MgSO_4$ 1.2, and aerated with 95% O_2-5%

CO_2. The rings were equilibrated for 2 hours at +37ºC with preload of 4.905 mN/mm, and challenged with 125 mmol/L KCl [18].

Responses to acetylcholine (ACh) in the absence and presence of 0.1 mmol/l N^G-nitro-L-arginine methyl ester (L-NAME) or 1 mmol/l L-arginine, norepinephrine (NE), and angiotensin II (Ang II) were studied in endothelium-intact rings, and to KCl and nitroprusside in endothelium-denuded rings. All vasorelaxations were studied after precontractions induced by 1 μmol/L NE. The presence of intact endothelium was confirmed by a clear relaxation to 1μmol/L ACh, and the absence of endothelium by the lack of this response [17,18]. Contractions were recorded using Grass equipment (FT-03 transducer, 7E Polygraph; Grass Instrument Co., Quincy, MA). Stock solutions of the compounds used to study arterial tone *in vitro* were freshly prepared in distilled water and protected from light.

Biochemical measurements

NOx concentration was measured by conversion of nitrite and nitrate to NO, quantified by the ozone-chemiluminescense method [19]. Plasma and urine samples were treated with ethanol at +20°C for 2 hours to precipitate proteins. Then a 20μl sample was injected into a cylinder containing saturated vanadium (III) chloride (VCl_3) in HCl (0.8g VCl_3 / 100ml of 1mol/L HCl) at 95°C, and NO formed under reducing conditions was measured (NOA 280 analyzer, Sievers Instruments, Boulder, CO) using sodium nitrate as the standard [20]. Measurements of plasma phosphate, PTH and ionized calcium were as recently described [14].

Autoradiography of tissue ACE

Frozen tissue sections (20 μm thick) were cut on a cryostat (-17°C), thaw mounted onto slides (Super Frost R Plus, Menzel-Gläser, Germany), dried in a desiccator (reduced pressure, +4°C) overnight, and stored at -80 °C with silica gel [14,21]. A tyrosyl residue of lisinopril

(MK351A, Merck, Sharp & Dohme Research Laboratories, West Point, PA) was iodinated by chloramine T method, purified (SP-Sephadex C-25 column, Pharmacia, Piscataway, NJ), and a previously described technique was applied [21,22]. For quantification, the sections were placed on a Fuji Imaging Plate BAS-TP2025 (Tamro, Finland) for 3 hours. The optical densities were quantified by an image analysis system (AIDA 2D densitometry) coupled to FUJIFILM BAS-5000 phosphorimager (Tamro, Finland), a total of 24 analyses per tissue sample. Specific binding was calculated as total binding minus non-specific binding.

Western blotting of aortic NOS and nitrated proteins

Frozen tissues were homogenized (Ultra-Turrax T25, Janke & Kunkel GmbH & Co, IKA®-Labortechnik, Germany) in 400 µl distilled H_2O containing protease inhibitors (Complete™ Mini EDTA-free, Roche Diagnostics GmbH, Germany). After centrifugation (12,000 g, 15 min, 4°C), protein concentrations of the supernatants were determined (Coomassie Plus™ Protein Assay Kit, Pierce, IL). SDS-PAGE was run on 8% resolving gel and 4% stacking gel, and proteins were transferred to Hybond-ECL nitrocellulose membrane (Amersham Biosciences Limited, Buckinghamshire, UK). The primary antibodies were: 1:2500 dilution of mouse eNOS antibodies (BD Biosciences-Pharmingen, CA), 1:4000 dilution of rabbit NOS2 polyclonal antibodies (Santa Cruz Biotechnology), and 1:3333 dilution of mouse nitrotyrosine monoclonal antibody (Cayman Chemical, MI). Antibody binding was detected using SuperSignal® West Pico chemiluminescent substrate (Pierce, IL), and signal was analysed using FluorChem 8800 imaging system (software version 3.1., Alpha Innotech Corporation, San Leandro, CA).

Aortic calcification

Calcifications were determined from von Kossa-stained aortic sections at 200X magnification. The total area and area of calcification was measured, and the index of

calcification for each rat was expressed as percentage of the calcified area related to the total area of the cross-section.

Drugs

The drugs were: ketamine (Parke-Davis Scandinavia AB, Solna, Sweden), ACh chloride, L-arginine, L-NAME hydrochloride, NE bitartrate, Ang II (Sigma Chemical Co, St. Louis, MO), sodium nitroprusside (Fluka Chemie AG, Buchs SG, Switzerland).

Data presentation and analysis of results

Contractions were expressed in mN/mm, and the EC_{50} for the contractions as the negative logarithm (pD_2) values. Vasorelaxation was presented as percentage of precontraction. Area under concentration response curve (AUC) analysis was applied to present the change in AUC by L-NAME to evaluate the contribution of NO to vasorelaxation. Statistics was by one-way analysis of variance (ANOVA), supported by post-hoc Tukey's test, or ANOVA for repeated measurements, as appropriate. If skewed variable distribution was observed, the Kruskal-Wallis and post-hoc Mann-Whitney U-test were applied. Results were presented as mean±SEM, and $P<0.05$ was considered significant.

Results

The 12-week pilot study

The results of quantitative *in vitro* autoradiography showed a decrease in aortic and cardiac ACE protein content after 8 weeks of phosphate binding with 3.0% calcium carbonate (Supplemental Figure S1). The analyses were performed from randomly selected 8-10 rats in each group.

The 27-week study

Animal data, plasma and urine determinations

At week 15 week after the operations, systolic BP was elevated in all NX groups (Table 1). At study week 27, BP was higher in all NX groups than in Sham rats, but BP in the NX-Ca group was lower than in NX and NX+Pi rats. There were no differences in body weight at week 15, but at week 27 body weights were lower in the NX+Ca and NX+Pi groups than in Sham rats, while no significant differences were detected between the NX groups. The heart/body weight ratios were increased, and creatinine clearance was decreased, in all NX rats versus Sham rats (Table 1).

Plasma phosphate and PTH were increased in the NX group, and further elevated in the NX+Pi group, while both phosphate and PTH were suppressed in the NX+Ca group. Plasma ionized calcium did not differ from Sham in the NX group, but was increased in the NX+Ca, and decreased in the NX+Pi group. Both plasma and urine NOx were increased in all NX groups when compared with Sham (Table 1).

Aortic ACE, endothelial NOS, nitrated proteins, and calcification

After 27 study weeks, aortic ACE protein content was higher in the NX and NX+Pi groups than in Sham rats. Notably, aortic ACE content was clearly lower in the NX+Ca group when compared with the NX and NX+Pi groups (Figures 1A and 1B).

Aortic eNOS protein content, determined using Western blotting, was similarly decreased in all NX groups when compared with Sham rats (Figure 2A). However, no difference was detected in aortic iNOS protein between the study groups, with average values ranging ±18% of the level observed in Sham rats (not shown). Aortic nitrated protein content (Western blotting) was higher in the NX and NX+Pi groups versus Sham, but was lower in the NX+Ca than in NX and NX+Pi rats (Figure 2B). The index of aortic calcification was increased in the NX and NX+Pi groups when compared with the NX+Ca and Sham groups (Figure 2C).

Endothelium-dependent and -independent vasorelaxation

The relaxations induced by ACh in NE-precontracted endothelium-intact mesenteric artery rings were impaired in the NX and NX+Pi groups, but did not differ from Sham in the NX+Ca group (Figure 3A). The NOS inhibitor L-NAME reduced the relaxations to ACh in all study groups, but the effect was more pronounced in the NX+Ca than the NX and NX+Pi groups, as the ACh-response no more differed between the NX groups in the presence of L-NAME (Figure 3B). The change in the AUC of the ACh-response induced by L-NAME suggested that the contribution of NO to the relaxation was reduced in the NX and NX+Pi groups, but did not differ from Sham in the NX+Ca group (Figure 3C). The addition of exogenous L-arginine (1 mmol/l) *in vitro* had no significant effects on the ACh-induced relaxations (data not shown).

Vasorelaxation to the NO donor nitroprusside in endothelium-denuded rings was slightly decreased in the NX+Pi group when compared with Sham and NX+Ca rats, but did not differ between the Sham, NX and NX+Ca groups (Figure 3D).

Vasoconstrictor responses

Vasoconstrictor sensitivity and maximal responses of mesenteric arterial rings to NE did not differ between the Sham, NX and NX+Ca groups, while sensitivity to NE was slightly higher in the NX+Pi than Sham and NX+Ca groups, and maximal response was lower in the NX+Pi than Sham group (Supplemental Table S1). The sensitivity and maximal responses to KCl did not significantly differ between the study groups. Vasoconstrictor sensitivity to Ang II was lower in the NX+Ca than Sham group, while maximal wall tension in response to Ang II was higher in the NX versus Sham group, and lower in the NX+Ca versus NX group (Supplemental Table S1).

Discussion

This study investigated the effects of dietary phosphate binding and loading on abdominal aortic ACE protein, eNOS content, and calcification, and vascular tone *in vitro* of isolated mesenteric arterial rings in experimental CRI. The two above sites of circulation are in close proximity of each other, so metabolic and functional changes in one probably well correspond to those in the other. In the 27-week study, elevated systolic BP, decreased creatinine clearance, and increased heart/body weight were seen in all NX groups (Table 1). However, phosphate-lowering diet blunted the increase in BP, while phosphate loading did not influence BP. In experimental studies, the lowering of BP after high calcium diet has been attributed to increased natriuresis, reduced sympathetic activity, and enhanced vasodilatation [4,15,23,24]. The present results suggest that reduction of tissue ACE might also play a role in the lowering of BP after increased calcium intake.

Abnormal calcium, phosphate, and PTH metabolism are known causes for increased cardiovascular calcification in CRI [1,2], and in the present study phosphate binding with calcium carbonate reduced aortic calcifications in NX rats, as expected [15]. Previously we have found that calcium-phosphorus balance also influences ACE content in kidney tissue [14,15], and the results of the 12-week pilot study showed that the phosphate binding calcium carbonate diet reduced the amount of ACE in the heart and aorta (Supplementary Figure 1). In the 27-week study aortic ACE protein was decreased after 12 weeks of oral calcium carbonate treatment. In our earlier study, the correlation between ACE protein and ACE mRNA content in kidney tissue was good (r=0.83) [14], and this suggests that changes in tissue ACE are probably explained by alterations at the level of gene expression. In contrast to our previous results on kidney ACE, the content of ACE in the aorta was not increased here after phosphate loading in NX rats [14]. This may be attributed to the abundant calcifications in the aortas of NX+Pi rats, as calcified tissue sections would not contain ACE

to bind the iodinated autoradiography-tracer. Of note, the autoradiography tracings showed that aortic ACE protein was present throughout the vascular wall in all study groups and was not limited to the endothelium (Figure 1).

Deficient endothelium-mediated vasodilatation is a common finding in CRI [24-27]. Previously, we observed that the correction of abnormal calcium, phosphate and PTH levels in NX rats improved endothelium-mediated vasorelaxation via K^+-channels in small 3rd order mesenteric arterial branches [4], and enhanced vasorelaxation via NO and K^+-channels in slightly larger 2nd order mesenteric arterial rings [24]. In the present study, we examined arterial tone in a conduit-size artery due to the greater contribution of endothelium-derived NO to vasodilatation in larger vessels [10,28], and found that phosphate binding normalized the impaired relaxation to ACh in the main branch of the mesenteric artery (Figure 3). As the improved vasorelaxation was entirely inhibited by the NOS inhibitor L-NAME, and the change in AUC induced by L-NAME was more pronounced in the NX+Ca than NX and NX+Pi groups, the beneficial effect could be attributed to enhanced NO-mediated component in the ACh response. Dietary phosphate loading did not decrease the relaxation to ACh, and the contribution of endothelium-derived NO to the vasorelaxation was corresponding in the NX and NX+Pi groups, as judged by the change in AUC induced by L-NAME (Figure 3C). Of note, enhanced vasorelaxation after calcium carbonate was not explained by changes in NO sensitivity in arterial smooth muscle, as the endothelium-independent response to nitroprusside did not differ in the Sham, NX and NX+Ca groups (Figure 3D). Moreover, vasorelaxation via exogenous NO was slightly impaired in the NX+Pi group.

Many studies have examined the effect of CRI on L-arginine metabolism and functional role of the NOS enzymes with somewhat contradictory results [29-32]. Here we found that eNOS content in the abdominal aorta was equally reduced in all NX groups (Figure 4A). Thus, the enhanced endothelium-mediated vasorelaxation in the Ca+NX group was not

explained by changes in the amount of eNOS, since the modulation of calcium-phophorus balance was without effect on the quantity of eNOS protein.

The major effector-peptide of RAS, Ang II, can reduce NO bioactivity through increased production of superoxide radicals, which rapidly inactivate NO and thus prevent its dilatory actions in vascular smooth muscle [13,33]. At the molecular level Ang II, generated predominantly via the action of ACE, up-regulates and activates NADPH oxidases in the vascular wall, resulting in increased superoxide release [34]. Today vascular oxidative stress is considered as one of the culprits leading to the loss of NO-mediated vasodilatation [34]. Furthermore, when superoxide radicals react with NO, the highly reactive radical peroxynitrite is formed, at a reaction rate that is several-fold faster than the scavenging of superoxide by superoxide dismutase [31,35,36]. Peroxynitrite, in turn, can modify tyrosine-residues in proteins to create nitrotyrosine, thus leaving a detectable footprint of oxidative stress in tissues [36]. Here we determined aortic nitrated proteins using Western blotting, and found that the levels were increased in the NX and NX+Pi group, but were significantly reduced in the NX+Ca group. Therefore, phosphate binding with calcium carbonate reduced oxidative stress in vascular tissue. One mechanism leading to reduced local Ang II and superoxide generation could be the reduced amount of arterial tissue ACE (Figure 1). Furthermore, reduced superoxide generation in the vascular wall would result in increased bioactivity of endothelium-derived NO, and this mechanism may explain the enhanced ACh response in the NX+Ca when compared with the NX group.

NO has a short half-life, and thereby NOx determination as the stable end-product of NO metabolism was used to evaluate NO production *in vivo*. Plasma NOx concentration was increased in all NX rats after 27 weeks of CRI, in agreement with previous results in experimental and clinical CRI [30,31]. Urine NOx was also increased in all NX groups. The elevated NOx is considered to reflect oxidative stress and inflammation in CRI [29,31]. The

source of NOx remains unknown from the present results, as we detected reduced eNOS and no differences in abdominal aortic iNOS content after 27 weeks of CRI. Previously, studies examining NO release have shown increased production, whereas those examining NO bioactivity have shown attenuated responses in CRI, and even endothelial cells cultured with uremic plasma *in vitro* have shown increased NO release [for a review, see 31]. Thus, elevated plasma NOx could result from the effects of uremic milieu on NOS activity *in vivo,* while reduced NO bioactivity in uremia has been strongly related to excess NO consumption due to oxidative stress [31]. Of note, elevated NOx could also result from the increased oxidative stress in CRI, as peroxynitrite can break down to form NOx [29,37].

The arterial contractions were examined to uncover possible differences in vasoconstrictor sensitivity that would interfere with the interpretation of the relaxation experiments. No differences were found in responses elicited by membrane depolarisation with KCl, and contractions elicited by NE were also corresponding in the Sham, NX and NX+Ca groups. Therefore, alterations in vasoconstrictor sensitivity did not explain enhanced vasorelaxation in NX+Ca rats when compared with NX rats. The NX+Pi group exhibited lower maximal response but higher sensitivity to NE when compared with Sham rats (Supplementary Table S1), and increased vasoconstrictor sensitivity to NE may thus partially explain impaired vasodilator response to exogenous NO after phosphate loading. Finally, mesenteric arterial rings in the NX group exhibited increased maximal wall tension induced by Ang II, while the response in the NX+Ca group did not differ from Sham rats, and contractile sensitivity to Ang II was even lower in NX+Ca than Sham rats. This implies that phosphate binding with oral calcium carbonate reduced Ang II-mediated responses in arterial tissue even at the level of the AT_1 receptor or its signal transduction cascade.

In conclusion, this study showed that elevated BP in the 5/6 nephrectomy rat model of CRI was associated with impaired vasorelaxation via endothelium-derived NO in the

mesenteric artery, and decreased eNOS, and increased ACE and nitrated proteins in the aorta, and elevated levels of plasma and urine NO metabolites. Phosphate binding with 3.0% calcium carbonate reduced ACE and nitrated proteins in the aorta, and enhanced vasorelaxation via increased bioactivity of endothelium-derived NO. Thus, correction of the disturbances of calcium-phosphorus metabolism could beneficially influence vascular pathophysiology in CRI.

Disclosure

The authors declare no conflicts of interest.

Acknowledgments

The excellent technical assistance of Marja-Leena Koskinen, Riina Hatakka, and Riikka Kosonen are sincerely acknowledged. This study was supported by Finnish Kidney Foundation, Finnish Foundation for Cardiovascular Research, Competitive State Research Financing of the Expert Responsibility Area of Tampere University Hospital, Paavo Nurmi Foundation, Emil Aaltonen Foundation, Pirkanmaa Regional Fund of the Finnish Cultural Foundation, Sigrid Jusélius Foundation, Finska Läkaresällskapet, Liv och Hälsa, and Competitive Research Funding of the Hospital District of Helsinki and Uusimaa.

References

1 Tyralla K, Amann K: Morphology of the heart and arteries in renal failure. Kidney Int Suppl 2003:S80-83.

2 Marco MP, Craver L, Betriu A, Belart M, Fibla J, Fernandez E: Higher impact of mineral metabolism on cardiovascular mortality in a european hemodialysis population. Kidney Int Suppl 2003:S111-114.

3 Safar ME, London GM, Plante GE: Arterial stiffness and kidney function. Hypertension 2004;43:163-168.

4 Jolma P, Kööbi P, Kalliovalkama J, Saha H, Fan M, Jokihaara J, Moilanen E, Tikkanen I, Pörsti I: Treatment of secondary hyperparathyroidism by high calcium diet is associated with enhanced resistance artery relaxation in experimental renal failure. Nephrol Dial Transplant 2003;18:2560-2569.

5 Slatopolsky E, Brown A, Dusso A: Role of phosphorus in the pathogenesis of secondary hyperparathyroidism. Am J Kidney Dis 2001;37:S54-57.

6 Amann K, Tyralla K, Gross ML, Eifert T, Adamczak M, Ritz E: Special characteristics of atherosclerosis in chronic renal failure. Clin Nephrol 2003;60 Suppl 1:S13-21.

7 Nolan CR, Qunibi WY: Treatment of hyperphosphatemia in patients with chronic kidney disease on maintenance hemodialysis. Kidney Int Suppl 2005:S13-20.

8 Moncada S, Higgs A: The l-arginine-nitric oxide pathway. N Engl J Med 1993;329:2002-2012.

9 Geiger M, Stone A, Mason SN, Oldham KT, Guice KS: Differential nitric oxide production by microvascular and macrovascular endothelial cells. Am J Physiol 1997;273:L275-281.

10 Garland CJ, Plane F, Kemp BK, Cocks TM: Endothelium-dependent hyperpolarization: A role in the control of vascular tone. Trends Pharmacol Sci 1995;16:23-30.

11 Raij L: Workshop: Hypertension and cardiovascular risk factors: Role of the angiotensin II-nitric oxide interaction. Hypertension 2001;37:767-773.

12 Ceconi C, Fox KM, Remme WJ, Simoons ML, Deckers JW, Bertrand M, Parrinello G, Kluft C, Blann A, Cokkinos D, Ferrari R: ACE inhibition with perindopril and biomarkers of atherosclerosis and thrombosis: Results from the pertinent study. Atherosclerosis 2008

13 Enseleit F, Hurlimann D, Luscher TF: Vascular protective effects of angiotensin converting enzyme inhibitors and their relation to clinical events. J Cardiovasc Pharmacol 2001;37 Suppl 1:S21-30.

14 Eräranta A, Riutta A, Fan M, Koskela J, Tikkanen I, Lakkisto P, Niemelä O, Parkkinen J, Mustonen J, Pörsti I: Dietary phosphate binding and loading alter kidney angiotensin-converting enzyme mRNA and protein content in 5/6 nephrectomized rats. Am J Nephrol 2012;35:401-408.

15 Pörsti I, Fan M, Kööbi P, Jolma P, Kalliovalkama J, Vehmas TI, Helin H, Holthöfer H, Mervaala E, Nyman T, Tikkanen I: High calcium diet down-regulates kidney angiotensin-converting enzyme in experimental renal failure. Kidney Int 2004;66:2155-2166.

16 Kööbi P, Kalliovalkama J, Jolma P, Rysä J, Ruskoaho H, Vuolteenaho O, Kähönen M, Tikkanen I, Fan M, Ylitalo P, Pörsti I: AT1 receptor blockade improves vasorelaxation in experimental renal failure. Hypertension 2003;41:1364-1371.

17 Arvola P, Porsti I, Vuorinen P, Pekki A, Vapaatalo H: Contractions induced by potassium-free solution and potassium relaxation in vascular smooth muscle of hypertensive and normotensive rats. Br J Pharmacol 1992;106:157-165.

18 Kööbi P, Jolma P, Kalliovalkama J, Tikkanen I, Fan M, Kähönen M, Moilanen E, Pörsti I: Effect of angiotensin II type 1 receptor blockade on conduit artery tone in subtotally nephrectomized rats. Nephron Physiol 2004;96:p91-98.

19 Kalliovalkama J, Jolma P, Tolvanen JP, Kähönen M, Hutri-Kahonen N, Saha H, Tuorila S, Moilanen E, Pörsti I: Potassium channel-mediated vasorelaxation is impaired in experimental renal failure. Am J Physiol 1999;277:H1622-1629.

20 Braman RS, Hendrix SA: Nanogram nitrite and nitrate determination in environmental and biological materials by vanadium (III) reduction with chemiluminescence detection. Anal Chem 1989;61:2715-2718.

21 Bäcklund T, Palojoki E, Grönholm T, Eriksson A, Vuolteenaho O, Laine M, Tikkanen I: Dual inhibition of angiotensin converting enzyme and neutral endopeptidase by omapatrilat in rat in vivo. Pharmacol Res 2001;44:411-418.

22 Kohzuki M, Johnston CI, Chai SY, Jackson B, Perich R, Paxton D, Mendelsohn FA: Measurement of angiotensin converting enzyme induction and inhibition using quantitative in vitro autoradiography: Tissue selective induction after chronic lisinopril treatment. J Hypertens 1991;9:579-587.

23 Hatton DC, McCarron DA: Dietary calcium and blood pressure in experimental models of hypertension. A review. Hypertension 1994;23:513-530.

24 Kööbi P, Vehmas TI, Jolma P, Kalliovalkama J, Fan M, Niemelä O, Saha H, Kähönen M, Ylitalo P, Rysä J, Ruskoaho H, Pörsti I: High-calcium vs high-phosphate intake and small artery tone in advanced experimental renal insufficiency. Nephrol Dial Transplant 2006;21:2754-2761.

25 Joannides R, Richard V, Haefeli WE, Benoist A, Linder L, Luscher TF, Thuillez C: Role of nitric oxide in the regulation of the mechanical properties of peripheral conduit arteries in humans. Hypertension 1997;30:1465-1470.

26 van Guldener C, Lambert J, Janssen MJ, Donker AJ, Stehouwer CD: Endothelium-dependent vasodilatation and distensibility of large arteries in chronic haemodialysis patients. Nephrol Dial Transplant 1997;12 Suppl 2:14-18.

27 Rabelink TJ, Koomans HA: Endothelial function and the kidney. An emerging target for cardiovascular therapy. Drugs 1997;53 Suppl 1:11-19.

28 Boegehold MA: Heterogeneity of endothelial function within the circulation. Curr Opin Nephrol Hypertens 1998;7:71-78.

29 Thuraisingham RC, Roberts NB, Wilkes M, New DI, Mendes-Ribeiro AC, Dodd SM, Yaqoob MM: Altered l-arginine metabolism results in increased nitric oxide release from uraemic endothelial cells. Clin Sci (Lond) 2002;103:31-41.

30 Aiello S, Noris M, Todeschini M, Zappella S, Foglieni C, Benigni A, Corna D, Zoja C, Cavallotti D, Remuzzi G: Renal and systemic nitric oxide synthesis in rats with renal mass reduction. Kidney Int 1997;52:171-181.

31 Thuraisingham RC, Yaqoob MM: Oxidative consumption of nitric oxide: A potential mediator of uremic vascular disease. Kidney Int Suppl 2003:S29-32.

32 Vaziri ND, Ni Z, Wang XQ, Oveisi F, Zhou XJ: Downregulation of nitric oxide synthase in chronic renal insufficiency: Role of excess PTH. Am J Physiol 1998;274:F642-649.

33 Chabrashvili T, Kitiyakara C, Blau J, Karber A, Aslam S, Welch WJ, Wilcox CS: Effects of Ang II type 1 and 2 receptors on oxidative stress, renal NADPH oxidase, and SOD expression. Am J Physiol Regul Integr Comp Physiol 2003;285:R117-124.

34 Förstermann U: Nitric oxide and oxidative stress in vascular disease. Pflugers Arch 2010;459:923-939.

35 Bouloumie A, Bauersachs J, Linz W, Scholkens BA, Wiemer G, Fleming I, Busse R: Endothelial dysfunction coincides with an enhanced nitric oxide synthase expression and superoxide anion production. Hypertension 1997;30:934-941.

36 Beckman JS, Koppenol WH: Nitric oxide, superoxide, and peroxynitrite: The good, the bad, and ugly. Am J Physiol 1996;271:C1424-1437.

37 Moncada S, Higgs EA: Endogenous nitric oxide: Physiology, pathology and clinical relevance. Eur J Clin Invest 1991;21:361-374.

Figure Legends

Figure 1. Representative original tracings (A) and mean±SEM plots (B) of aortic angiotensin-converting enzyme (ACE) content determined using autoradiography; NX=5/6 nephrectomized rats, Ca=high-calcium diet (3.0%), Pi=high-phosphorus diet (1.5%); n=8-10 in each group, **P*<0.05 versus Sham, †*P*<0.05 versus NX, ‡*P*<0.05 versus NX+Pi.

Figure 2. Bar graphs and representative bands of aortic eNOS protein (A), and nitrated proteins (B), determined using Western blotting, and index of aortic calcification (percent of cross section) determined using von Kossa stain (C); mean±SEM, groups as in Figure 1, n=7-11 in each group, intensity of white bands represents binding to specific antibody (A, B); **P*<0.05 versus Sham, †*P*<0.05 versus NX, ‡*P*<0.05 versus NX+Pi.

Figure 3. Relaxations to acetylcholine in endothelium-intact mesenteric arterial rings in the absence (A) and presence (B) of 0.1 mmol/L L-NAME; bar graphs showing the change induced by NOS inhibition with L-NAME (C) in the area under concentration response curve (AUC, arbitrary units) of the acetylcholine response; relaxations to nitroprusside (D) in endothelium-denuded mesenteric arterial rings; mean±SEM, groups as in Figure 2, n=7-11 in each group; **P*<0.05, ANOVA for repeated measurements (A, B, D); **P*<0.05 versus Sham, †*P*<0.05 versus NX, ‡*P*<0.05 versus NX+Pi (C), one-way ANOVA.

Figure 1.

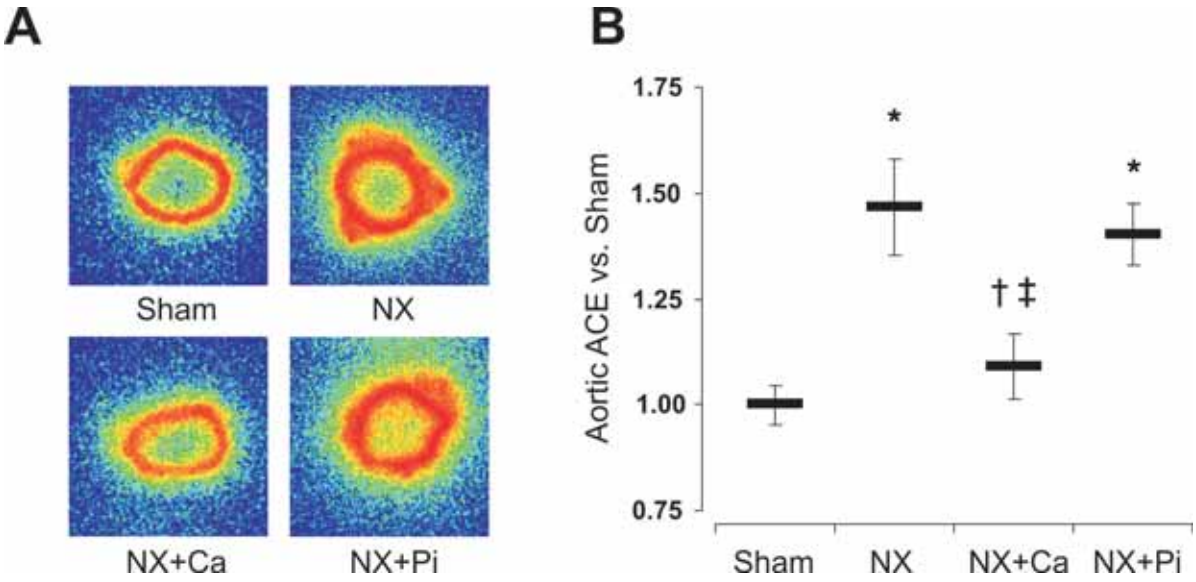
A
Sham
NX
NX+Ca
NX+Pi
B
Aortic ACE vs. Sham
1.75
1.50
1.25
1.00
0.75
*
*
† ‡
Sham
NX
NX+Ca
NX+Pi

Figure 2.

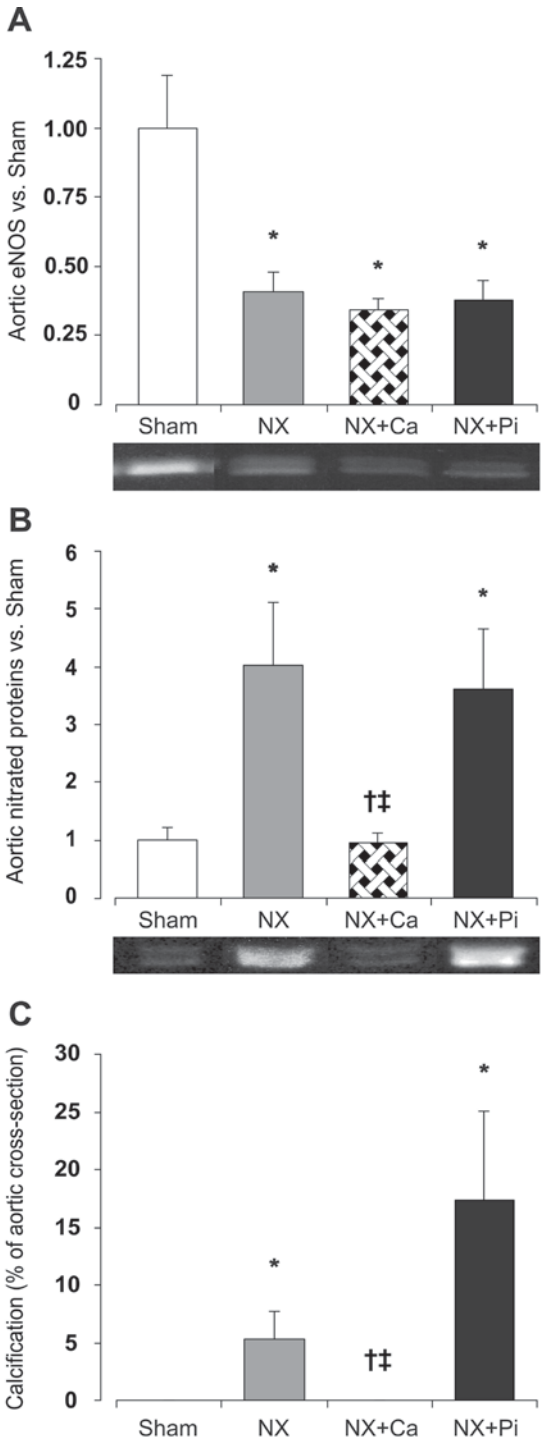
A
Aortic eNOS vs. Sham
1.25
1.00
0.75
0.50
0.25
0
*
*
*
Sham
NX
NX+Ca
NX+Pi
B
Aortic nitrated proteins vs. Sham
6
5
4
3
2
1
0
*
*
††
Sham
NX
NX+Ca
NX+Pi
C
Calcification (% of aortic cross-section)
30
25
20
15
10
5
0
*
*
††
Sham
NX
NX+Ca
NX+Pi

Figure 3.

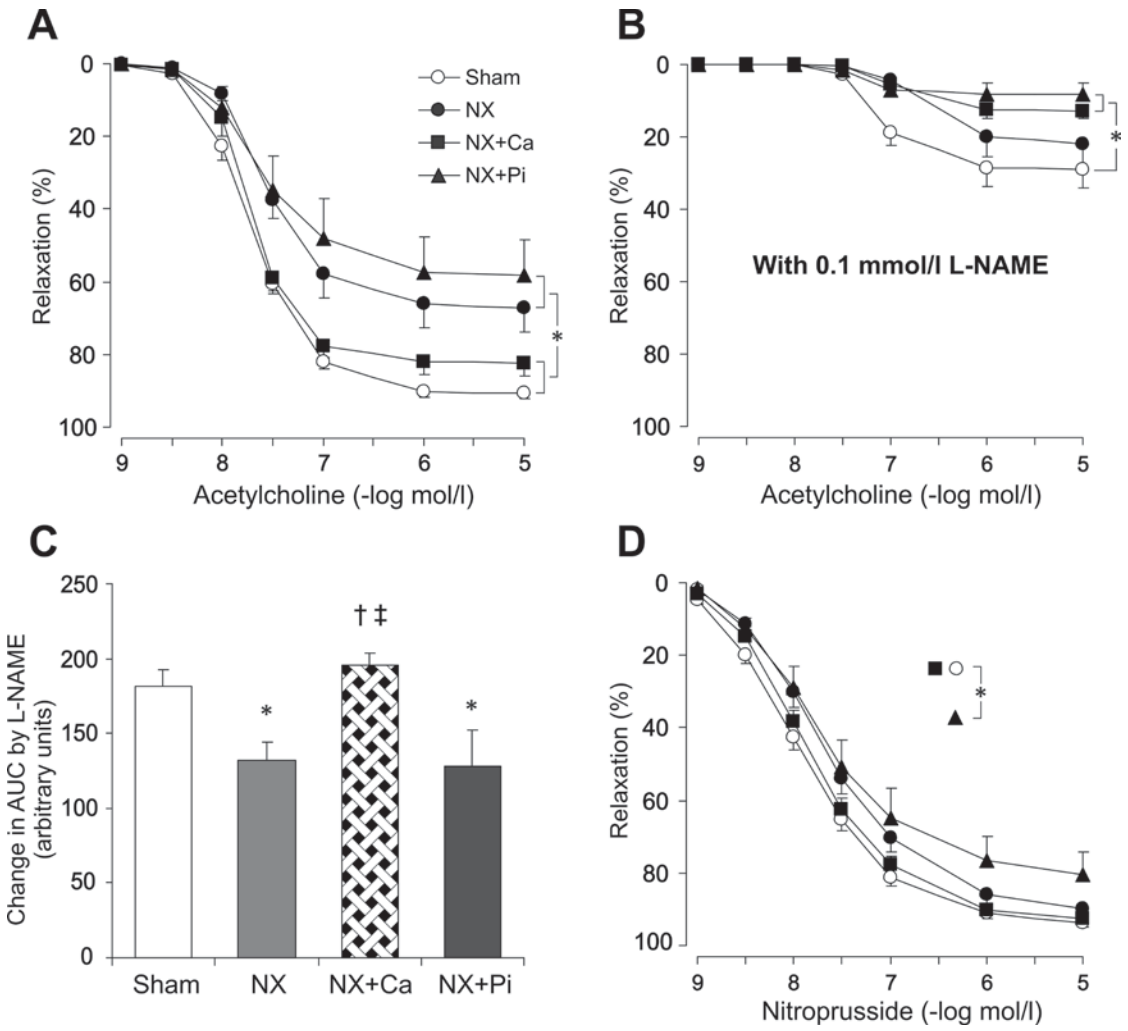
A
Sham
NX
NX+Ca
NX+Pi
Relaxation (%)
Acetylcholine (-log mol/l)
B
With 0.1 mmol/l L-NAME
Relaxation (%)
Acetylcholine (-log mol/l)
C
Change in AUC by L-NAME (arbitrary units)
Sham
NX
NX+Ca
NX+Pi
D
Relaxation (%)
Nitroprusside (-log mol/l)

Table 1. Experimental animal data and laboratory findings in the experimental groups

	Sham	NX	NX+Ca	NX+Pi
Systolic blood pressure				
at week 15 (mmHg)	133±2	154±6*	153±4*	152±4*
at week 27 (mmHg)	129±2	173±4*	145±3*†	161±4*
Body weight at week 15 (g)	499±8	476±9	478±9	484±11
Body weight at week 27 (g)	557±7	507±38	488±13*	431±35*
Heart weight / body weight (g/kg)	3.21±0.03	4.19±0.43*	4.03±0.13*	4.46±0.40*
Creatinine clearance week 27 (µmol/ml/100 g)	327±19	167±34*	177±16*	145±29*
Plasma				
Phosphate (mmol/l)	1.16±0.06	2.52±0.46*	0.81±0.08*†	5.47±1.12*†‡
PTH (pg/ml)	88±12	1172±343*	3.7±0.5*†	3620±236*†‡
Ionized calcium (mmol/l)	1.36±0.06	1.34±0.03	1.55±0.03*†	0.93±0.09*†‡
NOx (µmol/l)	8.9±0.4	11.4±0.9*	14.2±5.1*	18.4±5.1*
Urine				
NOx (µmol/24h)	0.03±0.01	1.36±0.66*	1.49±0.84*	0.80±0.36*

Values are mean ± SEM, n=7-14 for all groups, *P<0.05 versus Sham, †P<0.05 versus NX, ‡P<0.05 versus NX+Ca.